Department of Chemistry

Imperial College London

Towards the Development of Modulators of LRH-1 as Potential Anti-Cancer Therapeutic Leads

Thesis submitted for the partial fulfilment of a PhD degree

Melanie Mueller

Acknowledgements

First of all, I would like to thank Prof. Alan Spivey for adopting me as his student after my previous group "dissolved". I thank him for his constant support and motivation. His door was always open to seek advice. He is a brilliant teacher particularly during the group meetings we have.

The Spivey group, which includes all the past and present members, was a fantastic group to work with. I had a lot of fun discussing all sorts of things over lunch or in the lab. Without you guys, the PhD would only have been half as good!

I would like to thank Prof. Simak Ali and his group for allowing me to carry out the testing of my compounds in their lab. I am also grateful to Prof. Paul Freemont and his group who helped me express the LRH-1 protein that I used in my biological assays. I thank Katie Chapman for her help to get started with the assay.

I thank Prof. Chris Frampton (Pharmorphix, Cambridge) for solving my X-ray crystal structure of one of my compounds, Pete Haycock and Dick Sheppard for help with running NMR spectra and Lisa Haigh for many attempts to run my mass spec samples.

Thank you to my family and friends for their support during all my studies. In particular I would like to thank my sister Melina Bielka, for being such a caring sister.

Finally, I would like to thank my good friend Miguel Navascués for his constant motivation when things did not work according to plan and his patience when I endlessly moaned about that. It is to him that I dedicate this thesis.

Abbreviations

AF-1 activation function-1

AF-2 activation function-2

Ar aryl

Bn benzyl

BnBr benzyl bromide

Boc *tert*-butyloxycarbonyl

Bpin pinacolborane

Bu butyl

Bz benzoyl

CBI co-factor binding inhibitor

Cbz benzyloxy carbamate

CDI carbonyldiimidazole

CTE carboxy terminal extension

DAX-1 dosage-sensitive sex reversal-1

DBD DNA binding domain

DIBAL-H di*iso*butylaluminium hydride

DCIS ductal carcinoma *in situ*

DLPC dilauroyl phosphatidylcholine

DMA dimethylacetamide

DMAP dimethylaminopyridine

DMF dimethylformamide

DMSO dimethyl sulfoxide

DNA deoxyribonucleic acid

dppf 1,1'-bis(diphenylphosphino)ferrocene

DUPC diundecanoyl phosphatidylcholine

E. coli Eschericha coli

EC_{50} half maximal effective concentration

e.g. exempli gratia

ELISA enzyme-linked imunosorbant assay

eq. equivalents

ER estrogen receptor

EtOAc ethyl acetate

EtOH ethanol

FDA food and drug administration

FPLC fast protein liquid chromatography

Ftz-F1 Fushi tarazu factor 1

g grams

GC gas chromatography

GR glucocorticoid receptor

h hours

HDL-cholesterol high density lipoprotein cholesterol

HER2 human epidermal growth factor receptor-2

HRMS high resolution mass spectrometry

IBC inflammatory breast cancer

IDC invasive ductal carcinoma

ILC invasive lobular carcinoma

IPTG isopropyl β-D-1 thiogalactopyranoside

kDa kiloDalton

LB lysogeny broth

LBD ligand binding domain

LBP ligand binding pocket

LCIS lobular carcinoma *in situ*

LDA lithium diisopropylamide

LDL-cholesterol low density lipoprotein cholesterol

LRH-1 liver receptor homologue-1

LRMS low resolution mass spectrometry

M molar

MBP maltose binding protein

m-CPBA *meta*-chloroperoxybenzoic acid

Me methyl

MeCN acetonitrile

MeOH methanol

mg milligramm

mmol millimoles

mL millilitres

mp melting point

MS mass spectrometry

NMP *N*-methyl-2-pyrrolidone

nm nanometer

NR nuclear receptor

PE petrol ether

PGC-1α peroxisome proliferator-activated receptor gamma coactivator-1 alpha

PGE$_2$ prostaglandine E$_2$

PPARγ peroxisome proliferator activated receptor γ

Ph phenyl

1,10-phen 1,10-phenanthroline

PPI protein-protein interaction

PR progesterone receptor

rpm rounds per minute

RT room temperature

SAR structure-activity relationship

SDS-PAGE SDS polyacrylamide gel electrophoresis

sec second

SEM 2-(trimethylsilyl)ethoxymethyl

SERM selective estrogen receptor modulator

SF-1 steroidogenic factor-1

SM starting material

SRC-1 steroid receptor co-factor-1

SRC-3 steroid receptor co-factor-3

TBAF tetrabutylammonium fluoride

TBAI tetrabutylammonium iodide

TEV tobacco etch virus

TFA trifluoroacetic acid

TFAA trifluoroacetic anhydride

THF tetrahydrofuran

TIF-2 transcriptional intermediary factor-2

TLC thin layer chromatography

TR thyroid hormone receptor

TrCl trityl chloride

TR-FRET time resolved fluorescence resonance energy transfer

UV ultra violet

VS virtual screening

Abstract

Breast cancer is the most common cancer in women worldwide and afflicts about 30 % of all women between 35 and 50 years. The majority of breast cancers are estrogen dependent. This means that they need estrogen for their development and growth. Estrogen dependent breast cancers can be treated with hormone therapy to block estrogen action and prevent cancer growth. Unfortunately, there are many side effects associated with this treatment and therefore, there is a great need for the development of new therapies for breast cancer. Liver receptor homologe-1 (LRH-1) is a nuclear receptor that recently came into focus for its implications in breast cancer development and growth. Targeting LRH-1 could present an alternative approach for the treatment of breast cancer. There are two potential sites to target nuclear receptors: the ligand binding pocket or the co-activator binding site. Both sites are known to be crucial for the transcriptional activity of nuclear receptors.

This thesis gives an overview about breast cancer and the role of nuclear receptors in this disease. In particular, approaches to the regulation of nuclear receptors using small molecule antagonists are discussed both in terms of traditional "ligand binding pocket" inhibitors and the more recently explored "co-activator binding inhibitors". Both approaches are explained generally and in the context of LRH-1.

The work described here is divided into two parts: The first part describes the synthesis and evaluation of a library of benzimidazole-based potential antagonists of LRH-1. These molecules are expected to bind into the ligand binding pocket and act as traditional antagonists.

The second part of this thesis explains the synthesis of an α-helix mimetic. A previous PhD student in the group developed a route for the synthesis of an α-helix mimetic. The mimetic targeted here was anticipated to bind competitively to the co-activator binding site of LRH-1 and prevents co-activators from binding and consequently blocks transcriptional activity.

Declaration: Hereby I declare that I personally prepared this thesis. I conducted the work described here, unless otherwise stated. Other information used for the preparation of this thesis are acknowledged by means of references.

Contents

Contents

1. Introduction

1.1 Introduction to Breast Cancer

1.1.1 The Normal Breast

The breast consists of fat, connective tissue and glandular tissue. The glandular tissue contains the lobes (milk glands), where the milk is produced, and milk ducts, which connect the lobes to the nipple (**figure 1.1**).
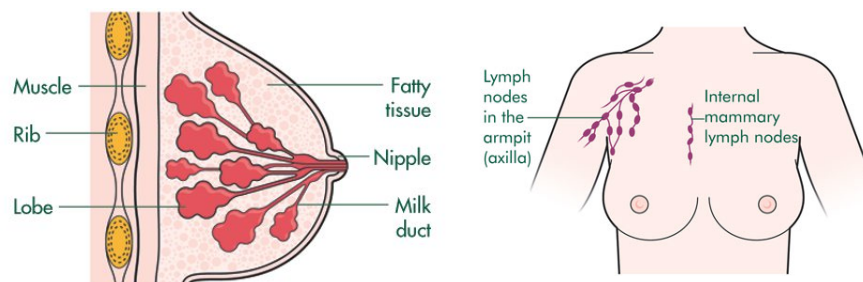
Figure 1.1: Structure of the breast (illustrations from Macmillan Cancer Support). [1]

The area of breast tissue extends into the axilla, the breast bone and the collar bone, where lymph nodes can be found that connect the breast to the lymphatic system. [2]

1.1.2 Breast Cancer

Breast cancer is a malignant tumour that originates in the breast tissue, most commonly in the ducts or lobes. [2]

In the western world, the incidences of breast cancer have doubled since 1940. [3] World-wide, a yearly incidence rate of nearly one million new cases has been estimated. Breast cancer constitutes 30% of all cancers in women between 35 and 55 years of age. [3]

1.1.2.1 Types of Breast Cancer

Traditionally, breast cancers are classified according to their origin. There are 5 main types of breast cancer subdivided into 3 classes: ductal carcinomas, lobular carcinomas and rare types.

Ductal Carcinomas

Ductal carcinoma *in situ* (DCIS)
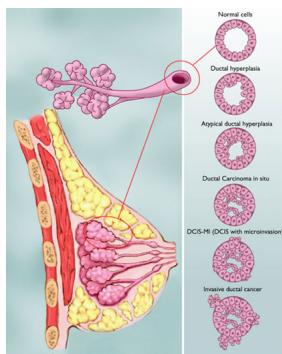
20% of breast cancers are DCISs. This type of cancer is made of irregular cells found in the ductal system of the breast (**figure 1.2**). DCISs are the most common non-invasive breast cancer. It is a non-metastatic breast cancer, but around 50% of DCISs progress to become malignant. Between 50 and 75% are ER/PR positive and have a good prognosis. The remaining 30-50% are HER2 positive with a worse prognosis than the ER/PR positive cancers. [4]

Figure 1.2: Illustration of DCIS (Image used with kind permission from breastcancer.org) [4]

Invasive ductal breast cancer (IDC)

With about 80% of cases, IDCs are the most common type of invasive breast cancers. Originated in the milk ducts, this cancer invades the surrounding tissue. IDCs move to other parts of the body through the blood stream or the lymphatic system. Women over 40 years have an increased risk of developing invasive ductal carcinomas. [4]

Lobular Carcinoma

Lobular carcinoma *in situ* (LCIS)

LCIS is a benign type of breast cancer, which starts in the milk producing glands. It is often referred to as lobular neoplasia. Unlike the DCIS, it does not progress to its invasive type. LCIS are most commonly found in pre-menopausal women aged 40-50. They are usually HER2 negative but ER/PR positive and can therefore be treated with hormone therapy. [4]

Invasive lobular breast cancer (ILC)
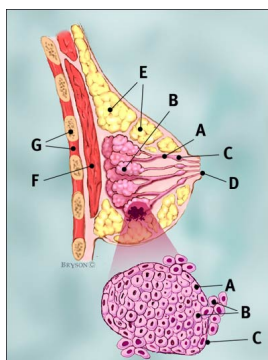
This type develops in the milk-producing glands of the breast (**figure 1.3**). Like the IDCs, it invades the surrounding tissue and has the ability to metastasise. It presents as an abnormal feeling in the breast. ILCs are most common in women between 45 and 56 years. [4]

Figure 1.3: Illustration of ILC: **Breast profile: A:** ducts; **B:** lobules; **C:** dilated section of duct to hold milk; **D:** nipple; **E:** fat; **F:** pectoralis major muscle; **G:** chest wall/ rib cage; **Enlargement: A:** normal cells; **B:** lobular cancer cells breaking through basement membrane; **C:** basement membrane (Image used with kind permission from breastcancer.org) [4]

1.1.2.2 Rare Types of Breast Cancer

Inflammatory Breast Cancer (IBC)

In inflammatory breast cancer, the cancer cells grow along small lymph vessels in the skin of the breast and block these vessels. The body reacts to this blockage with symptoms similar to an inflammation: the breast becomes swollen sore and often develops an orange-peel like skin.

With only 1-4% of breast cancer patients affected by IBC, it is a rare but aggressive form of breast cancer. [1]

Paget's Disease

Paget's disease affects less than 5% of breast cancer patients and shows with an eczema-like change of the nipple and areola. The majority of patients with Paget's disease have underlying DCISs or a type of invasive cancer. [4]

Breast Cancer in Men

Breast cancer in men is very rare. As for women, age is a major risk factor. Additional risk factors are exposure to estrogen, radiation to the chest and Klinefelter's syndrome. This syndrome is a set of symptoms that result from the presence of an additional of X chromosome, which can cause an increased concentration of circulating estrogen and hence more feminie body features and a higher risk to develop brest cancer.

1.1.2.2 Molecular Classification of Breast Cancers

More modern classification methods also take other relevant information such as the grade and receptor status into account. The grade is determined by microscopic analysis and gives information about the appearance of the breast cancer cells. A low grade corresponds to well differentiated cancer cells, that appear similar to healthy cells in shape and organisation. Low grade cancers are associated with slowly growing tumours and a good prognosis. In contrast, high grade breast cancer cells are not differentiated and exhibit an abnormal shape and a non-tissue like organisation. High grade breast cancers are associated with fast growing tumours and a worse prognosis.

The receptor status defines which receptors are expressed in the breast cancer. Nuclear receptors are transcription factors that regulate the expression of their target genes. In the context of breast cancer, there are three important nuclear receptors: the estrogen receptor (ER), the progesterone receptor (PR) and HER2 (Human Epidermal Growth Factor Receptor

2). ER/PR positive breast cancers express the estrogen receptor and the progesterone receptor. ER/PR positive breast cancers are estrogen dependent tumours and require estrogen for their growth. Due to this dependency, ER positive tumours can be treated by hormone therapy, which generally improves the prognosis. Tumours that express HER2 are termed HER2 positive. This can be in conjunction with ER/PG, so that all three receptors are present. Breast cancers which express the HER2 receptor have a worse prognosis than the only ER/PR positive cancers as they tend to be of higher grade and more proliferative. Additionally, there are breast cancers where none of the mentioned receptors are expressed. These "triple negative" cancers are generally associated with a bad prognosis.

By taking into account more factors, a more accurate classification of the breast cancer is possible which allows for a more individual treatment and can prevent over- or under-treatment of breast cancer patients.

1.1.3 Risk Factors for Breast Cancer

The greatest risk factor for breast cancer is gender. The occurrence of breast cancer in women is 100 times higher than in men. [5] The risk to develop breast cancer increases steadily with age. The vast majority of patients are women over 50 years of age.

Although only 5-10% of cases are considered hereditary, genetics are a risk factor. [3] Alterations in the BRCA-1 and BRCA-2 genes are the most common mutations accounting for the development of breast cancer. Closely related to the hereditary risk factor is the family history. The risk increases the more close relatives developed breast cancer.

An important risk aspect is the hormonal history. The exposure to estrogen and progesterone for a long period of time has been linked to an increased risk of developing breast cancer. The use of hormone replacement therapy or the contraceptive pill increases estrogen levels and contributes to this hormonal history. Further aspects include early menarche, late menopause, having no children or having children late in life and not having breastfeed children. [6]

After the menopause, when the ovary has stopped the production of estrogen, adipose tissue is the major source of estrogen. It is produced from androgens by the aromatase enzyme. Therefore, obesity is a risk factor for the development of breast cancer. There is evidence that a lack of physical activity increases the risk of breast cancer, independent of the menopausal status. [7] Other common risk factors are smoking and excessive alcohol consumption.

1.1.4 Treatments for Breast Cancer

The first line of treatment is surgery where parts of the breast (lumpectomy) or the whole breast (mastectomy) are removed. To reduce the risk of reoccurrence, radiation therapy is routinely used as adjuvant therapy after the surgical removal of the tumour. Chemotherapy is only indicated for invasive types of cancer. [6] Another adjuvant therapy is hormone therapy. In ER positive breast cancers, where estrogen is required for the tumour growth, blocking estrogen from binding to the estrogen receptor or reducing estrogen production are important methods of treatment. This can be achieved with selective estrogen receptor modulators, which prevent estrogen from binding to the estrogen receptor or aromatase inhibitors that reduce the local estrogen production.

In HER2 positive breast cancers, adjuvant therapy can also consist of treatment with a monoclonal antibody which blocks HER2 action such as Trastuzumab (Herceptin®).

1.1.4.1 Hormone Therapy-Estrogen and the Estrogen Receptor

Estrogen is a steroidal hormone that is produced by the female ovaries. It is involved in cell proliferation in the breast inner lining and the uterine inner lining (endometrium) to prepare the female body for a possible pregnancy. At the end of the menstrual cycle the concentration of circulating estrogen decreases dramatically and the endometrium is shed out as menstruation. Additionally, estrogen is involved in maintaining bone density, lowers LDL-cholesterol and increases HDL-cholesterol. Estrogen has been shown to slow down the development of dementia and has a positive effect on cognitive functions (**figure 1.4**).
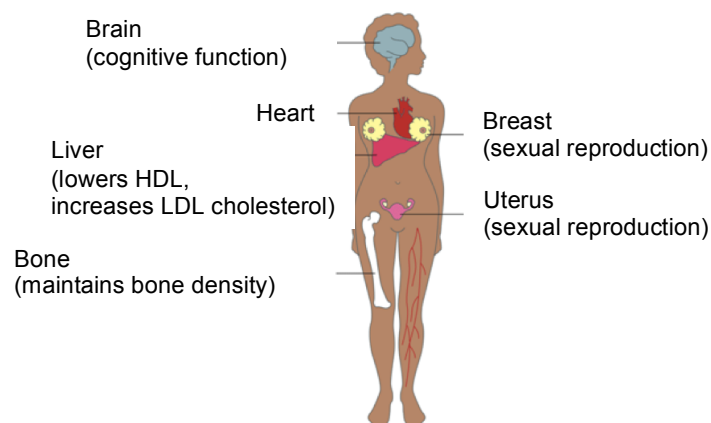

Figure 1.4: Sites of estrogen action. [8]

The actions of estrogen are mediated by the ER, a nuclear receptor of the family of ligand-activated transcription factors. Upon estrogen binding the estrogen receptor is activated and controls the expression of its target genes.

Selective Estrogen Receptor Modulators (SERMs)

SERMs stimulate or inhibit the action of estrogen in different tissues. The most famous example is Tamoxifen (Nolvadex®). It has anti-estrogenic properties in breast tissue and prevents cell growth and therefore reduces the risk of breast cancer (**figure 1.5**).

Tamoxifen (Nolvadex®, Istubal®, Valodex®)   Toremifene   GW5638
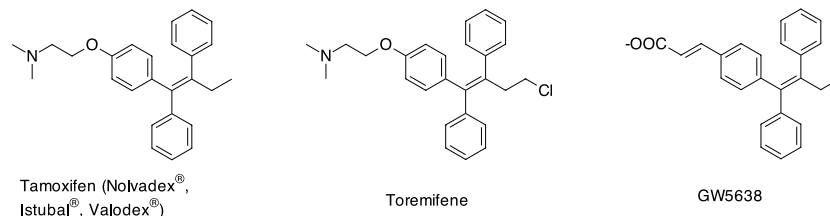
Figure 1.5: Structures of selected SERMs.

Additionally, Tamoxifen has beneficial estrogen-like properties in the bone, where it preserves bone mineral density, and in the liver, where it affects cholesterol metabolism. [9] In 1977 the FDA approved Tamoxifen for the treatment of advanced breast cancer and in 1998 Tamoxifen was approved for the reduction of risk of breast cancer in pre-and postmenopausal women. [9, 10] To date, Tamoxifen is the most prescribed anti-cancer drug. However, it exhibits severe side effects. Due to its estrogen-like behaviour, Tamoxifen increases the risk of uterine endometrial cancer and causes thromboembolic events in postmenopausal women.

Another problem occurring with Tamoxifen is that a high population of tumours that express the ER develop a resistance to Tamoxifen. This can lead to the rapid reoccurrence of the breast cancer when undetected. There are many possible explanations for this resistance. Some of which are mutations in the ER, limited ER saturation by Tamoxifen due to a reduced intracellular concentration, alterations in the co-regulator proteins or increased metabolism of Tamoxifen to its agonistic metabolites (*e.g.* 4-hydroxy-*N*-desmethyltamoxifen). [11, 12,13]

Raloxifene (Evista®) is a second generation SERM. It works in a similar fashion to Tamoxifen by acting as an anti-estrogen in breast tissue, and estrogen-like in bone and liver (**figure 1.6**).

Raloxifene (Evista®)   Arzoxifene   EM 652

Figure 1.6: Structure of Raloxifen and analogues- second generation SERMs.

After being originally approved for preventing osteoporosis in postmenopausal women, Raloxifene is now also approved for reduction of risk of breast cancer in postmenopausal

patients. Because of its poor bioavailability and short half life, the efficacy of Raloxifen in preventing breast cancer is slightly lower than of Tamoxifen. On the other hand, Raloxifen does not increase the risk of endometrial cancer.
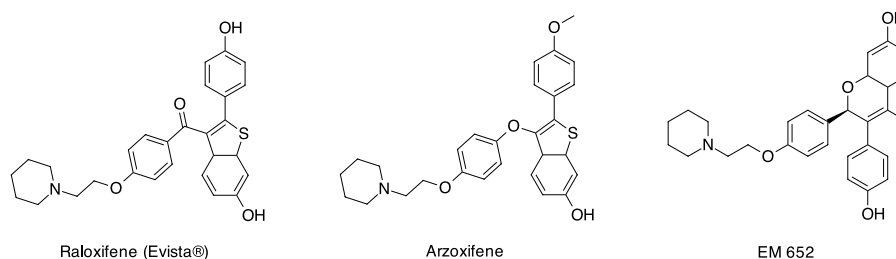
Aromatase Inhibitors

Aromatase is an enzyme of the P-450 superfamily. It is responsible for the final step in the conversion of androgens to estrogen. After the menopause the ovaries stop the production of estrogen. The residual estrogen production is solely from non-glandular sources, in particular subcutaneous fat.

Aromatase inhibitors are designed to reduce the risk of breast cancer in postmenopausal women. They act *via* the inhibition of aromatase and prevent the synthesis of estrogen. Aromatase inhibitors affect the estrogen production in the whole body and do not profit from the positive effects on the bones density of the SERMs. The most serious side effects include loss of bone density, an increased fracture rate and heart problems. There are two types of third generation aromatase inhibitors: the steroidal and non-steroidal type (**figure 1.7**).

Exemestane (Aromasin®)   Letrozole (Femara®)   Anastrazole (Arimidex®)

Steroidal aromatase inhibitor   non-steroidal aromatase inhibitor
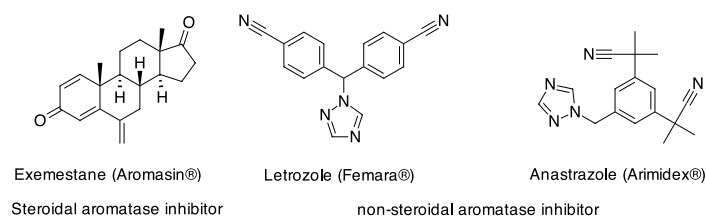
Figure 1.7: Structures of aromatase inhibitors.

The steroidal aromatase inhibitors such as Exemestane (Aromasin®), bind irreversibly to the aromatase enzyme and deactivate the enzyme. The non-steroidal aromatase inhibitors such as Letrozole (Femara®) or Anastrozole (Arimidex®) also bind to aromatase to prevent its actions, but do so in a reversible manner. Current trials are evaluating the use of aromatase inhibitors as first line adjuvant therapy in breast cancer.

Estrogen Receptor Downregulators

Estrogen receptor downregulators are used in patients with metastatic breast cancers and where other hormone therapies have stopped working. Fulvestrant (Faslodex®) is one of these downregulators (**figure 1.8**).

Fulvestrant (Faslodex®)
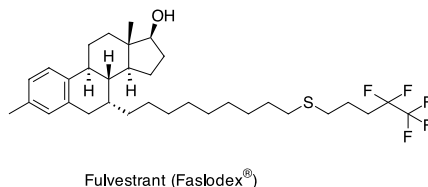
Figure 1.8: Structure of estrogen downregulator Fulvestrant.

Fulvestrant acts in two different ways: as an anti-estrogen, it binds to the ER and prevents estrogen from binding. This deactivates both co-activator binding sites (AF-1 and AF-2) and prevents dimerisation, both required for the receptor's action. Additionally, it destroys the ER and consequently decreases the concentration of the ER.

Antibody Therapy

Breast cancers, where HER2 is overexpressed can be treated with Trastuzumab (Herceptin®). This drug consists of a monoclonal antibody that blocks the action of a growth-promoting protein HER2/neu and prevents cell division and therefore, cancer growth.

The work presented in this thesis concerns the development of molecules designed to inhibit the action of nuclear receptors. For a better understanding of the action of nuclear receptors, a brief introduction into nuclear receptors is given here.

# 1.2 Nuclear Receptors

Nuclear receptors are the largest super family of intracellular transcription factors with 48 members identified in the human genome. [14] From these, 25 nuclear receptors are classified as orphan, [15] which means that no ligand has yet been identified. Nuclear receptors play important roles in key biological processes, ranging from development and reproduction to homeostasis and metabolism. [16] The nuclear receptor super family is divided into three classes. The steroid receptor class includes the progesterone receptor, estrogen receptor and androgen receptor, the thyroid/retinoid class that includes the thyroid receptor, vitamin D receptor and the orphan receptor class. [17] As indicated above, in the context of breast cancer, there have traditionally been considered three nuclear receptors of importance: the estrogen receptor, progesterone receptor and HER2. Recently, however, a fourth nuclear

receptor involved in breast cancer came into focus: Liver receptor homologue-1 (LRH-1 or NR5A2).

LRH-1 is a monomeric nuclear receptor that belongs to the Ftz-F1 subgroup of nuclear receptors. [18, 19] Its closest mammalian homolog is steroidogenic factor-1 (SF-1) Both LRH-1 and SF-1 are considered orphan nuclear receptors. However, recent studies suggest phosphatidyl inositols [20, 21] and phospholipids such as dilauryl phosphatidylcholine (DLPC) and diundecanoly phosphatidylcholine (DUPC) could be its endogenous ligands (**figure 1.9**). [22]

Dilauroyl phosphatidylcholine (DLPC)   Diundecanoyl phosphatidylcholine (DUPC)
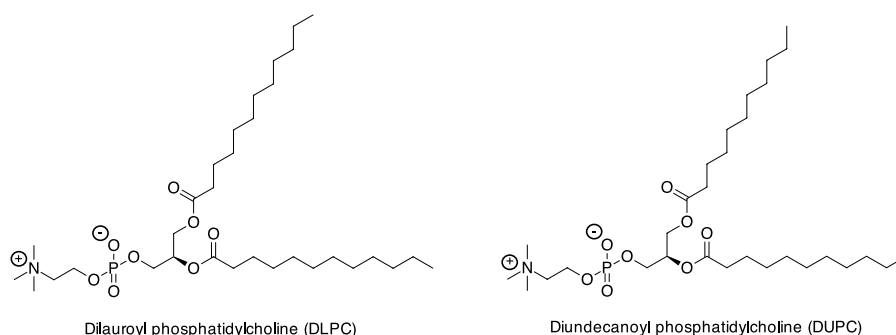
Figure 1.9: Structures of phospholipids DLPC and DUPC.

SF-1 expression is mainly restricted to steroidogenic tissue such as found in the ovary and adrenal cortex, [23] where it regulates the synthesis of various steroids. In adult mammals, LRH-1 is expressed in the liver, pancreas and intestine, [19] where it plays a key role in metabolic pathways, [24] which include the regulation of cholesterol metabolism, reverse cholesterol transport to the liver and bile acid synthesis. LRH-1 is also expressed at high levels in the ovaries, more specifically in the granulosa cells and corpora lutea, [18] where it is involved in steroid synthesis. [25] Additionally, LRH-1 is vital in early development by maintaining undifferentiated embryonic stem cells [26, 27] *via* controlling the expression of two transcription factors: Oct4 and Nanog. [21]

Recent studies showed that LRH-1 is also expressed in colon, gastric and breast cancers where, it is involved in tumour development and progression. [18, 28–31]

1.2.1 Structure of Nuclear Receptors

Like all nuclear receptors, members of the Ftz-F1 subfamily share a highly conserved domain structure (**figure 1.10**). [19]
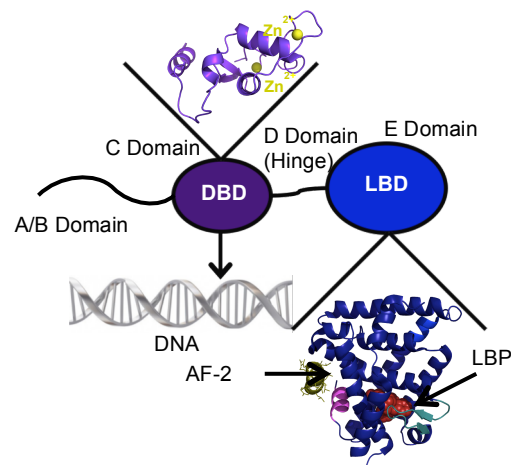
Figure 1.10: Domain structure of nuclear receptors: [16] **A/B domain:** contains the ligand independent activation function (AF-1); **C domain:** Contains the DNA binding domain, the CTE and the Ftz-F1 box; **D domain:** flexible hinge between DBD and LBD; **E domain:** contains ligand-dependent activation function (AF-2). (PDBs for zinc finger: 2A66, LRH-1: 3PLZ)

A/B domain

The N-terminal regions of nuclear receptors are highly variable in sequence and size and harbour potent transcription activation functions, known as activation function-1 (AF-1). [32] This function assists in the regulation of transcriptional activity and is independent from ligand binding. The AF-1 region of the protein is one of two sites involved in co-regulator binding. Additionally, it is an important site for posttranslational modification by processes such as phosphorylation and sumoylation. [15]

C domain

The C domain includes the DNA binding domain (DBD), which targets specific DNA sequences known as hormone response elements. [33] The DBD consists of two cysteine rich zinc fingers that mediate DNA binding. This region is also important for regulating the dimerisation of the nuclear receptor either to give a homodimer or a heterodimer. [15] Located at the C-terminal end of the zinc finger module, is the carboxy-terminal extension (CTE), which extends the contact surface between the receptor and the DNA (**figure 1.11**).
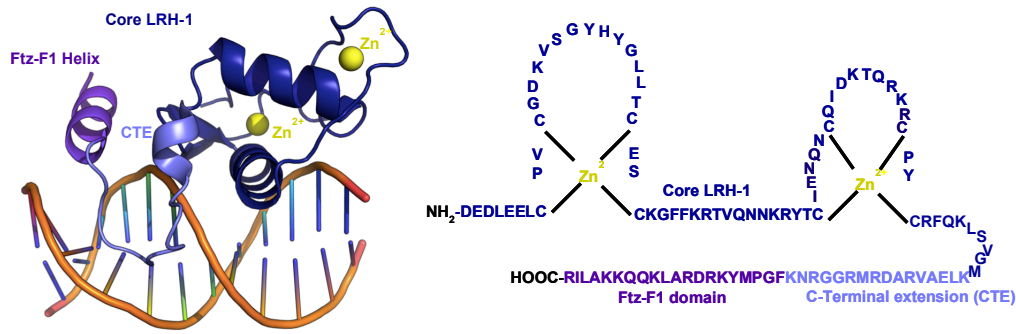
Figure 1.11: Crystal structure of zinc fingers (PDB: 2A66). [34]

Most nuclear receptors bind to DNA as dimers: either as homodimers, like the ER, or as heterodimers with retinoid X receptor. By contrast, LRH-1 and other members of the Ftz-F1 subfamily bind to DNA as monomers. Here, the specificity of DNA binding is dictated by the Ftz-F1 box, a unique feature of the members of the Ftz-F1 subfamily. This box is a sequence of 20 amino acids located immediately after the CTE. [34]

D domain

The region between the DBD and the ligand binding domain (LBD) is a flexible hinge region. This region allows for the accommodation of rotational differences, [35] but is also an important site for posttranslational modifications. [15]

E domain

The E domain or ligand binding domain (LBD) is located at the carboxy-terminal end of the protein and can be seen as a molecular switch, which, upon ligand binding shifts the receptor to a transcriptionally active state. [33]

The LBD of most nuclear receptors shows a common structure consisting of 12 α-helices and a short β turn, which form 3 antiparallel helical sheets that shape the so-called α-helical sandwich that forms the ligand binding pocket (LBP). [16] The ligand binding domain also includes a ligand-dependent activation function (AF-2), which is located at the carboxy-terminus of the LBD. Both the LBP and the AF-2 function are essential for the regulation of the transcriptional function of the nuclear receptor (**figure 1.12**).

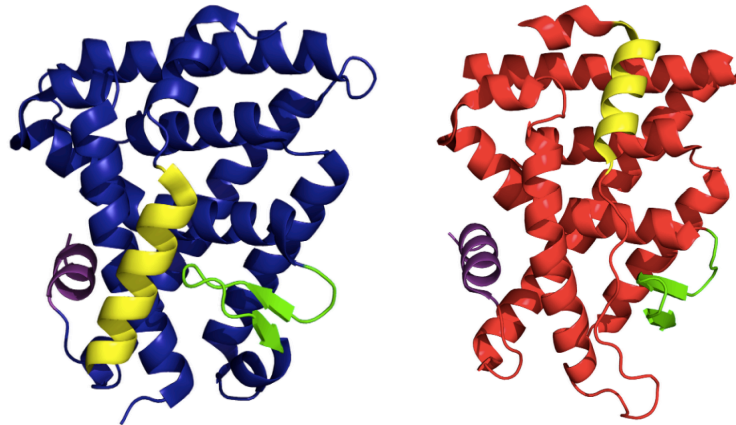**Figure 1.12: Left:** Crystal structure of LRH-1 with extended helix 2 (yellow) and the AF-2 function in an active conformation; **Right:** Crystal structure of LBD ER with helix 2 (yellow) (PBD LRH-1: 3PLZ, ER: 2QZO). [36]

The Crystal structure of mouse LRH-1 LBD shows a stable monomer with a large but empty LBP (blue crystal structure). [36] Additionally, at the N-terminal region of the LBD, the rigid structure of helix 2 (yellow) forms a fourth layer in the canonical fold of the LBD. In contrast, the LBD of the ER (red crystal structure) has a short helix 2 which does not form an additional layer. This difference in structure relative to most nuclear receptors confers LRH-1 with constitutional activity by indirectly stabilising the active position of helix 12 (purple) and so of the AF-2 function. This constitutional activity is also common among orphan receptors.

Co-Factors

Co-activators positively regulate a nuclear receptor and enable its transcriptional activity, whereas co-repressors dampen the transcriptional activity of nuclear receptors. Analysis of numerous nuclear receptors has revealed that the ligand dependent transcriptional activation function (AF-2) consists of a short LXXLL motif (where L is leucine and X is any amino acid) in a hydrophobic cleft on the surface of the ligand binding pocket. Residues adjacent to the LXXLL core encode domains with specificity for different nuclear receptors. [37]

The hydrophobic cleft is flanked by charged residues, the "charge clamp" on either side, that contributes to the orientation of the co-factor towards the LBD and its specificity. [37] In ligand-activated nuclear receptors, binding of ligands induces a conformational change that alters the orientation of several helices, in particular helix 12, which contains the AF-2 domain. This repositioning uncovers the hydrophobic binding cleft and enables co-activator binding, which results in an enhancement of transcriptional activity (**figure 1.13**). [15]
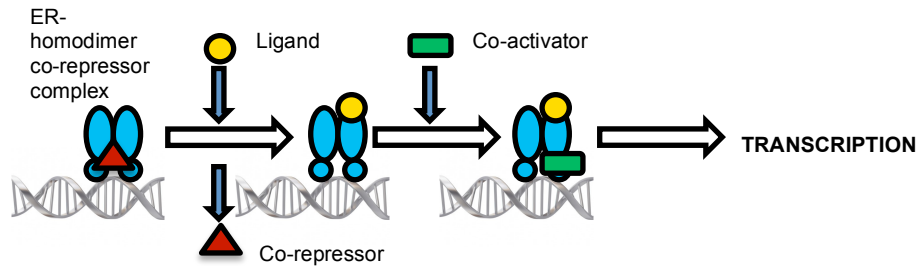
Figure 1.13: Schematic diagram of a ligand-dependent nuclear receptor: [38] Upon Ligand binding a conformational change is induced that leads to release of the co-repressor and recruitment of a co-activator and results in transcriptional activity.

Orphan receptors, such as LRH-1 and SF-1 are constitutively active and therefore exhibit slight differences in the LBD structure and mode of action. As their helix 12 is prepositioned for optimal co-activator binding, orphan receptors are particularly sensitive to co-activator proteins. Differential co-regulator binding can therefore directly affect the activity of the nuclear receptor (**figure 1.14**). [15]
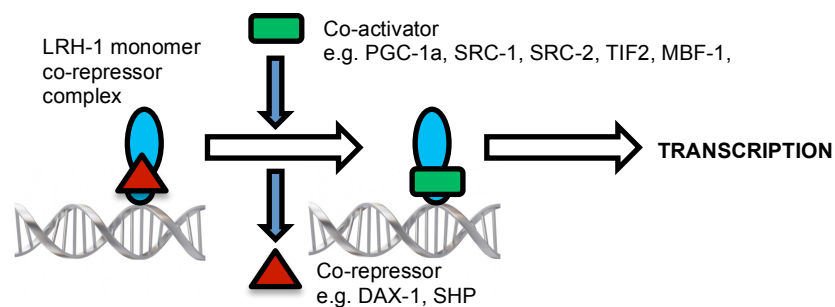
Figure 1.14: Schematic representation of orphan receptors: [38] Competitive binding of co-factors can lead to binding of a co-activator and transcriptional activity.

The transcritptional activity of LRH-1 strongly depends on the presence or absence of co-activators. They are expressed in a tissue specific manner and regulate the activity of LRH-1 by competitive binding to the receptor.

1.3 Implications of LRH-1 in Breast Cancer

As detailed above, estrogen is known to play a critical role in the development and progression of breast cancer. [39] Its action is mediated by the ER, which is expressed in the majority of breast cancers. [39] In healthy women, aromatase expression in adipose tissue is low and originates mainly from activation of the promoter called I.4. [39] In breast cancer surrounding adipose tissue, the gonadal type promoter pII is used. The most potent factor identified that stimulates the activity of promoter pII is prostaglandin E_2 (PGE_2), [30] which is produced by the breast tumour itself. Interestingly, LRH-1 is co-expressed with aromatase in

undifferentiated adipose stromal cells and has the ability to bind to the promoter pII and thus stimulate aromatase expression. At the same time, PGE_2 stimulates aromatase activity by inducing the expression of LRH-1. [30] As aromatase is a crucial factor for the conversion of androgens into estrogen, this results in an increase in estrogen levels in breast cancer surrounding adipose tissue.

In addition to these implications of LRH-activity in aromatase expression, LRH-1 is directly involved in the regulation of the expression of ERα. Furthermore, Annicotte *et al*. [18] have reported that LRH-1 contains a near perfect palindromic estrogen response element to which ERα binds and stimulates LRH-1 expression (**figure 1.15**). [25]
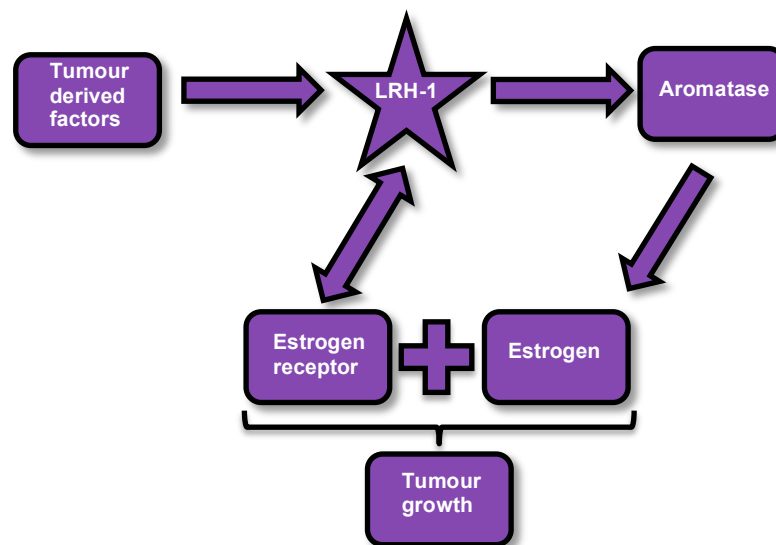
Figure 1.15: Connection between LRH-1, aromatase and the estrogen receptor.

Clyne *et al*. [40] showed that LRH-1 is directly implicated in cell migration and increases cell invasiveness in normal and malignant breast tissue, independent of the ER status.

Cell migration is important for cancer progression and is the initial step in tumour metastasis. The cells subsequently invade into adjacent tissue and start growing. [40]

In summary, LRH-1 locally induces the production of estrogen *via* the regulation of the expression of aromatase in adipose stromal cells. Within the tumour, LRH-1 regulates estrogen dependent cell proliferation [41] and is directly involved in the expression of ER, which in turn, regulates the expression of LRH-1. [24,39,40] These two properties of LRH-1 cause a steep increase in the local estrogen levels of the tumour surrounding tissue, which ultimately results in tumour growth. Additionally, LRH-1 is involved in cell migration and increases cell invasiveness in breast cancer. These implications make LRH-1 a very interesting target for the treatment of breast cancer.

1.4 History of Nuclear Receptors as Therapeutic Targets

Nuclear receptors are implicated in a variety of functions ranging from embryonic development to homeostasis. [42] Dysfunction of the nuclear receptor signalling can result in many pathological processes such as diabetes, cancer, rheumatoid arthritis and hormone resistance. [42] Therefore, nuclear receptors are of great interest in the development of new drugs.

The first drugs to target nuclear receptors were discovered before the discovery of the nuclear receptors themselves. One of these examples started as a treatment of Addinson's disease (glucocorticoid deficiency). [42] Extracts from adrenal glands had been shown to bring relief from stress-related disease and reduce inflammatory conditions; cortisone was identified as the active component of these extracts and used as a therapeutic.

With this early success further evolution of the first generation of steroidal glucocorticoids was started which led to the modern glucocorticoid steroids such as Prednisolone, Dexamethasone and Fluocotolone (**figure 1.16**). [42, 43]
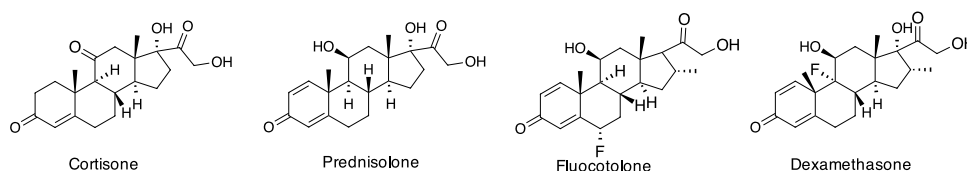
Figure 1.16: Examples of modern glucocorticoids.

In 1929 estrone was isolated independently by Doisy and Butenandt. The latter elucidated its structure in 1932. [44] Six years later, Inhoffen and Hohlweg [45] published the first synthesis of ethinyl-estradiol, which later became a cornerstone of modern female fertility control (**figure 1.17**).
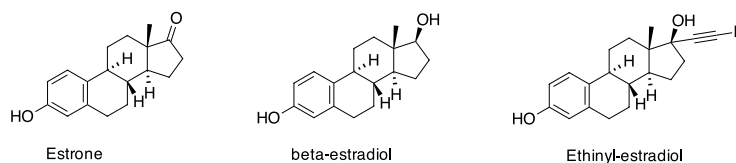
Figure 1.17: Structures of estrogens.

In the 1960s anti-estrogens were developed as contraceptives. Among these compounds were the non-steroidal anti-estrogens Ethamoxytriphetol, Clomiphene and Tamoxifen, which later became the gold standard of treatments for ER positive breast cancers.

1.4.1 Targeting Nuclear Receptors

Nuclear receptors have been studied for decades due to their interest as potential drug targets. Therefore it is not surprising that nuclear receptor agonists and antagonists such as Tamoxifen (ER), thiazolidinediones (PPARγ) and dexamethasone (glucocorticoid receptor) are amongst the most commonly used drugs. [46] The challenge for finding novel drugs is to generate a compound that addresses one or only a few physiological nuclear receptor functions to achieve the desired effects without causing side effects from the activation/deactivation of other nuclear receptor functions. To date, the vast majority of drug discovery programs have aimed to find structures that bind to the LBD of the NR and prevent transcriptional activity.

1.4.1.1 Targeting the Ligand Binding Pocket of Estrogen- SERMs

SERMs are a type of conventional anti-estrogens, with Tamoxifen as the most famous drug for the treatment of breast cancer. They bind to the ligand binding domain, more specifically in the ligand binding pocket, and cause a conformational change that prevents the binding of co-activators and therefore transcriptional activity of the receptor. However, as noted above it is known that that the efficiency of Tamoxifen decreases with time and can also result in Tamoxifen promoting breast cancer.
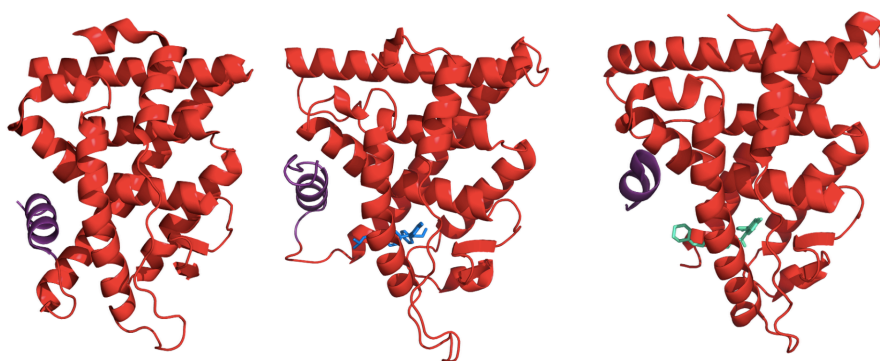
Figure 1.18: Left: The crystal structure of the ER in a active conformation; **Middle:** structure of ER bound to tamoxifen (blue), where helix 12 is shifted into a slightly different position; **Right:** Structure of the ER bound to raloxifene (teal), with position of helix 12 altered but still allowing for limited co-activator binding (PBD left: 2QZO; middle: 3ERT; right: 1QKN).

The anti-tumour effect of Tamoxifen is mediated by its competitive binding to the ER. This causes a conformational change (**figure 1.18**). [47] This change is different to the conformational change caused by estrogen binding. In the case of estrogen, the binding to the ER results in a change that seals the ligand binding domain and activates the AF-2 function of the ER. When Tamoxifen binds to the ER, the structure of Tamoxifen prevents the

sealing of the ligand binding domain and activation of the AF-2 function. [13] Similar conformational changes can be observed upon binding of Raloxifen.

1.4.1.2 The LRH-1 Ligand Binding Domain as Drug Target

As LRH-1 plays a vital role in a variety of biological functions and pathological processes which include early embryonic development, cholesterol metabolism, and steroidogenesis, [19,29,48–52] a great number of applications for both agonists and antagonists in medicine can be envisioned (**figure 1.19**).
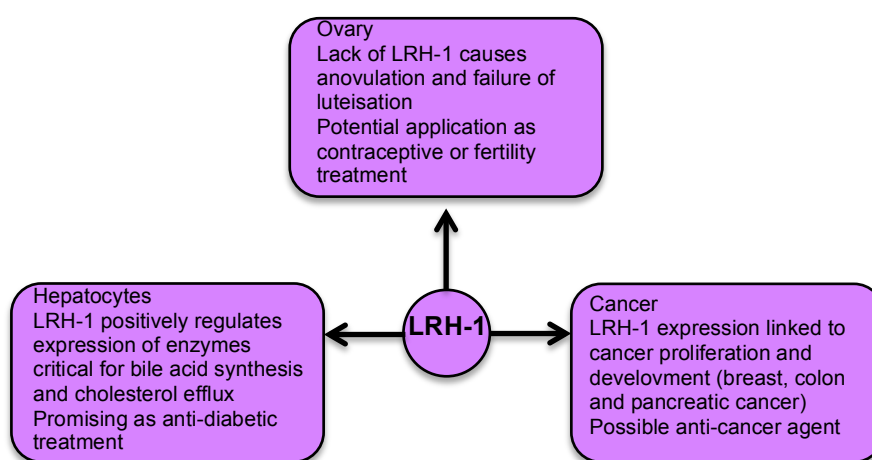
Figure 1.19: Summary of potential therapeutic applications of LRH-1. [25]

The major sites of action of LRH-1 are summarised in the chart above and some of them have been used as targets for potential drugs. Recent studies by Ortlund *et al*. [22] discovered that dilauroyl phosphatidylcholine (DLPC) and diundecanoyl phosphatidylcholine (DUPC) are potent selective agonists for LRH-1 and have a positive effect in diabetic and obese disease models. [20,53] Similarly, Whitby *et al*. [54,55] published two series of LRH-1 agonists aimed at the treatment of metabolic diseases (**figure 1.20**).
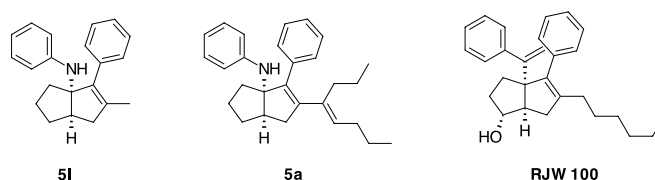
Figure 1.20: Whitby's LRH-1 agonists. [55, 54]

Earlier this year, Fletterick *et al*. [56] reported on the discovery of the first LRH-1 small molecule antagonists by virtual screening of a database of compounds (**figure 1.21**).
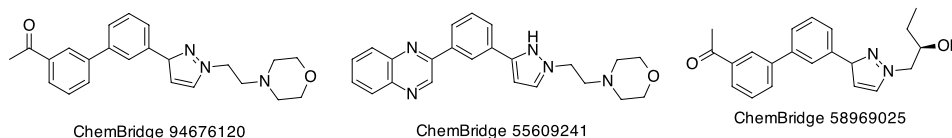
Figure 1.21: Most effective LRH-1 antagonists. [56]

These compounds have been shown to selectively inhibit the transcriptional activity of LHR-1 and exhibit no cytotoxicity. Additionally, these compounds have demonstrated anti-proliferative properties in breast, pancreatic, and colon cancer cells and could therefore be used as a molecular tool to further explore the involvement of LRH-1 in the development and growth of these types of cancer. [56]

1.4.2 Targeting the Co-Activator Binding Site

Co-activators bind with high selectivity to the AF-2 function of nuclear receptors. As indicated above, this selectivity is due to an amphipathic α-helix that contains the LXXLL motif and additional charged residues, which constitute the "charge clamps". [37]

McDonnell *et al*. [59, 60] noted that these well-defined features raise the possibility for the development of small synthetic molecules that bind to this AF-2 function and directly disrupt the nuclear receptor–co-factor interaction. [59] To fulfil all criteria mentioned above, the ideal co-activator binding inhibitor (CBI) would be a short α-helical sequence that constitutes the LXXLL motif as well as the polar functional groups that make the charge clamp. Initial approaches have employed short helical peptides, constrained peptides and peptidomimetics. [60]

1.4.2.1 The AF-2 Function of the Estrogen Receptor

In 2003, Leduc *et al*. [59] reported on a helix-stabilised cyclic peptide as a selective co-activator binding inhibitor for the estrogen receptor. Their results support the idea to design α-helical peptide fragments that contain the LXXLL motif as potential new antagonists for the estrogen receptor. Katzenellenbogen *et al*. [12] used a very similar approach. They established a FRET assay with streptavidin-europium labelled estrogen receptor ligand binding domain and a Cy5 dye labelled sequence of SRC3, a known co-activator for the estrogen receptor, to verify the possibility of peptides to function as CBIs (**figure 1.22**).
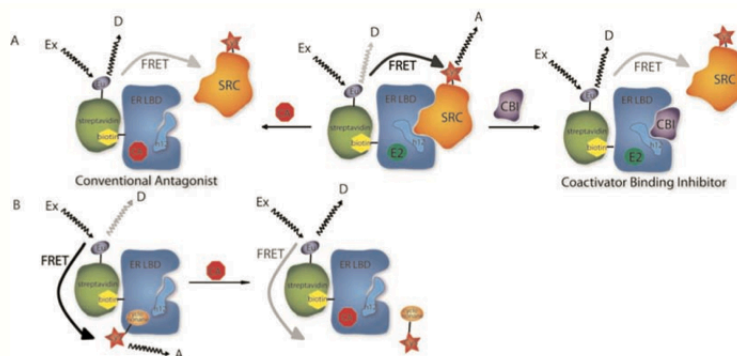
Figure 1.22: Schematic representation of time-resolved fluorescence resonance energy transfer (FRET)–based coactivator binding inhibitor (CBI) assay: **A:** ER in the presence of agonist estradiol (center), with a competing CBI (right), and with a competing conventional antagonist (CA; left). **B:** Schematic representation of FRET-based CA-binding assay. LBD, ligand-binding domain; SRC, steroid receptor co-activator. [12]

In the same year they published the synthesis and initial testing of proteomimetics as estrogen receptor co-activator binding inhibitors, which were tested using the FRET assay described above (**figure 1.23**). [60]
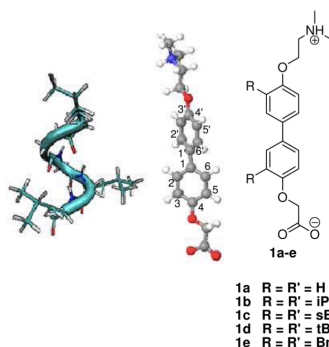
Figure 1.23: Structures of proteomics by Katzenellenbogen *et al*. [60]

The main features of peptide mimetics are their low molecular weight and their relative ease of modification to improve binding, selectivity, solubility and bioavailability. [59–61]

1.4.2.2 Targeting LRH-1's Co-Activator Binding Site

As an orphan receptor, LRH-1 is constitutively active and hence, primarily regulated by transcriptional co-regualtors. This feature suggests that it could be fruitful to selectively target the LRH-1 AF-2 site and regulate its transcriptional activity. Clyne *et al*. [23] started a project looking for an α-helical peptide as a potential CBI. Using phage display technology they found a series of peptides modulating the transcriptional activity of LRH-1.

It could be anticipated that LRH-1 agonists could have positive effects in the activation of LRH-1 in the liver as drugs for non-insulin dependent diabetes and obesity and in the ovary as potential agents to treat infertility. On the other hand, the activation of LRH-1 would cause

severe effects in various cancer types. At the same time, LRH-1 antagonists could be a key treatment for breast cancer, but the downregulation of LRH-1 could cause dramatic changes in lipid metabolism and cholesterol efflux. To address all implications of LRH-1 it is essential to find selective and tissue specific modulators, which act as agonists *e.g.* in the liver but antagonise LRH-1 in cancer.

The remainder of this chapter outlines our strategy to develop such agents.

1.5 Scientific Aims and Objectives

1.5.1 Synthesis of a Benzimidazole-based Compound Library and SAR Studies

The first half of this thesis describes a project based on the idea to find conventional antagonists that bind to the ligand binding pocket of LRH-1. In a previous project, Andrew Bayly (Spivey Group 2007-2011) [62] found through *in silico* screening that benzimidazole thioethers exhibit similar properties in terms of charge distribution, size and hydrogen bonds to the known LRH-1 agonists published by Whitby *et al*. [54,55] This benzimidazole scaffold was taken further by Andrew Bayly and displayed a good EC_{50} and no toxicity in cells (**scheme 1.1**).
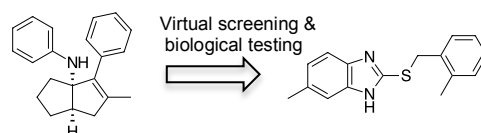
Scheme 1.1: Andrew Bayly's Approach towards a benzimidazole series. [62]

Therefore, this scaffold was to be employed as a new lead with the plan to synthesise a library of benzimidazoles to study the structure-activity relationship (SAR) of these compounds.

In the first instance we chose to explore three distinct sites in the benzimidazole structure that could be modified (**figure 1.24**):

Figure 1.24: Sites of possible modifications on the benzimidazole structure.

The first position selected for substitution on the benzimidazole core was at the R^1 position. These derivatives were envisaged to be prepared using transition metal catalysed cross-coupling of an appropriate aryl halide precursor. The second position for modification was on the benzyl ring. These analogues could be envisaged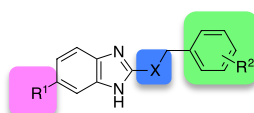 to be obtained by reacting an appropriate 2-substituted benzimidazole with a range of commercially available substituted benzyl bromides or benzyl alcohols.

As there was no evidence that the originally included thioether is required for the binding properties of the lead compound it was decided also to synthesise a series of analogues which an ether linkage instead of a thioether.

A retrosynthetic analysis for the synthesis of the envisaged compound library could start from the diamine and form the 2-mercapto or 2-hdroxy benzimidazole using carbon disulfide or CDI, which in the final step of the synthesis could be the converted to the corresponding benzyl ethers (**scheme 1.2**).
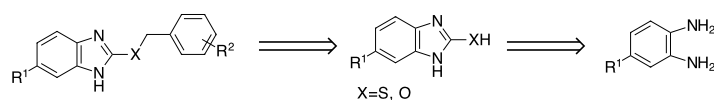
Scheme 1.2: Retrosynthetic analysis of the benzimidazole synthesis.

It was decided to select the substitution patterns on the benzyl ring according to the Topliss series of analogues. [63] This series is designed to empirically optimise the substitution pattern of substituents on aromatic rings when, no structural information about the mode of binding is available and takes steric factors, hydrophobicity and electronic effects into account.

To obtain an SAR, the second part of the research described in this thesis is dedicated to the testing of the synthesised compound library for binding to the ligand binding domain of LRH-1. Achieving this required the expression and purification of the ligand binding domain of LRH-1, the optimisation of the assay conditions and finally the testing of the compounds.

1.5.2 Towards the Synthesis of an α-Helix Mimetic

The final piece of research described in this thesis is based on the idea to design and synthesise nuclear receptor antagonists by targeting the co-activator binding site and consequently inhibit nuclear receptor action.

A prior PhD student in the research group, Andrew Bayly, had designed an α-helix mimetic which could potentially contain the required LXXLL motif for co-activator binding. [62] He had also conducted preliminary synthetic studies towards its synthesis. The aim of the research described herein was therefore to improve and continue of the synthesis of the α-helix mimetic (**scheme 1.3**).
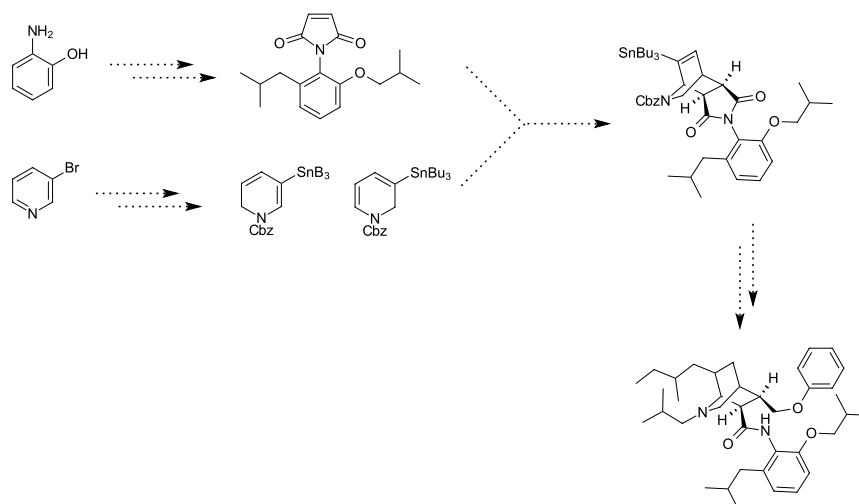
Scheme 1.3: Synthetic route towards α-helix mimetic. [62]

The first part of the synthetic pathway involves the synthesis of a substituted *N*-phenyl maleimide. In the second part of the synthesis a 1,6-dihydropyridine will be formed. Both parts will be combined *via* a hetero Diels-Alder reaction to give the scaffold of the α-helix mimetic. Then, further modification will give the final α-helix mimetic.

2. Results and Discussion

2.1 Synthesis of Potential LRH-1 Antagonists

2.1.1 Previous Work on Cresset Virtual Screen- Design of a New Lead

Previous PhD student in the research group Andrew Bayly (Spivey Group 2007-2011), in collaboration with Caroline Low (Drug Discovery Centre, Imperial College London) started the search for a new lead as potential LRH-1 antagonists or inverse agonists. [62] The search began by using the most active compound of a series of LRH-1 agonists published by Whitby *et al.* (**figure 2.1**). [54]
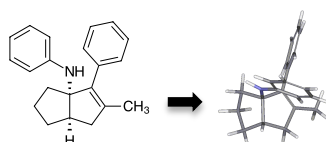
Figure 2.1: Structure of **5l** and energy minimised structure of **5l** as implemented by Andrew Bayly. [62]

This compound is a *cis*-fused [3.3.0] bicyclooctane derivative having an aniline substituent at the ring junction. Compounds of this type have been shown by X-ray crystallography to bind to the ligand binding pocket of LRH-1 and behave as agonists with EC_{50} values between 2 and 0.06 μM. [54]

Energy minimisation of the structrure of **5l** in the gas phase using the XED force field™ within the Cresset VS™ software suite gave a conformation very similar to the active conformation of this compound, as revealed in the aforementioned X-ray co-crystal structure. This energy minimised conformation was used as query to find a new series of agonists. By applying the Cresset FieldView[TM] Software (now TorchLite[TM]) field points for that structure were generated (**figure 2.2**).
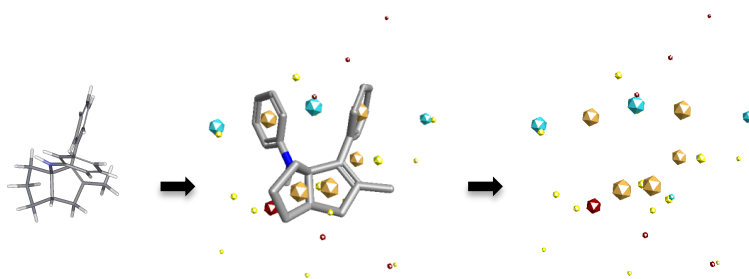
Figure 2.2: TorchLite™ field point structure of **5l** as generated by Bayly. [62]

The field points represent different areas of interactions within and around the molecule. The yellow field points correspond to van der Waals interactions, positive electrostatic interactions are represented as red field points and negative electrostatic interactions as blue field points. Hydrophobic areas are indicated as golden field points. The field points were then used to screen through a database of commercially available compounds using Cresset VS.

From the 200 obtained ranked hit compounds, those compounds, which were deemed to be unsuitable as medicinal chemistry leads, were discarded. Among the discarded structures were nitro and nitroso compounds, phosphines, organometallics, entirely hydrocarbon based compounds and compounds that did not match the positive field point derived from the aniline. After this library reduction process, the 143 compounds left were further refined by removal of potentially metabolically unstable primary amines and aniline-containing structures that exhibited a high structural and field point similarity to compounds with a higher score. This refinement resulted in 110 final compounds, of which 100 were purchased or synthesised by Andrew Bayly and tested *in vivo* for their ability to modulate LRH-1. The assay used was a cell-based luciferase and renilla reporter assay and was carried out by Dr Fiona Kyle (Department of Oncology, Hammersmith Campus, Imperial College London). The analysis showed 7 compounds with better agonistic properties than Whitby's **5a** compound, which is another LRH-1 agonist (**figure 2.3**).
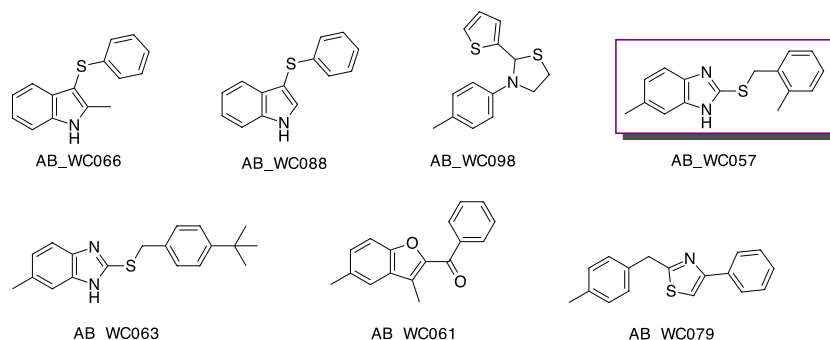
Figure 2.3: Structures of potential new lead compounds discovered by Bayly. [79]

One of these hits was **AB_WC057**. This compound showed a good EC_{50} in the µM range and most importantly, no toxicity as evidenced by a luciferase and renilla reporter assay (**figure 2.4**).
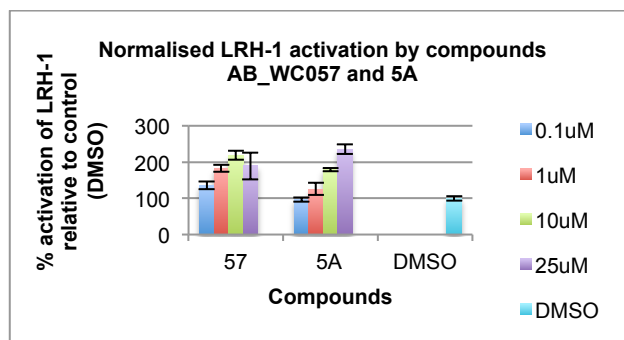
Figure 2.4: Activity of **5a** and **AB_WC057** in a cell-based assay as determined by Bayly. [62]

Overlapping the structure of **AB_WC057** with the field points of Whitby's **5l** compound shows a good similarity index of 0.69 (**figure 2.5**).
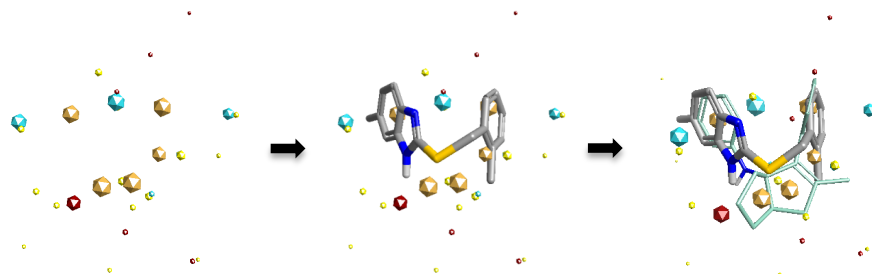
Figure 2.5: Overlapped structure of compounds **5l** and **AB_WC057**.

Due to its field points similarity to compound **5l**, its good EC_{50} and its non-toxicity, compound **AB_WC057** was selected as the new lead for the discovery of potential new LRH-1 antagonists.

From the overlapped structures of compound **5l** and the lead benzimidazole **AB_WC057**, we hoped that the benzimidazole would bind in a similar fashion to the LRH-1 LBD (**figure 2.6**).
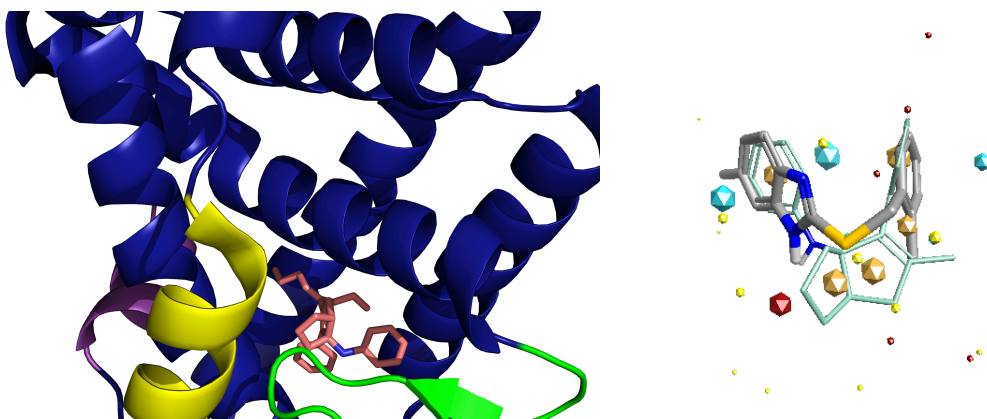
Figure 2.6: Left: compound **5a** (pink) bound to LRH-1 LBD (PDB: 3PLZ) [54,55], **Right:** overlapped structures **5l** and **AB_WC057**.

In this scenario the benzimidazole core takes the position of the aniline of compound **5l** and could point towards the β-sheet (green). The thioether bridge aligns with the bicyclic core of compound **5l** and would be positioned in the centre of the ligand binding pocket. The benzyl ring of the benzimidazole lead is in the same position as the phenyl ring of compound **5l** and would point towards the bottom of the ligand binding pocket.

The first task therefore was to devise a robust synthesis of benzimidazoles like **AB_WC057** that would allow the preparation of analogues varying in both the benzyl ring and phenyl core.

2.1.2 Benzimidazoles

2.1.2.1 Synthesis of Benzimidazoles

Historically, the first benzimidazole was synthesised by Hoebrecker *et al*. [64] in 1872 who obtained 2,5- and 2,6-dimethylbenzimidazole by reducing 2-nitro-4-methylacetanilide (**scheme 2.1**). [65]
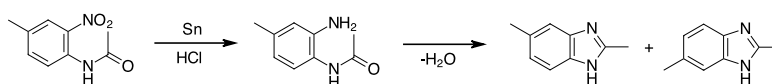
Scheme 2.1: Hoebrecker's synthesis of 2,6-dimethyl benzimidazole. [64]

Several years later, Ladenburg obtained the identical products by heating of 3,4-diaminotoluene and acetic acid to reflux (**scheme 2.2**). [66]
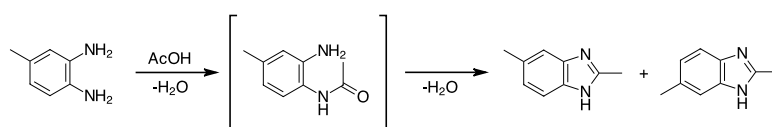
Scheme 2.2: Ladenburg's synthesis of 2,6-dimethylbenzimidazole. [66]

There are many other ways to synthesise benzimidazoles and therefore it is only possible to show a fraction of syntheses here (**scheme 2.3**).

X= I, Br; R^1= H, CO_2Me, pyridine ; R^3= aromatic, heteroaromatic, aliphatic; h): NaN_3, 5 mol% CuCl, 5 mol% TMEDA, DMSO, 120 °C, 12 h.

R1= EWG, EDG; R2= Bn; R3= Ar ; g) 1eq $Cu(OTf)_2$, toluene, 110 °C, 2.5-6h.

$R^{1,}$ R^2= H, Ph, Et; (f): Fe, NH_4Cl, 2-prOH/HCOOC (1:1), 80 °C, 1-3 h.

R^1= H (a): MsCl, NEt_3, CH_2Cl_2, 0 °C to RT, 6h.

X= Cl, Br, I; R^1= H, EWG, EDG; R^3= aryl, alkyl (e): Cu_2O, DMEDA, K_2CO_3, H_2O, 100 °C, 30 h.

Y= O, S, NH R^1= Cl, Br, CH_3, CO_2Me, H; R^2, R^3= alkyl (b): $BF_3 \cdot OEt$, CH_2Cl_2, RT, 2-4h.

R^1=H, Me, NO_2 ; R^3=Ar ; (d): 7 eq H_2O_2 (30% in H_2O), 3.5 eq HCl (37%), MeCN, rt, 30-50 min.

R1= Cl, Me, OMe, H ; R^2= H, alkyl; R^3= Ar, R= H, Me (c): i: $Cu(OAc)_2$, cat, NaOPiv, cat. air, DMF, 50 °C; ii: O_2, 120 °C.

Scheme 2.3: An overview of modern syntheses of benzimidazoles. [67–73]

The majority of syntheses start from the *o*-phenyl diamine and carboxylic acids or aldehydes. [67,74] Other methods use amidines, that react intramolecularly with a halide to close the ring and form the benzimidazole. Another method for the synthesis of substituted benzimidazoles was reported by Zhu *et al.* [71] This reaction employs a Chan-Lam-Evans *N*-arylation and C-H activation/C-N bond formation process to form the substituted benzimidazole.

2.1.2.2 Applications of Benzimidazoles

Reflecting the variety of syntheses, there is a diverse range in different applications for benzimidazoles. Benzimidazoles have a broad range of applications in medicinal chemistry and as pharmaceuticals for instance as anthelmintic, fungicides, antiviral, anticancer or antimicrobial agents [74] and are valuable precursors for the synthesis of ligands [75] and more complex structures (**figure 2.7**).
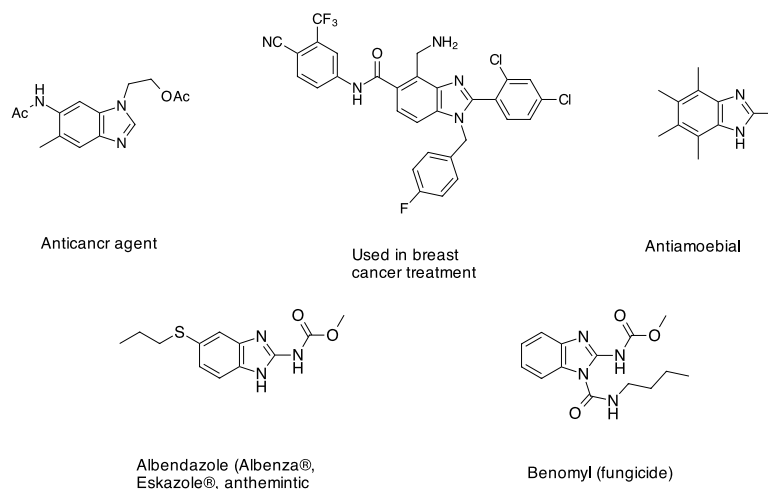
Figure 2.7: Selected examples of pharmaceutical relevant benzimidazoles as anticancer agent [76], treatment on breast cancer [77], as antiamoebial [78], anthemintic, or fungicide.

2.1.2.3 2-Mercaptobenzimidazoles

Important derivatives of benzimidazoles are 2-mercaptobenzimidazoles. These compounds have found many applications in medicine, for example as antiviral agents, [81, 82] anthelmintics or as luteinizing hormone-releasing hormone antagonists (**figure 2.8**). [81]
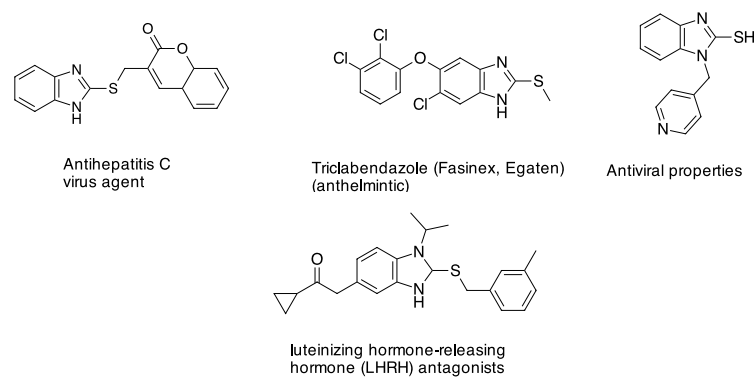
Figure 2.8: Examples of pharmaceutical relevant 2-mercaptobenzimidazoles.

Murzart *et al*. [82] reported a copper catalysed synthesis of unsymmetrically substituted 2-Mercaptobenzimidazoles **2** (**scheme 2.4**).

X: Br, I; R: alkyl
(a): CH$_2$Cl$_2$, RT, 16 h; (b): 1. Et$_3$N, R$_3$X; 2. CuI, 1,10-phenathroline, K$_2$CO$_3$, Dioxane 4 h.
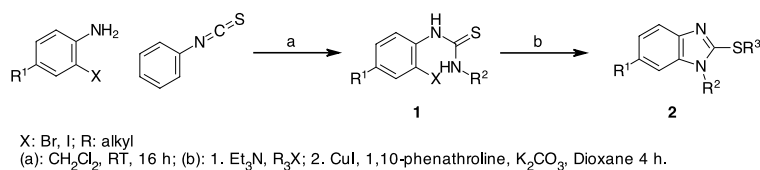
Scheme 2.4: Murzart's synthesis of unsymmetrical substituted 2-mercaptobenzimidazole **2**. [82,83]

Murzart's synthesis starts with the formation of the substituted thiourea **1**, which can be synthesised from the respective aniline and a thioisocyanate. [83] In the next step the thiourea undergoes *S*-alkylation followed by an intramolecular Cu-catalysed *N*-aryl amination to give the substituted 2-mercaptobenzimidazole **2**. [82]

The classical method for the synthesis of benzimidazole 2-thioethers **5** involves the reaction of *o*-phenyldiamine **3** with carbon disulfide and subsequent etherification of the 2-mercaptobenzimidazole **4** (**scheme 2.5**).

(a): CS$_2$, KOH, EtOH, reflux, 3 h; (b): benzyl bromide, Na, MeOH, DMF, RT, 2-8 h.
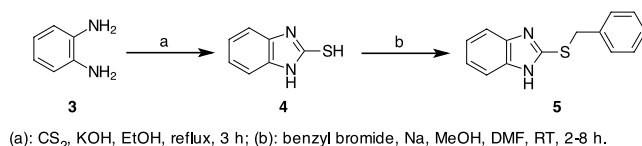
Scheme 2.5: Classical method of *S*-alkylated 2-mercaptobenzimidazole synthesis **5**. [84]

Among many, Klimesová *et al.* [84] suggested a mechanism for the reaction of carbon disulfide with *o*-phenyldiamine **3** (**scheme 2.6**).
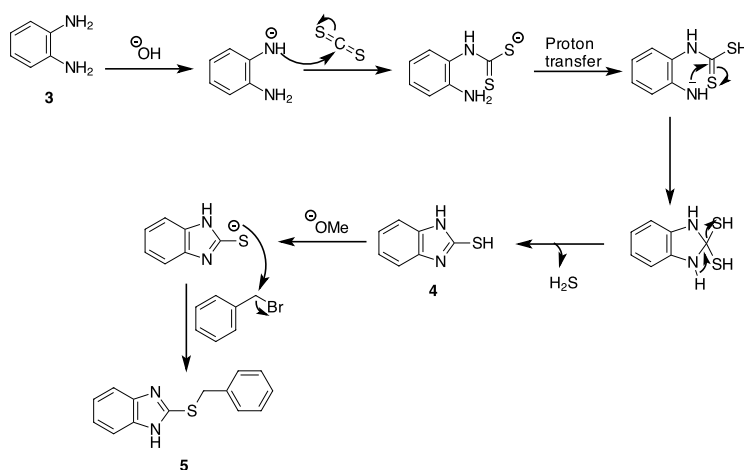
Scheme 2.6: Klimesová's proposed mechanism of *S*-alkylated 2-mercaptobenzimidazole **5** formation.

The reaction is initiated by the deprotonation of the diamine **3**, which then attacks the carbon of the carbon disulfide. A proton transfer produces another amide, which attacks the carbon of the carbon disulfide and closes the ring. The driving force of the following step is the loss of H$_2$S and the aromatisation, which gives the final 2-mercaptobenzimidazole **4**. In the second part of the synthesis the thiol is deprotonated and reaction with the benzyl bromide *via* an S$_N$2 reaction gives the final *S*-alkylated 2-mercaptobenzimidazole **5**.

The etherification can theoretically yield 3 different products: the desired *S*-alkylated product **5**, the *N*-alkylated product **6** and the *S*,*N*-dialkylated product **7** (**scheme 2.7**).
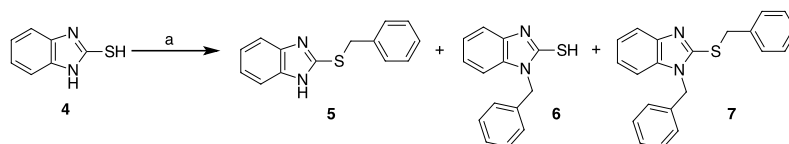
(a): Benzyl bromide, Na, MeOH, DMF, RT, 2-8 h.

Scheme 2.7: The three possible products of attempted alkylation of 2-mercaptobenzimidazole **4**.

Pearson's hard-soft-acid-base principle is a method to predict the pathways of reactions. It states that soft sites prefer to react with a soft counter part and hard moieties with hard counter parts. Soft moieties are large and easy polarisable. A hard moiety is small and hard to polarise. According to Pearson's principle the benzyl bromide is soft and threrefore should prefer to react with the soft thiol rather than the hard nitrogen. Additionally, the sulfur is sterically slightly less hindered and therefore should react faster.

2.1.3 Synthesis of AB_WC057 Analogues

With a plan for the synthetic approach in place, the synthesis of a compound library based on the lead benzimidazole was undertaken.

2.1.3.1 Analogues with Different Core Substituents

For the first analogues, different commercially available 4-substituted benzenediamines **8** were procured and used for the synthesis of a small series of core-substituted benzimidazole thioethers **10** (**table 2.1**).

(a): CS_2, NaOH, EtOH, H_2O, 70 °C, 4 h; (b): 2-Methyl BnBr, NaOMe, MeOH, DMF, RT, 16 h.

8, **9**, **10**: R= H
8a, **9a**, **10a**: R= ^{t}Bu
8b, **9b**, **10b**: R= Br
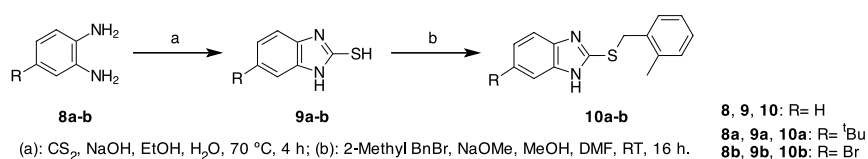
R	Yield benzimidazole	Yield thioether	Overall yield
H	51%	53%	27%
^{t}Bu	89%	66%	59%
Br	43%	30%	13%

Table 2.1: Synthesis of different core substituted benzimidazoles **10a-b**.

The synthesis was carried out following a procedure adapted from Klimesová *et al.* [84] As described above, the first step involved the formation of the 2-mercaptobenzimidazoles **9a-b**.

This product could be obtained in satisfactory yields. In the next reaction the sulfur was alkylated using 2-methylbenzyl bromide. There is a great variance in the yields for the individual compounds with the *tert*-butyl substituted benzimidazole **10a** giving the highest yield. It could be that the electron donating properties of the *tert*-butyl group result in a less stable but more nucleophilic thiol, which reacts faster with the benzyl bomide. This electron donation derives from hyperconjugation of the alkyl C-H bonds with the aromatic system.

At the same time, the deprotonation of the ring nitrogen is more difficult, due to the electron donating *tert*-butyl group, leading to fewer side products. The opposite appeared to be the case for the bromo-substituted benzimidazole **10b**. The electron withdrawing bromide could conceivably stabilise the thiol and make it less reactive towards S_N2 reactions. This is due to the inductive electron withdrawing effect of the bromide. At the same time the bromide exhibits a mesomeric donating effect which is significantly weaker than the inductive effect, resulting in a net electron withdrawing effect.

2.1.4 Benzimidazoles with Different Benzyl Ring Substitution

2.1.4.1 Topliss Series of Analogues

For the next series of benzimidazole analogues, the substitution pattern of the benzyl ring was modified. To select an array of substituents that is suitable for the synthesis of a compound library, the Topliss scheme was used as a guide.

The Topliss series is a tool for the optimisation of phenyl ring substitution in the context of medicinal chemistry. [63,85] The basis of this concept was developed by Hansch, [86] who established that the primary influences on activity of a compound result from lipophilic, electronic and steric properties of the substituents. His calculations are based on the partition coefficient log P of to give a substituent constant π (**equation 2.1**).

$$\pi = log P_X - log P_H$$

Equation 2.1: Hansch's substituent constant π with P_H: partition coefficient of parent substituent; P_X: partition coefficient of the derivative.

These calculations were taken further by Topliss, who developed a scheme for the optimisation of phenyl ring substitution (**figure 2.9**).
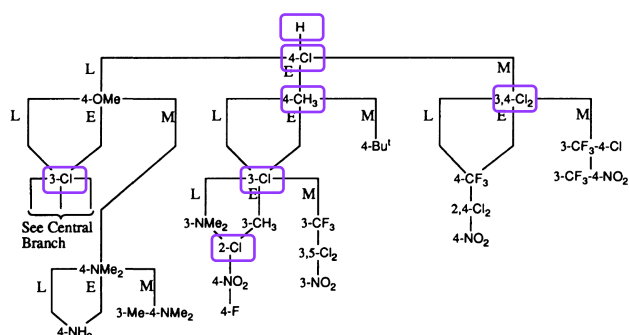
Figure 2.9: Topliss scheme for the optimisation of aryl substitution. [64]

For our series of analogues a set of 7 substituents has been chosen and include unsubstituted, 2-Me, 4-Me, 2-Cl, 3-Cl, 4-Cl and 3,4-Cl$_2$.

2.1.4.2. Synthesis of Benzimidazoles with Different Benzyl Ring Substitution Patterns

After choosing the substituents, the synthesis of the first series of Topliss analogues was carried out (**table 2.2**).

(a): Substituted BnBr, NaOMe, MeOH, DMF, RT, 16 h.

12: R= H
12a: R= 2-Me
12b: R= 4-Me
12c: R=2-Cl
12d: R= 3-Cl
12e: R= 4-Cl
12f: R= 3,4-Cl$_2$
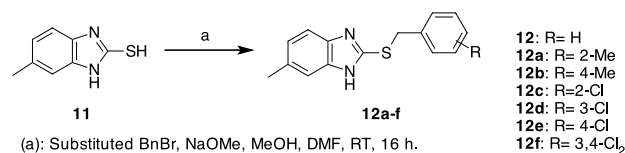
R	H	2-Me	4-Me	2-Cl	3-Cl	4-Cl	3,4-Cl$_2$
Yield	43%	53%	39%	28%	42%	27%	75%

Table 2.2: Synthesis of different benzyl substituted benzimidazole thioethers **12a-f**.

The syntheses were carried out as described above following the adapted procedure of Klimesová *et al.* [84] The analogues could be obtained in 27-75 % yield. The broad range in yields may be explained by the different electronic and steric properties of the benzyl bromides. The electron withdrawing property of the chloride substituent increases the reactivity of the benzyl bromide. The electron withdrawing effect is strong when the chloride is in *meta* position and weak in the *ortho* or *para* position. This is reflected by the obtained yields, where the 3-chloro substituted benzyl bromide gives a higher yield than the 2-chloro or 4-chloro benzyl bromide. The highest yield could be observed for the 3,4-dichlorobenzyl bromide, where the *meta* and *para* positions are occupied by a chloride. The methyl groups stabilise the transition state through hyperconjugation, where the *ortho* position is of greater importance than the *para* position.

2.1.5 Synthesis of *N*-Phenylbenzimidazole Thioether

It was also decided to target one benzimidazole having an *N*-phenyl substituent. This analogue was anticipated to allow us to evaluate if the nitrogen of the benzimidazole ring had any role in the binding to LRH-1.

Sreedhar *et al.* [87] published a Chan-Lam-Evans type reaction for the arylation of azoles using phenylboronic acid and copper oxide under air; we adapted this approach in our first attempt to prepare such a derivative (**scheme 2.8**).

12a   **13**

(a): phenylboronic acid, Cu$_2$O, MeOH, RT, 16 h.
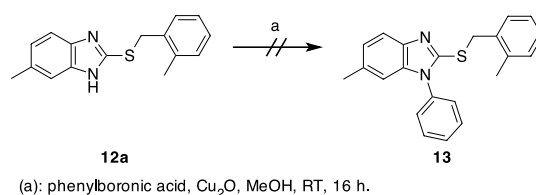
Scheme 2.8: Attempted synthesis of *N*-phenyl benzimidazole thioether **13** *via* Chan-Lam-Evans reaction. [87]

The reaction was performed using the conditions outlined in scheme 2.8 and monitored by TLC. After 16 hours at room temperature no product could be detected. Therefore, it was decided to increase the reaction temperature to 75 °C. Since after two hours still no product could be detected, the catalyst loading was increased from 5 mol% to 35 mol% and more phenylboronic acid was added. Heating the reaction mixture for another 24 hours did not yield any product.

Another method for the *N*-arylation of benzimidazoles is *via* Ullmann-type coupling. Buchwald *et al.* [88,89] have reported on a method for the arylation of this type of nitrogen heterocycles and so we opted to evaluate their method next (**scheme 2.9**).

12a   **13**

(a): bromobenzene, CuI, Cs$_2$CO$_3$, 1,10-phenanthroline DMF, 110 °C, 48 h.
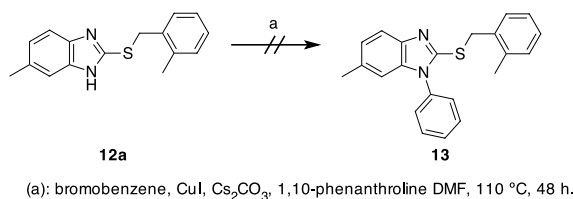
Scheme 2.9: Attempted synthesis of *N*-phenyl benzimidazole thioether *via* Ullmann-type coupling. [88,89]

The reaction was carried out in a sealed tube under an atmosphere of nitrogen and monitored periodically by TLC. After 48 hours no product has been formed. The reaction was repeated under the same conditions but with the more reactive iodobenzene instead of bromobenzene. As in the previous reaction, no product was formed. To find the best conditions for this arylation, the reaction conditions were optimised using benzimidazole **14** as a model system (**table 2.3**).

14   15
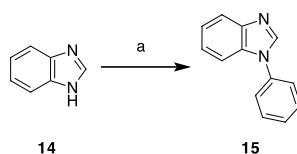
(a): Iodobenzene, CuI, Cs$_2$CO$_3$, 1,10-phenanthroline DMF, 110 °C, 48 h.

Entry	Iodobenzene	CuI	1,10-phen	Cs$_2$CO$_3$	Outcome
1	2.0 eq.	20 mol%	40 mol%	2.0 eq.	<2% product
2	2.0 eq.	50 mol%	100 mol%	2.0 eq.	100% conversion
3	2.0 eq.	100 mol%	200 mol%	2.0 eq.	100% conversion

Table 2.3: Optimisation of Ullmann-type coupling using benzimidazole **14** as model system.

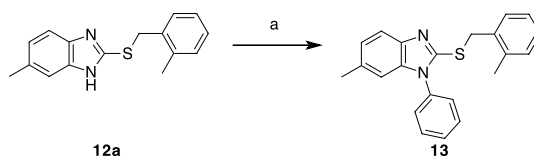Monitoring the reaction by GC showed a full conversion to *N*-phenylbenzimidazole **15** using 50 mol% copper iodide, caesium carbonate and 1 equivalent of phenanthroline in DMF (**table 2.3, entry 2**). The optimised conditions were transferred to the actual benzimidazole benzyl thioether system **12a** (**table 2.4**).

12a   13

(a): Iodobenzene (2 eq.), other conditions, see table

Entry	CuI	1,10-Phen	Base (2.0 eq.)	Solvent	Yield
1	1.0 eq.	2.0 eq.	Cs$_2$CO$_3$	DMF	16%
2	0.5 eq.	1.0 eq.	KO^{t}Bu	DMF	0%
3	0.5 eq.	1.0 eq.	K$_3$PO$_4$	Dioxane	16%
4	2.0 eq.	4.0 eq.	Cs$_2$CO$_3$	DMF	26%
5	2.0 eq.	4.0 eq.	Cs$_2$CO$_3$	DMA	16%
6	2.0 eq.	4.0 eq.	Cs$_2$CO$_3$	NMP	23%

Table 2.4: Optimisation of Ullmann-type coupling using the benzimidazole thioether system **12a**.

The initial reaction conditions gave only small quantities of the product **13** (**table 2.4, entry 1**). Therefore, further optimisation using benzimidazole thioether **12a** as the substrate was carried out. The best conditions found were using DMF with 2 equivalents copper iodide and 4 equivalents of phenanthroline (**table 2.4, entry 4**). Changing the base to KO^{t}Bu resulted in a complex mixture with no product detectable (**table 2.4, entry 2**). A screening of different solvents gave DMF and dioxane (**table 2.4, entries 3 and 4**) as the best solvents for this transformation. DMA and NMP also worked, but gave lower yields (**table 2.4, entries 5 and 6**).

From the results of the optimisation it is appears that the yield increases with the amount of catalyst used. The reason for this connection might be the ability of sulfur to form strong complexes with transition metals. [90] A more detailed discussion on this matter can be found in chapter 2.1.7.

It is possible that this problem might be overcome by using a ligand that is able to shield the metal and prevent the sulfur from binding to the copper centre during the Ullmann-type couplings. Here, phenathroline was used as the ligand. It has a flat structure and is not capable of protecting the metal centre from the sulfur. A possibility could be a 6,6-disubstituted-2,2'-bipyridyl complex, which still is flat but shields the copper ion from two sides.

2.1.6 Benzimidazole Ethers

The Cresset VS approach used to obtain the lead for this project primarily gives information relating to the structure and topology of potential binders and is not so prescriptive as to which atoms comprise these scaffolds. In order to test if the sulfur was crucial for the binding properties a series of oxygen analogues was synthesised. These analogues have the same substitution pattern as the thioether analogues. A possible retrosynthetic approach would follow a similar route as for the benzimidazoles thioethers (**scheme 2.10**).
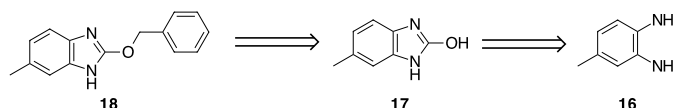

Scheme 2.10: Retrosynthetic approach for benzimidazole ethers **18**.

It was proposed that the synthesis could start with the 3,4-diaminotoluene **16**, which would be converted to the 2-hydroxybenzimidazole **17**. The next step would be the alkylation to give the benzimidazole ether **18**.
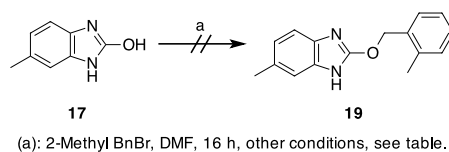
2.1.6.1 Synthesis of Benzimidazole Ethers

Intending to follow the method outlined above, the 2-hydroxybenzimidazole **17** was synthesised using CDI in anhydrous THF (**scheme 2.11**).

(a): CDI, THF, 0 °C to RT, 16 h (53%).
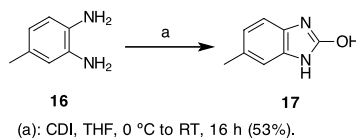
Scheme 2.11: Formation of 2-hydroxybenzimidazole **17**.

The reaction was carried out as described by Dannhardt *et al*. [91] The precipitated product was filtered and washed with THF. The reaction proceeded cleanly with no further purification required and gave the product in 53% yield.

With the 2-hydroxybenzimidazole in hand the alkylation was attempted using sodium methoxide or sodium hydride and benzyl alcohol in DMF (**table 2.5**).

(a): 2-Methyl BnBr, DMF, 16 h, other conditions, see table.

Entry	Solvent	Temperature	Base	Additive	Outcome
1	DMF	50 °C	NaOMe		No product
2	DMF	50 °C	NaOMe	NaI	No product
3	DMF	RT	NaH		No product

Table 2.5: Conditions for the synthesis of benzimidazole ether **19**.

Unfortunately, the reaction did not show any conversion to the product, even after heating the reaction mixture to 50 °C (**table 2.5, entry 1**). The reaction was repeated with 0.1 equivalents of sodium iodide to enable an *in situ* Finkelstein reaction and increase the reactivity of the benzyl bromide. Again, this attempt did not give the desired product (**table 2.5, entry 2**). A change in base to sodium hydride also was unsuccessful and no product could be detected (**table 2.5, entry 3**).

The reaction of 2-hydroxybenzimidazole **17** with benzyl bromide is expected to follow a S_N2 reaction mechanism with the deprotonated hydroxy group acting as the nucleophile (**scheme 2.12**).
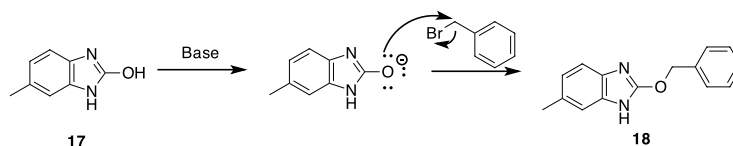
Scheme 2.12: Anticipated mechanism of the benzimidazole ether **18** formation *via* S_N2 reaction.

At the same time, deprotonation of the hydroxy group could also facilitate tautomerism within the benzimidazole, giving a cyclic urea-type structure **20**, which would be unreactive in the given conditions (**scheme 2.13**).
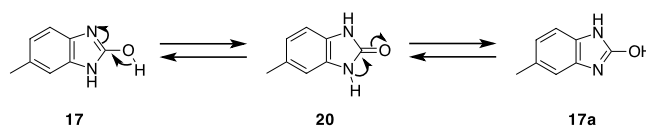
Scheme 2.13: Potential tautomerism of 2-hydroxybenzimidazole **17**. [65]

This tautomerism could be the main reason for the failure of the reactions.

A change in reaction mechanism could be a possibility to circumvent the unreactivity. Therefore, it was planned to convert the 2-hydroxybenzimidazole **17** to the 2-chlorobenzimidazole **21**. The reaction mechanism would then change from S_N2 to a nucleophilic aromatic substitution-type reaction, which we hoped would be successful irrespective of the tautomerism of the benzimidazole (**scheme 2.14**).
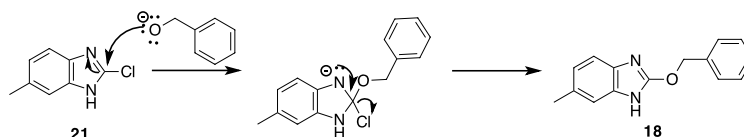
Scheme 2.14: Anticipated mechanism of benzimidazole ether **18** formation *via* nucleophilic aromatic substitution.

In this reaction mechanism the nucleophile is the benzyl alcohol. After deprotonation to the alkoxide it attacks the position 2 of the benzimidazole **21**, causing the chloride to be displaced.

## 2.1.6.2 Synthesis of Benzimidazole Ether *via* 2-Chlorobenzimidazole

The conversion of 2-hydroxybenzimidazole **17** to the 2-chlorobenzimidazole **21** was carried out using an adaptation of a procedure by Blythin *et al*. (**scheme 2.15**). [92]

(a): POCl$_3$, 100 °C, 4 h (40%).
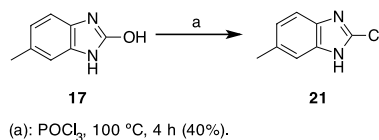
Scheme 2.15: Conversion of 2-hydroxybenzimidazole **17** to 2-chlorobenzimidazole **21**. [92]

This reaction gave the desired product in 40% yield, but it was decided not to further optimise the reaction conditions until the utility of the product had been established.

The next step towards the benzimidazole ether **18** was the alkylation (**table 2.6**).
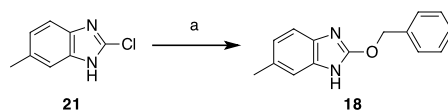
(a): NaH (2 eq.), benzyl alcohol (1.3 eq.), further conditions, see table.

Entry	Solvent	Temperature	Additive	Outcome
1	DMF	25 °C		No product
2	DMF	60 °C		No product
3	DMF	25-60 °C	DMAP	No product
4	DMF	25 °C	AgNO$_3$	No product
5	THF	25 °C	18 crown 6	No product

Table 2.6: Optimisation of benzimidazole ether **18** synthesis.

At first, the reaction was attempted using sodium hydride as base at 25 °C. This reaction did not lead to the formation of the desired product (**table 2.6, entry 1**). The reaction was therefore repeated at elevated temperature, but again, no product could be detected (**table 2.6, entry 2**). To increase the reactivity of the benzyl alcohol, DMAP was added to the reaction mixture. Even after heating the reaction to 60 °C, no product was detected (**table 2.6, entry 3**). In the next attempt silver nitrate was added to the reaction mixture. This was to convert the chloride to a better leaving group by forming silver chloride and to act as a mild Lewis acid to increase the reactivity of the benzyl alcohol. Unfortunately, this also did not lead to the desired product (**table 2.6, entry 4**). In a final attempt to induce a reaction, the solvent was changed to THF and 18 crown 6 was added. It was thought that this crown ether should increase the reactivity of the benzyl alcohol by removing the sodium counter ions from the vicinity. As before, no product was formed (**table 2.6, entry 5**).

A potential reason for the failure of the alkylation could be that the position 2 of the 2-chlorobenzimidazole **21** is too electron rich to allow for a nucleophilic attack of the benzyl alkoxide. The tautomerism of the 2-chlorobenzimidazole **21** consists of two isoforms: **21** and **21a** (**scheme 2.16**).
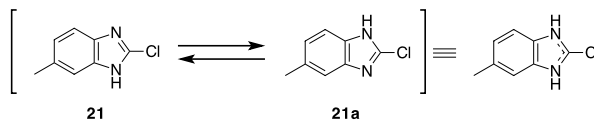
<div align="center">Scheme 2.16: Tautomerism of 2-chlorobenzimidazole 21.</div>

Superposition of the two tautomers **21** and **21a** gives a situation in which a high electron density resides at position 2, which makes this position difficult to attack with a nucleophile.

To minimise the possibility of tautomerism, it was decided to protect one of the nitrogens in the benzimidazole core. Furthermore, this measure would reduce the electron density on position 2, hopefully leaving it more susceptible towards nucleophilic attack.

2.1.6.3 Synthesis of Benzimidazole Ethers with Protected 2-Chlorobenzimidazole

There is a plethora of protecting groups available for the protection of amines and it is crucial for the success of the synthesis to find one that is appropriate for the particular circumstances. An ideal protecting group must be introduced selectively and under mild conditions. The protecting group needs to be stable during the synthesis and be cleaved under mild conditions and in a selective manner. [93] In the case of the synthesis of benzimidazole ethers, the protecting group needs to be stable under basic conditions.

Some of the most common base-stable protecting groups for amines are: Boc, Cbz, benzyl and trityl (**figure 2.10**).

<div align="center">Boc-Protecting group   Cbz-Protecting group   Benzyl-Protecting group   Trityl-Protecting group</div>
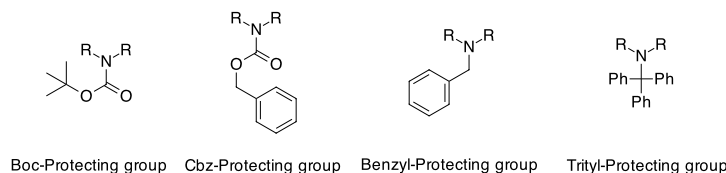
<div align="center">Figure 2.10: Potentially useful base-stable amine protecting groups.</div>

The benzyl and Cbz groups would be easy to install and stable under basic reaction conditions. As both groups are removed *via* hydrogenolysis, they are unsuitable for this synthesis because the benzyl ether may be cleaved in the same way.

A very common protecting group for amines is Boc. It fulfils all of the fundamental criteria, is stable under basic conditions and inert to many nucleophiles. The trityl group is another

suitable base-stable protecting group. It can be attached by using trityl chloride and removed under acidic conditions.

Synthesis of Benzimidazole Ether *via N*-Boc-protected 2-Chlorobenzimidazole

Due to its versatility and the mild procedures for its introduction and removal, the Boc group was chosen as the protecting group for the synthesis of benzimidazole ethers (**scheme 2.17**).

(a): Boc$_2$O, DMAP, Et$_3$N, MeCN, RT, 16 h (60%).
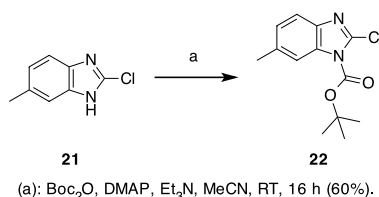
Scheme 2.17: Boc-protection of 2-chlorobenzimidazole **21**.

The protection was carried out using Boc-anhydride under standard conditions and gave the Boc-protected benzimidazole **22** in 60% yield.

The product was then used to find suitable reaction conditions to synthesise the Boc-protected benzimidazole benzyl ether **23** (**table 2.7**).

(a): Benzyl alcohol (1.3 eq.), further conditions see table.
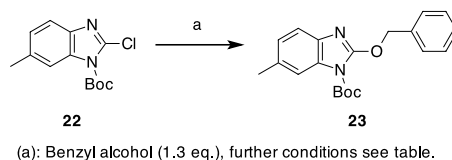
| Entry	Base	Solvent	Additive	Outcome
1	NaH (1.3 eq.)	DMF		No product
2	NaH (2.6 eq.)	DMF		No prduct
3	NaH (4.0 eq.)	DMF		No product,
4	NaH (1.5 eq.)	DMF	DMAP	No product
5	NaH (1.5 eq.)	THF	DMAP	Trace amounts, deprotected SM
6	Et$_3$N (1.3 eq.)	DMF	DMAP	No product
7	Et$_3$N (1.3 eq.)	THF	DMAP	No product
8	No base	DMF	AgNO$_3$	No product
9	No base	THF	AgNO$_3$	No product

Table 2.7: Conditions tried for the synthesis of benzimidazole ether **23**.

The optimisation was started with a series of reactions with increasing amounts of base employed. None of these reactions gave any amount of the desired benzimidazole **23** (**table 2.7, entries 1-3**). Then, to increase the reactivity of the benzyl alcohol two reactions were conducted where a catalytic amount (0.1 equivalents) of DMAP was added. While the reaction in DMF did not yield any product, the reaction in THF showed a trace amount of product (**table 2.7, entries 4 and 5**). Unfortunately, the reaction also yielded a large quantity of deprotected starting material. It was hypothesised, that deprotection could occur due to the hydroxy group attacking the carbonyl of the Boc group (**scheme 2.18**).
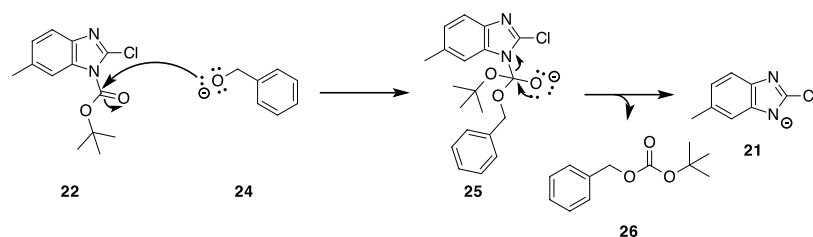
Scheme 2.18: Possible mechanism for the nucleophilic deprotection of 2-chloro-*N*-Boc benzimidazole **22**.

Thus, nucleophilic attack by the alkoxide **24** on the Boc group results in the formation of a carbonate-amide intermediate **25** that collapses to give back the 2-chlorobenzimidazole **21** and a *tert*-butyl-benzyl carbonate **26**.

To avoid the deprotection, the next reactions were carried out with triethylamine to neutralise the hydrochloric acid produced in this process. For both reactions, in THF as well as in DMF no conversion to the product occurred (**table 2.7, entries 6 and 7**). In the last trial reaction of this series, silver nitrate was used as an additive. This salt acts as a mild Lewis acid and should activate the benzyl alcohol, as well as leading to the formation of silver chloride, which precipitates, driving the reaction towards the product. Unfortunately, this was also not successful (**table 2.7, entries 8 and 9**).

After these unsuccessful attempts and the observed deprotection under the employed reaction conditions, it was anticipated that a change in protecting group might be the key to achieving a successful synthesis of the benzimidazoles.

Synthesis of Benzimidazole Ether *via N*-Trityl-Protected 2-Chlorobenzimidazole

Our second choice of protecting group for this reaction was the trityl group. This group is stable under basic conditions and can be cleaved under mild acidic conditions. The trityl protection was carried out as described in the patent by Matsoukas *et al*. (**scheme 2.19**). [94]

(a): TrCl, Et₃N, CH₂Cl₂, RT, 16 h (83%).
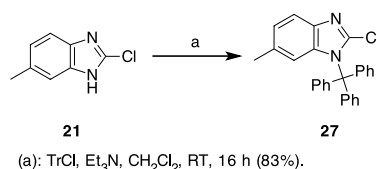
Scheme 2.19: Trityl protection of 2-chlorobenzimidazole **21**. [94]

This reaction was carried out with a slight excess of trityl chloride. The product was purified by column chromatography, but proved to be highly sensitive towards acid, which led to decomposition of the product during the chromatography.

Nevertheless, the etherification was attempted with the slightly impure starting material (**table 2.8**).

(a): Benzyl alcohol (1.3 eq.), further conditions, see table.
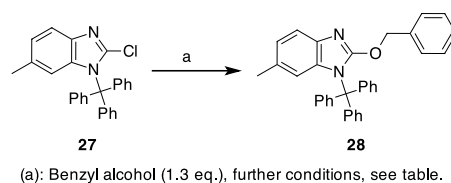
Entry	Base	Solvent	Temperature	Additive	Outcome
1	NaH	DMF	RT		<5% product
2	Et₃N	DMF	RT	DMAP	No product
3	NaH	THF	68 °C		No product
4	NaH	Neat	70 °C		No product
5	NaH	NMP	70 °C		Decomposition of SM
6	NaH	DMF	70 °C		≈10% Product

Table 2.8: Conditions for the synthesis of *N*-trityl protected benzimidazole ether **28**.

The optimisation was started with sodium hydride in DMF at room temperature. Encouragingly, a small amount of product was obtained (**table 2.8 entry 1**). To improve the yield a selection of different solvents was tried. Changing the base to triethylamine, and the addition of DMAP did not give any product (**table 2.8, entry 2**). Therefore, it was decided to continue with sodium hydride as the base. The reaction in THF did not yield any product and the starting material was recovered (**table 2.8, entry 3**). To eliminate any effects the solvent could have, the reaction was tried neat with benzyl alcohol as the nucleophile and solvent.

After removing the benzyl alcohol, no product could be detected (**table 2.8, entry 4**). In the following attempt NMP was employed as the solvent but these conditions led to the decomposition of the starting material (**table 2.8, entry 5**). The last reaction of this optimisation series was again run in DMF but at 70 °C. The product was formed but the yield was still very poor (**table 2.8, entry 6**).

Looking at the structure of the *N*-trityl-2-chlorobenzimidazole **27** more closely, it is noticeable that the trityl group is sterically very demanding (**figure 2.11**).
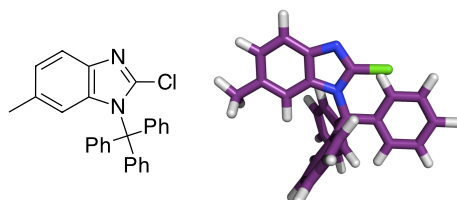

Figure 2.11: 3-Dimensional structure of *N*-trityl-2-chlorobenzimidazole **27** generated by using Chem 3D®.

The 3-dimensional structure shows that the three phenyl rings are organised like a propeller, with one of the phenyl rings very close to the envisaged reactive centre of the molecule. At elevated temperature the movements within the molecule should increase and allow the benzyl alcohol to attack at the position 2 of the benzimidazole **27**. However, the yield did not greatly increase when the reaction was carried out at higher temperature. Another possible problem with the trityl group could be the electron donating properties of the three phenyl rings. This could increase the electron density at C-2 and result in a reduced reactivity towards nucleophiles.

Even though some product could be obtained from this reaction, the conditions were still not good enough for the synthesis of a compound library. Therefore, the trityl protecting group was discarded as unsuitable.

Synthesis of Benzimidazole *via N*-SEM-protected 2-Chlorobenzimidazole

An extensive search in the literature suggested that a rather less commonly used protecting group could potentially be suitable for the present reaction: the trimethylsilylethoxymethyl (SEM) group. This protecting group is significantly smaller than the trityl group, inert to strong bases and nucleophiles and can be selectively removed with TBAF. Consequently, we decided to evaluate this form of *N*-protection (**scheme 2.20**).
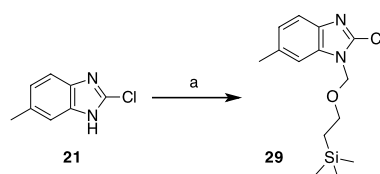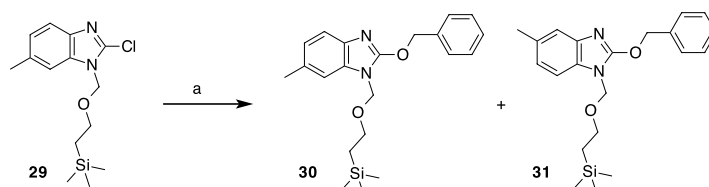
(a): NaH, SEM-Cl, DMF, RT, 16 h (75%).

Scheme 2.20: *N*-SEM-protection of 2-chlorobenzimidazole **21**.

The protection reaction was carried out by adapting a procedure described by Grice *et al.* [95] and gave the product in good yield.

The *N*-SEM protected benzimidazole **29** was then reacted with benzyl alcohol under the same conditions as before, with sodium hydride in DMF (**scheme 2.21**).

(a): Benzyl alcohol, NaH, DMF, RT, 16 h, (41%).

Scheme 2.21: Synthesis of the two regioisomeric products **30** and **31** of *N*-SEM-protected benzimidazole **29**.

The reaction in DMF gave the desired benzimidazole benzyl ether in 41% yield at the first attempt. Interestingly, as evidenced by ^{1}H-NMR spectroscopy, the *N*-SEM-protected benzimidazole ether is formed as a 1:1 mixture of two products. These two products derive from the tautomerism of the starting material and are the 6-methylbenzimidazole and 5-methylbenzimidazole respectively.

The deprotection was carried out utilising TBAF in THF, similarly to the conditions described by Bamberg *et al*. (**scheme 2.22**). [96]
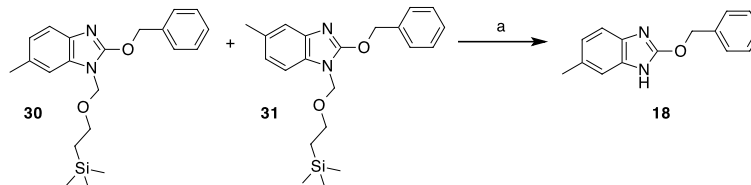
(a): TBAF, THF, 55 °C, 16 h (29%).

Scheme 2.22: SEM-deprotection to the final benzimidazole ether **18**. [96]

Heating the reaction mixture with 5 equivalents of TBAF at 55 °C gave the benzimidazole ether **18** as a single product in 29% yield.

With workable reaction conditions for the etherification and deprotection in hand, the synthesis of the analogues was carried out, giving the *N*-protected benzimidazole ethers **30a-f** in 49-86% yield and the final benzimidazole ethers **18a-f** between 10 and 54% overall yield (**table 2.9**).

(a): NaH, substituted benzyl alcohol, DMF, RT, 16 h; (b): TBAF, THF, 55 °C, 48 h.

30, 18: R= H
30a, 18a: R= 2-Me
30b, 18b: R= 4-Me
30c, 18c: R=2-Cl
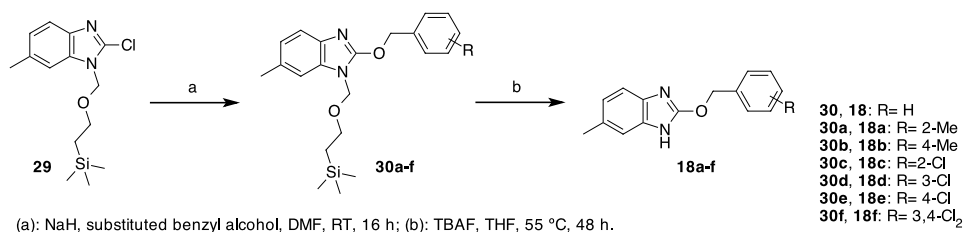**30d, 18d**: R= 3-Cl
30e, 18e: R= 4-Cl
30f, 18f: R= 3,4-Cl$_2$

Substituent R	H	2-Me	4-Me	2-Cl	3-Cl	4-Cl	3,4-Cl$_2$
Etherification	53%	77%	28%	49%	67%	83%	76%
Deprotection	29%	33%	35%	87%	42%	45%	71%
Overall	15%	25%	10%	43%	28%	37%	54%

Table 2.9: Yields for the synthesis of the series of benzimidazole ethers **18a-f**.

Due to the low yield in the test deprotection reaction, the amount of TBAF was increased to ten equivalents and the reaction time prolonged to 48 hours, when preparing the analogues. The compounds synthesised were analogous to those prepared in the thioether series. This would enable us to directly compare the binding effects of the oxygen analogues *versus* the thioether analogues.

2.1.7 Synthesis of 6-Aryl Substituted Benzimidazole Thioether

The final series of benzimidazole analogues contains an aryl group at position 6. As before, the substitution on the aryl ring was to be varied according to the Topliss series. [63]

The synthesis of the aryl substituted benzimidazoles **32** starts with the synthesis of 6-bromo 2-mercaptobenzimidazole **9b**. As discussed above, this can easily be synthesised from the corresponding diamine and carbon disulfide (**scheme 2.23**).

(a): 2-Methyl BnBr, NaOMe, DMF, MeOH, RT, 16 h.
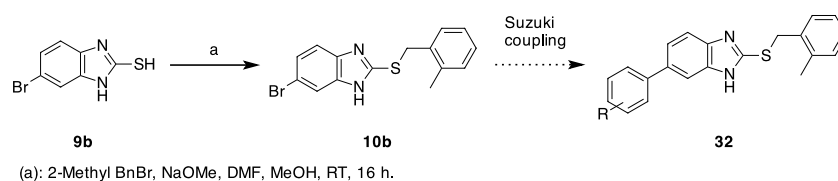
Scheme 2.23: Planned route for the synthesis of substituted 6-aryl benzimidazole thioethers **32**.

After formation of the 2-mercaptobenzimidazole **9b**, the next step is the conversion to the thioether **10b**. The final and crucial step is the introduction of the substituted aryl ring *via* Suzuki-Miyaura coupling (**scheme 2.23**).

This synthetic route has the advantage of a late-stage diversification. Therefore, the starting materials until the Suzuki coupling could be prepared on a large scale.

There are, of course, numerous types of palladium cross couplings known. [97] The most suitable cross coupling for this system however, was considered to be the Suzuki-Miyaura coupling, which is a powerful method for the synthesis of biphenyls and is mechanistically well-understood (**scheme 2.24**).
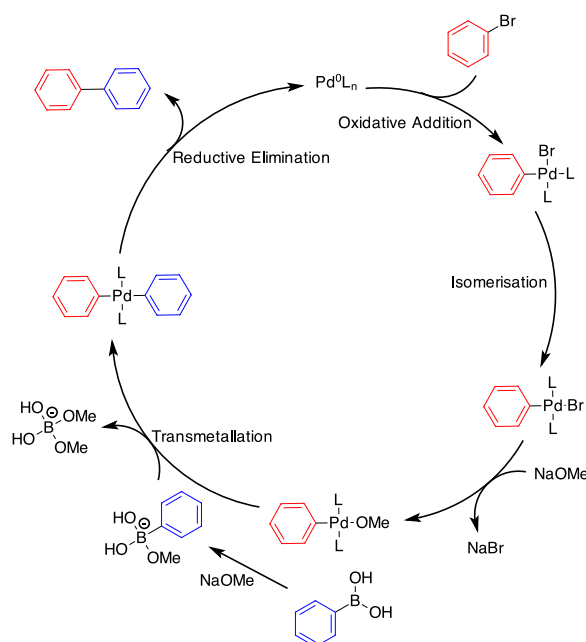
Scheme 2.24: Catalytic cycle of the Suzuki-Miyaura coupling. [98]

The catalytic cycle starts with the oxidative addition of the aryl bromide to the Pd(0). The *cis* Pd(II)-complex then isomerises to the *trans* isomer. Transmetallation with the boronic acid gives the Pd(II)-biphenyl complex that undergoes reductive elimination to give the biphenyl product and concomitantly regenerates Pd(0) to continue the catalytic cycle.

In the above reported copper catalysed Ullmann-type coupling it was noted that the thioether **12a** appeared to cause deactivation of the copper catalyst. A similar deactivation could be expected for the palladium catalyst. Maxted [90] has reported on the ability of sulfur-containing compounds to poison transition metal catalysts and deactivate them. Among the poisoning compounds are sulfites, organic thiols and organic sulfides. All these compounds have at least one free electron pair that can form a dative bond to the metal catalyst (**figure 2.12**).
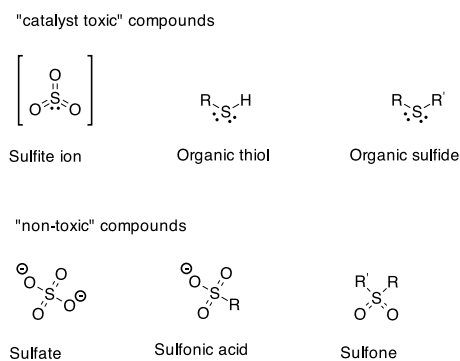
"catalyst toxic" compounds

Sulfite ion   Organic thiol   Organic sulfide

"non-toxic" compounds

Sulfate   Sulfonic acid   Sulfone

Figure 2.12: Examples of "catalyst toxic" and "non-toxic" sulfur-containing compounds. [90]

In contrast, sulfur containing compounds which lack a free electron pair are not capable of binding to the catalyst and hence, cannot deactivate the metal catalyst. To prevent the deactivation, it was therefore decided to mask the thioether sulfur as a non-catalyst toxic sulfone (**scheme 2.25**).

10b   **33**

(a): Peracetic acid, CH$_2$Cl$_2$, 40 °C, 3.5 h (58%).
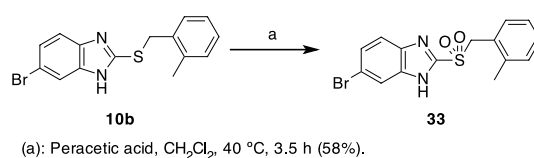
Scheme 2.25: Oxidation of the benzimidazole thioether **10b** to the corresponding sulfone **33**.

The oxidation was carried out with peracetic acid and gave the product in 58% yield.
Following the pathway outlined above, the sulfone was to be subjected to the Suzuki-Miyaura coupling, followed by the reduction to the thioether to give the final product **32** (**scheme 2.26**).

33   **34**   **32**
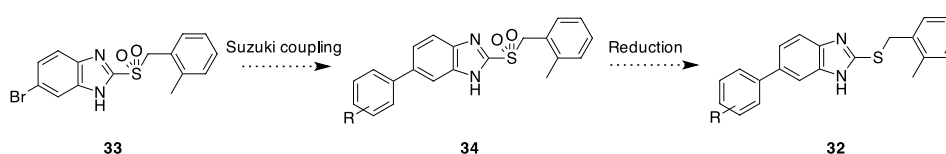
Scheme 2.26: Planned route for the synthesis of 6-aryl benzimidazoles **32** *via* the sulfone **34**.

This procedure would have two advantages: on the one hand, the oxidation masks the sulfur and reduces its ability to deactivate the palladium catalyst during the Suzuki coupling and on the other hand, the respective sulfones are also a series of compounds that may have the ability to modulate the action of LRH-1.

2.1.7.1 Suzuki Coupling of Benzimidazole Sulfone

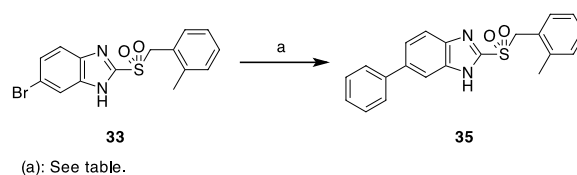The Suzuki reaction was carried out using a variety of different conditions (**table 2.10**).

33   **35**

(a): See table.

Entry	Pd(PPh$_3$)$_4$	Base (2.0 eq.)	PhB(OH)$_2$	Solvent	Outcome
1	10 mol%	NaHCO$_3$	1.5 eq.	THF	No product
2	10mol%	Na$_2$CO$_3$	1.5 eq.	Toluene	< 2%
3	10 mol%	Na$_2$CO$_3$	1.5 eq.	DME/H$_2$O (10:1)	No product
4	10 mol%	Na$_2$CO$_3$	1.5 eq.	Tol/H$_2$O (10:1)	No product
5	10 mol%	K$_2$CO$_3$	1.5 eq.	Tol/MeOH (10:1)	No product
6	10 mol%	Na$_2$CO$_3$	1.5 eq.	Tol/MeOH/H$_2$O (10:1:1)	No product
7	20 mol%*	K$_2$CO$_3$	2.0 eq.	Dioxane/H$_2$O (10:1)	< 2%
8	30 mol%*	K$_2$CO$_3$	2.0 eq.	DMF	No product
9	15 mol%*	K$_2$CO$_3$	2.0 eq.	DMF/MeOH/H$_2$O	No product

*Pd(PPh$_3$)$_4$ formed *in situ*.

Table 2.10: Suzuki coupling of the benzimidazole sulfone **33** with phenylboronic acid.

The coupling reaction was first attempted in THF and in toluene (**table 2.10, entries 1 and 2**). The reaction in toluene gave trace amounts of the product (**table 2.10, entry 2**). Then a selection of different solvents and solvent mixtures were tried, but none of these conditions proved successful (**table 2.10, entries 3-6**). Then it was decided to increase the amount of phenylboronic acid and the catalyst loading level (**table 2.10, entries 7-9**). From these experiments only the reaction in a dioxane/water mixture gave traces of the desired product (**table 2.10, entry 7**).

A possible reason for the failure of the reactions could be the decomposition of the catalyst. To address this possibility, in the last three reactions the Pd(PPh$_3$)$_4$ complex was formed *in situ* using Pd-acetate and triphenyl phosphine (**table 2.10, entries 7-9**).

Another reason for the lack of success of the reaction could be the electronic properties of the benzimidazole **33**. This electron rich aryl halide would undergo very slow oxidative addition. Due to the oxidation of the sulfur it is improbable that it is still able to deactivate the catalyst.

After none of the conditions tried gave the desired product in a satisfactory yield, it was necessary to search for an alternative route for the synthesis of 6-aryl benzimidazole thioethers **32**.

2.1.7.2 Alternative Route Towards 6-Aryl Benzimidazole Thioethers

An alternative route for the synthesis of the desired aryl benzimidazoles **32** was considered to be *via* an "early" Suzuki coupling prior the formation of the 2-mercaptobenzimidazole. A comparison of the two retrosynthetic pathways is presented below (**scheme 2.27**):
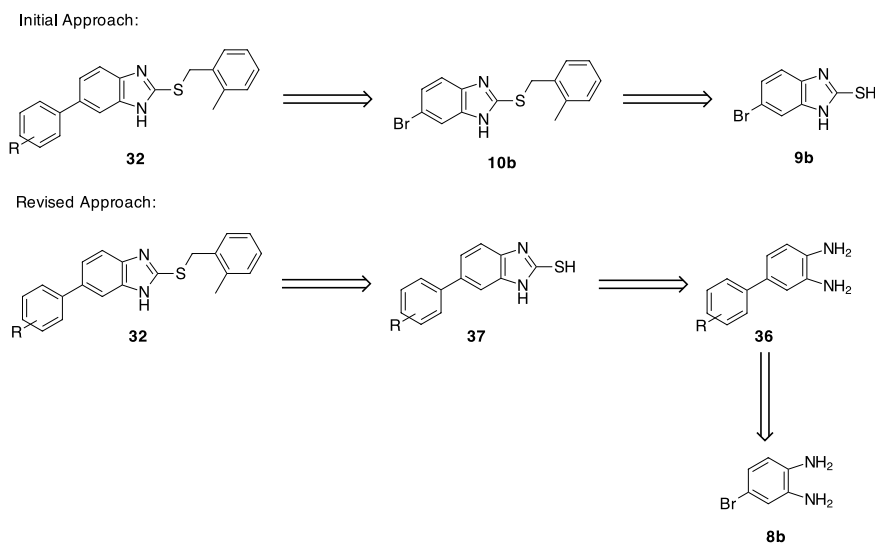
Scheme 2.27: Comparison of the initial and revised routes for the synthesis of 6-aryl benzimidazoles **32**.

The starting material for both routes is 4-bromo-1,2-diaminobenzene **8b**, but the order of events is reversed. The original approach started with the synthesis of the benzimidazole thioether **10b**, which was envisaged to be cross-coupled to give the 6-aryl benzimidazole **32**. The revised apporach begins with the Suzuki coupling to form the biaryl compound **36**. After that, the benzimidazole **37** is formed, using similar reaction conditions to those already described.

The new pathway was initiated with the *N*-Boc-protection of the 4-bromo-1,2-diaminobenzene **8b**, followed by the Suzuki coupling, using a procedure adapted from that described by Cheung *et al*. (**table 2.11**). [99]

8b **38** **39**
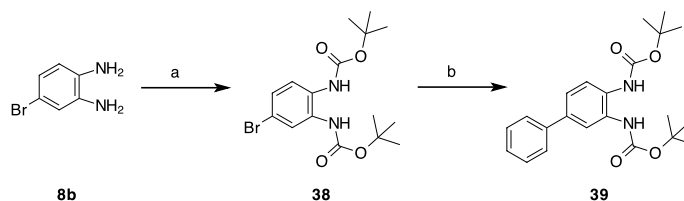
(a): Boc$_2$O, NaOH, CH$_2$Cl$_2$/H$_2$O, RT, 16 h (69%); (b): see table.

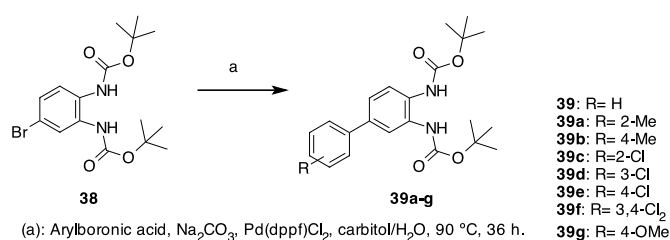| Entry	PhB(OH)$_2$	Pd(dppf)Cl$_2$	Na$_2$CO$_3$	Time	2-(2-ethoxy-ethoxy)ethanol /H$_2$O	Yield
1	2.0 eq.	20 mol%	8.0 eq.	11 h	1:0	< 2%
2	2.0 eq.	10 mol%	8.0 eq.	11 h	3:1	20%
3	2.0 eq.	20 mol%	8.0 eq.	36 h	1:1	77%
4	2.0 eq.	20 mol%	8.0 eq.	36 h	1.5:1	85%

Table 2.11: Optimisation of the Suzuki coupling with phenylboronic acid.

The protection was carried out in a mixture of water and dichloromethane with a high excess of Boc-anhydride. After purification by column chromatography the pure product **38** was obtained in good yield. The *N,N´*-di-Boc-protected 4-bromo diamide **38** was then used for the Suzuki coupling, which was optimised with phenylboronic acid. It was found that the Suzuki coupling was most efficient in a solvent mixture of 2-(2-ethoxyethoxy)ethanol/water (1.5:1) and a 20 mol% catalyst loading level.

With the key steps optimised the synthesis of analogues was carried out (**table 2.12**).

38 **39a-g**

39: R= H
39a: R= 2-Me
39b: R= 4-Me
39c: R=2-Cl
39d: R= 3-Cl
39e: R= 4-Cl
39f: R= 3,4-Cl$_2$
39g: R= 4-OMe

(a): Arylboronic acid, Na$_2$CO$_3$, Pd(dppf)Cl$_2$, carbitol/H$_2$O, 90 °C, 36 h.

R	H	2-Me	4-Me	2-Cl	3-Cl	4-Cl	3,4-Cl$_2$	4-OMe
Yield	29%	55%	49%	19%	53%	46%	20%	16%

Table 2.12: Yields for the Suzuki coupling.

All the biaryls **39a-g** could be obtained in yields ranging from 16 to 55%

With the key cross-coupling achieved, the Boc-deprotection was carried out with TFA in dichloromethane (**scheme 2.28**).

(a): TFA, CH$_2$Cl$_2$, RT, 15 min.
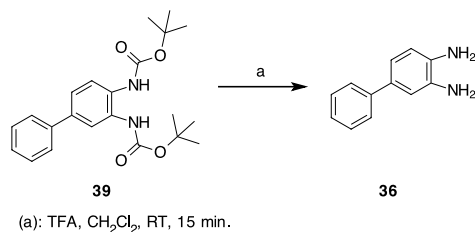
Scheme 2.28: Deprotection to the biaryl diamine **39**.

The reaction was complete after 15 min. In order to remove traces of TFA the crude product was purified by column chromatography. Unfortunately, the purified product proved to be very unstable and decomposed immediately. This event was quite unexpected as the commercially available diamines can be stored at room temperature in air. A possible reason for the rapid decomposition could be the increased stability of the Wheland intermediate due to the greater delocalisation of the electrons in the biaryl system and the amine groups formed by protonation.
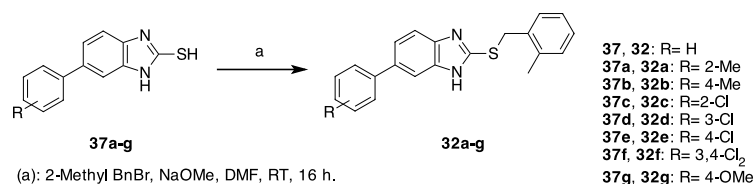
It was found, however, that the TFA salt **40** of the diamine **36** was stable. In the light of this finding, it was decided to use the diamine crude, as obtained from the deprotection reaction in the subsequent formation of the 2-mercaptobenzimidazole **37**. This reaction was carried out as described above, with one equivalent of base and gave only a poor yield of 16% (**scheme 2.29**).

(a): CS$_2$, NaOH, EtOH/H$_2$O, 50 °C, 4 h (16%).
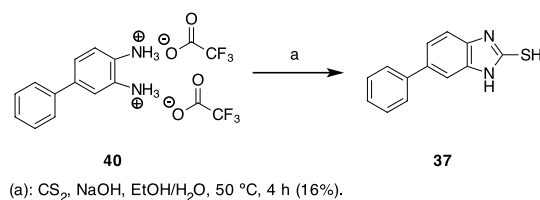
Scheme 2.29: Formation of the biaryl 2-meracpto benzimidazole **37**.

This very low yield can be explained by the fact that an insufficient amount of base to neutralise the TFA and deprotonate the diamine has been added. To increase the yield, the amount of base and carbon disulfide was increased to 10 equivalents and the temperature decreased to 50 °C to minimise the loss of the highly volatile carbon disulfide. With the improved reaction conditions in place, a significant increase in yield to up to 95% could be observed (**scheme 2.29**).

The final step of the synthetic sequence was the etherification of the thiol (**table 2.13**).

(a): 2-Methyl BnBr, NaOMe, DMF, RT, 16 h.

37, 32: R= H
37a, 32a: R= 2-Me
37b, 32b: R= 4-Me
37c, 32c: R=2-Cl
37d, 32d: R= 3-Cl
37e, 32e: R= 4-Cl
37f, 32f: R= 3,4-Cl$_2$
37g, 32g: R= 4-OMe

R	H	2-Me	4-Me	2-Cl	3-Cl	4-Cl	3,4-Cl$_2$	4-OMe
Overall Yield	11%	19%	20%	6%	4%	11%	4%	4%

Table 2.13: Overall yields of the synthesis of the final 6-aryl benzimidazole thioethers **32a-g**.

The alkylations were carried out as previously described with sodium methoxide in DMF. The reactions proceeded smoothly and yielded the desired final benzimidazoles **32a-g** in good to satisfactory yields.

For the 3-chloro analogue **32d**, a very small second signal in the benzyl region of the ^{1}H-NMR spectrum could be detected. This indicated that a small amount of the *N*-alkylated benzimidazole thioether was formed. The two products could be separated by preparative TLC. The separated products were recrystallised and a single crystal X-ray structure determination carried out by Chris Frampton (Pharmophix Ltd, Cambridge) on the major product. This confirmed that the major product of the alkylations is the expected *S*-alkylated benzimidazole (**figure 2.13**).
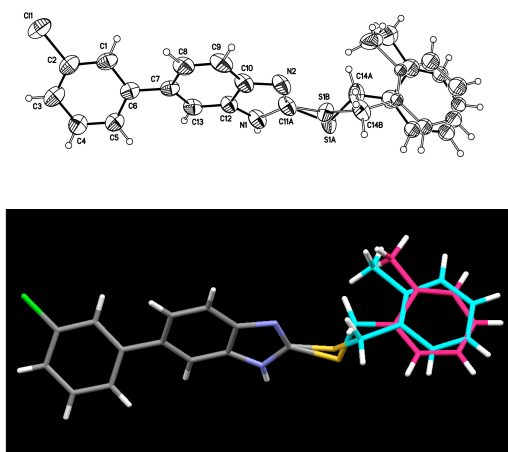

Figure 2.13: Molecular structure of *S*-benzylated thioether **32d** as determined by a single crystal X-ray experiment performed by Chris Frampton.

The crystal structure shows that the alkylation took place predominantly at the sulfur as we hoped for, and not at the nitrogen.

2.2. Biological Testing of the Compound Library

After the completion of the synthesis of this series of analogues, all of the compounds were tested for their binding properties to the LRH-1 ligand binding pocket. Eric Ortlund (Emory Hospital, Atlanta, Georgia, USA) kindly prepared and supplied us with an appropriate plasmid, which was used for the expression of LRH-1.

Plasmids are circular double stranded DNA molecules, which are distinct from the chromosomal DNA of the cell. The length can range from one to one hundred thousand DNA base pairs. Plasmids for genetic or biological work are called vectors. These vectors are used for instance to express particular genes (**scheme 2.30**).
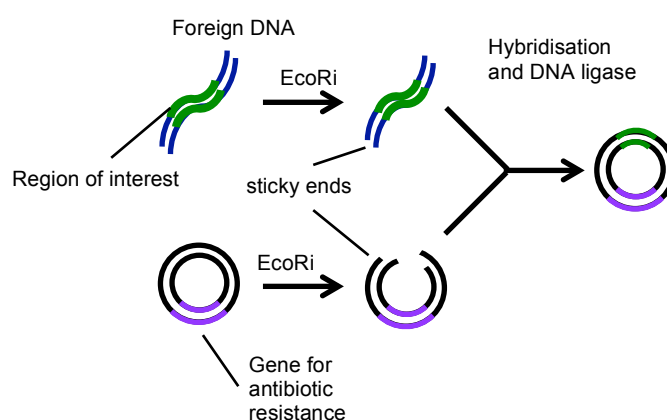
Scheme 2.30: Cartoon depicting the formation of a plasmid. [100]

The plasmid contains genes responsible for antibiotic resistance. The DNA strand contains the gene of interest. Both the DNA and the plasmid are opened with restriction endonuclease (EcoRi) and mixed with DNA ligase to reform the two pieces as recombinant DNA.
The plasmid used here encodes for the expression of a fusion protein consisting of the LRH-1 LBD and a maltose binding protein (MBP), connected through a histidine chain. The function of the MBP is to increase the solubility of the protein and prevent unwanted aggregation.

2.2.1 Expression of LRH-1

The fusion protein was expressed in *E.coli* bacterial cells (**scheme 2.31**).
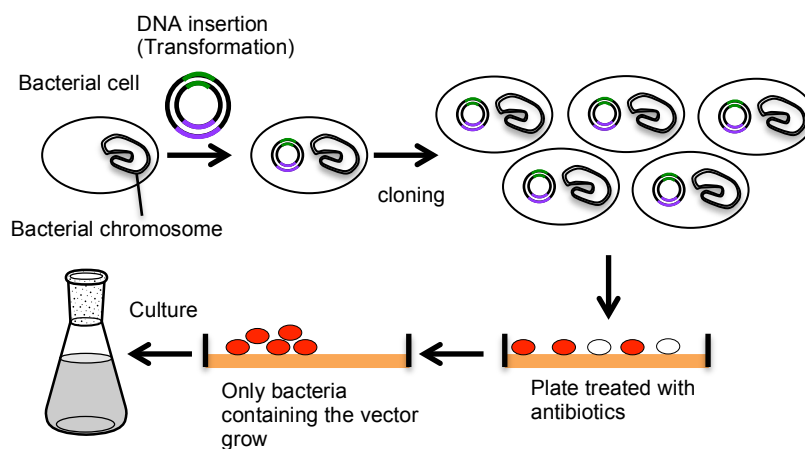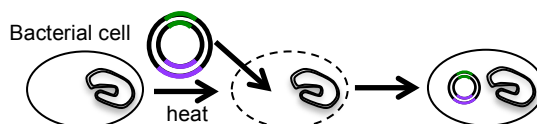

Scheme 2.31: Cartoon showing the steps involved in the expression of proteins from *E. coli* (picture adapted from accessexelence.org [100]).

The first step in the expression was to transfect the plasmid into the bacterial cells (transformation). The plasmid was added to a stock of bacterial cells in media and the cells were heat shocked (**scheme 2.32**).

Scheme 2.32: Principle of plasmid transfection *via* heat shock.

The heat shock procedure involved heating a mixture of *E.coli* cells and the plasmid to 42 °C for 45 seconds and then placing the tube on ice to minimise the damage to the cells.

The heating causes the cell walls to open slightly and allows the plasmid to enter the cell. After the heat-shock, the cells were incubated for 30 min at 37 °C and cloned. This stock of cells was then transferred to agar plates, in which the media was treated with antibiotics. Cells which contain the plasmid have immunity towards the antibiotics. Hence, only successfully transfected cells remain on the plate and are grown overnight. The following day a single colony was chosen and a culture grown. After 12 hours in 5 mL growth media, the cells were transferred into one litre of medium and grown for further 8 hours. This stock was then divided into 5 times 1 litre aliquots. These cultures were grown until an optical density of 0.6 was achieved. The optical density was monitored by measuring the UV absorption at 600 nm. This method can be used to estimate the concentration of a bacterial solution. When the target optical density was reached, the cells were induced with isopropyl β-D-1 thiogalactopyranoside (IPTG) and incubated at 25 °C overnight (**figure 2.14**).
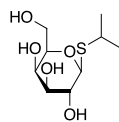
Figure 2.14: Structure of isopropyl β-D-1 thiogalactopyranoside (IPTG).

IPTG is a sugar derivative that cannot be metabolised and enables the expression of the desired protein.

After incubation for 24 hours the bacterial cells were centrifuged and the cells separated from the media solution. The supernatant was discarded and the cell pellet transferred into a smaller tube. The cell pellet was re-suspended in water and sonicated to destroy the bacterial cell walls and extract the protein. The suspension was treated with DNAse, an enzyme used to break up DNA and after centrifugation, the supernatant contained the crude protein.

The protein was purified by FPLC. Due to the structure of the fusion protein, the histidine residues could be used to aid the purification process. Therefore, it was possible to use a Hi-trap column, which contains nickel ions that bind to the His-tag of the protein. After the crude protein was loaded on the column, all impurities that did not have a histidine chain were washed away leaving only the protein on the column. Then, the protein was gradually eluted from the column by increasing the concentration of imidazole in the buffer. A SDS PAGE was run to determine the fractions that contained the protein and to determine the purity (**figure 2.15**).
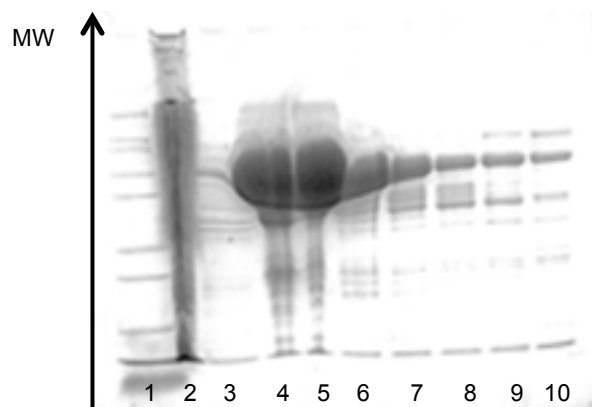
Figure 2.15: SDS PAGE of the expressed LRH-1 protein (1: Ladder, 2: flowthrough, 3-10 protein containing fractions).

The protein containing fractions were combined and dialysed to remove residual imidazole. For that process the protein solution was transferred into a permeable tube, that allowed only small molecules to pass through. These tubes were placed in a buffer solution, which was changed every 8 hours.

For the testing of the compounds, it was preferred to have only the LRH-1 LBD protein. At the outset it was not known whether the MBP would have an influence on the behaviour of the

LRH-1 LBD in terms of ligand binding or co-activator binding in particular, because the MBP is bigger than the LRH-1 LBD itself. Ideally, the protein used for the testing would only be the LRH-1 LDB rather than the fusion protein. Therefore, the dialysis was combined with the cleavage of the MBP.

This cleavage can be carried out with an enzyme derived form the tobacco etch virus (TEV). The enzyme recognises the specific sequence Glu-Asn-Leu-Tyr-Phe-Gln-(Gly/Ser) and cleaves the MBP fusion protein between the Gln and Gly/Ser residues, leaving the LRH-1 LBD and the His tagged MBP. This cleavage leaves the LRH-1 protein without a His-tag, which is required for some assays and therefore would limit the choice of potential assays.

For the TEV-cleavage the protein solution was split into three batches and each was treated with increasing amounts of the TEV enzyme. After the cleavage/dialysis a SDS PAGE showed that only a small fraction of the protein was cleaved. The cleavage was repeated with small quantities of the protein but again, no cleavage was observed. Due to the prolonged time the protein was at 4 °C and the general instability of proteins this batch was discarded and the expression repeated.

At the same time, Eric Ortlund provided us with a different plasmid, which only encodes for the LRH-1 LBD and a short His-tag. Expression of this protein under similar conditions as mentioned above was therefore attempted. The *E. coli* cells transfected with the plasmid grew well on the agar plate, but after inoculation of a single colony into LB broth, no further growth was observed. The procedure was repeated under close supervision of an experienced molecular biologist to detect any handling errors, but again, the cells did not grow. The great number of possible errors in the growth of bacterial cells makes the trouble shooting very challenging. Possible mistakes can be the wrong amount or type of antibiotics, bad condition of the cells, an alternative infection due to non-sterile handling or the wrong temperature and CO_2 content during the incubation.

Due to the failure in the TEV-cleavage and the unsuccessful attempts at expressing the short His-tag LRH-1 LBD protein it was decided to continue with the MBP fusion protein.

2.2.2 Testing of the Compound Library

2.2.2.1 Review of Most Common Assays [101]

There are many possible assays that can be used to evaluate the binding properties of small drug-like compounds to a protein. The most common types are ELISA assays, fluorescence polarisation assays, FRET assays and AlphaScreen® assays.

Enzyme-Linked Immunosorbant Assay (ELISA)

With the ELISA assay it is possible to measure the protein-protein interaction and effects of small molecule inhibitors (**figure 2.16**).
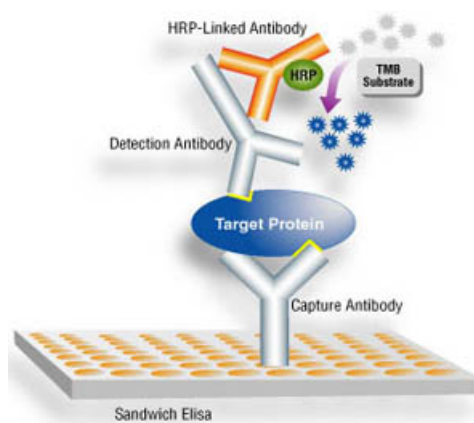

Figure 2.16: Cartoon showing the principle of the ELISA assay (picture from Iaszoology). [102]

One of the proteins is attached to the surface of a 96 well plate and the second protein allowed to bind to the first protein. The second protein is then allowed to bind an antibody, which is attached to an enzyme and as a result a, readout is produced that is proportional to the amount of the second protein bound to the first. For the case an inhibitor is bound, an decease in readout can be observed. Alternatively, an activator would increase the readout. The detection of the second protein can occur in several ways, such as direct labelling of the protein with a signal generating enzyme or binding of an enzyme labelled antibody. Depending on the method chosen, the readouts can be UV absorbance, fluorescence or luminescence.

Fluorescence Polarisation Assay

This assay enables the measurement of the association or dissociation between two molecules of which one has to be relatively small (**figure 2.17**).
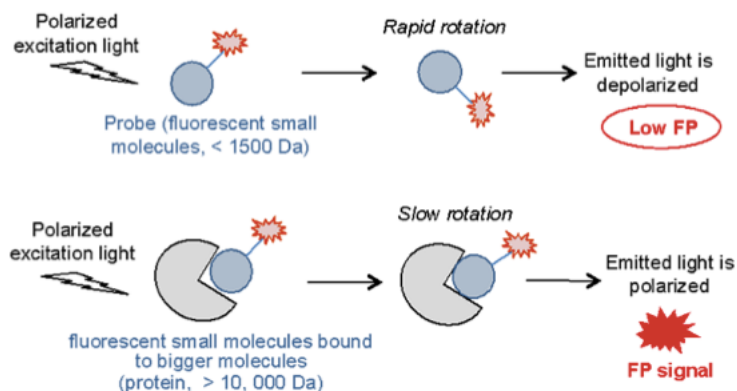

Figure 2.17: Cartoon depicting the principle of a fluorescence polarisation assay (picture from Arkin *et al*.). [101]

When a molecule labelled with a fluorophore is excited by polarised light it emits light with a degree of polarisation that is inversely proportional to the rate of molecular rotation. This molecular rotation is strongly dependent on the mass of the molecule. When a small molecule is fluorescently labelled and excited with polarised light, it will lose most of its polarisation due to rotation. However, when the small molecule is bound to a protein (bigger than 10 kDa), then the rotation is significantly reduced, which results in a higher intensity of polarised light being emitted. This differential can be quantified and forms the basis of this assay.

Time Resolved Fluorescence/Förster Resonance Energy Transfer (TR-FRET)

FRET is a phenomenon of non-radiative energy transfer between two fluorophores. For FRET to occur, the emission spectrum of the donor fluorophore must overlap with the excitation spectrum of the acceptor fluorophore. Additionally, the donor and acceptor need to be in close proximity (10-20 nm). When the donor is excited, energy can be transferred to the acceptor *via* long range dipole-dipole interactions. In TR-FRET the donor has very long emission half-live. This delay of 50-150 μsec between excitation and measured acceptor emission allows most of the background fluorescence to decay before the acceptor emission is measured giving a better signal-to-niose ratio than the standard FRET (**figure 2.18**).
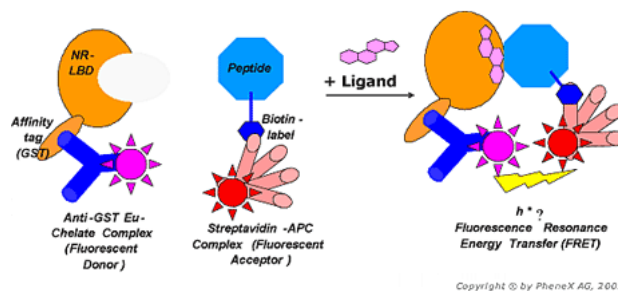
Figure 2.18: Cartoon depicting the principle of a TR-FRET assay (picture with kind permission taken from Phenex-Pharma). [103]

Amplified Luminescent Proximity Homogenous Assay (AlphaScreen®)

The AlphaScreen® was originally developed as LOCI (luminescent oxygen channelling immunoassay) by Dade Behring Inc. and is now a product of PerkinElmer. Like the FRET assay, the AlphaScreen® is a proximity assay. The two molecules to be observed are bound to beads. The donor bead contains a photosensitiser, phthalocyanine, that converts ambient oxygen into singlet oxygen upon illumination at 680 nm. Therefore, excitation of the donor results in the formation of singlet oxygen, which diffuses to the acceptor bead. When the acceptor bead is within range, energy is transferred to the thioxene containing acceptor bead and light is produced. The emission is measured at 520-620 nm (**figure 2.19**).
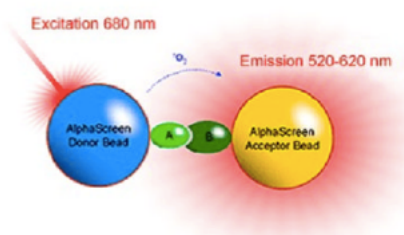

Figure 2.19: Cartoon depicting the principle of a AlphaScreen® assay (Image used with kind permission of PerkinElmer © 2014 PerkinElmer). [104]

The principle of the ELISA assay makes it unsuitable for the testing of the compounds prepared in this work. Additionally, several steps of washing make this assay impractical in a high throughput scenario. The FRET assay is also not suitable for the testing anticipated here, as it would require that one of the fluorophores is bound to the LRH-1 protein and the other to the co-activator peptide. Even though the former can be achieved by using the His-tag, the fluorophore would be too far away for FRET to occur. To have the fluorophore in proximity to the AF-2 site, significant molecular modifications to the protein would be required, which would impart unknown effects to the binding properties of the co-factor and the potential ligands.

The fluorescence polarisation assay could be used for the testing of the series of benzimidazoles. For this assay only one fluorophore is required that can be attached to a co-

activator peptide. When the compound is an agonist it would enhance co-factor binding and the polarisation of the emitted light would be increased. Alternatively, if the compound is an antagonist, the co-activator binding would be reduced and hence, the polarisation would decrease. A limitation of the fluorescence polarisation assay is that the fluorophores quench over time. The AlphaScreen® is a FRET-type assay, where the distance of donor and acceptor beads can be longer than in a conventional FRET assay, enabling us to use the His-tag to bind one of the fluorophore beads. The other bead can be attached to the peptide by a biotin linker. Due to previous experiments carried out by Dr Fiona Kyle on the AlphaScreen®, [105] it was decided to use this assay for the testing of this compound library.

Taking previous experiments into account, a panel of 4 co-factors was selected for incorporation into the AlphaScreen® assay and testing of the synthesised compound library. These comprised PGC-1α and TIF2 as co-activators and DAX-1 and a phage display derived peptide published by Clyne *et al.* [23] as co-repressors.

Unlike in other binding assays, the shape of the curves obtained from the AlphaScreen® are expected to follow a bell shape. This is because of the so-called hook effect (**figure 2.20**).
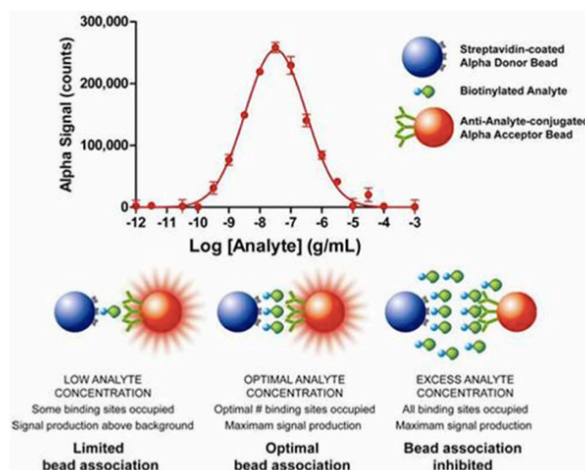

Figure 2.20: Explanation of the Hook effect (Image used with kind permission of PerkinElmer © 2014 PerkinElmer). [106]

When the protein and peptide are titrated, the beads become progressively saturated by binding to their respective target and the alpha signal increases. At the hook point either the donor or the acceptor bead is fully saturated and the signal reaches its maximum. At concentrations above the hook point an excess of target molecules for the donor or acceptor bead exists, which inhibits their association and cause a decrease in alpha signal. As a consequence the working region of the output is in the region where the concentrations are below the hook region.

2.2.2.2 Assay Optimisation

Before the testing was started the assay had to be optimised. To find an optimal ratio of protein to peptide, a titration was carried out with a 1:1 ratio of the LRH-1 protein to each of the selected peptides PGC-1α, Dax-1 TIF2 and the Clyne 4-16 peptide. As the LRH-1 protein binds its co-factor peptides in a 1:1 ratio, this ratio was used as a starting point for the optimisation (**figure 2.21**).

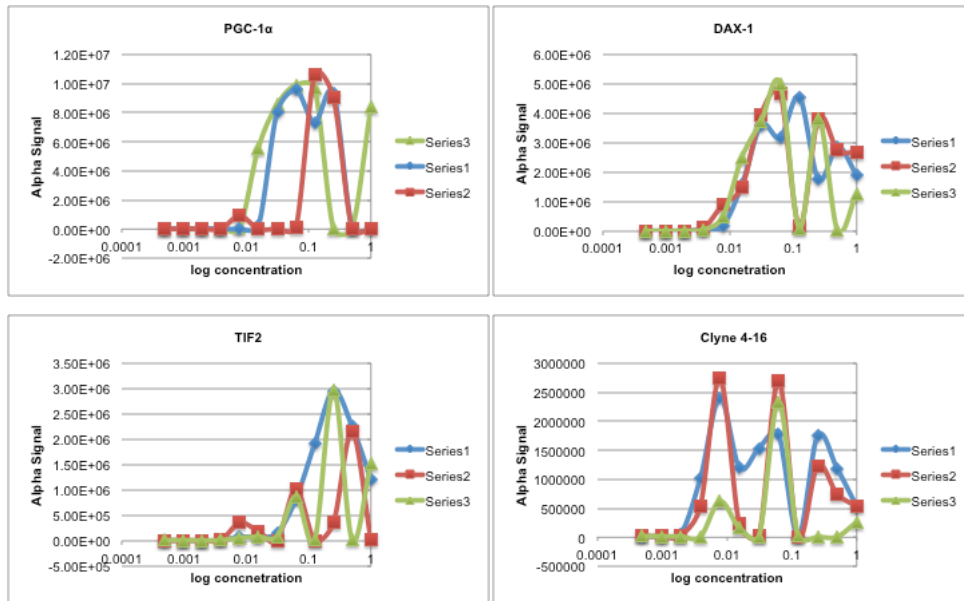**Figure 2.21:** Titration of LRH-1 and peptide in ratio 1:1.

The titration was carried out in triplicate and the results of each titration are plotted in the graphs. The graphs only vaguely resemble the expected bell-shaped curve. This result could be due to a too high concentration of either peptide or protein. Therefore, the titration was repeated with a 10:1 ratio of protein and peptide (**figure 2.22**).
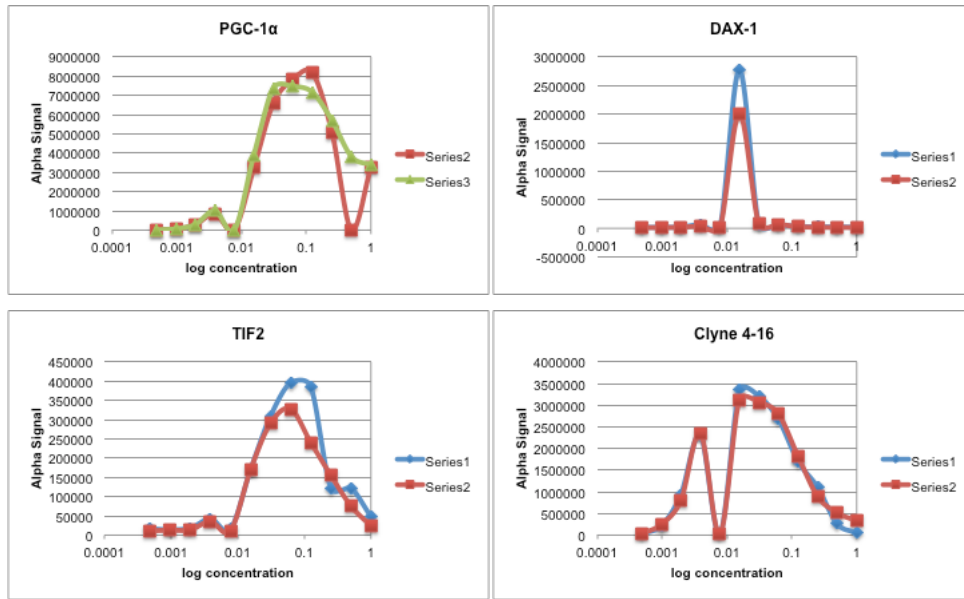
Figure 2.22: Titration of LRH-1 and peptide in ratio 10:1.

The graphs obtained are now significantly smoother and with reduced error. Still, these results are not satisfactory, as they still do not exhibit the bell shape. Particularly, the curve for DAX-1 appears erroneous, as it exhibits only one high readout point. In all traces it can be seen that for the fifth lowest concentration point the alpha signal plummets to zero. This could have two possible reasons: First, it may be that the plate reader used has a problem reading that particular column of the plate or second, it could be a pipetting error, which caused one of the components to be present in insufficient quantity, so that the reading drops. To explore both possibilities the titration was repeated a third time using the same ratio of protein and peptide (**figure 2.23**).
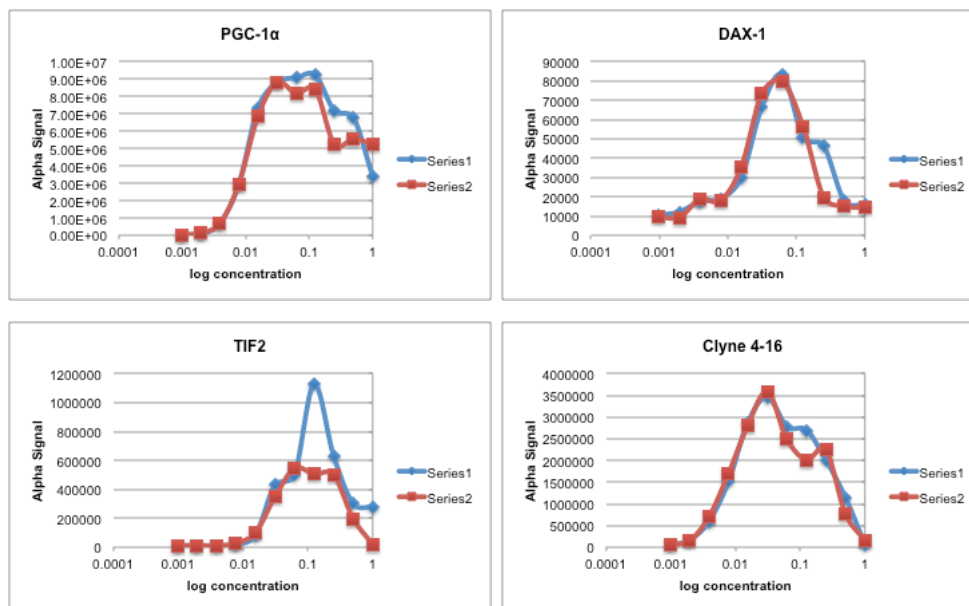

Figure 2.23: Repetition of the titration of LRH-1 and peptide in ratio 10:1.

A repetition of the titration gave the bell shaped curves confirming the chosen concentrations for protein and peptide and that the error seen in the graphs above was due to a pipetting error. Therefore, these titration curves were used for further considerations of the testing conditions.

With this ratio set it is necessary to chose a concentration of the protein and peptide mixture. During the testing it is expected that antagonistic behaviour of the compound leads to a drop of the alpha signal. To detect this difference in alpha signal it was required to choose a concentration of protein and peptide high enough to see a reduction in alpha signal. In contrast, an agonist compound would increase the binding of protein and peptide and hence, lead to an increase in alpha signal. To observe this change, it was required to run the testing at a concentration low enough to detect this increase.

To address both modes it was decided to run the assay against all peptides at one high and one low concentration (**figure 2.24**).

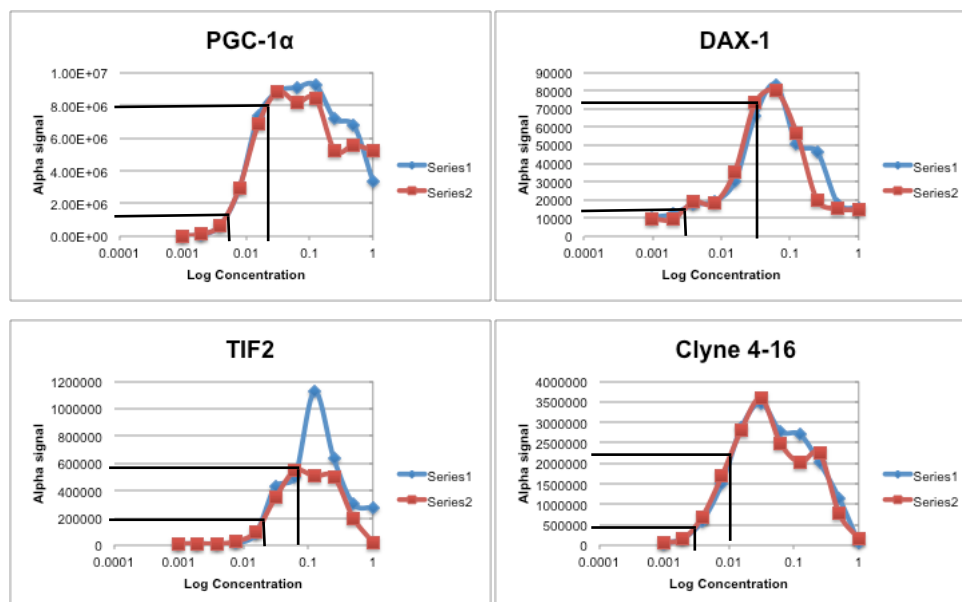Figure **2.24**: Determination of low and high concentration point for the assay.

These concentrations were determined form the titration curves by choosing a point with low alpha signal and low concentration of protein and peptide to test for agonism and a point with high readout and concentration to detect antagonism. The high concentration point had to be before the hook effect takes place.

The concentrations for the compounds are summarised in the table below (**table 2.14**).

Peptide	Low conc peptide [µM]	Low conc LRH-1 [µM]	High conc peptide [µM]	High conc LRH-1 [µM]
PGC-1a	0.004	0.04	0.02	0.2
DAX-1	0.003	0.03	0.03	0.3
TIF2	0.02	0.2	0.06	0.6
Clyne 4-16	0.003	0.03	0.01	0.1

Table 2.14: Summary of peptide and protein concentrations.

2.2.2.3 Assay Outline

During the assay the concentration of protein and peptide were kept constant, while a titration of the compound was carried out.

The assay was run on a 384 well plate with a standard format of the plate. Each plate was divided into 12 segments, where two segments contained one compound (**figure 2.25**).

Columns 1-12 protein and peptide at low concentration
Columns 1-2, 4 and 6-12: compound titration from 100 µM to 5 nM, column 3: control (purple), column 5: background (yellow)

Columns 13-24 protein and peptide at high concentration
Columns 13-14, 16 and 18-24: compound titration from 100 µM to 5 nM, column 15: control (purple), column 17: background (yellow)

Rows A-C: compound A
Rows D-F: compound B
Row G: control compound **5a** or **Scripps** compound
Rows H-J compound C
Rows K-M compound D
Rows N-P compound E

Figure 2.25: Outline of 384-well assay plate and structures of the controls.

On the left hand side of the plate was the low concentration and on the right hand side the high concentration of protein and peptide. In addition to the compounds, two known compounds were run to compare the tested compounds against them. For the testing for agonists, Whitby's **5a** compound [54] was used as standard. In the case of the testing for antagonists, the published **Scripps** compound was used (**figure 2.26**). [107]
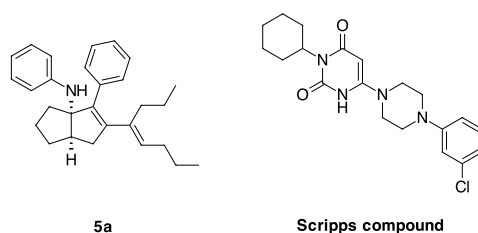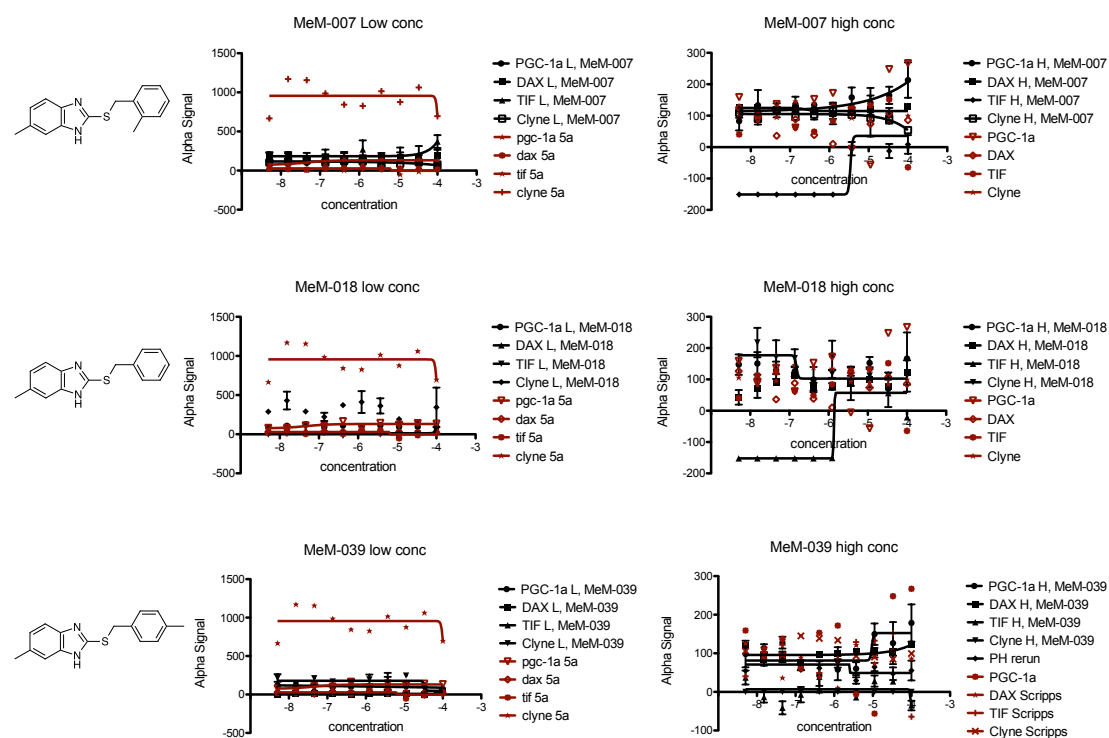
Figure 2.26: Controls used in the AlphaScreen® assay: Whitby's **5a** compound and a **Scripps** compound. [54,107]

At first a one-in-three serial dilution of the compounds in DMSO was carried out, starting from 100 µM to 5 nM as the lowest concentration over 10 concentration points. An aliquot of these dilutions were transferred to the measuring plate. Then buffer, the LRH-1 protein and the respective peptide were added to the wells. After addition of the Ni-chelate acceptor beads the plate was incubated for 30 minutes before the streptavidin donor beads were added. The plate was again incubated and the alphasignal measured using a Pherastar™ plate reader.

To normalise the data, one column was dedicated for the measurement of the background, and another column to the measurement of the signal when no compound was added (control). The latter can be used as the baseline for the assay.

2.2.3 Assay Results

The results for the AlphaScreen® testing of all benzimidazoles against all 4 peptides are outlined below (**figure 2.27**).

MeM-028D low conc

MeM-028D high conc

MeM-028B low conc

MeM-028B high conc

MeM-008 low conc

MeM-008 high conc

MeM-013 low conc

MeM-013 high conc

MeM-028A low conc

MeM-028A high conc

MeM-028C low conc

MeM-028C high conc

MeM-026 low conc

Mem-026 high conc

MeM-sulfone low conc

MeM-sulfone high conc

MeM-174A low conc

MeM-174A high conc

MeM-174B low conc

MeM-174B high conc

MeM-174C low conc

MeM-174C high conc

MeM-185Bn low conc

MeM-185Bn high conc

MeM-180B low conc

MeM-180B high conc

MeM-180C low conc

MeM-180C high conc

MeM-185Cl low conc

MeM-185Cl high conc

Figure 2.27: Summary of the AlphaScreen® data for the testing of the compounds **10-33**.

The raw data was normalised using the background and the control using the formula below (**equation 2.2**).

$$100\,\frac{(readout - background)}{(control - background)}$$

Equation **2.2:** Formula used for the normalisation of the raw assay data.

Despite the fact that all compounds and controls were run under the same conditions, there is a significant variance in the results. This can be clearly seen in the graphs of the controls. The Whitby **5a** compound [54] shows large error bars for the Clyne 4-16 peptide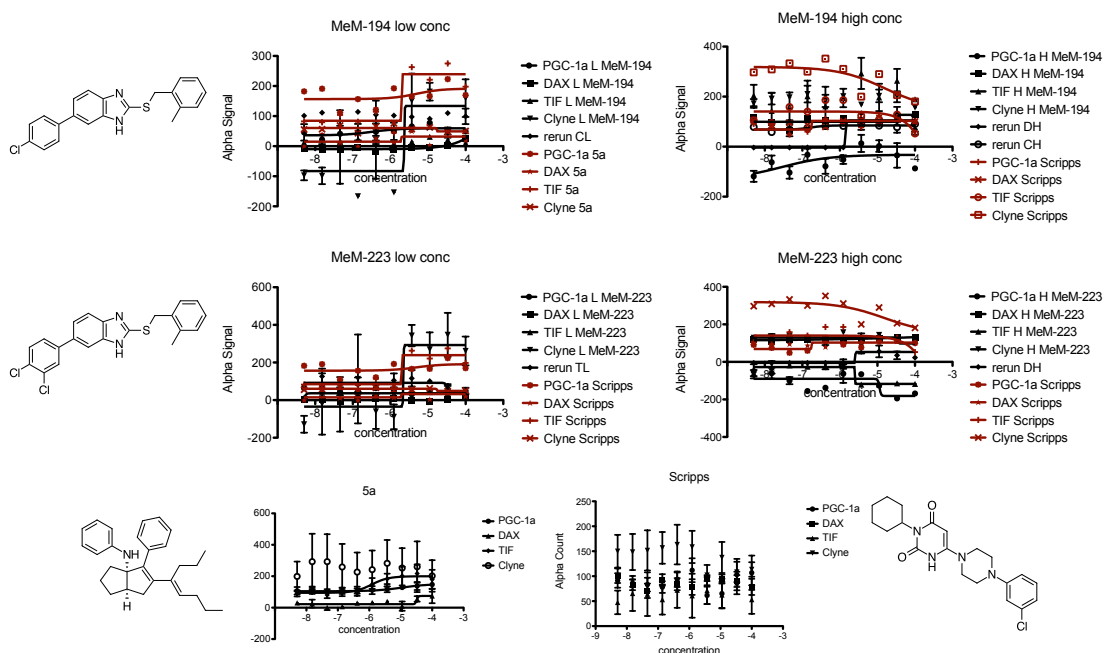 but appears consistent for the other peptides. On the other hand, the **Scripps** compound, which is a published LRH-1 antagonist [107] does not seem to have any effect on the binding of co-factor and protein. Ideally, compound **5a** and the **Scripps** compound would reproducibly show clear agonism and antagonism respectively. As this is not the case, it is difficult to evaluate the data and no other control molecules were available.

Interpreting the data here, it seems that the original lead compound (MeM-007) does indeed slightly increase the peptide binding for PGC-1α and TIF2, but has no effect on the Clyne peptide and DAX-1. Two close derivatives of the lead compound, MeM-028D and MeM-028B also show an increase in alpha signal for PGC-1α for the high concentration experiment. At the same time MeM-028B decreases the binding of TIF2 at low concentration and Clyne 4-16 at both concentrations. For compound MeM-013 the data appears contradictory: at low concentration the binding to DAX-1 increases, but it decreases for the high concentration. As the change in activity for both concentrations is very abrupt, it is more likely that this is due to an experimental error, rather than reflecting a true property of the compound. A steady

decline in activity can be found for MeM-026 at low concentrations for DAX-1. The compound MeM-174A causes a slight decrease in the binding of the Clyne peptide and an increase in the activity of DAX-1 at low concentration. At high concentration this compound greatly increases the binding of TIF2. Similar behaviour can be found for MeM-174B and MeM-185Bn although not as strongly. A steady increase in DAX-1 binding is also observed for MeM-174C and MeM-180C at low concentrations. Interestingly, MeM-185Cl seems to cause a slight increase in binding for all four tested peptides in the high concentration experiment.

Taking the results together, it appears that only a few of the compounds of the first series of analogues (different benzyl groups or commercial cores) have an effect on the binding of co-factors. The most significant effects in binding could be observed among the ether analogues but none affected the PGC-1α binding, which was affected by the thioether series. Among the aryl substituted compounds none of the compounds was able to cause a significant change in the binding between protein and peptide. Comparing the equivalent ether and thioether analogues, shows that the properties of these two sets are quite different. While the thioether series has a stronger effect on PGC-1a and DAX, the ether series did not affect PGC-1α, but did effect TIF2, DAX and Clyne peptide. Also, the ether series contained more compounds that showed any activity.

Due to the high levels of error and the fact that the controls did not perform consistently throughout the testing, any conclusions must be drawn with great care. The results of this testing could be used to select compounds for further testing, but the results need to be re-validated before any firm conclusions can be drawn.

Some of the compounds have negative values for their normalised data. It is unclear how to interpret these data. Negative values can occur when the background signal is higher than the compound or control signal, but this should not be the case at any time.

There can be many factors that contribute to the inconsistency of the data of this assay. The most obvious point of error or mistake is during the pipetting. Pipetting errors would only affect one small part of the plate *e.g.* one row and should not affect the whole plate. Other handling related errors could also be mistakes while preparing the protein/peptide dilutions or in the incubation times. A prolonged incubation leads to a decrease in signal. Another factor that changes the signal strength is the duration of light exposure: The beads are sensitive to light, in particular the donor beads. Therefore, the light exposure was kept as short as possible.

Other problems could arise from the configuration of the assay itself. The assay is designed to measure the fluorescence of the acceptor beads. It may be that be signal of a particular well is either contaminated with the bleeding through from adjacent wells or is not recorded properly by the plate reader. Other problems may arise from the fact that a fusion protein is

used for the testing. It is possible that the His-tag, used to attach the donor bead to the Ni-chelate bead, is too far away for the energy transfer to be efficient and consistent enough. This would cause a permanently reduced signal. Furthermore, the MBP could influence the binding of the compound into the LBD.

Some suggestions as to how to systematically address these questions are presented in the conclusions and future work sections of this thesis.

The remainder of this chapter describes a separate project that was carried out in parallel to the aforementioned work.

2.3 Towards the synthesis of α-Helix Mimetic as LRH-1 Co-Activator Binding Inhibitor

The ability to control protein-protein interactions (PPI) is of great importance in modern drug discovery. [108–110] Until recently, protein-protein interactions were considered "undruggable". [111] A potential way to target this type of interaction is with peptides. Unfortunately, there are many shortcomings associated to peptides as drugs, such as short duration of activity, lack of receptor subtype specificity and poor oral bioavailability. [112] Peptidomimetics are small protein-like compounds that mimic a natural peptide or protein and interact with the biological target. [113–115] They are designed to overcome the disadvantages of the peptide. Additionally, they can be designed to have improved potency or selectivity. Hamilton *et al.* [116] were the first to described completely non-peptidic synthetic molecules capable of mimicking the peptide's α-helical structure. They developed a terphenyl based system able to mimic the *i* *i*+3 and *i*+7 positions of an α-helix (**figure 2.28**).
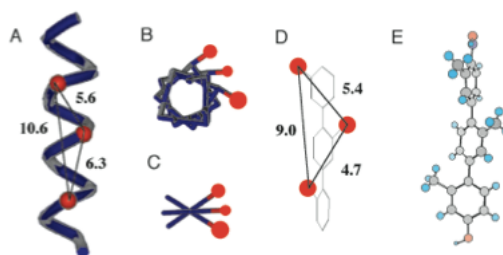

Figure 2.28: A: Schematic representation of an R-helical 12-mer peptide with *i*, *i* + 3, and *i* + 7 substituents, side view; **B:** top view; **C:** 3,2″,2″- trisubstituted terphenyl, top view; **D:** side view; **E:** X-ray crystal structure. [116]

Several other designs followed targeting different PPIs. One example is the work of Katzenellenbogen *et al.* [12] who established a system to prevent the co-activator binding onto the AF-2 site of the estrogen receptor. Taking this idea forward, Andrew Bayly (Spivey Group 2007-2011) [62] developed an α-helix mimetic designed to target the AF-2 site of LRH-1 and therefore prevent co-activator binding and transcriptional activity of the nuclear receptor. His α-helix mimetic is based on the atypical nuclear receptor small heterodimer partner (SHP), which is known to selectively repress LRH-1 activity (**table 2.15**). [23]

i-4	*i*-3	*i*-2	*i*-1	*i*+1	*i*+2	*i*+3	*i*+4	*i*+5	*i*+6	*i*+7	*i*+8	*i*+9	
R	P	A	I	L	Y	A	L	L	S	S	S	L	**SHP NR Box 1**
V	P	S	I	L	K	K	I	L	L	E	E	P	**SHP NR Box 2**

Table 2.15: Residues of the SHP NR Box with the LXXLL motif (red). [23]

The residues of importance of the SHP-1 box are the *i*-1, *i*+1, *i*+2, *i*+3, *i*+4 and *i*+5 residues, which include the LXXLL motif required for co-activator binding. After selection of the appropriate scaffold [62] the final α-helix mimetic had the following structure (**figure 2.29**):
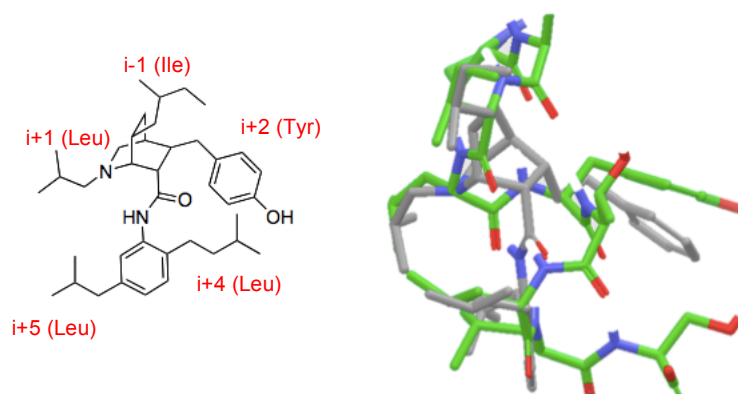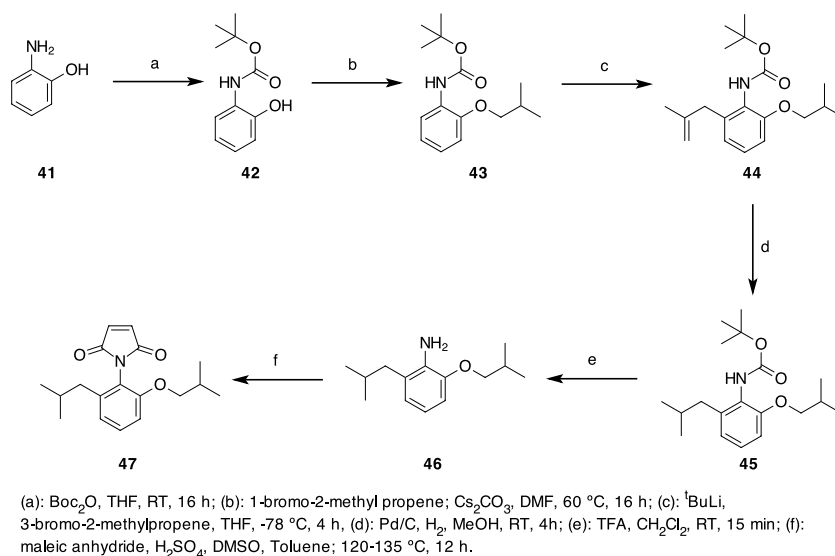

Figure 2.29: Left: Structure of Andrew Bayly's proposed helix mimetic; **Right:** the overlap of the mimetic (gray) with SHP-1 box (green). [62]

The displayed overlap with the SHP-1 box shows a good match in terms of 3-dimensional topology.
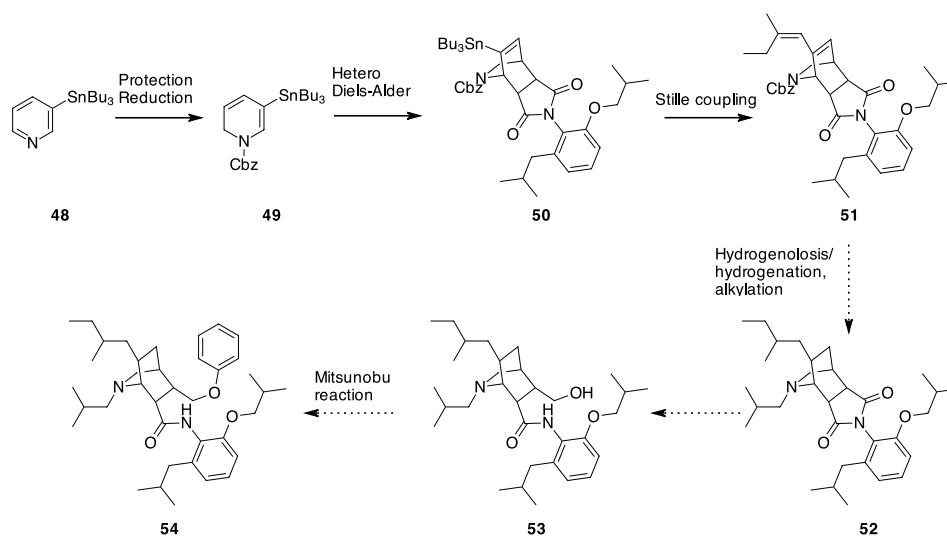
2.3.1 Synthesis of α-Helix Mimetic

The α-helix mimetic consists of an azabicyclo[2.2.2]octane scaffold, that can potentially be modified to have all required residues in place. The synthetic route Andrew Bayly developed commences with the synthesis of the dialkyl substituted maleimide which contains the *i*+4 and *i*+5 leucine residues (**scheme 2.33**).

(a): Boc$_2$O, THF, RT, 16 h; (b): 1-bromo-2-methyl propene; Cs$_2$CO$_3$, DMF, 60 °C, 16 h; (c): ^{t}BuLi, 3-bromo-2-methylpropene, THF, -78 °C, 4 h, (d): Pd/C, H$_2$, MeOH, RT, 4h; (e): TFA, CH$_2$Cl$_2$, RT, 15 min; (f): maleic anhydride, H$_2$SO$_4$, DMSO, Toluene; 120-135 °C, 12 h.

Scheme 2.33: Andrew Bayly's synthesis of *N*-phenyl maleimide **47**. [62]

The starting material is the 2-hydroxyaniline **41**, which in the first step was *N*-Boc-protected, before the hydroxy group was alkylated, putting the first leucine mimetic residue in place. Then, the aryl ring was alkylated *via ortho*-directed lithiation and quenching with the alkyl bromide. The C-C double bond was hydrogenated, using palladium on charcoal and gaseous hydrogen. After that, the *N*-Boc group was removed and the resulting aniline **46** was treated with maleic anhydride and a catalytic amount of sulfuric acid to give the final substituted *N*-phenyl maleimide **47**.

In the next part of the synthesis the other part of the α-helix mimetic, which will undergo a Diels-Alder reaction with the maleimide **47** was prepared. This heterodiene **49** is required to participate in a hetero-Diels-Alder reaction to establish the key core azabicyclooctane unit of the mimetic, which requires further modification to access the final α-helix mimetic (**scheme 2.34**).

Scheme 2.34: Proposed synthetic route of the final helix mimetic **54** incorporating early progress by Andrew Bayly. [62]

This part of the synthesis was also initiated by Andrew Bayly and involved the formation of the dihydropyridine **49**. The plan for my work was to combine this dihydropyridine with the previously synthesised substituted *N*-phenyl maleimide **47** *via* a hetero Diels-Alder reaction. The remaining steps are to install the *i*-1 moiety by Stille coupling. The *N*-Cbz group is then removed by hydrogenolysis and the free amine alkylated, constituting the *i*+1 residue mimetic. At the same time, the double bonds are hydrogenated. The maleimide **52** is then reductively opened and the phenyl group installed *via* Mitsunobu reaction to give the final α-helix mimetic **54**. Clearly, there are a number of regio- and stereochemical issues associated with these steps. It was planned to address them on a case-by-case basis as the synthetic studies progressed.

2.3.2 Current Work on the Synthesis of α-Helix Mimetics

2.3.2.1 Synthesis of *N*-Phenyl Maleimide

The first task towards developing this chemistry was the synthesis of a substantial amount of the substituted maleimide **47** following the synthetic route outlined above, established by Andrew Bayly (**scheme 2.32**). [62] The synthesis was started with the *N*-Boc protection, followed by alkylation of the hydroxy group (**scheme 2.35**).
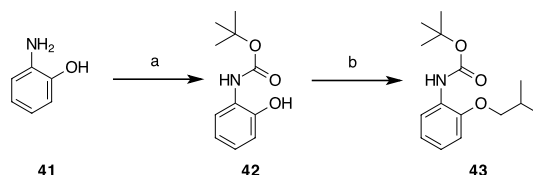
Scheme 2.35: *N*-Boc-protection and alkylation of 2-hydroxyaniline **41**.

The *N*-Boc protection and subsequent alkylation gave the product in good yields. The following step was the *ortho*-directed lithiation to introduce the second leucine mimetic group (**table 2.16**).
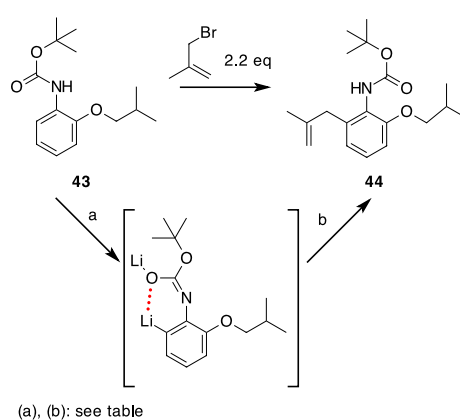

(a), (b): see table

Entry	^tBuLi	Time (a)	Temp (a)/(b)	Time (b)	Additive	Yield
1	2.4 eq.	20 min	-65 °C/-15 °C	2 h	-	45%
2	2.4 eq.	1 h	-65 °C/0 °C	1 h	-	10%
3	4.4 eq.	1 h	-65 °C/-10 °C	1.5 h	-	74%
4	2.4 eq.	1 h	-65 °C/-10 °C	1.5 h	TBAI	56%

Table 2.16: Optimisation of *ortho*-directed lithiation/alkylation of aniline **43** to give dialkylated aniline **44**.

The reaction was carried out as described by Andrew Bayly, but gave the product in just 45% yield (**table 2.16, entry 1**). Therefore, optimisation of the reaction conditions was undertaken. An increase in reaction temperature to 0 °C reduced the yield to 10% (**table 2.16, entry 2**). The addition of TBAI to enable an *in situ* Finkelstein reaction, only modestly increased the yield to 56% (**table 2.16, entry 4**). However, the use 4.4 equivalents of *tert*-BuLi resulted in a dramatic increase in yield to 74% (**table 2.16, entry 3**).

After the alkylation, the double bond was reduced using hydrogen gas over 10% (w/w) palladium on carbon with concomitant deprotection of the aniline *N*-Boc group (**scheme 2.36**).

(a): Pd/C (10% w/w), H$_2$, MeOH, RT, 4 h (99%); (b): TFA, CH$_2$Cl$_2$, RT, 15 min (52%).
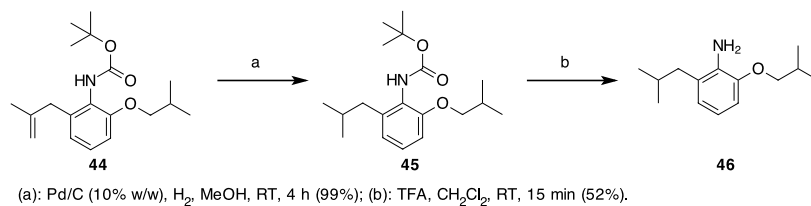
Scheme 2.36: Synthesis of dialkyl aniline **46**.

The hydrogenation as well as the deprotection were carried out as described by Andrew Bayly [62] and gave the product in quantitative and 52% yield respectively, without any purification required. In the final step the substituted *N*-phenyl maleimide **47** was formed by condensation of the di-*ortho* substituted aniline **46** with maleic anhydride (**scheme 2.37**).


(a): i:maleic anydride, neat, 120 °C, 1 h; ii: H$_2$SO$_4$, DMSO, toluene,135 °C, 18 h (88%).
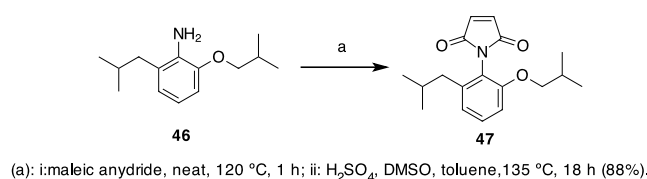
Scheme 2.37: Synthesis of alkylated *N*-phenyl maleimide **47**.

This reaction was carried out as a two-step process. First, the maleic anhydride and aniline **46** were heated neat to 120 °C for one hour to obtain a glassy compound. This was then dissolved in a toluene/DMSO solvent mixture with a catalytic amount of sulfuric acid and heated to 135 °C for 18 hours to give the desired substituted *N*-phenyl maleimide **47** in 88% isolated yield.

2.3.2.2 Synthesis of 1,6-Dihydropyridine

The next part of the synthesis towards the α-helix mimetic is the Diels-Alder reaction of the substituted maleimide **47** and 1,6-dihydropyridine **49**. The preparation of the heterodiene compound required 3-bromopyridine **55** to be converted to 3-tributylstannyl pyridine **48** (**scheme 2.38**).

(a): i: ^{n}BuLi, Et$_2$O, -78 °C, 1 h; ii: SnBu$_3$Cl, 0 °C, 1h (37%).
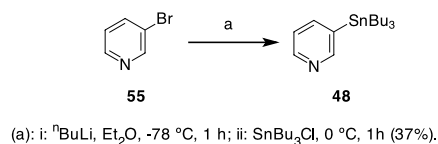
Scheme 2.38: Synthesis of 3-tributylstannyl pyridine **48**.

The reaction gave the desired product in 37% yield. Despite the poor yield it was decided not to further optimise the reaction conditions at this juncture.

The selective reduction of 3-tributyl stannly pyridine **48** was then attempted (**table 2.17**).

(a): See table
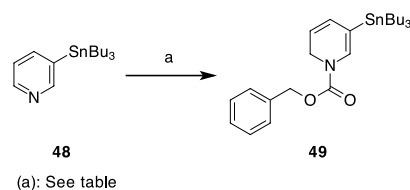
Entry	Reducing Agent	CbzCl	Warming up Time	Outcome
1	N-selectride (2.1 eq.)	1.2 eq.	-	No product
2	N-selectride (2.1 eq.)	1.2 eq.	-	No product
3	Li(^{t}OBu)$_3$AlH (2.1 eq.)	1.1 eq.	1 h	Product formed, NMR not clean
4	Li(^{t}OBu)$_3$AlH (2.1 eq.)	1.1 eq.	4 h	Product looks very unclean
5	Li(^{t}OBu)$_3$AlH (2.1 eq.)	1.1 eq.	6 h	No product

Table 2.17: Reduction conditions for the formation of 1,6-dihydropyridine **49**.

The first attempt of the reduction of the stannylated pyridine **48** was by using N-selectride. The CbzCl was added at -78 °C and the reaction mixture stirred at that temperature for one hour. Then, N-selectride was added and the reaction mixture stirred for another 3 hours at -78 °C, before stirring it at room temperature for another 30 min. Quenching the reaction involved the addition of a basic solution of hydrogen peroxide. The quenched reaction mixture was stirred overnight. A ^{1}H-NMR spectrum of the crude reaction mixture did not indicate the presence of product (**table 2.17, entry 1**). The reaction was therefore repeated using the same procedure but again, no product was obtained (**table 2.17, entry 2**). The reason for the failure of this procedure appeared to be that hydrogen peroxide caused destannylation of the formed dihydropyridine **49**. Therefore, another reducing agent was evaluated.

Sundberg *et al*. [117] reported the selective reduction of substituted pyridines to the corresponding 1,6-dihydropyridines by using Li(^{t}BuO)$_3$AlH. This method was applied to the 3-stannyl pyridine **48** (**table 2.17, entries 3-5**). The reaction mixture was cooled to -78 °C, before CbzCl and Li(^{t}BuO)$_3$AlH were slowly added. Then, the reaction mixture was warmed to 0 °C and stirred for another hour (**table 2.17, entry 3**). The reaction gave the product as a mixture of the 1,2- and 1,6-dihydropyridine and the ^{1}H-NMR spectrum of the crude product mixture revealed many additional side products. To increase the amount of the 1,6-dihydropyridine **49** the warming up time was prolonged to 4 hours (**table 2.17, entry 4**). The ^{1}H-NMR spectrum of the crude reaction mixture still showed a mixture of the two possible products and many impurities. After extending the time to warm up the reaction mixture and stirring overnight at room temperature the product could not be detected possibly due to decomposition *in situ* (**table 2.17, entry 5**).

Attempted purification of the product by column chromatography led to destannylation of the product. Treating the silica gel with triethylamine prior to the column chromatography, unfortunately, did not change the outcome.

As the stannylated dihydropyridine **49** is very unstable and was proving impossible to purify, another method for the synthesis of the 1,6-dihydropyridine was sought.

Suginome *et al*. [118] have reported on a Rh-catalysed hydroboration for the synthesis of 1,2-dihydropyridines with pinacolborane (Bpin). This reaction was tried on 3-picoline **56** as a model system (**table 2.18**).


(a): Toluene, further conditions, see table.
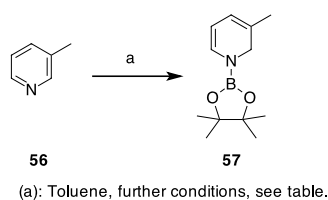
Entry	Solvent	Bpin	[RhCl(cod)]₂	PCy₃	Outcome
1	Toluene	0.5 eq.	1 mol%	4 mol%	No product
2	Toluene	1.0 eq.	1 mol%	4 mol%	No product
3	Toluene	2.0 eq.	1 mol%	4 mol%	Decomposition
4	Toluene	1.5 eq.	5 mol%	20 mol%	No product
5	Toluene	1.5 eq.	10 mol%	40 mol%	No product

Table 2.18: Attempted hydroboration of 3-picoline **56** according to the method of Suginome. [118]

In the first attempt, the reaction conditions employed were exactly as described by Suginome *et al*. [118] As it appeared that the amount of Bpin is very low, the reaction was also set up with greater amounts of Bpin. Interestingly, in the reaction with 2 equivalents of Bpin the decomposition of the starting material could be seen immediately after the addition of the Bpin (**table 2.18, entry 3**). As the catalyst load in the original procedure is also very low, two experiments were started using 5 and 10 mol% of the catalyst respectively. As before, no product was formed (**table 2.18, entries 4 and 5**).

A way to circumvent the problems arising form the use of the tributylstannyl pyridine **48** is to use the already alkylated pyridine. In her Masters thesis, Fiona Lee (Spivey Group 2010-2011) [119] synthesised the required pyridine derivative by lateral deprotonation of 3-picoline **56** with LDA followed by alkylation (**scheme 2.39**). [119]
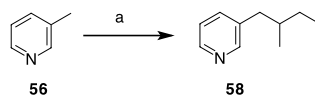
(a): i: LDA, -78 C; ii: 2-bromo butane, RT, 2 h.

Scheme 2.39: Synthesis of 3-(2-methyl butyl) pyridine **58**. [119]

She found that the only hydride source capable of reducing this alkylated pyridine **58** was sodium borohydride, which gave a mixture of the 1,2-, 1,4- and 1,6-dihydropyridines; the sterically more demanding N-selectride and Li(^{t}BuO)$_3$AlH, did not yield any product (**scheme 2.40**). [119]

Ratio of products: 75   :   5   :   20

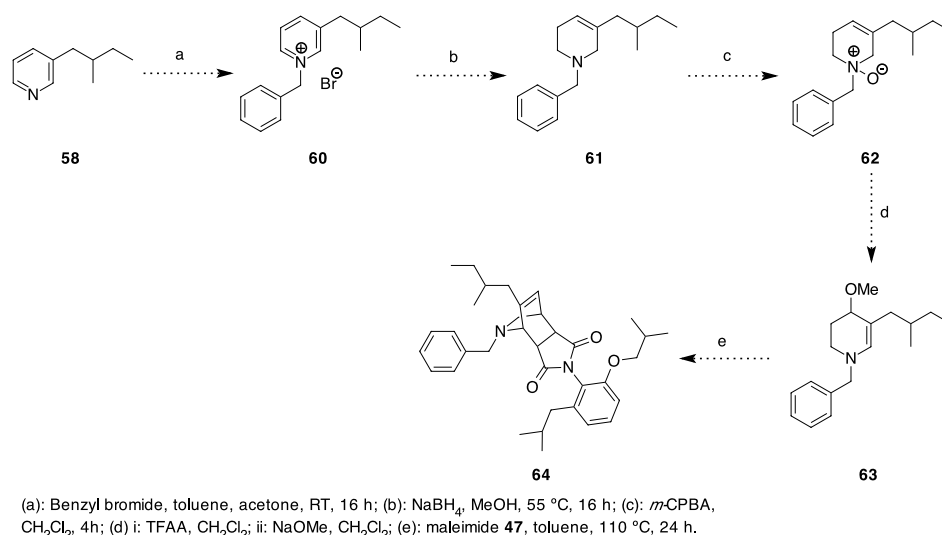(a): CbzCl, NaBH$_4$, MeOH, -78 °C, 2h.
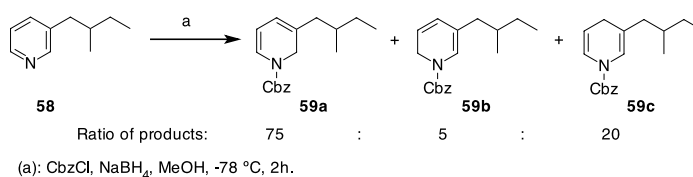
Scheme 2.40: Fiona Lee's best conditions for the formation of 1,6-dihydropyridine **59**. [119]

Clearly, a new method had to be found for the synthesis of the desired alkylated 1,6-dihydropyridine **59**.

## 2.3.3 Alternative Pathway for the Synthesis of Alkylated 1,6-Dihydropyridine

Maranzano *et al*. [120] have reported on a facile synthesis of 1,6-dihydropyridines, which were then trapped *in situ* with a dienophile present in the reaction mixture. This method, in the context of how it could be applied to access our target 1,6-dihydropyridine, is shown below (**scheme 2.41**).

(a): Benzyl bromide, toluene, acetone, RT, 16 h; (b): NaBH$_4$, MeOH, 55 °C, 16 h; (c): m-CPBA, CH$_2$Cl$_2$, 4h; (d) i: TFAA, CH$_2$Cl$_2$; ii: NaOMe, CH$_2$Cl$_2$; (e): maleimide **47**, toluene, 110 °C, 24 h.

Scheme 2.41: Outline of proposed new pathway for the synthesis of α-helix mimetic scaffold **64**. [120]

The sequence starts with the formation of the benzyl pyridinium salt **60**, which would then be reduced to the tetrahydropyridine **61** using sodium borohydride. This compound would then be treated with m-CPBA to give the N-oxide **62**. Treatment with trifluoroacetic anhydride followed by sodium methoxide would then hopefully give p-methoxy tetrahydropyridine **63** as a precursor to the 1,6-dihydropyridine, which we would plan to directly trap via a hetero Diels-Alder reaction to give the azabicyclooctane scaffold of the α-helix mimetic **64**. Although this sequence is longer than the direct reduction of the pyridine and subsequent Diels-Alder reaction, each step here appears simple and was hoped to give the product in acceptable yield with complete selectively for the desired 1,6-dihydropyridine.

The exploration of this sequence started with the benzylation of 3-(3-methylbutyl)pyridine **58** (**scheme 2.42**).

(a): Benzyl bromide, toluene, acetone, RT, 48 h (81%); (b): NaBH$_4$, MeOH, 60 °C, 10 h (53%).
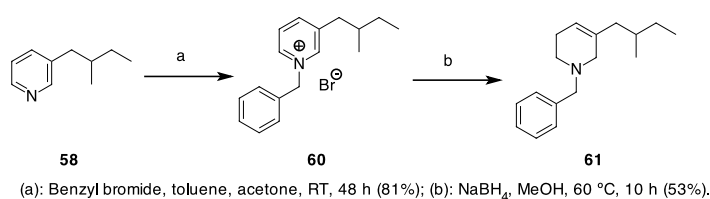
Scheme 2.42: Synthesis of the N-benzyl tetraydropyridine **61**.

The benzylation reaction was carried out using benzyl bromide in toluene and gave the product in 81% yield. This salt was directly subjected to the reduction reaction with sodium borohydride as the reducing agent. After purification the product could be obtained in 53% yield.

The next step in the sequence is the formation of the N-oxide (**scheme 2.43**).

(a): *m*-CPBA, CH₂Cl₂, RT, 16 h (42%).
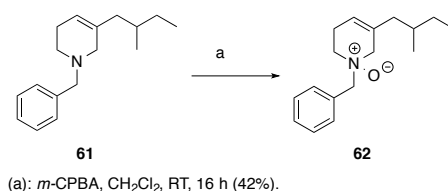
Scheme 2.43: Formation of the 3-alkylated *N*-benzyl *N*-oxide **62**.

The reaction was carried out by modification of the method published by Gil *et al.* [121] Due to the high polarity of the *N*-oxide product **62**, the purification consisted of a short column chromatography with basic alumina, that quenches any remaining *m*-CPBA. The solvent system was chosen as a gradient of methanol in dichloromethane. Using this method, all impurities were removed before the product was eluted off the alumina giving the product in 42% yield. During the reaction, a considerable amount of a single byproduct was formed, which could not be identified.

With the *N*-oxide **62** in hand, the next reaction was carried out which involved treatment with trifluoroacetic anhydride followed by sodium methoxide (**scheme 2.44**).

(a): TFAA, CH₂Cl₂, 0 ºC, 1 h; (b): MaOMe, CH₂Cl₂/MeOH, RT, 1.5 h (14%).
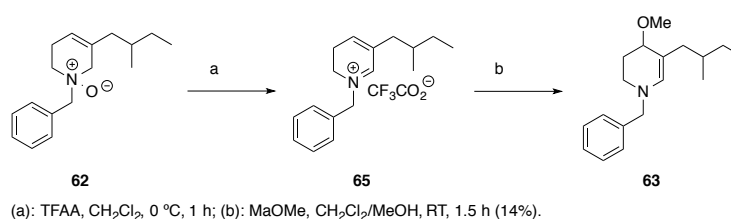
Scheme 2.44: Formation of *p*-methoxy tetrahydropyridine **63**.

After the formation of the TFA salt **65** all residues of trifluoroacetic anhydride or TFA were removed under reduced pressure and by co-evaporation with toluene. Next, the TFA salt was treated with sodium methoxide to give the *p*-methoxy tetrahydropyridine **63**. Due to the high instability of the product, it was used crude in the following Diels-Alder reaction (**scheme 2.45**).

(a): Substituted maleimide **47**, toluene, 120 °C, 24 h (5%).
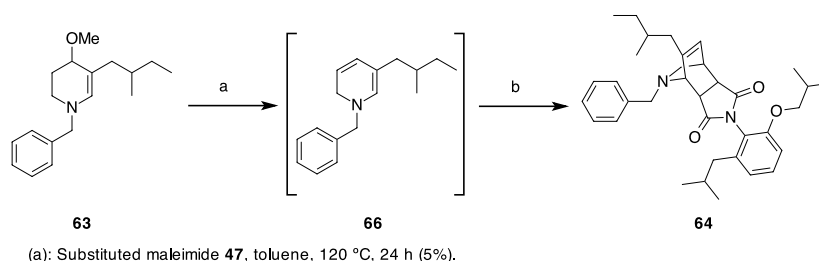
Scheme 2.45: Diels-Alder reaction towards the α-helix mimetic scaffold precoursor **64**.

By heating the *p*-methoxy tetrahydropyridine **63** to reflux, it should be converted to the 1,6-dihydropyridine **66** as the only product, which should immediately react further with the

substituted *N*-phenyl maleimide **47** to give the desired Diels-Alder adduct. The selectivity for the 1,6-dihydropyridine **66** and the corresponding Diels-Alder adduct can be explained by the proposed mechanism of this transformation (**scheme 2.46**).
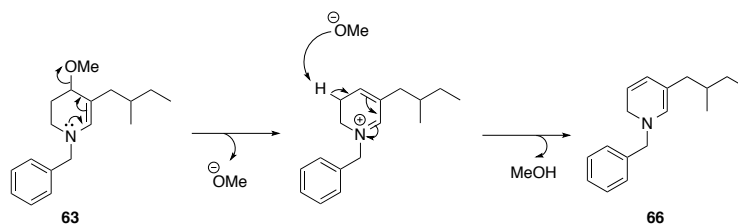

Scheme 2.46: Proposed mechanism of 1,6-dihydropyridine **66** formation. [120]

The nitrogen lone pair donates its electrons towards the methoxy group, which departs and acts as a base to effect the elimination reaction that gives the 1,6-dihydropyridine **66**.

Maranzano *et al.* [120] claim that any subsequent Diels-Alder reaction is completely *endo* selective. Unfortunately, the amount of the Diels-Alder product obtained was not sufficient to verify that this was also the case for our reaction.

From this point onwards the route outlined by Andrew Bayly towards the final α-helix would comprise three further steps (**scheme 2.47**).
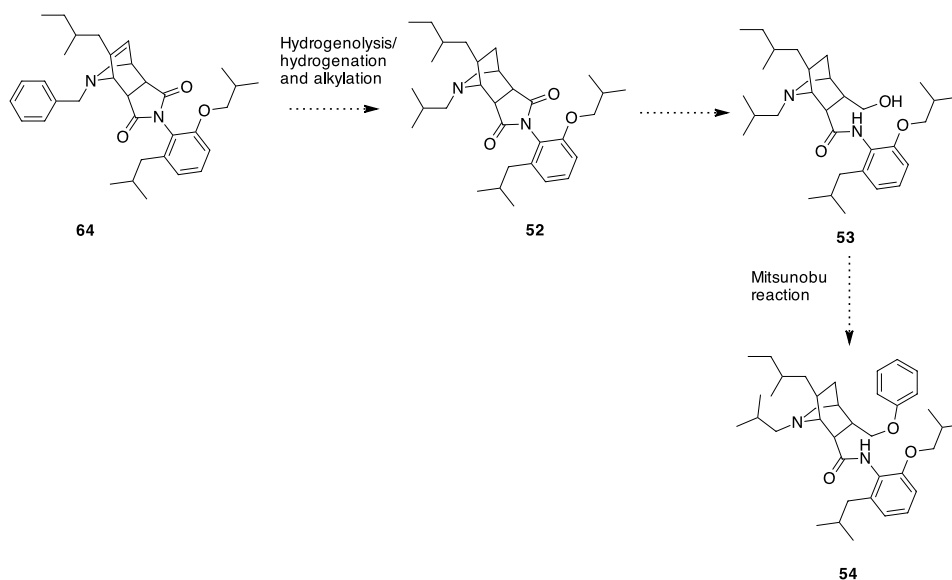
Scheme 2.47: Proposed remaining steps towards the synthesis of the α-helix mimetic **54**. [62]

Unfortunately, time constraints prevented exploration of these steps, but the next step would be the hydrogenolysis/hydrogenation to remove the *N*-benzyl group and reduce the double bond followed by *N*-alkylation. Then, reductive opening of the maleimide ring and subsequent Mitsunobu reaction should give the final α-helix mimetic **54**. The prospects for achieving this

hopefully in the near future are evaluated in the conclusions and future work sections of this thesis.

3. Conclusions

3.1 Synthesis and Testing of Potential Benzimidazole-based LRH-1 Antagonists

The first aim of this project was to find a new antagonist or inverse agonist of LRH-1 as a lead towards a potential breast cancer treatment. Starting from a lead found by Andrew Bayly, [62] three series of analogues have been synthesised and tested for their binding to the LRH-1 LBD. The first series comprised benzimidazole thioether analogues with different benzyl substitution patters. The synthesis work went smoothly and the products could be obtained in acceptable yields.

For the second series, the substitution pattern was kept the same, but the sulfur atom was exchanged for an oxygen atom. The synthesis proved difficult and a novel route for the synthesis of this series had to be found, which finally led to the synthesis of the desired benzimidazole ether analogues.

In the third series a substituted aryl group was introduced into the benzimidazole structure. By developing a new route towards these analogues the synthesis of this series could be successfully accomplished.

After the completion of the synthesis the prepared analogues were tested for their binding properties to the LRH-1 LBD. The assay used was an AlphaScreen® proximity assay. To address the testing for both agonists and antagonists the assay was run at two different concentrations. The testing results show a significant variance in the readout which makes it impossible do draw firm conclusions. Nevertheless, a few compounds could be identified which appeared to display weak agonistic properties. These compounds need to be submitted for further evaluation to confirm their status as interesting new leads.

3.2 Synthesis of a α-Helix Mimetic as Potential Co-Activator Binding Inhibitor

The second aim of the research presented in this thesis was the synthesis of an α-helix mimetic as a potential co-activator binding inhibitor for LRH-1.

Andrew Bayly (Spivey group 2007-2011) had already outlined a route for a synthesis of the α-helix mimetic. [62]

The first task of this project was therefore to synthesise a large quantity of the substituted *N*-phenyl maleimide **47** following the route established by Andrew Bayly. [62] The synthesis went smoothly and the maleimide **47** could be obtained in good yield.

The second task was the synthesis of a 3-stannylated 1,6-dihydropyridine **49**, which was then to be combined with the substituted *N*-phenyl maleimide **47**, to give the scaffold of the α-helix mimetic. This synthesis proved difficult and a new route for the preparation of the desired 1,6-dihydropyridine based on the synthesis of a 1,6-dihydropyridine by Maranzano *et al*. [120] was established. Although this route does not provide access to the target α-helix mimetic, it gives a firm foundation for future work to hopefully achieve this synthetic goal in the near future (**scheme 3.1**).
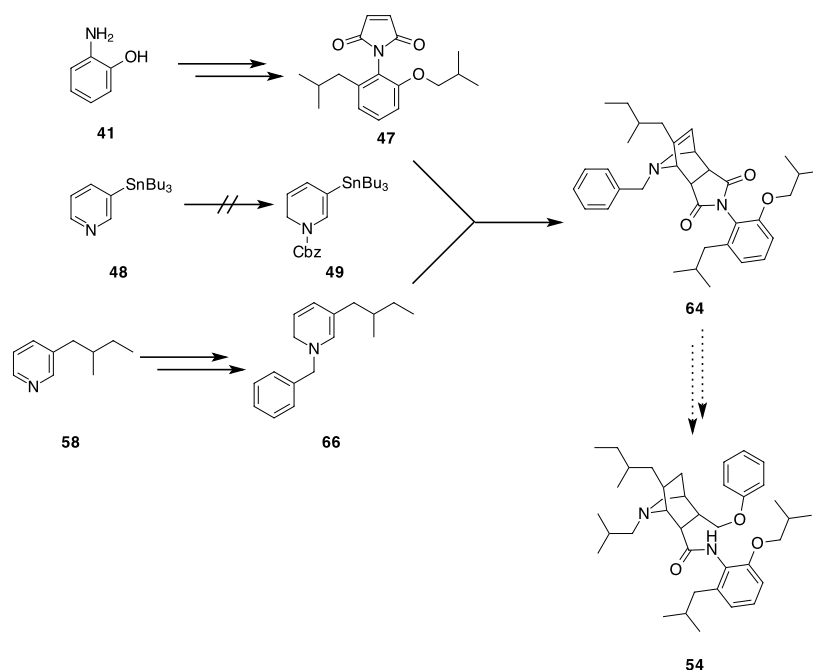
Scheme 3.1: Summary of progress so far towards the synthesis of α-helix mimetic **54**.

In conclusion, during this work two different approaches towards modulating the activity of LRH-1 have been targeted. In the first approach, the synthesis of a conventional antagonist, which was designed to bind to the ligand binding pocket was attempted and some promising compounds were identified. In the second approach, an α-helix mimetic designed to bind to the AF-2 binding site and prevent co-activator binding was investigated. Although the synthetic route was not completed, progress was made towards that end.

4. Future Work

4.1 Further Development of Benzimidazole-based LRH-1 Modulators

After the completion of the synthesis of the series of benzimidazole analogues and their evaluation as potential agonists or antagonists, it appears that compounds MeM-028B, MeM-028D and MeM-185Cl increase the binding of co-activator PGC-1α to LRH-1. These compounds should therefore be subjected to further testing to confirm their binding activity to LRH-1. As the results from the testing are inconclusive, it is necessary to further improve the assay conditions to obtain reproducible and reliable data. The controls used for the testing seem unsuitable, as the results for these compounds could not be reproduced consistently throughout the experiments. Whitby's compound **5a** is a LRH-1 agonist [54] and was used as a control during the testing. The assay results obtained for compound **5a** do not reflect this ability. Similarly, the **Scripps** compound, [107] a known LRH-1 antagonist, appears to have no effect on the binding of LRH-1 to the co-factor peptides used in our assay. Therefore, part of the ongoing assay optimisation has to be to find more suitable controls. With the optimised conditions in place, the mentioned compounds MeM-028B, MeM-028D and MeM-185Cl can be tested again to verify the data. Additionally, a complimentary assay based on activity rather than binding should be established to exclude false hits.

To find a compound with antagonistic rather than agonistic properties another series could be synthesised with substituents protruding towards the helix 12 (purple) of the LRH-1 LBD (**figure 4.1**).
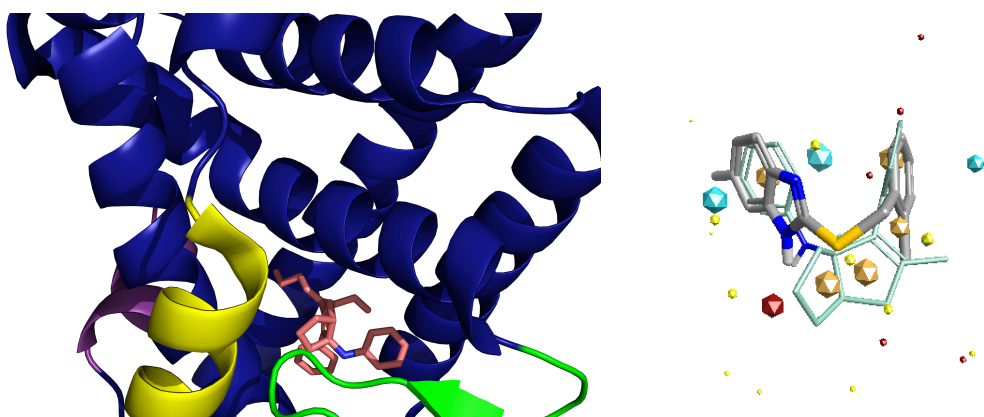

Figure 4.1: Left: image of the crystal structure of Whitbys compound **5a** bound into the entrance of the ligand binding pocket of the LBD of LRH-1 (PDB: 3PLZ). **Right:** overlay of the structures of Whitby's compound **5l** and **AB_WC057**. [54,55,62]

Assuming that compound AB_WC057 binds in an analogus fashion to that revealed in the crystal structure of Whitby's compound **5a** bound to the LBD of LRH-1, in order for a substituent to point towards helix 12 (purple), it will need to be situated at the benzyl ring of the benzyl thioether. To test this possibility several alkyl substituted benzyl thioethers with different chain topologies will need to be prepared (**scheme 4.1**).

R= ethyl, 'propyl, propyl, ''butyl, 'butyl, 'butyl, hexyl
(a): alkylated benzyl bromides, NaOMe, DMF.
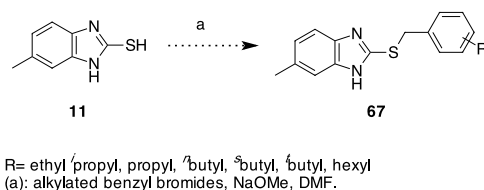
Scheme 4.1: Proposed synthesis of alkyl-substituted benzimidazole thioethers **67**.

Additionally, it would be interesting to evaluate a naphthyl group and other fused aromatic ring systems in place of the benzyl ring (**scheme 4.2**).

(a): 2-(Bromomethyl)naphthalene, NaOMe, DMF.
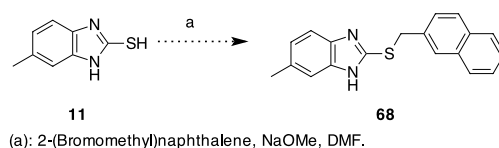
Scheme 4.2: Proposed synthesis of naphthyl benzimidazole **68**.

These syntheses could be carried out as described previously: it should be possible to alkylate the 2-mercapto function of benzimidazole **11** under basic conditions using substituted benzyl halides for example 2-(bromomethyl)naphthalene in combination with sodium methoxide in DMF. These lipophilic and bulky groups would be anticipated to point towards helix 12, once bound to LRH-1 and could displace it, resulting in an inability to allow co-activator binding.

As the ether series generally appeared to perform better in the binding assay than the thioether series, it will be interesting to change the ether linkage to an amine linkage. Synthetically, the same route as for the ether analogues could probably be employed (**scheme 4.3**).

(a): Substituted benzyl amine, NaH, DMF; (b): TBAF, THF.
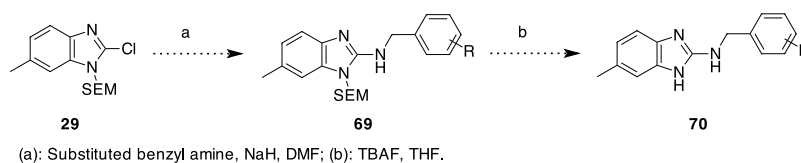
**Scheme 4.3:** Proposed synthesis of amino benzimidazoles **70**.

Starting from the SEM-protected 2-chlorobenzimidazole **29**, the secondary amine could probably be formed using benzyl amine. The resulting benzimidazole benzyl amine **69** should be deprotected with TBAF in THF.

These proposed compounds should then be tested for their binding using the AlphaScreen®, to obtain an indication of their binding to the LRH-1 LBD and the most promising derivatives also be tested in an activity assay. Clearly however, the aforementioned optimisation of the AlphaScreen® assay needs to be completed before this can be accomplished.

4.2 Synthesis of the α-Helix Mimetic

Notwithstanding the results obtained in the abovementioned work towards benzimidazole based LRH-1 antagonists, a potentially complimentary approach to prevent the transcriptional activity of LRH-1 is by targeting the AF-2 site. This was addressed by the synthesis work carried out towards the α-helix mimetic **54**.

However, further optimisation of the key Diels-Alder reaction is required. Prior to this, it will be necessary to optimise the reaction conditions for the preparation of the 1,6-dihydropyridine **66** and in particular the formation of the *p*-methoxy tetrahydropyridine **63**, which currently gives the product in poor yield (**scheme 4.4**).
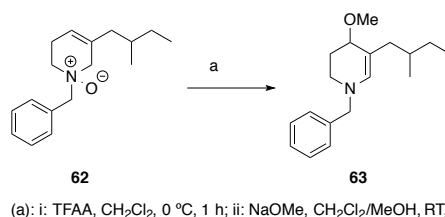
(a): i: TFAA, CH$_2$Cl$_2$, 0 ºC, 1 h; ii: NaOMe, CH$_2$Cl$_2$/MeOH, RT, 1.5 h (14%).

Scheme 4.4: Formation of *p*-methoxy tetrahydropyridine **63**.

After the optimisation of the Diels-Alder reaction, the next step will be the deprotection of the *N*-benzyl group and hydrogenation of the double bond. These two transformations will hopefully be carried out in one step using standard hydrogenolysis conditions (**scheme 4.5**).
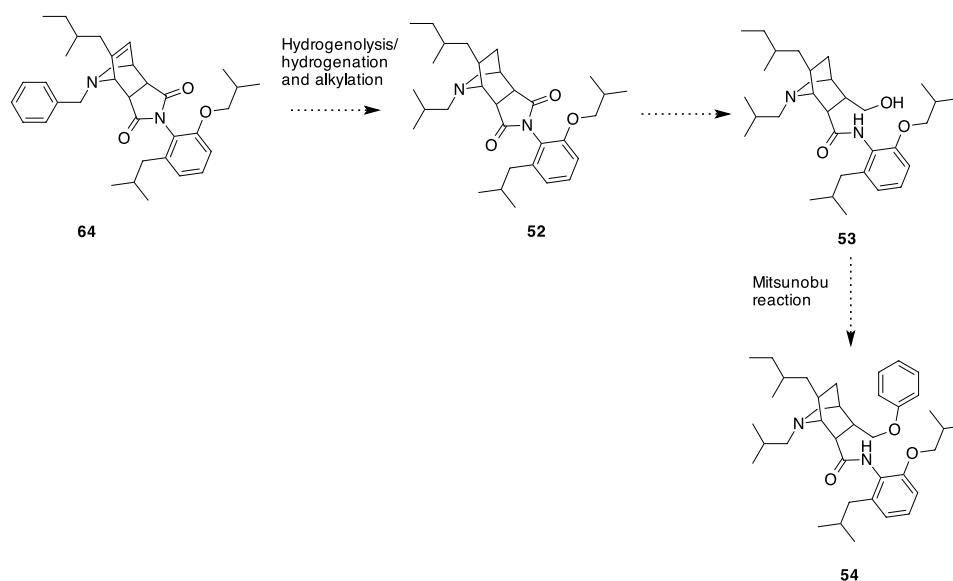
Scheme 4.5: Proposed synthesis of the final α-helix mimetic **54**.

These reactions are followed by the alkylation of the just deprotected nitrogen, which can be anticipated to successfully be carried out with 1-bromo-3-methyl propane. After the alkylation, the former maleimide ring is to be subjected to a reductive ring opening using sodium borohydride at elevated temperature. The resulting primary alcohol needs to be converted to the aryl ether, which mimics the *i*+2 tyrosine residue (**figure 2.26**). There are several possibilities to carry out this reaction. The most straight-forward method will involve a Mitsunobu reaction with a phenol. A fallback route will be to convert the hydroxy group to a better leaving group such as tosylate or mesylate and carry out a nucleophilic substitution reaction.

Once the synthetic route for the α-helix mimetic has been established, a series of analogues with varying substituents will be prepared and tested for their efficacy to prevent co-activator binding.

It is envisioned that this testing should be possible using the same AlphaScreen® method as used for the benzimidazole derivatives mentioned above, once optimised. Development beyond this will strongly depend on the results of these studies, but will undoubtedly reflect the fact that α-helix mimetics hold the prospect of being deployed for the disruption of numerous protein-protein interactions of crucial importance in a plethora of therapeutically important signal transduction cascades. In this context it is important to note that the majority of protein-protein interactions are mediated by α-helices. [122]

# 5. Experimental

General Directions

All reactions were performed under anhydrous conditions, in oven-dried or flame-dried glassware and under a nitrogen atmosphere. **Anhydrous Solvents:** MeCN, toluene, Et_2O, CH_2Cl_2 and THF were used directly after passage through Al_2O_3 columns in a Grubb dry-solvent system (Innovative Technology Inc.). Solvents were degassed using a freeze-pump-thaw cycle. **Reagents:** were purchased from commercial suppliers and handled according to COSHH regulations. **Chromatography**: column chromatography was performed on silica gel (Merck Kieselgel 60 F_{254} 230-400 mesh) or basic alumina following the method of W. C. Still. [123] Thin Layer Chromatography (TLC) was carried out on Merck aluminium-backed plates pre- coated with silica (0.2 mm, 60 F_{254}). The plates were visualised either by quenching of ultraviolet fluorescence ($λ_{max}$ = 254 nm) or by charring with $KMnO_4$, phosphomolybdic acid, vanillin or ninhydrin TLC dip. **Melting points:** were determined on a Reichardt hot stage apparatus. **Infra red spectra:** were recorded neat on Perkin-Elmer Paragon 1000 Fourier transform spectrometer. Only selected absorbances (v_{max}) are reported. **^{1}H-NMR spectra:** were recorded at 400 MHz on a Bruker AV 400 spectrometer. Chemical shifts ($δ_H$) are given in parts per million (ppm) and are referenced to the residual solvent peak of $CDCl_3$, DMSO-d_6 or MeOD-d_4. Coupling constants (J) are reported in Hz and to the nearest 2 significant figures. **^{13}C-NMR spectra:** were recorded at 100 MHz on a Bruker 400 AV spectrometer. Chemical shifts ($δ_C$) are given in ppm and referenced to the residual solvent peaks of $CDCl_3$, DMSO-d_6 or MeOD-d_4. **Mass spectra:** low resolution mass spectra (m/z) and high resolution mass spectra were recorded on either a VG platform II or VG AutoSpec spectrometers, using electron ionization (EI) or chemical ionization (CI). High Resolution Mass Spectrometry measurements are valid to ± 5ppm.

Note on Regional Assignments

Throughout this thesis benzimidazoles having a substituent in the "benzo" ring are designated as being 6-substituted, when in fact they are a ~1:1 mixture of 5-and 6-substituted isomers (for the *N*-substituted case) or a single undetermined isomer (for the *N*-H case)

General Procedure A [84]

The diamine was dissolved in a 10:1 mixture of EtOH and H_2O. NaOH was added and the reaction stirred for 5 min. CS_2 was added and the reaction heated to 70 °C for 3.5 h. After that time activated charcoal was added and the reaction mixture heated to reflux for another 15 min. The reaction mixture was cooled to RT and filtered. The filtrate was acidified with acetic acid (50%) and the precipitate was filtered and washed with H_2O to give the pure product.

2-Mercapto-6-methylbenzimidazole 11 [84]
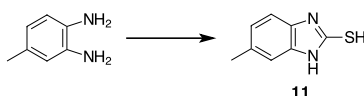
The reaction was carried out as described in the general procedure A, with 3,4-diaminotoluene (0.51 g, 4.15 mmol, 1.0 eq.), CS_2 (0.25 mL, 4.09 mmol, 1.0 eq.), and NaOH (0.18 g, 4.37 mmol, 1.0 eq.) in H_2O (3 mL) and EtOH (30 mL) to give the 2-mercaptobenzimidazole **11** as a gray powder (389 mg, 58%). R_f:0.1 (1% MeOH/CH_2Cl_2); mp: 193-200 °C; v/cm^{-1} (neat) 3122, 2580, 1574, 1495, 1329, 798, 718, 665; δ_H (DMSO-d_6, 400 MHz) 2.32 (3H, s, CH_3), 6.83-6.98 (2H, m, H-5 and H-7), 7.01 (1H, dd, J 7.9 and 3.3 Hz, H-4), 12.45 (2H, br s, SH and NH); δ_C (DMSO-d_6, 100 MHz) 20.9, 109.4, 110.1, 123.2, 130.3, 131.6, 132.5, 167.8; MS (ES$^+$) m/z 165 (M+H$^+$, 34%), M+CH_3COOH^+, 27%); HRMS (ES$^+$) 165.0486 calculated for $C_8H_9N_2S^+$ (M+H$^+$) found 165.0476, Δ= -6.1 ppm.

2-Mercaptobenzimidazole 4 [84]
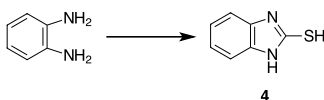
The synthesis was carried out using the general procedure A, with phenylenediamine (2.00 g, 18.49 mmol, 1.0 eq.), CS_2 (1.10 mL 18.49 mmol, 1.0 eq.) NaOH (0.78 g, 19.50 mmol, 1.05 eq.) in H_2O (3 mL) and EtOH (30 mL) to give the 2-mercaptobenzimidazole **4** as a light brown powder (1.42 g, 9.45 mmol, 51%). R_f: 0.1 (1% MeOH/CH_2Cl_2); mp: 200-205 °C; v/cm^{-1} (neat) 3110, 2572, 1667, 1510, 1464, 1356, 1177, 740, 702, 658; δ_H (DMSO-d_6, 400 MHz) 7.17-7.07 (4H, m, Ar-H), 12.53 (2H, s, NH, SH); δ_C (DMSO-d_6, 100 MHz) 109.5, 122.3, 132.2, 168.1; MS (ES$^+$) m/z 151 (M+H$^+$, 35%), 300 (M+M$^+$, 14%); HRMS (ES$^+$) 151.0330 calculated for $C_7H_7N_2S^+$ (M+H$^+$) found 151.0341, Δ= +7.3 ppm.

6-*tert*-Butyl-2-mercaptobenzimidazole 9a
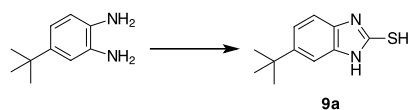
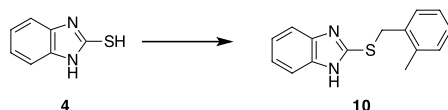The synthesis was carried out as described in the general procedure A using 4-(*tert*-butyl)-1,2-diaminobenzene (1.00 g, 6.09 mmol, 1.0 eq.), CS_2 (1.00 ml, 16.92 mmol, 2.8 eq.) and NaOH (0.25 g, 6.25 mmol, 1.0 eq.) in H_2O (1.5 mL) and EtOH (15 mL) to give the substituted 2-mercaptobenzimidazole **9a** as a light brown powder (1.13 g, 5.48 mmol, 89%). R_f: 0.2 (1% MeOH/CH_2Cl_2); mp: 216-219 °C; v/cm^{-1} (neat) 3076, 2958, 1488, 1324, 1243, 1191, 856, 808, 753, 710; δ_H (DMSO-d_6, 400 MHz) 1.27 (9H, s, C(CH_3)$_3$), 7.10-7.03 (2H, m, H-5 and H-7), 7.18 (1H, dd, J 8.4, 1.7 Hz, H-4), 12.42 (2H, br s, SH and NH); δ_C (DMSO-d_6, 100 MHz) 31.5, 34.5, 105.9, 109.0, 119.8, 130.1, 132.3, 145.3, 167.9; MS (ES$^+$) m/z 207(M+H$^+$, 100%); HRMS (ES$^+$) 207.0956 calculated for $C_{11}H_{15}N_2S^+$ (M+H$^+$) found 207.0957, Δ= +0.5 ppm.
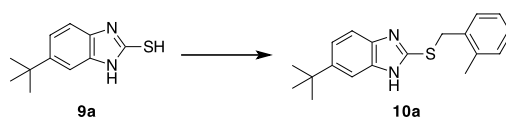
6-Bromo-2-mercaptobenzimidazole 9b
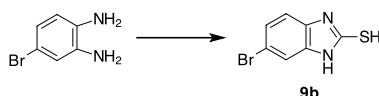
The synthesis was carried out as described in the general procedure A using 4-bromo-1,2-benzenediamine (2.00 g, 10.7 mmol, 1.0 eq.) CS_2 (0.64 mL, 10.7 mmol, 1.0 eq.) and NaOH (0.50 g, 12.5 mmol, 1.1 eq.) in H_2O (3 mL) and EtOH (30 mL) to give the 6-bromo-2mercaptobenzimidazole **9b** as a brown powder (1.05 g, 4.58 mmol, 43%). R_f: 0.2 (1% MeOH/CH_2Cl_2); mp: 205-210 ºC; v/cm^{-1} (neat) 3109, 1577, 1521, 1477, 1373, 1055, 912, 845, 796; δ_H (DMSO-d_6, 400 MHz) 7.08 (1H, d, J 8.9 Hz, H-5), 7.32-7.22 (2H, m, H-4, H-7); δ_C (DMSO-d_6, 100 MHz) 111.0, 111.9, 114.3, 124.9, 131.7, 133.8, 169.1; MS (ES$^+$) m/z 228/230 (M+H$^+$, 100%), 246 (M+NH$_4^+$, 50%); HRMS (ES$^+$) 228.9435 calculated for $C_7H_6N_2S^{79}Br^+$ (M+H$^+$) found 228.9437, Δ= +0.9 ppm
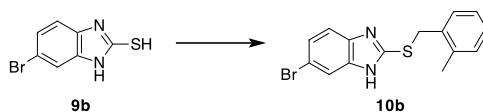
General Procedure B [84]

The 2-mercaptobenzimidazole was dissolved in dry DMF. A solution of NaOMe in MeOH was added. The reaction mixture was stirred at RT for 30 min. Then the desired benzyl bromide was added to the reaction mixture, which was stirred at RT for another 16 h. After that time H_2O was added and the mixture extracted with CH_2Cl_2. The organic layer was dried over Na_2SO_4 and the solvent removed *in vacuo*. The crude product was purified by column chromatography to afford the desired product.

### 2-{[(2-Methylphenyl)methyl]sulfanyl}-1*H*-benzimidazole 10

The reaction was carried out as described in the general procedure B, using 2-mercaptobenzimidazole **4** (800 mg, 5.32 mmol, 1.0 eq.), NaOMe (0.34 g, 6.38 mmol, 1.2 eq. in 2 mL MeOH), and 2-methylbenzyl bromide (0.71 mL, 5.32 mmol, 1.0 eq.) in DMF (6 mL). The crude product was purified by flash column chromatography (CH_2Cl_2) to give the benzimidazole thioether **9** as white crystals (0.72 g, 2.83 mmol, 53%). R_f: 0.7 (10% MeOH/CH_2Cl_2); mp: 148-150 ºC; v/cm^{-1} (neat) 3045, 2961, 2869, 2803, 1436, 1400, 1350, 1269, 1229, 982, 740; δ_H (CDCl$_3$, 400 MHz) 2.48, (3H, s, CH_3), 4.66, (2H, PhCH_2), 7.19 (1H, td, J 7.0, 2.2 Hz, Ar-H), 7.29-7.23 (2H, m, Ar-H), 7.30-7.32 (2H, m, Ar-H), 7.47-7.35, m, Ar-H), 7.81 (1H, br s, Ar-H), 10.00 (1H, s, NH); δ_C (CDCl$_3$, 100 MHz) 19.3, 35.7, 122.6, 126.4, 128.2, 130.2, 130.7, 134.30, 137.2, 150.1; MS (ES$^+$) m/z 255 (M+H$^+$, 100%); HRSM (ES$^+$) 255.0956 calculated for $C_{15}H_{14}N_2S^+$ (M+H$^+$) found 255.0955, Δ= -0.4 ppm.

6-*tert*-Butyl-2-{[(2-methylphenyl)methyl]sulfanyl}-1*H*-benzimidazole 10a

The reaction was carried out as described in the general procedure B, with 2-mercaptobenzimidazole **9a** (600 mg, 2.91 mmol, 1.0 eq.), NaOMe (188 mg, 3.49 mmol, 1.2 eq. in 2 mL MeOH), 2-methylbenzyl bromide (427 µL, 3.20 mmol, 1.1 eq.) in DMF (3.3 mL). After purification by column chromatography (CH_2CH_2) the benzimidazole thioether **10a** was obtained as a white crystalline solid (600 mg, 1.93 mmol, 66%) of the R_f: 0.4 (2% MeOH/CH_2Cl_2); mp: 108-111 °C; v/cm^{-1} (neat) 3031, 2957, 2801, 1629, 1390, 1280, 1233, 986, 811, 731, 652; δ_H (CDCl$_3$, 400 MHz) 1.46 (9H, s, C(CH_3)$_3$), 2.48 (3H, s, CH_3), 4.65 (2H, s, PhCH_2), 7.20 (1H, td, *J* 6.9 and 2.4 Hz, Ar-*H*), 7.25-7.30 (2H, m, Ar-*H*), 7.34-7.43 (2H, m. Ar-*H*), 7.60 (1H, br s, Ar-*H*), 9.68 (1H, br s, N*H*); δ_C (CDCl$_3$, 100 MHz) 19.3, 31.9, 34.9, 35.8, 120.5, 126.4, 128.2, 130.2, 130.7, 134.4, 137.2, 146.1, 149.7; MS (ES$^+$) *m/z* 311 (M+H$^+$, 100%); HRMS (ES) 311.1582 calculated for C$_{19}$H$_{23}$N$_2$S$^+$ (M+H$^+$) found 311.1568, Δ= -4.5 ppm.

### 6-Bromo-2-{[(2-methylphenyl)methyl]sulfanyl}-1*H*-benzimidazole 10b

The synthesis was conducted in accordance with the general procedure B, utilising 6-bromo-2-mercaptobenzimidazole **9b** (800 g, 3.49 mmol, 1.0 eq.), NaOMe (249 mg, 4.54 mmol, 1.3 eq. in 1.60 mL MeOH) and 2-methylbenzyl bromide (0.51 mL, 3.84 mmol, 1.1 eq.) in DMF (4 mL). After purification by column chromatography (CH_2Cl_2) the pure benzimidazole thioether **10b** was obtained as a white solid. (0.34 g, 1.03 mmol, 30%); R_f: 0.3 (CH_2Cl_2); mp: 165-166 °C; v/cm^{-1} (neat) 3021, 2927, 2813, 2675, 1387, 1331, 1268, 1225, 1048, 984, 909, 800, 730; δ_H (CDCl$_3$, 400 MHz) 2.42 (3H, s, CH_3), 4.57 (2H, s, PhCH_2), 7.14 (1H, td, *J* 7.1 and 2.3 Hz, Ar-*H*), 7.17-7.26 (2H, m, Ar-*H*), 7.28-7.45 (3H, m, Ar-*H*), 7.68 (1H, br s, Ar-*H*); δ_C (CDCl$_3$, 100 MHz) 19.4, 35.7, 115.7, 125.7, 126.5, 128.4, 130.2, 130.8, 134.1, 137.2, 151.3; MS (ES$^+$) *m/z* 333/335 (M+H$^+$, 90%); HRMS (ES) 333.0061 calculated for C$_{15}$H$_{14}$N$_2$S^{79}Br$^+$ (M+H$^+$) found 333.0071, Δ= +3.0 ppm.

6-Methyl-2-{[phenylmethyl]sulfanyl}-1*H*-benzimidazole 12
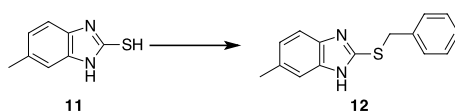
The compounds was synthesised as described in the general procedure B, using 2-mercapto-6-methylbenzimidazole **11** (150 mg, 0.91 mmol, 1.0 eq.), NaOMe (66 mg, 1.18 mmol, 1.3 eq.

in 0.5 mL MeOH), benzyl bromide (0.13 mL, 1.00 mmol, 1.1 eq.) in DMF (1.5 mL). Purification by column chromatography (CH$_2$Cl$_2$) afforded the benzimidazole thioether **12** as white crystals (99.1 mg, 0.39 mmol, 43%). R$_f$: 0.1 (CH$_2$Cl$_2$); mp: 138-143 ºC; v/cm^{-1} (neat) 3029, 2924, 2860, 2797, 2624, 1494, 1438, 1394, 1338, 1275, 1228, 987, 802, 700; δ$_H$ (CDCl$_3$, 400 MHz) 2.45 (3H, s, C*H*$_3$), 4.51 (2H, s, PhC*H*$_2$), 7.04 (1H, dd, *J* 8.4 and 1.5 Hz, H-7), 7.32-7.21 (4H, m, Ar-*H*), 7.38-7.32 (2H, m, Ar-*H*), 7.42 (1H, d, H-4); δ$_C$ (CDCl$_3$, 100 MHz) 21.8, 37.6, 123.9, 127.8, 128.8, 129.1, 132.5, 136.9, 149.2; MS (ES$^+$) *m/z* 255 (M+H$^+$, 100%), HRMS (ES$^+$) 255.0956 calculated for C$_{15}$H$_{15}$N$_2$S$^+$ (M+H$^+$) found 255.0947, Δ= -3.5 ppm.

6-Methyl-2-{[(2-methylphenyl)methyl]sulfanyl}-1*H*-benzimidazole 12a
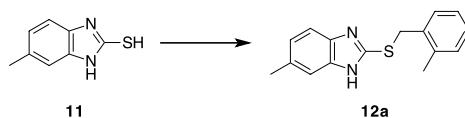
The reaction was carried out as described in the general procedure B, with 2-mercapto-6-methylbenzimidazole **11** (600 mg, 3.65 mmol, 1.0 eq.), NaOMe (0.26 g, 4.8 mmol, 1.3 eq. in 2 mL MeOH) and the 2-methylbenzyl bromide (0.49 mL, 3.65 mmol, 1.0 eq.) in DMF (6 mL). The crude product was purified by column chromatography (10:1 PE/EtOAc) to give the benzimidazole thioether **12a** as a white solid (86.6 mg, 0.32 mmol, 53%). R$_f$: 0.2 (PE/EtOAc 10:3); mp: 117-123 ºC; v/cm^{-1} (neat) 3027, 2921, 2863, 2794, 2618, 1392, 1275, 987, 801, 729; δ$_H$ (CDCl$_3$, 400 MHz) 2.40 (3H, s, C*H*$_3$), 2.48 (3H, s, C*H*$_3$), 4.56 (2H, s, PhC*H*$_2$), 7.06 (1H, dd, *J* 8.3 and 1.6 Hz, Ar-*H*), 7.11 (1H, td, *J* 7.0, 2.3 Hz, Ar-*H*), 7.23-7.15 (2H, m, Ar-*H*), 7.28-7.31 (2H, m, Ar-*H*), 7.45 (1H, br s, Ar-*H*); δ$_C$ (CDCl$_3$, 100 MHz) 19.3, 21.8, 35.9, 123.9, 126.4, 128.2, 130.1, 130.7, 132.4, 134.5, 137.1, 149.4; MS (ES$^+$) *m/z* 269 (M+H$^+$, 100%); HRSM (ES$^+$) 269.1112 calculated for C$_{16}$H$_{17}$N$_2$S$^+$ (M+H$^+$) found 269.1110, Δ= -0.7 ppm.

6-Methyl-2-{[(4-methylphenyl)methyl]sulfanyl}-1*H*-benzimidazole 12b
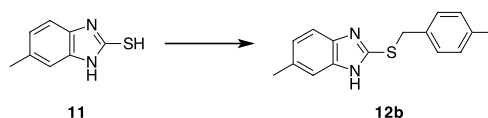
The synthesis was carried out as described in the general procedure B, using 2-mercaptobenzimidazole **11** (100 mg, 0.609 mmol, 1 eq.), NaOMe (40.0 mg, 0.73 mmol, 1.2 eq.) and α-bromo-*p*-xylene (135.0 mg, 0.73 mmol, 1.2 eq.) in DMF (2 mL) and MeOH (0.3 mL). Purification by column chromatography afforded the pure benzimidazole thioether **12b** as a white crystalline solid (64.4 mg, 0.24 mmol, 39%). R$_f$: 0.4 (2% MeOH/CH$_2$Cl$_2$); mp: 146-150 °C; v/cm^{-1} (neat) 3022, 2922, 2856, 1513, 1394, 1339, 1275, 1229, 980, 801, 729; δ$_H$ (CDCl$_3$, 400 MHz) 2.33 (3H, s, C*H*$_3$), 2.47 (3H, s, C*H*$_3$), 4.52 (2H, s, PhC*H*$_2$), 7.07 (1H, d, *J* 8.3 Hz, Ar-*H*), 7.11 (2H, d, *J* 7.8 Hz, Ar-*H*), 7.24-7.28 (2H, m, Ar-*H*), 7.32 (1H, br s, Ar-*H*), 7.44 (1H, d, *J* 8.2 Hz, Ar-*H*); δ$_C$ (CDCl$_3$, 100 MHz) 21.3, 21.8, 37.5, 124.1, 128.9, 129.6,

132.6, 133.8, 137.6, 149.2; MS (ES$^+$) *m/z* 269 (M+H$^+$, 100%); HRMS (ES$^+$) 269.1112 calculated for C$_{16}$H$_{17}$N$_2$S$^+$ (M+H$^+$) found 289.1114, Δ= +0.7 ppm.

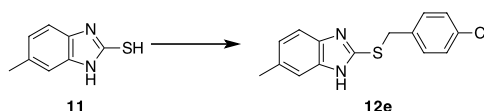## 6-Methyl-2-{[(2-chlorophenyl)methyl]sulfanyl}-1*H*-benzimidazole 12c
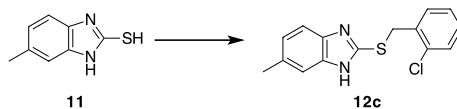
The synthesis was conducted according the general procedure B, using 2-mercaptobenzimidazole **11** (100 mg, 0.61 mmol, 1.0 eq.), NaOMe (40 mg, 0.76 mmol, 1.3 eq. in 0.3 mL MeOH), 2-chlorobenzyl bromide (106 µL, 0.73 mmol, 1.2 eq.), in DMF (2 mL). The crude product was purified by column chromatography to afford the benzimidazole thioether **12c** as a white solid (49.2 mg, 0.17 mmol, 28%). R$_f$: 0.5 (2% MeOH/CH$_2$Cl$_2$); mp: 108-111 °C; v/cm^{-1} (neat) 3056, 2921, 2792, 2629, 1443, 1392, 1337, 1276, 1229, 1055, 987, 803, 758, 734, 670; δ$_H$ (CDCl$_3$, 400 MHz) 2.44 (3H, s, C*H*$_3$), 4.59 (2H, s, PhC*H*$_2$), 7.03 (1, d, *J* 8.5 Hz, Ar-*H*), 7.07 (1H, td, *J*, 7.46 and 1.4 Hz, Ar-*H*), 7.13 (1H, td, *J* 7.7 and 1.8 Hz, Ar-*H*), 7.29-7.31 (2H, m, Ar-*H*), 7.36 (1H, dd, *J* 7.6 and 1.8 Hz, Ar-*H*), 7.42 (1H, d, *J* 8.2 Hz, Ar-*H*); δ$_C$ (CDCl$_3$, 100 MHz) 21.8, 35.4, 124.3, 127.2, 129.3, 129.8, 131.2, 132.8, 134.9, 143.6; MS (ES$^+$) *m/z* 289/291 (M+H$^+$, 100%); HRMS (ES$^+$) 289.0566 calculated for C$_{15}$H$_{14}$N$_2$S^{35}Cl$^+$ (M+H$^+$) found 289.0574, Δ= +2.8 ppm.
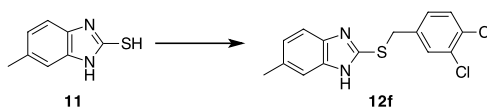
## 6-Methyl-2-{[(3-chlorophenyl)methyl]sulfanyl}-1*H*-benzimidazole 12d
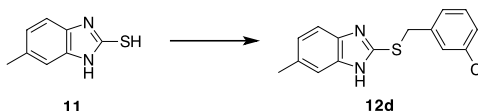
The synthesis was conducted according the general procedure B, using 2-mercaptobenzimidazole **11** (100 mg, 0.61 mmol, 1.0 eq.), NaOMe (40 mg, 0.77 mmol, 1.3 eq. in 0.3 mL MeOH), 3-chlorobenzyl bromide (106 µL, 0.73 mmol, 1.2 eq.), in DMF (2 mL). The crude product was purified by column chromatography to afford the benzimidazole thioether **12d** as a white solid (73.9 mg, 0.26 mmol, 42%). R$_f$: 0.5 (2% MeOH/CH$_2$Cl$_2$); mp: 132-136 °C; v/cm^{-1} (neat) 3053, 2924, 2858, 1597, 1576, 1432, 1391, 1336, 1272, 1226, 804, 732, 690; δ$_H$ (CDCl$_3$, 400 MHz) 2.44 (3H, s, C*H*$_3$), 4.48 (2H, s, PhC*H*$_2$), 7.05 (1H, dd, *J* 8.1 and 1.5, Ar-*H*), 7.11-7.25 (3H, m, Ar-*H*), 7.29 (1H, t, *J* 1.8 Hz, Ar-*H*), 7.42 (1H, d, *J* 8.2 Hz, Ar-*H*); δ$_C$ (CDCl$_3$, 100 MHz) 21.8, 36.9, 124.2, 127.2, 127.9, 129.1, 130.0, 132.8, 134.5, 139.0, 148.5; MS (ES$^+$) *m/z* 289/291 (M+H$^+$, 100%); HRMS (ES$^+$) 289.0566 calculated for C$_{15}$H$_{14}$N$_2$S^{35}Cl$^+$ (M+H$^+$) found 289.0571, Δ= +1.7 ppm.

6-Methyl-2-{[(4-chlorophenyl)methyl]sulfanyl}-1*H*-benzimidazole 12e

The synthesis was conducted according the general procedure B, using 2-mercaptobenzimidazole **11** (100 mg, 0.61 mmol, 1.0 eq.), NaOMe (41 mg, 0.77 mmol, 1.3 eq. in 0.3 mL MeOH), 4-chlorobenzyl bromide (106 μL, 0.73 mmol, 1.2 eq.), in DMF (2 mL). The crude product was purified by column chromatography to afford the benzimidazole thioether **12e** as a white solid (47.5 mg, 0.16 mmol, 27%). R_f: 0.4 (2% MeOH/CH$_2$Cl$_2$) mp: 168-172 °C; v/cm^{-1} (neat) 2786, 2719, 2606, 1490, 1394, 1277, 1226, 1088, 1013, 991, 829, 805, 722, 676; δ_H (CDCl$_3$, 400 MHz) 2.44 (3H, s, C*H*$_3$), 4.49 (2H, s, PhC*H*$_2$), 7.00-7.13 (1H, m, Ar-*H*), 7.21 (2H, d, *J* 8.5 Hz, Ar-*H*), 7.26-7.30 (3H, m, Ar-*H*), 7.42 (1H, d, *J* 8.2 Hz, Ar-*H*); δ_C (CDCl$_3$, 100 MHz) 21.8, 36.9, 124.5, 128.9, 130.4, 133.1, 133.7, 135.5, 148.4; MS (ES$^+$) *m/z* 289/291 (M+H$^+$, 100%); HRMS (ES$^+$) 289.0566 calculated for C$_{15}$H$_{14}$N$_2$S^{35}Cl$^+$ (M+H$^+$) found 289.0577, Δ= +3.8 ppm.

### 6-Methyl-2-{[(3,4-dichlorophenyl)methyl]sulfanyl}-1*H*-benzimidazole 12f

The synthesis was conducted according the general procedure B, using 2-mercaptobenzimidazole **11** (100 mg, 0.61 mmol, 1.0 eq.), NaOMe (41 mg, 0.77 mmol, 1.3 eq. in 0.3 mL MeOH), 3,4-dichlorobenzyl bromide (106 μL, 0.73 mmol, 1.2 eq.), in DMF (2 mL). The crude product was purified by column chromatography to afford the benzimidazole thioether **12f** as a white solid (147.63 mg, 0.46 mmol, 75%). R_f:0.5 (2% MeOH/CH$_2$Cl$_2$); mp: 101-104 °C; v/cm^{-1} (neat) 2923, 2859, 2794, 1470, 1394, 1338, 1274, 1132, 1031, 986, 904, 802, 726; δ_H (CDCl$_3$, 400 MHz) 2.44 (3H, s, C*H*$_3$), 4.44 (2H, s, PhC*H*$_2$), 7.05 (1H, dd, *J* 8.2 and 1.5 Hz, Ar-*H*), 7.15 (1H, dd, *J* 8.2 and 2.1 Hz, Ar-*H*), 7.22-7.32 (2H, m, Ar-*H*), 7.37-7.48 (2H, m Ar-*H*); δ_C (CDCl$_3$, 100 MHz) 21.8, 36.2, 124.3, 128.4, 130.7, 130.9, 131.9, 132.7, 132.9, 137.4, 148.1; MS (ES$^+$) *m/z* 323/325/327 (M+H$^+$, 100%); HRMS (ES$^+$) 232.0177 calculated for C$_{15}$H$_{13}$N$_2$S^{35}Cl$_2^+$ (M+H$^+$) found 232.0181, Δ= +1.2 ppm.

N-Phenyl benzimidazole 13
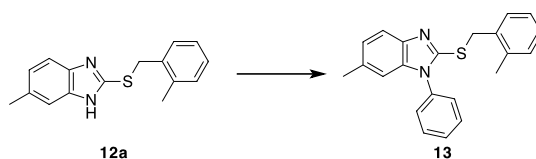
The reaction was carried out following a modified procedure by Buchwald *et al*. [88] Benzimidazole **12a** (50 mg, 0.19 mmol, 1.0 eq.) was dissolved in DMF (0.4 mL) in a

microwave tube. Iodobenzene (42 µL, 0.38 mmol, 2.0 eq.), phenathroline (67 mg, 0.38 mmol, 2.0 eq.), CuI (36 mg, 0.29 mmol, 1.0 eq.) and Cs_2CO_3 (121 mg, 0.38 mmol, 2.0 eq.) were added, the lid was closed and the gas was exchanged to nitrogen. The vial was heated to 110 °C for 16 h. After that, the reaction mixture was cooled to RT and water added. The mixture was extracted with CH_2Cl_2. The crude product was purified by column chromatography to afford the *N*-phenyl benzimidazole **13** as a yellow solid (17 mg, 0.05 mmol, 25%). R_f: 0.5 (2% MeOH/CH_2Cl_2); mp: 186-191 °C; v/cm^{-1} (neat) 2921, 1596, 1498, 1433, 1363, 1293, 1217, 798, 760, 732, 696; δ_H (CDCl$_3$, 400 MHz) 2.38 (3H, s, C*H*$_3$, 2.49 (3H, s, C*H*$_3$), 4.62 (2H, d, *J* 4.8 Hz, PhC*H*$_2$), 7.02 (1H, s br, Ar-*H*), 7.11 (2H, ddd, *J* 10.0, 5.3 and 2.0 Hz, Ar-*H*), 7.13-7.16 (1H, m, Ar-*H*), 7.30-7.39 (3H, m, Ar-*H*), 7.48-7.54 (3H, m, Ar-H), 7.58 (1H, s, Ar-H); δ_D (CDCl$_3$, 100 MHz) 19.3, 21.7, 35.5, 109.2, 109.6, 110.1, 118.2, 124.0, 126.4, 127.1, 128.2, 129.0, 129.9, 130.4, 130.7, 137.4; MS (ES$^+$) *m/z* 345 (M+H$^+$, 100%); HRMS (ES$^+$) 345.1425 calculated for $C_{22}H_{21}N_2S^+$ (M+H$^+$) found 345.140, Δ= 1.4 ppm.

2-Hydroxy-6-methylbenzimidazole 17
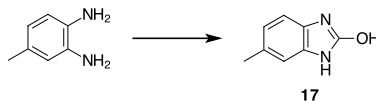
The reaction was carried out in analogy to a procedure by Dannhardt *et al*. [91] 3,4-Diaminotoluene (200 mg, 1.64 mmol, 1.0 eq.) was dissolved in THF (5 mL) the reaction mixture was cooled to 0 °C prior the addition of carbonyldiimidazole (384 mg, 2.37 mmol, 1.4 eq.). The reaction was stirred at RT for 16 h. The precipitated product was filtered and washed with THF to afford the pure 2-hydroxybenzimidazole **17** as a white solid (128 mg, 0.86 mmol, 53%). R_f: 0.2 (4% MeOH/CH_2Cl_2); mp: 213-217 °C; v/cm^{-1} (neat) 2999, 1722, 1672, 1637, 1612, 1506, 1477, 1374, 1279, 1210, 1026, 885, 848, 786, 766, 748; δ_H (DMSO-d$_6$, 400 MHz) 2.26 (3H, s, C*H*$_3$), 6.72 (2H, d, *J* 7.7 Hz, Ar-*H*), 6.78 (1H, d, *J* 7.8 Hz, Ar-*H*), 10.45 (1H, s, N*H*), 10.48 (1H, s, O*H*); δ_C (DMSO-d$_6$, 100 MHz) 21.1, 108.2, 109.0, 120.9, 127.4, 129.4, 129.8, 155.4; No mass spectrum could be obtained.

2-Chloro-6-methylbenzimidazole 21
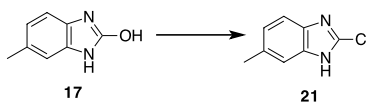
The reaction was carried out in analogy to the procedure described by Blythin *et al*. [92] 2-Hydroxy-6-methylbenzimidazole **17** (1.05 g, 7.10 mmol, 1.0 eq.) was added to phosphorous oxychloride (5.00 mL, 53.6 mmol, 7.6 eq.) the neat reaction mixture was heated to 100 °C for 4.5 h. The reaction mixture was carefully poured onto ice and the remaining phosphorous oxychloride neutralised with NaOH solution. The pH was adjusted to 9 when a white precipitate formed. The precipitate was filtered and washed with CH_2Cl_2 to get the product. Purification by column chromatography (dry loaded, 4% MeOH/CH_2Cl_2) afforded the 2-chlorobenzimidazole **21** as a white solid (38 mg, 2.27 mmol, 32%) R_f: 0.2 (4% MeOH/CH_2Cl_2);

v/cm^{-1} (neat) 2872, 2806, 2179, 2028, 1960, 1441, 1344, 1296, 1229, 988, 800; δ$_H$ (DMSO-d$_6$, 400 MHz) 2.39 (3H, s, C*H$_3$*), 7.03 (1H, dd, *J* 8.5, 1.6 Hz, Ar-*H*), 7.20-7.60 (2H, m, Ar-*H*), 137.07 (1H, s br, O*H*); (DMSO-d$_6$, 100 MHz) 21.2, 123.8, 131.8, 137.9; *m/z* 167/169 (M+H, 100%); HRMS (ES$^+$) 167.0376 calculated for C$_8$H$_8$N$_2$^{35}Cl$^+$ (M+H$^+$), found 167.0369, Δ= -4.2 ppm.

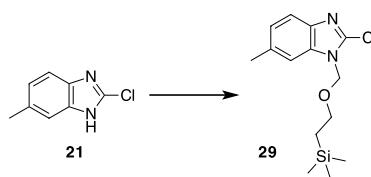### *N*-Boc-2-chloro-6-methylbenzimidazole 22

2-Chloro-6-methylbenzimidazole **21** (10 mg, 0.06 mmol, 1.0 eq.) was dissolved in dry MeCN (0.5 mL). DMAP (0.7 mg, 0.006 mmol, 0.1 eq.) and Et$_3$N (10 µL, 0.075 mmol, 1.25 eq.) were added to the reaction mixture, which was stirred at RT for 17 h. Purification by column chromatography afforded the *N*-boc protected 2-chlorobenzimidazole **22** as a greenish powder (10 mg, 0.04 mmol, 60%); R$_f$: 0.2; mp: 67-72 °C; v/cm^{-1} (neat) 2979, 1744, 1496, 1480, 1369, 1341, 1318, 1296, 1269, 1202, 1147, 1133, 1123, 1076, 1030, 847, 804, 763; δ$_H$ (CDCl$_3$, 400 MHz) 1.71 (18H, 2 s, 2×C(C*H$_3$*)$_3$), 2.45 (3H, s, C*H$_3$*), 2.48 (3H, s, C*H$_3$*), 7.13-7.19 (2H, m, Ar-*H*), 7.44 (1H, s br, Ar-*H*), 7.53 (1H, d, *J* 8.2 Hz, Ar-*H*), 7.74-7.78 (2H, m, Ar-*H*); δ$_C$ (CDCl$_3$, 100 MHz) 21.5, 22.1, 28.2, 86.6, 86.7, 114.4, 115.0, 119.1, 119.6, 126.1, 126.5, 134.7, 135.4, 141.3, 147.5; No mass spectrum could be obtained.

N-Trityl-2-chloro-6-methylbenzimidazole 27
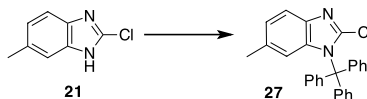
The reaction was carried out as described in the patent by Matsoukas *et al*. [94] 2-Chloro-6-methyl benzimidazole **21** (20 mg, 0.12 mmol, 1.0 eq.) and trityl chloride (50 mg, 0.18 mmol, 1.5 eq.) were dissolved in CH$_2$Cl$_2$ (0.5 mL). Et$_3$N (42 µL, 0.3 mmol, 2.5 eq.) was added and the reaction mixture was stirred at ambient temperature for 16 h. The crude product was attempted to purify by column chromatography (7:3 CH$_2$Cl$_2$/Hex) but the product decomposes. Attempts to recrystallise the product failed. Therefore the product is only verified by 1H-NMR and mass spectroscopy and used crude. The product **27** was obtained as a yellow solid (42 mg, 0.10 mmol, 83%). Rf: 0.2; δ$_H$ (CDCl$_3$, 400 MHz) 2.14 (3H, s, C*H$_3$*), 7.18-7.26 (1H, m, Ar-H), 7.18-7.26 (37H, m, Ar-*H* and trityl chloride), 7.48 (1H, d, J 2.0 Hz, Ar-H), 7.57 (1H, d, J 8.2 Hz, Ar-H); *m/z* 409/411 (M+H, 22%).

2-Chloro-6-methyl-1-{[2-{trimethylsilyl)ethoxy]methyl}-benzimidazole 29

The reaction was carried out following a modified procedure by Grice *et al.* [95] 2-Chloro-6-methyl benzimidazole **21** (1.5 g, 9.00 mmol, 1.0 eq.) was dissolved in DMF (30.00 mL). NaH (47 mg, 11.7 mmol, 1.3 eq.) was added slowly and the reaction mixture stirred for 30 min. Then, SEM-Cl (1.91 mL, 10.80 mmol, 1.2 eq.) was added and the reaction stirred at RT for another 16 h. The crude product was purified by column chromatography to afford the pure *N*-SEM-protected 2-chlorobenzimidazole **29** as a yellow oil (1.50 g, 5.58 mmol, 62%). R$_f$: 0.4 (2% Acetone/CH$_2$Cl$_2$); v/cm^{-1} (neat) 2958, 1718, 1470, 1356, 1330, 1263, 1248, 1081, 939, 917, 833, 805, 693; δ$_H$ (CDCl$_3$, 400 MHz) -0.05 (18H, 2 s, 2×SiC(C*H*$_3$)$_3$), 0.74-1.10 (4H, m, SiC*H*$_2$), 2.47 (6H, d, *J* 6.3 Hz, 2×C*H*$_3$), 3.38-3.79 (4H, m, 2×OC*H*$_2$), 5.51 (2H, s, NC*H*$_2$), 7.11 (2H, td, *J* 8.3 and 1.5 Hz, Ar-*H*), 7.23 (1H, s br, Ar-*H*), 7.32 (1H, d, *J* 8.3 Hz, Ar-*H*), 7.45-7.48 (1H, m, Ar-*H*), 7.56 (1H, d, *J* 8.2 Hz, Ar-*H*); δ$_C$ (CDCl$_3$, 100 MHz) -1.4, 17.8, 21.6, 21.9, 66.7, 73.0, 73.2, 109.8, 110.1, 119.1, 119.4, 124.8, 125.1, 133.0, 133.2, 133.9, 135.3, 139.9, 140.4, 142.1; *m/z* 297/299 (M+H, 100%); HRMS (ES$^+$) 297.1190 calculated for C$_{14}$H$_{21}$N$_2$OSi^{35}Cl$^+$ (M+H$^+$), found 297.1182, Δ= -2.7 ppm.
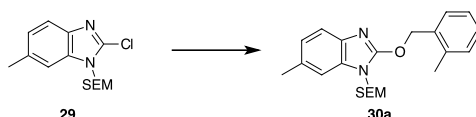
General Procedure C

In an oven-dried round-bottom flask benzyl alcohol was dissolved in dry DMF. NaH was added slowly and the reaction mixture stirred for 30 min. A solution of the *N*-SEM-protected 2-chlorobenzimidazole in DMF was added to the reaction mixture, which was stirred at RT for 48 h. Then, the reaction mixture was quenched with H$_2$O and extracted with CH$_2$Cl$_2$. The combined organic layer was dried over Na$_2$SO$_4$ and the solvent removed under reduced pressure. The crude product was purified by column chromatography to afford the pure product.

2-(Benzyloxy)-6-methyl-1-{[2-(trimethylsilyl)ethoxy]methyl}-benzimidazole 30
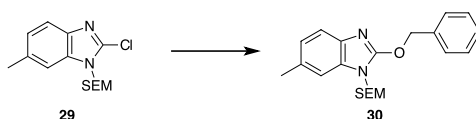
The reaction was carried out as described in general procedure C, using *N*-SEM-protected 2-chlorobenzimidazole **29** (300 mg, 1.02 mmol, 1.0 eq.), benzyl alcohol (188 mg, 1.32 mmol, 1.3 eq.), NaH (83 mg, 2.09 mmol, 1.8 eq.) in DMF (10 mL). Column chromatography of the crude product (2% acetone/CH$_2$Cl$_2$) gave the pure benzimidazole ether **30** as a colourless, oil (196 mg, 0.53 mmol, 53%) R$_f$: 0.6 (2% acetone/CH$_2$Cl$_2$); v/cm^{-1} (neat) 3178, 2952, 1703, 1632, 1543, 1502, 1473, 1355, 1286, 1248, 1080, 858, 835, 798, 696; δ$_H$ (CDCl$_3$, 400 MHz) -0.06 (9H, s, Si(C*H*$_3$)$_3$), -0.07 (9H, s, Si(C*H*$_3$)$_3$), 0.86-0.93 (4H, m, alkyl), 2.46 (3H, s, C*H*$_3$),

3.49-3.57 (4H, m, alkyl), 5.37 (4H, s, PhCH_2), 5.60 (4H, d, J 2.1 Hz, OCH_2), 7.02 (2H, dd, J 12.5 and 8.1 Hz, Ar-H), 7.14 (1H, s br, Ar-H), 7.21 (2H, d, J 8.1 Hz, Ar-H), 7.34-7.45 (7H, m, Ar-H), 7.48 (4H, d, J 7.7 Hz, Ar-H); δ_C (CDCl$_3$, 100 MHz) -1.4, 17.8, 21.7, 66.3, 71.1, 71.2, 108.7, 109.4, 117.4, 118.1, 122.6, 123.4, 128.20, 128.7, 131.4, 131.6, 131.8, 133.7, 135.7, 137.9, 140.3, 156.9, 157.2; MS (ES$^+$) m/z 369 (M+H, 100%); HRMS (ES$^+$) 369.1998 calculated for C$_{21}$H$_{29}$N$_2$O$_2$Si$^+$ (M+H$^+$), found 369.1988, Δ= -2.7 ppm.

6-Methyl-2-[(2-methylphenyl)methoxy]-1-{[2-trimethylsilyl)ethoxy]methyl}-benzimidazole 30a

The reaction was carried out as described in general procedure C, using *N*-SEM-protected 2-chlorobenzimidazole **29** (301 mg, 1.01, 1.0 eq.), 2-methylbenzyl alcohol (161 mg, 1.32 mmol, 1.3 eq.), NaH (78 mg, 1.96 mmol, 1.9 eq.) in DMF (10 mL). Column chromatography of the crude product (2% acetone/ CH$_2$Cl$_2$) gave the pure benzimidazole ether **30a** as a colourless oil (298 mg, 0.78 mmol, 77%). R$_f$: 0.5 (2% acetone/CH$_2$Cl$_2$); v/cm^{-1} (neat) 2955, 2922, 2892, 1629, 1597, 1540, 1462, 1433, 1360, 1280, 1248, 1079, 988, 833, 745, 690; δ_H (CDCl$_3$, 400 MHz) -0.07 (9H, s, Si(CH_3)$_3$), -0.08 (9H, s, Si(CH_3)$_3$), 0.80-0.93 (4H, m, alkyl chain), 2.43 (6H, s, CH_3), 2.46 (6H, s, CH_3), 3.44-3.58 (4H, m, alkyl), 5.36 (4H, s, PhCH_2), 5.60 (4H, s, OCH_2), 7.03 (2H, m, Ar-H), 7.14 (0.5H, s, br, Ar-H), 7.23 (5H, dd, J 15.6 and 7.4 Hz, Ar-H), 7.32-7.27 (2H, m, Ar-H), 7.40 (1H, s br, Ar-H), 7.46 (3H, dd, J 7.7 and 4.5 Hz, Ar-H); δ_C (CDCl$_3$, 100 MHz) -1.4, 17.9, 19.2, 21.7, 21.8, 66.3, 70.4, 71.2, 71.3, 108.7, 109.5, 117.4, 118.3, 122.6, 123.4, 126.2, 128.9, 129.3, 129.4, 130.6, 131.4, 131.6, 131.8, 133.7, 133.8, 137.2, 138.0, 140.4, 156.9, 157.2; MS (ES$^+$) m/z 383 (M+H, 100%); HRMS (ES$^+$) 383.2155 calculated for C$_{22}$H$_{31}$N$_2$O$_2$Si$^+$ (M+H$^+$), found 383.2137, Δ= -4.7 ppm.
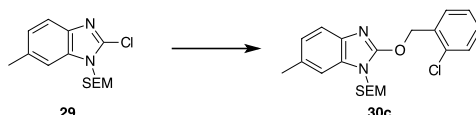
6-Methyl-2-[(4-methylphenyl)methoxy]-1-{[2-trimethylsilyl)ethoxy]methyl}-benzimidazole 30b
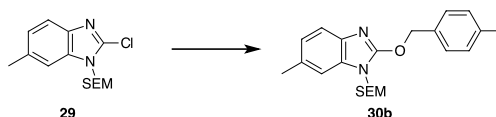
The reaction was carried out as described in general procedure C, using *N*-SEM-protected 2-chlorobenzimidazole **29** (300 mg, 1.01, 1.0 eq.), 4-methylbenzyl alcohol (162 mg, 1.32 mmol, 1.3 eq.), NaH (62 mg, 1.56 mmol, 1.6 eq.) in DMF (10 mL). Column chromatography of the crude product (2% acetone/ CH$_2$Cl$_2$) gave the pure benzimidazole ether **30b** as a colourless (119 mg, 0.31 mmol, 28%). R$_f$: 0.5 (2% acetone/CH$_2$Cl$_2$); v/cm^{-1} (neat) 2951, 1718, 1631, 1597, 1540, 1463, 1436, 1360, 1281, 1247, 1078, 989, 833, 805, 751, 688; δ_H (CDCl$_3$, 400 MHz) -0.05 (18H, 2 s, 2×Si(CH_3)$_3$), 0.84-0.97 (4H, m, alkyl), 2.38 (6H, s, CH_3), 2.47 (6H, s, CH_3), 3.47-3.58 (4H, m, alkyl), 5.35 (4H, d, J 1.5 Hz, PhCH_2), 5.57 (4H, d, J 1.7 Hz, OCH_2),

6.98-7.09 (2H, m, Ar-*H*). 7.15 (1H, s br, Ar-*H*), 7.21 (5H, dd, *J* 8.0 and 3.9 Hz, Ar-*H*), 7.40 (5H, d, *J* 7.8 Hz, Ar-*H*), 7.49 (1H, d, *J* 8.1 Hz, Ar-*H*); δ_C (CDCl$_3$, 100 MHz) -1.5, 17.7, 21.3, 21.6, 21.7, 66.1, 70.9, 71.1, 71.8, 108.6, 109.4, 117.3, 118.0, 122.5, 123.3, 128.4, 129.3, 131.2, 131.5, 131.7, 132.6, 133.7, 137.9, 138.4, 140.3, 156.9, 157.2; MS (ES$^+$) *m/z* 383 (M+H, 92%); HRMS (ES$^+$) 383.2160 calculated for C$_{22}$H$_{31}$N$_2$O$_2$Si$^+$ (M+H$^+$), found 383.2137, Δ= 1.3 ppm.

2-[(2-Chlorophenyl)methoxy]-6-methyl-1-{[2-(trimethylsilyl)ethoxy]methyl}-benzimidazole 30c

The reaction was carried out as described in general procedure C, using *N*-SEM-protected 2-chlorobenzimidazole **29** (301 mg, 1.01, 1.0 eq.), 2-chlorobenzyl alcohol (188 mg, 1.32 mmol, 1.3 eq.), NaH (70 mg, 1.75 mmol, 1.8 eq.) in DMF (10 ml). Column chromatography of the crude product (2% acetone/ CH$_2$Cl$_2$) gave the pure benzimidazole ether **30c** as a pale yellow oil (201 mg, 0.49 mmol, 49%). Rf 0.6 (2% acetone/CH$_2$Cl$_2$); v/cm^{-1} (neat) 2953, 1634, 1595, 1540, 1466, 1438, 1361, 1361, 1079, 1058, 941, 856, 833, 752, 680; δ_H (CDCl$_3$, 400 MHz) 0.08 (18H, 2 s, 2×Si(C*H$_3$*)$_3$), 0.73-0.95 (4H, m, alkyl), 2.45 (6H, d, *J* 2.2 Hz, C*H$_3$*), 3.46-3.59 (4H, m, alkyl), 5.38 (4H, s, PhC*H$_2$*), 5.69 (4H, s, OC*H$_2$*), 6.98-7.06 (1H, m, Ar-*H*), 7.13-7.16 (1H, m, Ar-*H*), 7.21 (4H, d, *J* 8.1 Hz, Ar-*H*), 7.30 (4H, d *J* 0.7 Hz, Ar-*H*), 7.39 (1H, s br, Ar-*H*), 7.41-7.48 (3H, m, Ar-*H*), 7.57 (1H, dd, *J* 7.3 and 1.9 Hz, Ar-*H*); δ_C (CDCl$_3$, 100 MHz) -1.4, 17.9, 21.8, 66.4, 69.3, 71.4, 108.8, 109.5, 117.5, 118.2, 122.7, 123.4, 127.1, 129.8, 130.0, 130.3, 131.5, 131.6, 131.9, 133.5, 133.8, 134.1, 137.9, 140.4, 156.7, 157.0; MS (ES$^+$) *m/z* 403/405 (M+H, 100%); HRMS (ES$^+$) 403.1609 calculated for C$_{21}$H$_{28}$N$_2$O$_2$Si^{35}Cl$^+$ (M+H$^+$), found 403.1599, Δ= -2.5 ppm.
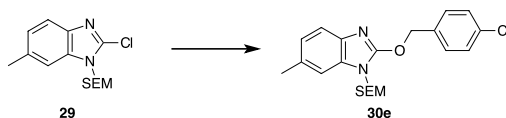
2-[(3-Chlorophenyl)methoxy]-6-methyl-1-{[2-(trimethylsilyl)ethoxy]methyl}-benzimidazole 30d
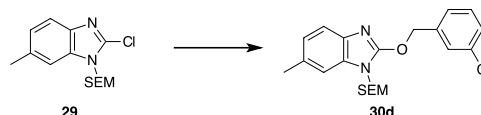
The reaction was carried out as described in general procedure C, using *N*-SEM-protected 2-chlorobenzimidazole **29** (303 mg, 1.02, 1.0 eq.), 3-chlorobenzyl alcohol (188 mg, 1.32 mmol, 1.3 eq.), NaH (83 mg, 2.09 mmol, 1.8 eq.) in DMF (10 mL). Column chromatography of the crude product (1% acetone/ CH$_2$Cl$_2$) gave the pure benzimidazole ether **30d** as a pale yellow oil (273 mg, 0.68 mmol, 67%). R$_f$: 0.6 (2% acetone/CH$_2$Cl$_2$); v/cm^{-1} (neat) 2958, 1635, 1595, 1541, 1467, 1425, 1361,1281, 1248, 1080, 1009, 858, 835, 783, 704, 682; δ_H (CDCl$_3$, 400 MHz) -0.07, (9H, s, Si(C*H$_3$*)$_3$), -0.08, (9H, s, Si(C*H$_3$*)$_3$), 0.78-0.95 (4H, m, alkyl), 2.45 (6H, d, *J* 2.7 Hz, C*H$_3$*), 3.42-3.61 (4H, m, alkyl), 5.37 (4H, s, PhC*H$_2$*), 5.56 (4H, d, *J* 2.2 Hz, OC*H$_2$*),

7.02 (2H, t, *J* 9.6 Hz, Ar-*H*), 7.14 (1H, s, Ar-*H*), 7.20 (1H, d, *J* 8.1 Hz, Ar-*H*), 7.31-7.39 (7H, m, Ar-*H*), 7.41-7.51 (3H, m, Ar-*H*); δ_C (CDCl$_3$, 100 MHz) -1.3, 17.8, 21.8, 66.4, 70.9, 71.3, 108.8, 109.5, 117.5, 118.2, 122.8, 123.5, 126.2, 128.2, 128.8, 130.1, 131.6, 131.9, 133.8, 134.7, 137.7, 137.8, 140.2, 156.6, 156.9; MS (ES$^+$) *m/z* 403/405 (M+H, 88%); HRMS (ES$^+$) 403.1609 calculated for C$_{21}$H$_{28}$N$_2$O$_2$Si^{35}Cl$^+$ (M+H$^+$), found 403.1593, Δ= -4.0 ppm.

2-[(4-Chlorophenyl)methoxy]-6-methyl-1-{[2-(trimethylsilyl)ethoxy]methyl}-benzimidazole 30e

The reaction was carried out as described in general procedure C, using *N*-SEM-protected 2-chlorobenzimidazole **29** (303 mg, 1.02, 1.0 eq.), 4-chlorobenzyl alcohol (188 mg, 1.32 mmol, 1.3 eq.), NaH (88 mg, 2.20 mmol, 1.8 eq.) in DMF (10 mL). Column chromatography of the crude product (2% acetone/ CH$_2$Cl$_2$) gave the pure product **30e** as a colourless oil (340 mg, 0.84 mmol, 83%). R$_f$: 0.3 (2% acetone/CH$_2$Cl$_2$); v/cm^{-1} (neat) 2952, 1718, 1631, 1596, 1540, 1463, 1441, 1360, 1280, 1248, 1080, 937, 834, 804, 756, 691; δ_H (CDCl$_3$, 400 MHz) -0.08 (9H, s, Si(C*H*$_3$)$_3$), -0.09 (9H, s, Si(C*H*$_3$)$_3$), 0.79-0.91 (4H, m, alkyl), 2.45, (6H, s, C*H*$_3$), 3.46-3.56 (4H, m, alkyl), 5.35 (4H, s, PhC*H*$_2$), 5.55 (4H, s, OC*H*$_2$), 6.98-7.05 (2H, m, Ar-*H*), 7.13 (1H, s br, Ar-*H*), 7.19 (1H, d, *J* 8.1 Hz, Ar-*H*), 7.33-7.46 (10H, m, Ar-*H*); δ_C (CDCl$_3$, 100 MHz) -1.4, 17.9, 21.8, 66.4, 71.0, 108.7, 109.5, 117.5, 118.2, 122.7, 123.5, 128.9, 129.7, 131.6, 131.9, 133.8, 134.2, 134.6, 137.9, 140.2, 156.9; MS (ES$^+$) *m/z* 403/405 (M+H, 100%); HRMS (ES$^+$) 403.1609 calculated for C$_{21}$H$_{28}$N$_2$O$_2$SiCl^{35+} (M+H$^+$), found 403.1598, Δ= -2.7 ppm.

2-[(3,4-Dichlorophenyl)methoxy]-6-methyl-1-{[2-(trimethylsilyl)ethoxy]methyl}-benzimidazole 30f
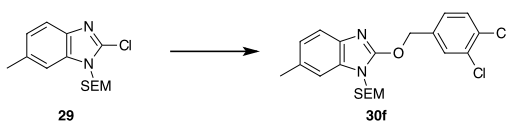

The reaction was carried out as described in general procedure C, using *N*-SEM-protected 2-chlorobenzimidazole **29** (303 mg, 1.02, 1.0 eq.), 2-chlorobenzyl alcohol (188 mg, 1.32 mmol, 1.3 eq.), NaH (83 mg, 2.09 mmol, 1.8 eq.) in DMF (10 mL). Column chromatography of the crude product (2% acetone/CH$_2$Cl$_2$) gave the pure benzimidazole ether **30f** as a yellow oil (338 mg, 0.77 mmol, 76%). R$_f$: 0.3 (2% acetone/CH$_2$Cl$_2$); v/cm^{-1} (neat) 2952, 1633, 1597, 1540, 1469, 1396, 1356, 1341, 1280, 1248, 1078, 1029, 833, 754, 690; δ_H (CDCl$_3$, 400 MHz) -0.07, (9H, s, Si(C*H*$_3$)$_3$), -0.08, (9H, s, Si(C*H*$_3$)$_3$), 0.83-0.94 (4H, m, alkyl), 2.45 (6H, d, *J* 2.9 Hz, C*H*$_3$), 3.46-3.57 (4H, m, alkyl), 5.36 (4H, s, PhC*H*$_2$), 5.53 (4H, d, *J* 2.2 Hz, OC*H*$_2$), 7.02 (2H, t, *J* 8.8 Hz, Ar-*H*), 7.13 (1H, s, br, Ar-*H*), 7.20 (1H, d, *J* 8.1 Hz, Ar-*H*), 7.29-7.38 (3H, m, Ar-*H*), 7.45 (3H, dd, *J* 11.6 and 8.2 Hz, Ar-*H*), 7.58 (2H, s br, Ar-*H*); δ_C (CDCl$_3$, 100 MHz) -1.4, 17.9, 21.8, 66.5, 70.2, 71.3, 108.8, 109.5, 117.6, 118.2, 122.9, 123.6, 127.5, 130.1, 130.8,

131.7, 132.1, 132.8, 132.9, 133.9, 135.9, 137.8, 140.1, 156.5, 156.8; MS (ES$^+$) m/z 437/439/441 (M+H, 100%); HRMS (ES$^+$) 437.1219 calculated for $C_{21}H_{27}N_2O_2SiCl^{35}{}_2{}^+$ (M+H$^+$), found 437.1216, Δ= -0.7 ppm.
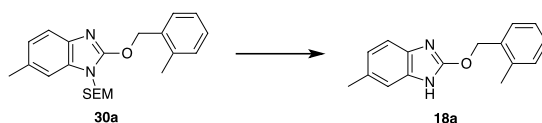
General Procedure D [96]

The SEM-protected benzimidazole was added to a 1M solution of TBAF in THF. The reaction mixture was heated to 55 °C for 18 h. Then, the reaction mixture was cooled to RT and H_2O was added. The mixture was extracted with Et_2O. The combined organic layer was dried over Na_2SO_4 and the solvent removed under reduced pressure. The product was purified by column chromatography to give the pure product.

2-(Benzyloxy)-6-methyl-1*H*-benzimidazole 18
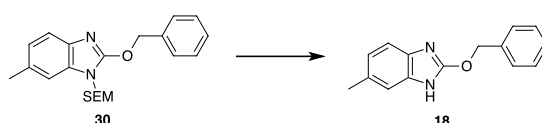
The synthesis was carried out according to the general procedure D, using *N*-SEM-protected benzimidazole benzyl ether **30** (196 mg, 0.53 mmol, 1.0 eq.) and TBAF (1 M in THF, 5.30 mL, 5.3 mmol, 10.0 eq.). Purification by column chromatography afforded the deprotected benzimidazole **18** as a white solid (36 mg, 0.15 mmol, 29%). R$_f$: 0.5 (2% acetone/CH_2Cl_2); mp: 149-155 °C; v/cm^{-1} (neat) 3032, 2922, 1634, 1532, 1449, 1429, 1345, 1277, 1213, 1049, 1028, 969, 918, 865, 834, 792, 756, 713, 696; δ$_H$ (CDCl$_3$, 400 MHz) 2.43 (3H, s, C*H$_3$*), 5.54 (2H, s, PhC*H$_2$*), 6.98 (1H, d, *J* 8.0 Hz, Ar-*H*), 7.19, (1H, s br, Ar-*H*), 7.24-7.33 (1H, m, Ar-*H*), 7.37 (3H, d, *J* 5.6 Hz, Ar-*H*), 7.43 (2H, s, Ar-*H*); δ$_C$ (CDCl$_3$, 100 MHz) 21.8, 71.8, 122.9, 128.5, 128.4, 128.7, 131.5, 135.6, 157.6; MS (ES$^+$) m/z 239 (M+H, 100%); HRMS (ES$^+$) 239.1184 calculated for $C_{15}H_{15}N_2O^+$ (M+H$^+$), found 239.1184, Δ= 0.0 ppm.
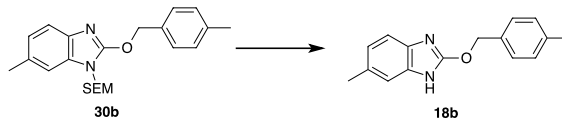
6-Methyl-2-[(2-methylphenyl)methoxy]-1*H*-benzimidazole 18a

The synthesis was carried out according to the general procedure D, using *N*-SEM-protected benzimidazole ether **30a** (286 mg, 0.75 mmol, 1.0 eq.) and TBAF (1M in THF, 7.50 mL, 7.50 mmol, 10.0 eq.). After column chromatography (2% acetone/CH_2Cl_2) the pure deprotected benzimidazole **18a** was obtained as a white solid (65 mg, 0.26 mmol, 33%). R$_f$: 0.5 (2% acetone/CH_2Cl_2); mp: 127-132 °C; v/cm^{-1} (neat) 3043, 2932, 1696, 1635, 1551, 1454, 1350, 1275, 1315, 1062, 1029, 969, 937, 800, 736, 703; δ$_H$ (CDCl$_3$, 400 MHz) 2.36 (3H, s, C*H$_3$*), 2.43 (3H, s, C*H$_3$*), 5.54 (2H, s, PhC*H$_2$*); 6.94-7.02 (1H, m Ar-*H*), 7.04 (0.5H, s, Ar-*H*), 7.11 (0.5H, d, *J* 8.0 Hz, Ar-*H*), 7.17-7.24 (2H, m, Ar-*H*), 7.25-7.32 (1H, m, Ar-*H*), 7.36-7.50 (2H, m, Ar-*H*), 8.75 (1H, s, N*H*); δ$_C$ (CDCl$_3$, 100 MHz) 19.0, 21.8, 70.3, 109.2, 109.9, 117.4, 118.0, 122.7, 123.0, 126.2, 129.1, 129.6, 130.6, 131.5, 132.3, 133.6, 137.4, 138.9, 141.3, 157.7,

158.1; MS (ES$^+$) *m/z* 253 (M+H, 100%); HRMS (ES$^+$) 253.1341 calculated for C$_{16}$H$_{17}$N$_2$O$^+$ (M+H$^+$), found 369.1340, Δ= -0.4 ppm.

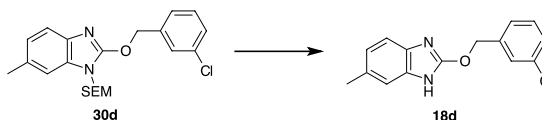### 6-Methyl-2-[(4-methylphenyl)methoxy]-1*H*-benzimidazole 18b

The synthesis was carried out according to the general procedure D, using *N*-SEM-protected benzimidazole ether **30b** (110 mg, 0.29 mmol, 1.0 eq.) and TBAF (1 M in THF, 2.40 mL, 2.4 mmol, 8.3 eq.). Purification by column chromatography (2% acetone/CH$_2$Cl$_2$) afforded the pure deprotected benzimidazole **18b** as a while solid (29 mg, 0.11 mmol, 35%). R$_f$: 0.4 (2% acetone/CH$_2$Cl$_2$); mp: 155-160 °C; v/cm^{-1} (neat) 3032, 2919, 1634, 1552, 1453, 1349, 1313, 1273, 1218, 1063, 972, 938, 846, 802, 714; δ$_H$ (CDCl$_3$, 400 MHz) 2.35 (3H, s, C*H*$_3$), 2.42 (3H, s, C*H*$_3$); 5.49 (2H, s, PhC*H*$_2$), 6.94-7.01 (1H, m, Ar-*H*), 7.15 (3H, d, *J* 7.8 Hz, Ar-*H*), 7.27-7.43 (3H, m, Ar-*H*), 9.44 (1H, s br, N*H*); δ$_C$ (CDCl$_3$, 100 MHz) 21.4, 21.7, 71.8, 122.8, 128.6, 129.4, 131.3, 132.5, 138.5, 158.0; MS (ES$^+$) *m/z* 253 (M+H, 100%); HRMS (ES$^+$) 253.1341 calculated for C$_{16}$H$_{17}$N$_2$O$^+$ (M+H$^+$), found 253.1348, Δ= 2.8 ppm.
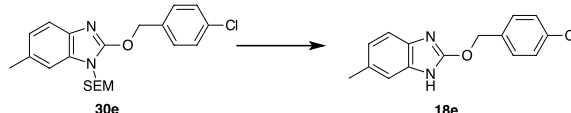
2-[(2-Chlorophenyl)methoxy-6-methyl-1*H*-benzimidazole 18c
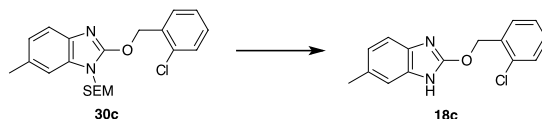
The synthesis was carried out according to the general procedure D, using *N*-SEM-protected benzimidazole ether **30c** (190 mg, 0.47 mmol, 1.0 eq.) and TBAF (1 M in THF, 2.40 mL, 2.4 mmol, 5.1 eq.). After purification by column chromatography the deprotected benzimidazole **18c** was obtained as a white solid (116 mg, 0.43 mmol, 87%). R$_f$: 0.5 (2% acetone/CH$_2$Cl$_2$); mp: 110-120 °C; v/cm^{-1} (neat) 3062, 2927, 1638, 1550, 1444, 1351, 1315, 1273, 1217, 1029, 941, 800, 748, 681; δ$_H$ (CDCl$_3$, 400 MHz) 2.42 (3H, s, C*H*$_3$), 5.64 (2H, s, PhC*H*$_2$), 6.92-702 (1H, m, Ar-*H*), 7.13-7.25 (3H, m, Ar-*H*), 7.27-7.39 (2H, m, Ar-*H*), 7.43 (1H, dt, *J* 7.6 and 1.6 Hz, Ar-*H*); δ$_C$ (CDCl$_3$, 100 MHz) 21.7, 69.1, 122.9, 126.9, 129.7, 129.9, 130.1, 131.4, 133.3, 133.9, 157.8; MS (ES$^+$) *m/z* 273/275 (M+H, 100%); HRMS (ES$^+$) 273.0795 calculated for C$_{15}$H$_{14}$N$_2$OCl^{35+} (M+H$^+$), found 273.0800, Δ= 1.8 ppm.

2-[(3-Chlorophenyl)methoxy-6-methyl-1*H*-benzimidazole 18d

The synthesis was carried out according to the general procedure D, using *N*-SEM-protected benzimidazole ether **30d** (263 mg, 0.65 mmol, 1.0 eq.) and TBAF (1 M in THF, 6.50 mL, 6.5 mmol, 10.0 eq.). Purification by column chromatography gave the deprotected benzimidazole

18d as a white solid (74 mg, 0.27 mmol, 42%). R_f: 0.5 (2% acetone/CH_2Cl_2); mp: 109-118 °C; v/cm^{-1} (neat) 3048, 2923, 1635, 1551, 1456, 1428, 1349, 1272, 1215. 1068, 981, 866, 787, 737, 682; δ_H (CDCl$_3$, 400 MHz) 2.45 (3H, s, CH_3), 5.51 (2H, s, PhCH_2), 6.99-7.05 (1H, m, Ar-H), 7.19-7.26 (3H, m, Ar-H), 7.28-7.34 (2H, m, Ar-H), 7.38 (1H, t, J 1.8 Hz, Ar-H), 10.02 (1H, s, br, NH); δ_C (CDCl$_3$, 100 MHz) 21.7, 70.7, 122.9, 126.1, 128.1, 128.7, 129.9, 131.6, 134.5, 137.5, 157.7; MS (ES$^+$) m/z 273/275 (M+H, 100%); HRMS (ES$^+$) 273.0795 calculated for C$_{15}$H$_{14}$N$_2$OCl^{35+} (M+H$^+$), found 273.0790, Δ= -1.8 ppm.

2-[(4-Chlorophenyl)methoxy-6-methyl-1H-benzimidazole 18e

The synthesis was carried out according to the general procedure D, using *N*-SEM-protected benzimidazole ether **30e** (327 mg, 0.81 mmol, 1.0 eq.) and TBAF (1 M in THF, 8.10 mL, 8.1 mmol, 10 eq.). Purification by column chromatography gave the deprotected benzimidazole **18e** as a white solid (105 mg, 0.38 mmol, 45%). R_f: 0.5 (2% acetone/CH_2Cl_2); mp: 163-167 °C; v/cm^{-1} (neat) 3049, 2923, 1634, 1551, 1492, 1454, 1407, 1347, 1313, 1271, 1217, 1091, 1065, 1016, 977, 939, 840, 802, 737; δ_H (CDCl$_3$, 400 MHz) 2.45 (3H, s, CH_3), 5.48 (2H, s, PhCH_2), 6.96-7.06 (1H, m, Ar-H), 7.06-7.61 (6H, m, Ar-H), 10.25 (1H, s br, NH); δ_C (CDCl$_3$, 100 MHz) 21.72 (s), 70.88 (s), 122.93 (s), 128.84 (s), 129.63 (s), 131.53 (s), 133.89 (s), 134.53 (s), 157.85 (s); MS (ES$^+$) m/z 273 (M+H, 100%); HRMS (ES$^+$) 273.0795 calculated for C$_{15}$H$_{14}$N$_2$OCl$^+$ (M+H$^+$), found 273.0786, Δ= -3.3 ppm.

## 2-[(3,4-Dichlorophenyl)methoxy-6-methyl-1H-benzimidazole 18f
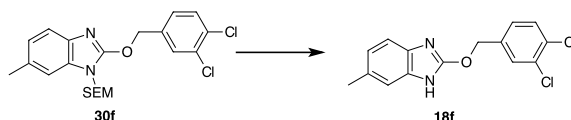
The synthesis was carried out according to the general procedure D, using *N*-SEM-protected benzimidazole ether **30f** (326 mg, 0.74 mmol, 1.0 eq.) and TBAF (1 M in THF, 7.40 mL, 7.40 mmol, 5.1 eq.). After purification by column chromatography the product **18f** was obtained as a white solid (168 mg, 0.55 mmol, 71%). R_f: 0.5 (2% acetone/CH_2Cl_2); mp: 53-65 °C; v/cm^{-1} (neat) 3061, 2927, 1632, 1553, 1463, 1399, 1350, 1278, 1261, 1217, 1130, 1067, 1028, 974, 819, 797, 747, 688; δ_H (CDCl$_3$, 400 MHz) 2.46 (3H, s, CH_3), 5.46 (2H, PhCH_2), 7.01-7.06 (1H, m, Ar-H), 7.09 (1H, dd, J 8.2 and 2.0 Hz, Ar-H), 7.24 (1H, s, Ar-H), 7.29-7.38 (2H, m, Ar-H), 7.39 (1H, d, J 1.9 Hz, Ar-H); δ_C (CDCl$_3$, 100 MHz) 21.7, 70.1, 123.1, 127.1, 129.7, 130.6, 131.7, 132.7, 135.5, 157.7; MS (ES$^+$) m/z 307/309/311 (M+H, 100%); HRMS (ES$^+$) 307.0405 calculated for C$_{15}$H$_{13}$N$_2$OCl$^{35}_2{}^+$ (M+H$^+$), found 307.0424, Δ= 6.2 ppm.

tert-Butyl N-(5-bromo-2-{[(tertbutoxy)carbonyl]amino}phenyl)carbamate 38 [99]
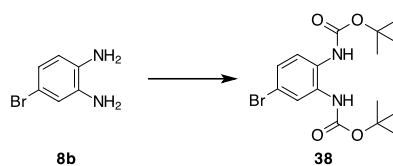
The synthesis was carried out as described by Cheung *et al*. [99] 6-Bromo diaminophenyl **8b** (50 mg, 0.27 mmol, 1.0 eq.) and Boc-anhydride (295 mg, 1.35 mmol, 5 eq.) were dissolved in CH_2Cl_2 (0.75 mL). An aqueous solution of NaOH (27 mg, 0.67 mmol, 2.5 eq. in 0.35 mL H_2O) was added to the reaction mixture, which was vigorously stirred at RT for 16 h. The fractions were separated and the aqueous layer was extracted with CH_2Cl_2. The combined organic layer was dried over Na_2SO_4 and the solvent removed under reduced pressure. Purification by column chromatography afforded the pure Boc-protected diamine **38** as a white solid (73 mg, 0.19 mmol, 69%). R_f: 0.1 (7:3 CH_2Cl_2/Hex), mp: 160-170 °C; v/cm^{-1} (neat) 3273, 2978, 1695, 1595, 1537, 1508, 1481, 1392, 1304, 1278, 1254, 1158, 1085, 1053, 859, 769; δ_H (CDCl$_3$, 400 MHz) 1.53 (18H, s, 2×C(CH_3)$_3$), 6.73 (2H, d, *J* 70.2 Hz Ar-*H*), 7.19 (1H, dd, *J* 8.6 and 2.2 Hz, Ar-*H*), 7.28-7.40 (1H, m, Ar-*H*), 7.73 (1H, s br, Ar-*H*); *m/z* 411 (M+Na, 25%); HRMS (ES$^+$) 409.0739 calculated for $C_{16}H_{23}N_2O_4BrNa^+$ (M+Na$^+$), found 409.0738, Δ= -0.2 ppm. The spectrum is in agreement to the published spectral data. [99]
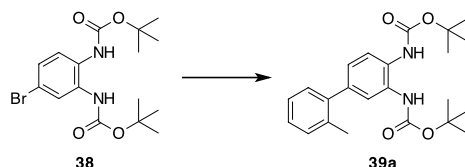
General Procedure E [99]

This general procedure describes a method which is in analogy to the described procedure by Cheung *et al*. [99] Boc-protected 4-bromo-1,2-benzenediamine was dissolved in degassed 2-(2-ethoxyethoxy)ethanol. Then Pd(dppf)Cl$_2$ and boronic acid were added. The atmosphere was exchanged to nitrogen and an aqueous solution of NaHCO$_3$ was added to the reaction mixture, which was heated to 90 °C for 48 h. After that time the reaction was cooled to RT and H_2O was added. The aqueous layer was extracted with CH_2Cl_2. The combined organic layer was dried over Na_2SO_4 and the solvent removed *in vacuo*. The product was purified by column chromatography.

tert-Butyl N-(2-{[(tert-butoxy)carbonyl]amino}-5-phenylphenyl)carbamate 39
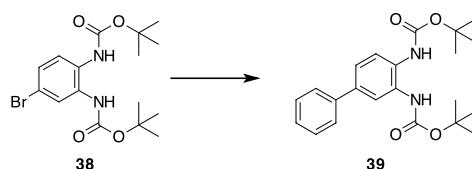
The synthesis was performed as outlined in the general procedure E in two vials, each with 4-Br di-Boc diamine **38** (300 mg, 0.67 mmol, 1.0 eq.), phenylboronic acid (192 mg, 1.33 mmol, 2.0 eq.), Pd(dppf)Cl$_2$ (126 mg, 0.12 mmol, 0.2 eq.), NaHCO$_3$ (656 mg, 5.26 mmol, 8.0 eq. in 5.5 mL H_2O) in 2-(2-ethoxyethoxy)ethanol (8 mL). The crude product was purified by column chromatography (CH$_2$Cl$_2$/Hex 6:4) to give the biaryl **39** as a pale yellow solid (171 mg, 0.45 mmol, 29%). R_f: 0.1 (4:6 Hex/CH$_2$Cl$_2$); mp: 58-65 °C; v/cm^{-1} (neat) 3310, 2978, 1701, 1594,

1494, 1414, 1392, 1239, 1154, 1048, 1023, 863, 758, 735, 696; δ_H (CDCl$_3$, 400 MHz) 1.57 (18H, s, 2×C(CH_3)$_3$), 6.80 (2H, s, br, NH), 7.32-7.41 (2H, m, Ar-H), 7.42-7.49 (2H, m, Ar-H), 7.55-7.63 (2H, m, Ar-H), 7.76 (1H, s br, Ar-H); δ_c (CDCl$_3$, 100 MHz) 28.4, 81.1, 127.2, 127.4, 128.8, 140.4, 153.9; MS (ES$^+$) m/z 407 (M+Na, 55%); HRMS (ES$^+$) 407.1947 calculated for C$_{22}$H$_{28}$N$_2$O$_4$Na$^+$ (M+Na$^+$), found 407.1938, Δ= -2.2 ppm.

tert-Butyl *N*-(2-{[(tert-butoxy)carbonyl]amino}-5-(2-methylphenyl)phenyl)carbamate 39a

The synthesis was carried out according to the general procedure E in two separate vials, each using 4-Br di-Boc diamine **38** (300 mg, 0.77 mmol, 1.0 eq.), 2-Methylphenylboronic acid (210 mg, 1.54 mmol, 2.0 eq.), Pd(dppf)Cl$_2$ (125 mg, 0.15 mmol, 0.2 eq.), NaHCO$_3$ (653 mg, 6.16 mmol, 8.0 eq. in 5.5 mL H$_2$O) in 2-(2-ethoxyethoxy)ethanol (8 mL). The crude product was purified by column chromatography (CH$_2$Cl$_2$/Hex 7:3) to give the biaryl **39a** as a pale yellow solid (339 mg, 0.85 mmol, 55%). R$_f$: 0.2 (4:6 Hex/CH$_2$Cl$_2$); mp: 55-59 °C; v/cm^{-1} (neat) 3305, 2978, 1702, 1455, 1484, 1367, 1247, 1154, 1049, 1023, 757, 735; δ_H (CDCl$_3$, 400 MHz) 1.51 (9H, s, C(CH_3)$_3$), 1.54 (9H, s, C(CH_3)$_3$), 2.28 (3H, s, CH_3), 6.77 (1H, br s, Ar-H), 7.09 (1H, dd, J 8.2 and 1.9 Hz, Ar-H), 7.18-7.22 (2H, m, Ar-H), 7.22-7.25 (2H, m, Ar-H), 7.45 (1H, br s, NH), 7.52 (1H, br s, NH); δ_C (CDCl$_3$, 100 MHz) 20.7, 28.4, 81.1, 125.9, 126.4, 127.4, 129.9, 130.4, 135.5, 141.1, 153.9; MS (ES$^+$) m/z 421 (M+Na$^+$, 100%), 199 (M-2×boc$^+$, 32%); HRMS (ES$^+$) 421.2103 calculated for C$_{23}$H$_{30}$N$_2$O$_4$Na$^+$ (M+Na$^+$) found 421.2092, Δ= -2.6 ppm.

tert-Butyl *N*-(2-{[(tert-butoxy)carbonyl]amino}-5-(4-methylphenyl)phenyl)carbamate 39b
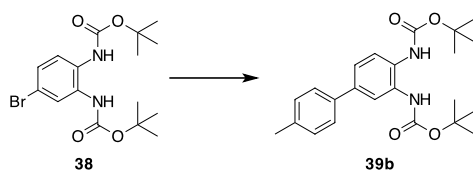
The reaction was conducted according to the general procedure E in two vials, each with 4-Br di-Boc diamine **38** (300 mg, 0.77 mmol, 1.0 eq.), 4-methylphenylboronic acid (211 mg, 1.54 mmol, 2.0 eq.), Pd(dppf)Cl$_2$ (125 mg, 0.15 mmol, 0.2 eq.), NaHCO$_3$ (653 mg, 6.16 mmol, 8.0 eq. in 5.5 mL H$_2$O) in 2-(2-ethoxyethoxy)ethanol (8 mL). The crude product was purified by column chromatography (CH$_2$Cl$_2$/Hex 7:3) to give the biaryl **39b** as a pale yellow solid (301 mg, 0.76 mmol, 49%). R$_f$: 0.1 (4:6 Hex/CH$_2$Cl$_2$); mp: 61-66 °C; v/cm^{-1} (neat) 3307, 2977, 2931, 1696, 1506, 1366, 1240, 1155, 1050, 1024, 808, 770, 736; δ_H (CDCl$_3$, 400 MHz) 1.53 (18H, s, 2×C(CH_3)$_3$), 2.38 (2H, s, CH_3), 6.76, (2H, br s, Ar-H), 7.22 (2H, d, J 7.9, Ar-H), 7.33 (1H, dd, J 8.4 and 2.1, Ar-H), 7.42-7.48 (2H, m, Ar-H), 7.53 (1H, br s, Ar-H), 7.70 (1H, br s,

Ar-H); δ_c (CDCl$_3$, 100 MHz) 21.2, 28.4, 81.1, 126.9, 129.6, 137.3, 153.9; MS (ES$^+$) m/z 421 (M+Na$^+$, 90%), 199 (M-2×boc$^+$, 43%); HRMS (ES$^+$) 421.2103 calculated for C$_{23}$H$_{30}$N$_2$O$_4$Na$^+$ (M+Na$^+$) found 421.2107, Δ= 0.9 ppm.

tert-Butyl *N*-(2-{[(tert-butoxy)carbonyl]amino}-5-(2-chlorophenyl)phenyl)carbamate 39c
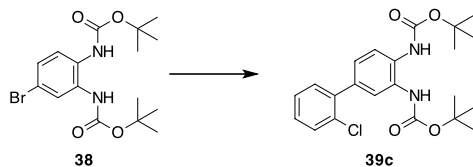
The reaction was carried out as described in the general procedure E in two identical batches, each with 4-Br di-Boc diamine **38** (251 mg, 0.65 mmol, 1.0 eq.), 2-chlorophenylboronic acid (204 mg, 1.30 mmol, 2.0 eq.), Pd(dppf)Cl$_2$ (100 mg, 0.13 mmol, 0.2 eq.), NaHCO$_3$ (557 mg, 5.3 mmol, 8.2 eq. in 4.8 mL H$_2$O) in 2-(2-ethoxyethoxy)ethanol (7.5 mL). The crude product was purified by column chromatography (CH$_2$Cl$_2$/Hex 7:3) to give the biaryl **39c** as a pale yellow solid (103.4 mg, 0.25 mmol, 19%). R$_f$: 0.1 (4:6 Hex/CH$_2$Cl$_2$); mp: 65-70 °C; v/cm^{-1} (neat) 3308, 2978, 1701, 1525, 1478, 1367, 1241, 1153, 1050, 1023, 756, 736; δ_H (CDCl$_3$, 400 MHz) 1.53 (18H, s, 2×C(CH_3)$_3$), 6.77 (2H, br s, Ar-H), 7.29-7.38 (2H, m, Ar-H), 7.38-7.44 (2H, m, Ar-H), 7.52-7.59 (2H, m, Ar-H), 7.73 (1H, br s, Ar-H); δ_c (CDCl$_3$, 100 MHz) 28.4, 81.1, 127.2, 127.4, 128.8, 140.4, 153.9; MS (ES$^+$) m/z 441/443 (M+Na$^+$, 100%), 199 (M-2×boc$^+$, 43%); HRMS (ES$^+$) 441.1557 calculated for C$_{22}$H$_{27}$N$_2$O$_4$Cl^{35}Na$^+$ (M+Na$^+$) found 441.1538, Δ= -4.3 ppm.

tert-Butyl *N*-(2-{[(tert-butoxy)carbonyl]amino}-5-(3-chlorophenyl)phenyl)carbamate 39d
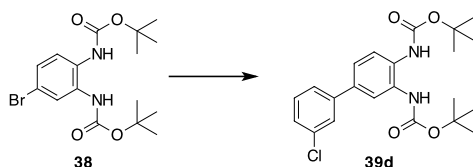
The synthesis was conducted as outlined in general procedure E in two vials, both with 4-Br di-Boc diamine **38** (300 mg, 0.77 mmol, 1.0 eq.), 3-chlorolphenylboronic acid (234 mg, 1.54 mmol, 2.0 eq.), Pd(dppf)Cl$_2$ (125 mg, 0.15 mmol, 0.2 eq.), sodium bicarbonate (655 mg, 6.17 mmol, 8.0 eq. in 5.5 mL H$_2$O) in 2-(2-ethoxyethoxy)ethanol (8 mL). The crude product was purified by column chromatography (CH$_2$Cl$_2$/Hex 7:3) to give the product **39d** as a pale yellow solid (283 mg, 0.68 mmol, 53%). R$_f$: 0.1 (4:6 Hex/CH$_2$Cl$_2$) mp: 60-63 °C; v/cm^{-1} (neat) 3304, 2978, 2933, 1698, 1527, 1478, 1391, 1366, 1241, 1151, 1047, 1024, 778, 693; δ_H (CDCl$_3$, 400 MHz) 1.53 (18H, s, 2×C(CH_3)$_3$), 6.76 (2H, br s, Ar-H), 7.29-7.34 (2H, m, Ar-H), 7.41-7.45 (1H, m, Ar-H), 7.48-7.55 (2H, m, Ar-H), 7.60-7.65 (1H, m, Ar-H), 7.69-7.74 (1H, m Ar-H); δ_c (CDCl$_3$, 100 MHz) 28.4, 77.4, 81.2, 125.4, 127.2, 127.4, 127.5, 134.7, 142.2, 153.9; MS (ES$^+$) m/z 441 (M+Na$^+$, 19%); HRMS (ES$^+$) 441.1557 calculated for C$_{22}$H$_{27}$N$_2$O$_4$Cl^{35}Na$^+$ (M+Na$^+$), found 441.1550, Δ= -1.6 ppm.

tert-Butyl *N*-(2-{[(tert-butoxy)carbonyl]amino}-5-(4-chlorophenyl)phenyl)carbamate 39e
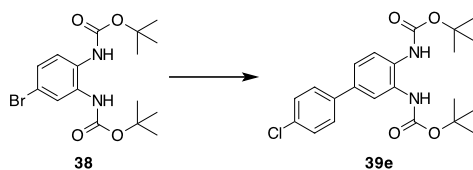
The reaction was carried out as described in general procedure E in two vials, both with 4-Br di-Boc diamine **38** (250 mg, 0.65 mmol, 1.0 eq.), 2-methylphenylboronic acid (201 mg, 1.29 mmol, 2.0 eq.), Pd(dppf)Cl$_2$ (100 mg, 0.13 mmol, 0.2 eq.), NaHCO$_3$ (553 mg, 5.22 mmol, 8.0 eq. in 4.8 mL H$_2$O) in 2-(2-ethoxyethoxy)ethanol (7.5 mL). The crude product was purified by column chromatography (CH$_2$Cl$_2$/Hex 7:3) to give the biaryl **39e** as a yellow solid (250.5 mg, 0.59 mmol, 46%). R$_f$: 0.1 (4:6 Hex/CH$_2$Cl$_2$); mp: 66-75 °C; v/cm^{-1} (neat) 3307, 2978, 1701, 1486, 1367, 1239, 1153, 1092, 1051, 1023, 1012, 812, 735; δ$_H$ (CDCl$_3$, 400 MHz) 1.53, (18H, s, 2×C(C*H$_3$*)$_3$), 6.75 (2H, br s, Ar-*H*), 7.30 (1H, dd, *J* 8.4 and 2.1 Hz, Ar-*H*), 7.35-7.39 (2H, m, Ar-*H*), 7.47-7.48 (2H, m, Ar-*H*), 7.55 (1H, d, *J* 8.5 Hz, Ar-*H*), 7.71 (1H, br s, Ar-*H*); δ$_c$ (CDCl$_3$, 100 MHz) 28.4, 77.4, 81.2, 127.4, 127.6, 128.4, 128.9, 133.5, 138.8, 153.9; MS (ES$^+$) *m/z* 441/443 (M+Na$^+$, 32%); HRMS (ES$^+$) 441.1557 calculated for C$_{22}$H$_{27}$N$_2$O$_4$Cl^{35}Na$^+$ (M+Na$^+$), found 441.1564, Δ= 1.6 ppm.

***tert*-Butyl N-(2-{[(tert-butoxy)carbonyl]amino}-5-(3,4-dichlorophenyl)phenyl)carbamate 39f**
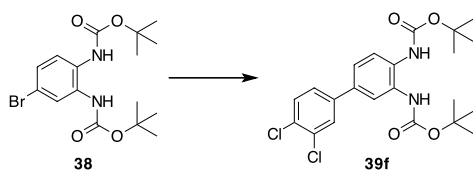
The synthesis was performed as described in the general procedure E in two separated vials, both with 4-Br di-Boc diamine **38** (250 mg, 0.66 mmol, 1.0 eq.), 3,4-dichloroboronic acid (300 mg, 1.55 mmol, 2.0 eq.), Pd(dppf)Cl$_2$ (127 mg, 0.13 mmol, 0.2 eq.), NaHCO$_3$ (560 mg, 5.28 mmol, 8.1 eq. in 4.8 mL H$_2$O) in 2-(2-ethoxyethoxy)ethanol (7.5 mL). The crude product was purified by column chromatography (CH$_2$Cl$_2$/Hex 6:4) to give the biaryl **39f** as an orange solid (142 mg, 0.31 mmol, 20%). R$_f$: 0.1 (4:6 Hex/CH$_2$Cl$_2$); mp: 64-70 °C; v/cm^{-1} (neat) 3305, 2979, 1699, 1593, 1474, 1367, 1241, 1152, 1050, 1025, 871, 813, 736; δ$_H$ (CDCl$_3$, 400 MHz) 1.53 (18H, s, 2×C(C*H$_3$*)$_3$), 6.77 (2H, s br, Ar-*H*), 7.28, (1H, dd, *J* 8.5 and 2.3 Hz, Ar-*H*), 7.35-7.40 (1H, m, Ar-*H*), 7.46 (1H, d, *J* 8.3 Hz, Ar-*H*), 7.46 (1H, d, *J* 8.3 Hz, Ar-*H*), 7.62 (1H, d, *J* 2.1 Hz, Ar-*H*); δ$_c$ (CDCl$_3$, 100 MHz) 28.3, 126.3, 128.7, 128.9, 129.9, 129.9, 130.7, 132.8, 140.3, 153.8; No Mass spectrum could be obtained from that compound.

tert-Butyl N-(2-{[(tert-butoxy)carbonyl]amino}-5-(4-methoxyphenyl)phenyl)carbamate 39g


38   **39g**
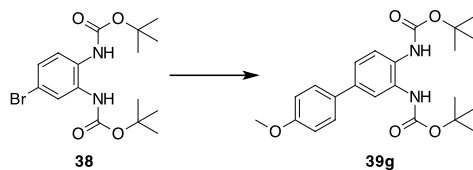
The reaction was carried out according to general procedure E in two vials, both with 4-Br di-Boc diamine **38** (257 mg, 0.67 mmol, 1.0 eq.), 4-methoxyphenylboronic acid (202 mg, 1.33 mmol, 2.0 eq.), Pd(dppf)Cl$_2$ (102 mg, 0.12 mmol, 0.2 eq.), NaHCO$_3$ (557 mg, 5.26 mmol, 8.0 eq. in 4.80 mL H$_2$O) in 2-(2-ethoxyethoxy)ethanol (7.50 mL). The crude product was purified by column chromatography (CH$_2$Cl$_2$/Hex 6:4) to give the biaryl **39g** as a yellow solid (85 mg, 0.21 mmol, 16%). R$_f$: 0.1 (4:6 Hex/CH$_2$Cl$_2$); mp: 58-63 °C; v/cm^{-1} (neat) 3314, 2976, 1709, 1508, 1367, 1244, 1162, 1042, 820; δ$_H$ (CDCl$_3$, 400 MHz) 1.53 (18H, s, 2×C(CH$_3$)$_3$), 3.84 (3H, s, OCH$_3$), 6.75 (2H, s br, NH), 6.92-6.98 (2H, m, Ar-H), 7.30 (1H, dd, J 8.8 and 1.8 Hz, Ar-H), 7.44-7.57 (2H, m, Ar-H), 7.69 (1H, s, Ar-H); δ$_c$ (CDCl$_3$, 100 MHz) 28.4, 55.5, 77.4, 81.0, 114.3, 128.2, 132.9, 154.0, 159.3; MS (ES$^+$) m/z 437 (M+Na, 52%); HRMS (ES$^+$) 437.2052 calculated for C$_{23}$H$_{30}$N$_2$O$_5$Na$^+$ (M+Na$^+$), found 437.2041, Δ= -2.5 ppm.

General Procedure F

The Boc-protected biaryl compound was dissolved in CH$_2$Cl$_2$. An excess of TFA was added and the reaction mixture stirred for 15 min. and the solvent and remaining TFA was removed under reduced pressure. The TFA salt was directly used for the next reaction. The TFA salt was dissolved in a 10:1 mixture EtOH and H$_2$O. Then 10 eq. of NaOH were added. The reaction mixture was stirred for 10 minutes before 10 eq. of carbon disulfide were added. The reaction mixture was heated to 50 °C for 4 h. After that time the reaction mixture was cooled to RT and the solvent and remaining carbon disulfide was removen in vacuo. The crude product was purified by flash column chromatography.

6-Phenyl-1H-2-mercaptobenzimidazole 37

39   **37**
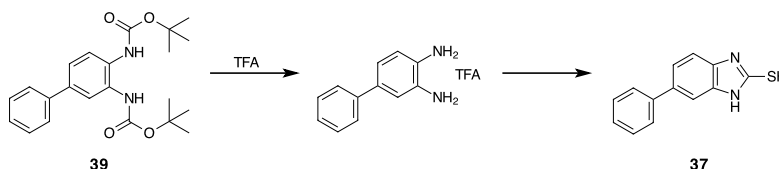
The synthesis was carried out according to general procedure F, using N-N'-di-Boc protected biaryl **39** (152 mg, 0.39 mmol, 1.0 eq.), TFA (0.5 mL, high excess), CS$_2$ (0.6 mL 9.88 mmol, 24.9 eq.), NaOH (161 mg, 4.03 mmol, 10.3 eq. in 1 mL H$_2$O) in EtOH (2 mL). Purification by column chromatography gave the 2-mercaptobenzimidazole **37** as a light brown solid (91 mg, 0.4 mmol, 100%) R$_f$: 0.4 (EtOAc/Hex, 4:6); mp: >240 °C; v/cm^{-1} (neat) 3065, 2339, 1598, 1465, 1301, 1184, 856, 807, 754, 659; δ$_H$ (MeOD-d$_4$, 400 MHz) 7.27 (1H, dd, J 8.2 and 0.8 Hz, Ar-H), 7.37 (1H, tt, J 7.4 and 1.3, Ar-H), 7.41-7.43 (2H, m, Ar-H), 7.44-7.45 (2H, m, Ar-H),

7.55-7.62 (2H, m, Ar-*H*); δ$_c$ (MeOD-d$_4$, 100 MHz) 107.8, 109.7, 121.7, 126.8, 128.5, 131.8, 133.1, 136.7, 140.9, 150.5, 168.4; No mass spectrum could be obtained.

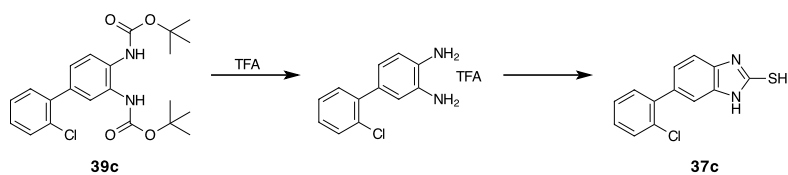### 6-(2-Methylphenyl)-1*H*-2-mercaptobenzimidazole 37a
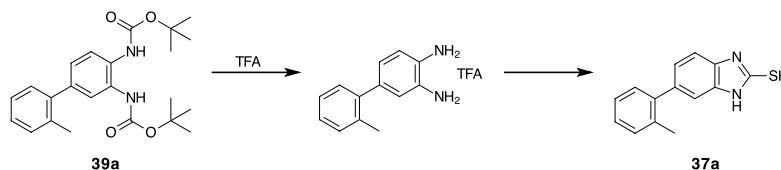
The reaction was carried out as described in the general procedure F, using *N,N'*-di-Boc protected 2-metyl biaryl **39a** (338.7 mg, 0.85 mmol, 1. 0 eq.), TFA (0.5 mL high excess) in CH$_2$Cl$_2$ (2.00 mL), CS$_2$ (0.77 mL, 12.75 mmol, 15.0 eq.), NaOH (340 mg, 8.5 mmol, 10.0 eq.) in EtOH (4 mL), H$_2$O (2 mL). The crude product was purified by column chromatography (dry loaded, gradient EtOAc/Hex 4:6 to 8:2) to give the 2-mercaptobenzimidazole **37a** as a pale yellow solid (146 mg, 0.61 mmol, 71%). R$_f$: 0.5 (EtOAc/Hex, 4:6); mp: >240 °C; v/cm^{-1} (neat) 3164, 3075, 3010, 2951, 2308, 1600, 1525, 1495, 1471, 1322, 1183, 983, 924, 857, 813, 753, 725; δ$_H$ (DMSO-d$_6$, 400 MHz) 2.21 (3H, s, C*H$_3$*), 7.02 (1H, d, *J* 1.5 Hz, Ar-*H*), 7.07 (1H, dd, *J* 8.1 and 1.6 Hz, Ar-*H*), 7.16-7.22 (2H, m, Ar-*H*), 7.22-7.30 (3H, m, Ar-*H*), 12.57 (2H, s br, N*H* and S*H*); δ$_c$ (DMSO-d$_6$, 100 MHz) 20.2, 109.1, 109.7, 123.5, 125.9, 127.2, 129.7, 130.3, 131.3, 132.4, 134.8, 135.6, 141.2, 168.5; MS (CI$^+$) *m/z* 240 (M, 18%); HRMS (CI$^+$) 240.0721 calculated for C$_{14}$H$_{12}$N$_2$S$^+$ (M), found 240.0729, Δ= 3.3 ppm.

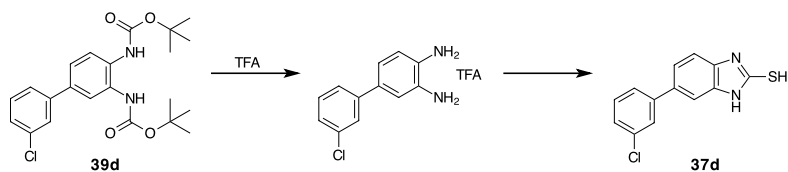### 6-(4-Methylphenyl)-1*H*-2-mercaptobenzimidazole 37b
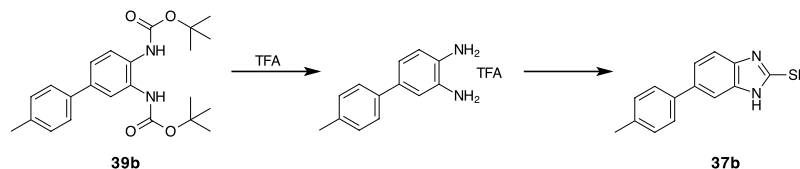
The synthesis was carried out as described in the general procedure F, using *N-N'*-di-Boc protected 4-methyl biaryl **39b** (301.7 mg, 0.75 mmol, 1.0 eq.), TFA (2.00 mL, high excess) in CH$_2$Cl$_2$ (2.00 mL), CS$_2$ (1.0 mL, 16.52 mmol, 21.7 eq.), NaOH (300 mg, 7.60 mmol, 10.1 eq.), EtOH (2 mL), H$_2$O (1 mL). Purification by column chromatography (dry loaded, gradient (EtOAc/Hex 4:6 to 8:2) afforded the 2-mercaptobenzimidazole **37b** as a white solid (137 mg, 0.72 mmol, 95%) R$_f$: 0.4 (EtOAc/Hex, 4:6); mp: >240 °C; v/cm^{-1} (neat) 3047, 2958, 2857, 2578, 2303, 1617, 1481, 1465, 1301, 1187, 791, 706, 620; δ$_H$ (MeOD-d$_4$, 400 MHz) 2.36 (3H, s, C*H$_3$*), 7.24 (3H, ddd, *J* 8.2, 4.1 and 0.8 Hz, Ar-*H*), 7.38 (1H, m, Ar-*H*), 7.41 (1H, dd, *J* 8.2 and 1.7 Hz, Ar-*H*), 7.45-7.49 (2H, m, Ar-*H*); δ$_c$ (MeOD-d$_4$, 100 MHz) 19.7, 107.5, 109.6, 121.8, 126.5, 129.1, 131.6, 133.0, 136.6, 136.7, 137.9, 168.2; MS (CI$^+$) *m/z* 241 (M+H$^+$, 35%); HRMS (CI$^+$) 241.0779 calculated for C$_{14}$H$_{13}$N$_2$S$^+$ (M+H$^+$), found 241.0791, Δ= -3.3 ppm.

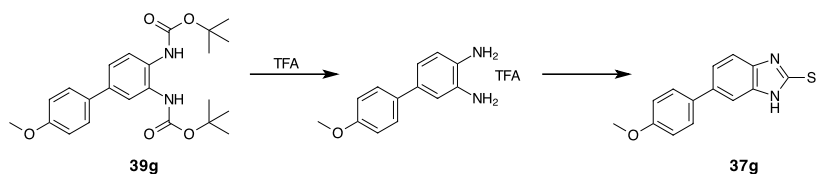### 6-(2-Chlorophenyl)-1*H*-2-mercaptobenzimidazole 37c

The reaction was carried out as described in the general procedure F, using *N-N'*-di-Boc protected 2-chloro biaryl **39c** (50 mg, 0.12 mmol, 1.0 eq.), TFA (1.00 mL, high excess) in CH_2Cl_2 (2.00 mL), CS_2 (0.11 mL, 1.8 mmol, 15 eq.), NaOH (50 mg, 1.2 mmol, 10 eq.) in EtOH (2 mL) and H_2O (1 mL). Column chromatography (dry loaded, EtOAc/Hex, 4:6 to 8:2) of the crude product afforded the pure 2-mercaptobenzimidazole **37c** as a pale yellow solid (33 mg, 0.51 mmol, 104%). R_f: 0.5 (4:6 EtOAc/Hex); mp: >240 °C; v/cm^{-1} (neat) 3068, 2317, 1598, 1441, 1185, 858, 808, 754, 696, 632; δ_H (MeOD-d$_4$, 400 MHz) 7.27 (1H, dd, *J* 8.2 and 0.8 Hz, Ar-*H*), 7.30-7.36 (1H, m, Ar-*H*), 7.39-7.46 (3H, m, Ar-*H*), 7.54-7.62 (2H, m, Ar-*H*); δ_c (MeOD-d$_4$, 100 MHz) 107.8, 109.7, 121.9, 126.7, 126.8, 128.5, 131.8, 133.1, 136.7, 140.9, 153.7, 168.4; No mass spectrum could be obtained from this compound.

6-(3-Chlorophenyl)-1*H*-2-mercaptobenzimidazole 37d

The reaction was carried out as described in the general procedure F, using *N-N'*-di-Boc protected 3-chloro biaryl **39d** (283 mg, 0.68, 1.0 eq.), TFA (2.00 mL, large excess) in CH_2Cl_2 (3.00 mL), CS_2 (0.7 mL 11.61 mmol, 17.1 eq.) NaOH (300 mg, 7.5 mmol, 11.0 eq.) in EtOH (4.00 mL) and H_2O (2.00 mL). The crude product was purified by column chromatography (dry loaded, gradient EtOAc/Hex 4:6 to 8:2) to give the pure 2-mercaptobenzimidazole **37d** as a white solid (149 mg, 0.57 mmol, 84%). R_f: 0.4 (EtOAc/Hex, 4:6); mp: >240 °C; v/cm^{-1} (neat) 3063, 2325, 1594, 1498, 1465, 1186, 770, 686, 635; δ_H (DMSO-d$_6$, 400 MHz) 7.22 (1H, d, *J* 8.3 Hz, Ar-*H*), 7.34-7.42 (2H, m, Ar-*H*), 7.43-7.46 (2H, m, Ar-*H*), 7.60 (1H, dt, *J* 7.8 and 1.4 Hz, Ar-*H*), 7.68 (1H, t, *J* 1.9 Hz, Ar-*H*), 12.67 (2H, s, N*H* and S*H*); δ_c (DMSO-d$_6$, 100 MHz) 107.6, 109.9, 121.7, 125.5, 126.4, 126.9, 130.8, 132.3, 133.1, 133.7, 142.5, 168.9; MS (ES$^+$) *m/z* 261/263 (M+H$^+$, 100%); HRMS (ES$^+$) 261.0253 calculated for $C_{13}H_{10}N_2SCl^{35+}$ (M+H$^+$), found 261.0255, Δ= 0.8 ppm.

### 6-(3,4-Dichlorophenyl)-1*H*-2-mercaptobenzimidazole 37f
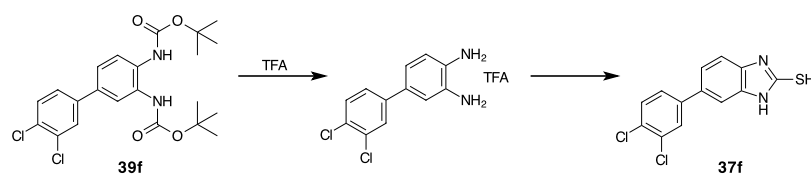
The synthesis was conducted in accordance with the general procedure F, using *N-N'*-di-Boc protected 3,4-dichloro biaryl **39f** (132 mg, 0.29 mmol, 1.0 eq.), TFA (0.50 mL, high excess) in CH_2Cl_2 (2.00 mL), CS_2 (0.5 mL, 8.40 mmol, 28.9 eq.), NaOH (120 mg, 3.00 mmol, 10.3 eq.) in EtOH (4.00 mL) and H_2O (2.00 mL). Purification by column chromatography (dry loaded, gradient (EtOAc/Hex, 4:6 to 8:2) afforded the pure 2-mercaptobenzimidazole **37f** as a light yellow solid (84 mg, 0.28 mmol, 98%). R_f: 0.4 (EtOAc/Hex, 4:6); mp: >240 °C; v/cm^{-1} (neat) 3099, 2578, 1465, 1188, 1135, 797, 749, 620; (DMSO-d$_6$, 400 MHz) 7.21 (1H, d, *J* 8.3 Hz, Ar-*H*), 7.36-7.41 (1H, m, Ar-*H*), 7.46 (1H, dd, *J* 8.2 and 1.7 Hz, Ar-*H*), 7.63 (1H, dd, *J* 8.4 and 2.0 Hz, Ar-*H*), 7.68 (1H, d, *J* 8.3 Hz, Ar-*H*), 7.90 (1H, d, *J* 2.1 Hz, Ar-*H*), 12.68 (1H, s, N*H*), 12.73 (1H, s, br, S*H*); δ_c (DMSO-d$_6$, 100 MHz) 108.1, 110.3, 122.1, 127.4, 128.9, 130.2, 131.4, 132.1, 132.9, 133.5, 141.4, 168.5; No mass spectrum could be obtained.

### 6-(4-Methoxyphenyl)-1*H*-2-mercaptobenzimidazole 37g

The reaction was carried out as described in the general procedure F, using *N-N'*-di-Boc protected 4-methoxy biaryl **39g** (75 mg, 0.49 mmol, 1.0 eq.), TFA (1.50 mL, high excess), in CH_2Cl_2 (2.00 mL), CS_2 (0.23 mL, 4.9 mmol, 10 eq.), NaOH (196 mg, 4.9 mmol, 10 eq. in 1.50 mL H_2O) in EtOH (4.00 mL). Column chromatography of the crude product afforded the pure 2-mercaptobenzimidazole **37g** as a pale yellow solid (133 mg, 0.51 mmol, 104%). R_f: 0.5 (4:6 EtOAc/Hex); mp: 215-220 °C; v/cm^{-1} (neat) 3534, 3110, 2835, 1608, 1530, 1486, 1285, 1249, 1205, 1176, 1035, 1018, 833, 805; (MeOD-d$_4$, 400 MHz) 3.83 (3H, s, OC*H*$_3$), 6.95-7.01 (2H, m, Ar-*H*), 7.24 (1H, dd, *J* 8.3 and 0.8 Hz, Ar-*H*), 7.36 (1H,dd, *J*, 1.7 and 0.7 Hz, Ar-*H*), 7.39 (1H, dd, *J* 1.7 and 0.7 Hz, Ar-*H*), 7.47-7.56 (2H, m, Ar-*H*); δ_c (MeOD-d$_4$, 100 MHz) 55.8, 108.7, 111.0, 115.3, 123.0, 129.1, 132.8, 134.5, 137.8, 160.7; No Mass spectrum could be obtained for this compound.
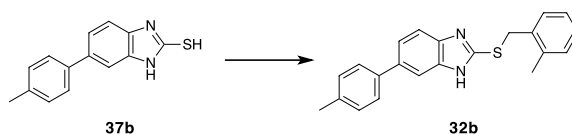
General Procedure G [84]

The 2-mercapto-6-aryl benzimidazole was dissolved in DMF. NaOMe was added and the solution stirred for 30 min. Then 2-methylbenzyl bromide was added and the reaction mixture stirred for 16 h. After that, H_2O was added and the mixture extracted with CH_2Cl_2. The combined organic layer was dried over Na_2SO_4 and reduced *in vacuo*. The crude product was purified by column chromatography.

2-{[(2-Methylphenyl)methyl]sulfanyl}-6-phenyl-1*H*-benzimidazole 32
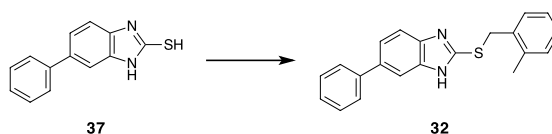
The reaction was performed as outlined in the general procedure G, using 6-aryl-2-mercaptobenzimidazole **37** (81 mg, 0.35 mmol, 1.0 eq.), NaOMe (25 mg, 0.47 mol, 1.3 eq.) and 2-methylbenzyl bromide (63 µL, 0.47 mmol, 1.3 eq.) in DMF (2 mL). After purification *via* column chromatography (CH$_2$Cl$_2$) the pure benzimidazole thioether **32** was obtained as a white solid (44 mg, 0.13 mmol, 37%). R$_f$ 0.2 (CH$_2$Cl$_2$); mp: 197-208 °C; v/cm^{-1} (neat) 3379, 3045, 2941, 2859, 2757, 1599, 1444, 1389, 1282, 1227, 982, 732, 697; δ$_H$ (CDCl$_3$, 400 MHz) 2.43 (3H, s, C*H*$_3$), 4.60 (2H, s, PhC*H*$_2$), 7.13 (1H, td, *J* 6.6 and 3.0 Hz, Ar-*H*), 7.17-7.23 (2H, m, Ar-*H*), 7.34 (2H, dd, *J* 8.9 and 7.2 Hz, Ar-*H*), 7.41-7.53 (3H, m, Ar-*H*), 7.56-7.67 (3H, m, Ar-*H*), 7.71 (1H, s br, Ar-*H*); δ$_C$ (CDCl$_3$, 100 MHz) 19.4, 35.8, 122.5, 126.5, 127.1, 127.5, 128.3, 128.9, 130.2; MS (ES$^+$) *m/z* 331 (M+H, 100%); HRMS (ES$^+$) 331.1269 calculated for C$_{21}$H$_{19}$N$_2$S$^+$ (M+H$^+$), found 331.1285, Δ= 4.8 ppm.

6-(2-Methylphenyl)-2-{[(2-methylphenyl)methyl]sulfanyl}-1*H*-benzimidazole 32a
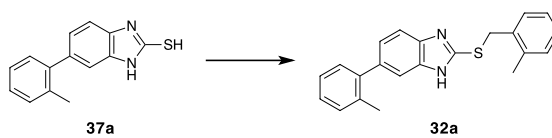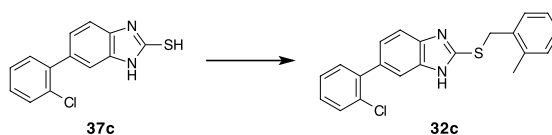

The synthesis was carried out according to general procedure G, using 6-aryl-2-mercaptobenzimidazole **37a** (134 mg, 0.55 mmol, 1.0 eq.), NaOMe (39 mg, 0.72 mmol, 1.3 eq.), 2-methylbenzyl bromide (96 µL, 0.72 mmol, 1.3 eq.) in DMF (4 mL). The crude product was purified by column chromatography to give the benzimidazole thioether **32a** as a yellow solid (92 mg, 0.27 mmol, 49%). R$_f$ 0.3 (CH$_2$Cl$_2$); mp: 183-186 °C; v/cm^{-1} (neat) 3025, 2929, 2625, 1632, 1447, 1393, 1327, 1266, 1229, 988, 816, 756, 730; δ$_H$ (CDCl$_3$, 400 MHz) 2.27, (3H, s, C*H*$_3$), 2.36 (3H, s, C*H*$_3$), 4.59 (2H, PhC*H*$_2$), 7.08 (1H, td, *J* 7.2 and 1.9 Hz, Ar-*H*), 7.12-7.15 (1H, m, Ar-*H*), 7.17 (2H, td, *J* 8.4 and 1.6 Hz, Ar-*H*), 7.23-7.33 (5H, m, Ar-*H*), 7.49 (1H, d, *J* 1.6 Hz, Ar-*H*), 7.57 (1H, d, *J* 8.2 Hz, Ar-*H*); δ$_C$ (CDCl$_3$, 100 MHz) 19.3, 20.7, 35.8, 124.3, 125.8, 126.4, 127.2, 128.2, 130.1, 130.3, 130.4, 130.7, 134.1, 135.7, 136.8, 137.2, 142.27 (s), 150.6; MS (ES$^+$) *m/z* 345 (M+H, 100%); HRMS (ES$^+$) 345.1425 calculated for C$_{22}$H$_{21}$N$_2$S$^+$ (M+H$^+$), found 345.1443, Δ= 5.2 ppm.

6-(4-Methylphenyl)-2-{[(2-methylphenyl)methyl]sulfanyl}-1*H*-benzimidazole 32b

The synthesis was performed using the general procedure G, with 6-aryl-2-mercaptobenzimidazole **37b** (162 mg, 0.67 mmol, 1.0 eq.) NaOMe (47 mg, 0.88 mmol, 1.3

eq.) and 2-methylbenzyl bromide (120 µL, 0.88 mmol, 1.3 eq.) in DMF (5 mL). The product was purified by column chromatography (CH_2Cl_2) to give the benzimidazole thioether **32b** as a yellow glassy solid (99 mg, 0.29 mmol, 43%). R$_f$: 0.3 (CH_2Cl_2); mp: 208-212 °C; v/cm^{-1} (neat) 3069, 2301, 1601, 1469, 1306, 1187, 861, 810; δ$_H$ (CDCl$_3$, 400 MHz) 2.40 (3H, s, CH_3), 2.41 (3H, s, CH_3), 4.59 (2H, s, PhCH_2), 7.11 (1H, td, *J* 6.9 and 2.6 Hz, Ar-*H*), 7.16-7.23 (2H, m, Ar-*H*), 7.25 (2H, d, *J* 7.6 Hz, Ar-*H*), 7.31 (1H, d, *J* 7.31 Hz, Ar-*H*), 7.46 (1H, dd, *J* 8.4 and 1.7 Hz, Ar-*H*), 7.51 (1H, d, *J* 8.1 Hz, Ar-*H*), 7.57 (1H, s br, Ar-*H*); δ$_C$ (CDCl$_3$, 100 MHz) 19.4, 21.2, 35.8, 122.3, 126.5, 127.3, 128.3, 129.6, 130.2, 130.8, 134.4, 136.3, 136.8, 137.2, 138.9, 150.4; MS (ES$^+$) *m/z* 345 (M+H, 100%); HRMS (ES$^+$) 345.1425 calculated for $C_{22}H_{21}N_2S^+$ (M+H$^+$), found 345.1436, Δ= 3.2 ppm.

6-(2-Chlorophenyl)-2-{[(2-methylphenyl)methyl]sulfanyl}-1*H*-benzimidazole 32c

The reaction was conducted as describes in the general procedure G, using 6-aryl-2-mercaptobenzimidazole **37c** (26.6 mg, 0.10 mmol, 1.0 eq.), NaOMe (7.01 mg, 0.13 mmol, 13 eq.), 2-methybenzyl bromide (17 µL, 0.13 mmol, 1.3 eq.) in DMF (0.5 mL). The crude product was purified by column chromatography (CH_2Cl_2) affording the benzimidazole thioether **32c** as a white solid (11 mg, 0.03 mmol, 32%). R$_f$: 0.2 (CH_2Cl_2); mp: 177-179 °C; v/cm^{-1} (neat) 3026, 1603, 1523, 1431, 1386, 1270, 1229, 982, 820, 753, 373, 697, 668, 639; δ$_H$ (CDCl$_3$, 400 MHz) 2.41, (3H, s, CH_3), 4.60 (2H, s, PhCH_2), 7.11 (1H, td, *J* 6.9 and 2.5 Hz, Ar-*H*), 7.16-7.22 (2H, m, Ar-*H*), 7.31 (1H, d, *J* 8.73 Hz, Ar-*H*), 7.33-7.37 (1H, m, Ar-*H*), 7.41-7.51 (2H, m, Ar-*H*), 7.57-7.62 (2H, m, Ar-*H*), 7.62 (1H, d, *J* 1.5 Hz, Ar-*H*), 7.73 (1H, s br, Ar-*H*); δ$_C$ (CDCl$_3$, 100 MHz) 19.3, 35.7, 122.5, 126.4, 126.9, 127.4, 128.2, 128.8, 130.1, 134.1, 136.4, 137.1, 141.5, 150.4; MS (ES$^+$) *m/z* 331 (M-Cl, 100%), 365 (M+H$^+$, 3%); HRMS (ES$^+$) 365.0879 calculated for $C_{21}H_{18}N_2SCl^+$ (M+H$^+$), found 365.0875, Δ= -1.1 ppm.

6-(3-Chlorophenyl)-2-{[(2-methylphenyl)methyl]sulfanyl}-1*H*-benzimidazole 32d
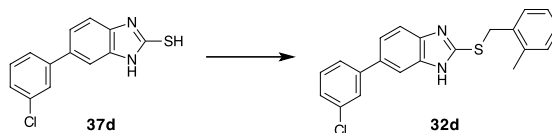
The synthesis was carried out in accordance to the general procedure G, using 6-aryl-2-mercaptobenzimidazole **37d** (139 mg, 0.53 mmol, 1.0 eq.), NaOMe (37 mg, 0.69 mmol, 1.3 eq.), 2-methylbenzyl bromide (92 µL, 0.69 mmol, 1.3 eq.) in DMF (4 mL). After the purification by column chromatography (CH_2Cl_2) the benzimidazole thioether **32d** was obtained as a pale yellow glassy solid (19 mg, 0.05 mmol, 10%). R$_f$: 0.2 (CH_2Cl_2); mp: 50-56 °C; v/cm^{-1} (neat) 2923, 2851, 2802, 2624, 1592, 1563, 1427, 1383, 1336, 1279, 1097, 1079, 1029, 983, 886, 816, 777, 730, 693, 642; δ$_H$ (CDCl$_3$, 400 MHz) 2.43 (3H, s, CH_3), 4.62 (2H, s, PhCH_2), 7.09-7.16 (1H, m, Ar-*H*), 7.17-7.22 (1H, m, Ar-*H*), 7.30-7.44 (3H, m, Ar-*H*), 7.38-7.57 (3H, m, Ar-*H*),

7.48-7.70 (2H, m, Ar-*H*), 7.80 (1H, s, Ar-H); MS (ES$^+$) *m/z* 365/367 (M+H$^+$, 100%); HRMS (ES$^+$) 365.0879 calculated for $C_{21}H_{18}N_2SCl^{35+}$ (M+H$^+$), found 365.0895, Δ= 4.4 ppm.

6-(4-Chlorophenyl)-2-{[(2-methylphenyl)methyl]sulfanyl}-1*H*-benzimidazole 32e
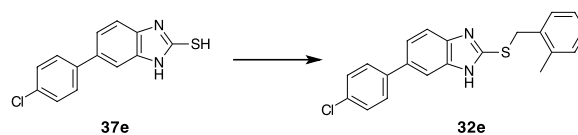

The reaction was carried out as described in the general procedure G, using 6-aryl-2-mercaptobenzimidazole **37e** (44 mg, 0.17 mmol, 1.0 eq.), NaOMe (13 mg, 0.24 mmol, 1.4 eq.), 2-methylbenzyl bromide (29 μL, 0.22 mmol, 1.3 eq.), in DMF (2 mL) After purification by column chromatography (CH$_2$Cl$_2$) the benzimidazole thioether **32e** was obtained as a white solid (16 mg, 0.04 mmol, 24%). R$_f$: 0.4 (CH$_2$Cl$_2$); mp: 186-192 °C; δ$_H$ (CDCl$_3$, 400 MHz) 2.43 (3H, s, C*H*$_3$), 5.55 (2H, s, PhC*H*$_2$), 6.50 (1H, d, *J* 7.8 Hz, Ar-*H*), 7.06 (1H, t, *J* 7.5 Hz, Ar-*H*), 7.19-7.31 (3H, m, Ar-*H*), 7.40 (4H, q, *J* 9.8, Ar-*H*), 7.53-7.64 (1H, m, Ar-*H*), 7.98 (1H, d, *J* 8.6 Hz, Ar-*H*); δ$_H$ (CDCl$_3$, 400 MHz) 19.3, 46.6, 109.3, 122.2, 123.8, 125.2, 126.8, 128.2, 128.9, 129.1, 130.8, 132.8, 133.8, 134.8, 136.5, 138.3, 139.5, 140.9; MS (ES$^+$) *m/z* 365/367 (M+H, 21%); HRMS (ES$^+$) 365.0879 calculated for $C_{21}H_{18}N_2SCl^{35+}$ (M+H$^+$), found 365.0866, Δ= -3.6 ppm.

**6-(3,4-Dichlorophenyl)-2-{[(2-methylphenyl)methyl]sulfanyl}-1*H*-benzimidazole 32f**
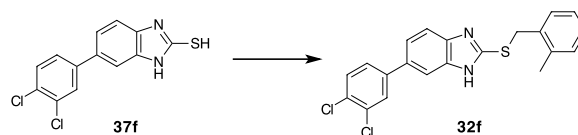
The reaction was carried out as described in general procedure G, using 6-aryl-2-mercaptobenzimidazole **37f** (70 mg, 0.24 mmol, 1.0 eq.), NaOMe (16.6 mg, 0.31 mmol, 1.3 eq.), 2-methylbenzyl bromide (41 μL, 0.31 mmol, 1.3 eq.) in DMF (2 mL). Purification by column chromatography gave the benzimidazole thioether **32f** as a yellow solid (21 mg, 0.05 mmol, 22%). R$_f$: 0.5 (CH$_2$Cl$_2$); mp: 67-73 °C; v/cm^{-1} (neat) 3387, 3019, 2921, 2853, 2803, 2619,1628, 1591, 1554, 1433, 1333, 1280, 1225, 1133, 1093, 1028, 985, 807, 732; δ$_H$ (CDCl$_3$, 400 MHz) 2.40 (3H, s, C*H*$_3$), 4.60 (2H, s, PhC*H*$_2$), 7.12 (1H, dt, *J* 9.2 and 4.6 Hz, Ar-*H*), 7.15-7.23 (2H, m, Ar-*H*), 7.31 (1H, dt, *J* 7.4 and 2.2 Hz, Ar-*H*), 7.40 (2H, td, *J* 8.8 and 1.9 Hz, Ar-*H*), 7.50 (2H, dd, *J* 15.0 and 8.4 Hz, Ar-*H*), 7.55-7.61 (1H, m, Ar-*H*), 7.67 (1H, dd, *J* 6.3 and 2.2 Hz); δ$_C$ (CDCl$_3$, 100 MHz) 19.4, 35.7, 122.0, 126.5, 126.7, 128.4, 128.7, 129.2, 130.8, 132.9, 133.7, 134.1, 137.2, 141.8, 151.4; MS (ES$^+$) *m/z* 399/401/404 (M+H, 100%); HRMS (ES$^+$) 399.0490 calculated for $C_{21}H_{17}N_2SCl^{35}_2{}^+$ (M+H$^+$), found 399.0501, Δ= 2.8 ppm.

6-(4-Methoxyphenyl)-2-{[(2-methylphenyl)methyl]sulfanyl}-1*H*-benzimidazole 32g
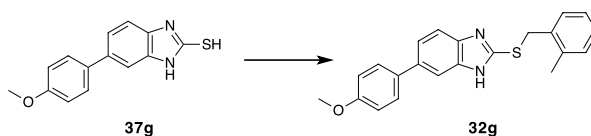
The synthesis was conducted according to the general procedure G, using 6-aryl-2-mercaptobenzimidazole **37g** (133 mg, 0.51 mmol, 1.0 eq.), NaOMe (36 mg, 0.66 mmol, 1.3 eq.), 2-methylbenzyl bromide (9 µL, 0.66 mmol, 1.3 eq.) in DMF (4.3 mL). Purification by column chromatography (2% MeOH/CH$_2$Cl$_2$) afforded the pure benzimidazole thioether **32g** as a pale yellow solid (40 mg, 0.11 mmol, 22%). R$_f$: 0.2 (CH$_2$Cl$_2$); mp: 190-194 °C; v/cm^{-1} (neat) 2935, 1733, 1608, 1527, 1437, 1387, 1227, 1178, 1034, 981, 833, 809, 735; δ$_H$ (CDCl$_3$, 400 MHz) 2.46 (3H, s, C*H$_3$*), 3.88 (3H, s, OC*H$_3$*), 4.62 (2H, s, PhC*H$_2$*), 7.01 (2H, d, *J* 8.7 Hz, Ar-*H*), 7.11-7.18 (1H, m, Ar-*H*), 7.22 (2H, dd, *J* 4.0 and 1.7 Hz, Ar-*H*), 7.31-7.37 (1H, m, Ar-*H*), 7.45 (1H, dd, *J* 8.4 and 1.7 Hz, Ar-*H*), 7.57 (2H, d, *J* 8.7 Hz, Ar-*H*), 7.67 (1H, s br, Ar-*H*); δ$_C$ (CDCl$_3$, 100 MHz) 19.0, 29.7, 55.3, 114.2, 114.3, 126.4, 128.4, 130.1, 130.6, 137.3, 137.5, 150.1, 159.1; MS (ES$^+$) *m/z* 361 (M+H, 100%); HRMS (ES$^+$) 361.1375 calculated for C$_{22}$H$_{21}$N$_2$OS$^+$ (M+H$^+$), found 361.1376, Δ= 0.3 ppm.

6-Bromo-2-{[(2-methylphenyl)methyl]sulfonly}-1*H*-benzimidazole 33
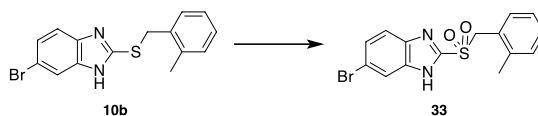

6-Bromo benzimidazole benyl ether **10b** (279 mg, 0.84 mmol, 1.0 eq.) was dissolved in CH$_2$Cl$_2$. Peracetic acid (0.6 mL, high excess) was added to the reaction mixture, which was heated to 40 °C for 2 h. After that time the solvent and remaining acid was removed under reduced pressure. The cure product was purified by column chromatography (dry loaded, 1% MeOH/CH$_2$Cl$_2$) to give the product **33** as a white solid (115 mg, 0.32 mmol, 38%). R$_f$: 0.6 (1% MeOH/CH$_2$Cl$_2$) mp: 175-181 °C; v/cm^{-1} (neat) 2929, 2461, 2352, 2198, 2146, 2034, 2003, 1331, 1132, 915, 812, 785, 748; δ$_H$ (CDCl$_3$, 400 MHz) 2.33 (3H, s, C*H$_3$*), 4.83 (2H, s, PhC*H$_2$*), 6.84-7.06 (2H, m, Ar-*H*), 7.17 (2H, dd, *J* 6.1 and 1.8 Hz, Ar-*H*), 7.51 (1H, dd, *J* 8.7 and 1.9 Hz, Ar-*H*), 7.59 (1H, d, *J* 8.7 Hz, Ar-*H*), 7.83 (1H, d, *J* 1.8 Hz, Ar-*H*); *m/z* 366 (M+H, 100%); HRMS (ES$^+$) 364.9959 calculated for C$_{15}$H$_{14}$N$_2$O$_2$SBr$^+$ (M+H$^+$), found 364.9946, Δ= -3.6 ppm.

N-Boc-2-hydroxyaniline 42 [62]
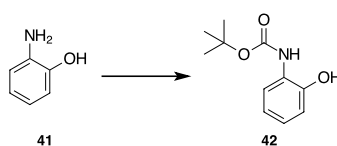
2-Hydroxyaniline **41** (500 mg, 4.58 mmol, 1.0 eq.) was dissolved in THF (10 mL). Then, Boc$_2$O (1.99 g, 9.16 mmol, 2.0 eq.) was added to the reaction mixture, which was stirred at RT for 16 h. The crude product was recrystallised from Et$_2$O and hexane to give the product

42 as pale brown crystals (929.5 mg, 4.44 mmol, 97%). The spectrum is in agreement with the already obtained data. [62] δ_H (CDCl$_3$, 400 MHz) 1.53 (9H, s, C(CH_3)$_3$), 6.69 (1H, s br, NH), 6.85 (1H, ddd, J 7.9, 7.2 and 1.6 Hz, Ar-H), 6.96 (1H, dd, J 8.1, 1.6 Hz, Ar-H), 7.03 (1H, ddd, J 8.7, 7.3 and 1.6 Hz, Ar-H), 7.10 (1H, dd, J 7.8, 1.6 Hz, Ar-H), 8.15 (1H, s br, OH); m/z 209 (M+Na, 25%).

tert-Butyl *N*-[2-(2-methylpropoxy)phenyl]carbamate 43 [62]
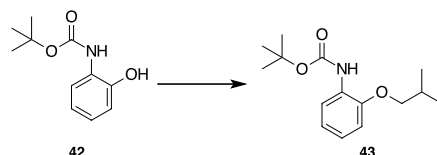
The reaction was carried out as described by Andrew Bayly. *N*-Boc 2-Hydroxyaniline **42** (500 mg, 2.39 mmol, 1.0 eq.) was dissolved in dry DMF (12.4 mL). 1-Bromo-2-methyl propane (0.39 mL, 3.59 mmol, 1.5 eq.) and Cs$_2$CO$_3$ (1.25 g, 3.82 mmol, 1.6 eq.) were added and the reaction mixture heated to 60 °C for 6 h. After that time the reaction mixture was cooled down to RT and H$_2$O was added. The phases were separated and the aqueous layer extracted with EtOAc. The combined organic layer was dried over Na$_2$SO$_4$ and the solvent removed *in vacuo*. Purification by column chromatography (Hex/EtOAc, 6:1) gave the product **43** as a yellow oil (367.8 mg, 1.38 mmol, 58%). The spectral data correspond to the data reported by Andrew Bayly. [62] δ_H (CDCl$_3$, 400 MHz) 1.06 (6H, d, J 6.7 Hz, CH(CH_3)$_2$), 1.55 (9H, s, C(CH_3)$_3$), 2.15 (1H, dq, J 6.8 and 6.7 Hz, CH$_2$CH), 3.78 (2H, d, J 6.6 Hz, Ar-OCH_2), 6.79-6.88 (1H, m, Ar-H), 6.91-6.99 (2H, m, Ar-H), 7.08 (1H, s br, N-H), 8.08 (1H, s br, Ar-H); m/z 265 (M, 100%).
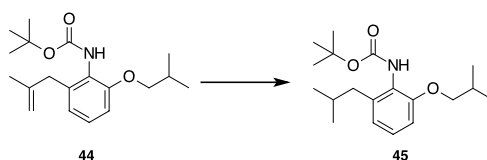
tert-Butyl *N*-[2-(2-methylprop-2-en-1-yl)-6-(2-methylpropoxy)phenyl] carbamate 44 [62]
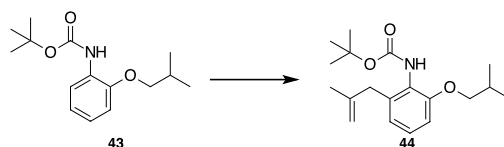
The reaction was carried out in analogy to the procedure described by Andrew Bayly. *tert*-Butyl *N*-[2-(2-methylpropoxy)phenyl]carbamate **43** (500 mg, 1.88 mmol, 1.0 eq.) was dissolved in dry THF (4 mL). The reaction mixture was cooled to -78 °C before ^{t}BuLi (1.6 M, 5.17 mL, 8.27 mmol, 4.4 eq.) was added slowly. The reaction mixture was warmed up to -10 °C and stirred for 1.5 h. Then, 3-bromo-2-methyl propene (0.42 mL, 4.14 mmol, 2.2 eq.) was added and the reaction mixture stirred at -10 °C for another 1.5 h. The reaction was quenched by adding saturated NH$_4$Cl solution. The phases were separated and the aqueous phase extracted with EtOAc. The combined organic layer was dried over Na$_2$SO$_4$ and removed under reduced pressure. Purification by column chromatography afforded the pure product **44** as a pale yellow oil (446 mg, 1.39 mmol, 74%). The spectra are in agreement with the data reported by Andrew Bayly. [62] δ_H (CDCl$_3$, 400 MHz) 1.02 (6H, d, J 6.7 Hz, CH(CH_3)$_2$),

1.47 (9H, s, C(C*H*₃)₃), 1.64 (3H, s, C(=C)C*H*₃), 2.09 (1H, dq, *J* 6.8, 6.6 Hz, CH₂C*H*), 3.39 (2H, s, Ar-C*H*₂), 3.72 (2H, d, *J* 6.5 Hz, OC*H*₂), 4.49-4.94 (1H, m, C=C*H*₂), 5.93 (1H, s br, N*H*), 6.75 (1H, dd, *J* 8.1, 1.3 Hz, Ar-*H*), 6.80 (1H, dd, *J* 7.9, 1.3 Hz, Ar-*H*), 7.11 (1H, t, *J* 7.9 Hz, Ar-*H*); *m/z* 320 (M+H, 10%).

tert-Butyl *N*-[2-(methylpropoxy)-6-(2-methylpropyl)phenyl] carbamate 45 [62]

The reaction was carried out as described in the PhD thesis by Andrew Bayly. In a two-neck flask *tert*-butyl *N*-[2-(2-methylprop-2-en-1-yl)-6-(2-methylpropoxy)phenyl] carbamate **44** (1.61 g, 5.01 mmol, 1.0 eq.) was dissolved in MeOH (4 mL). Pd/C (10 mol%, 182 mg, 0.1 eq.) was added to the reaction mixture. The flask was evacuated and carefully filled with hydrogen. This was repeated and a balloon with hydrogen was left connected to the flask. The reaction mixture was stirred for 4 h at RT. After that time the solution was filtered through Celite™ and washed with CH₂Cl₂. The solvent was removed to give the pure product as colourless **45** crystals (1.57 g, 4.91 mmol, 98%). The spectra correspond to the reported data by Andrew Bayly. [62] δ$_H$ (CDCl₃, 400 MHz) 0.88 (6H, d, *J* 6.5 Hz, Ar-CH₂CH(C*H*₃)₂), 1.02 (6H, d, *J* 6.7 Hz, OCH₂(C*H*₃)₂), 1.47 (9H, s, C(C*H*₃)₃), 1.89 (1H, dq, *J* 6.8, 6.7 Hz, CH₂C*H*) 2.08 (1H, dq, *J* 6.6, 6.7 Hz, OCH₂C*H*), 2.51 (2H, d, *J* 7.2 Hz, Ar-C*H*₂), 3.45 (3H, s, C*H*₃), 3.71 (2H, d, *J* 6.5 Hz, OC*H*₂), 5.86 (1H, s br, N*H*), 6.71 (1H, dd, *J* 8.3, 1.3 Hz, Ar-*H*), 6.76 (1H, dd, *J* 7.8 and 1.3 Hz, Ar-*H*), 7.10 (1H, t, *J* 7.9 Hz, Ar-*H*); *m/z* 222 (M-Boc⁺, 100%).
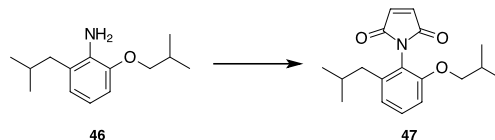
2-(2-Methylpropoxy)-6-(2-methylpropyl)aniline 46 [62]
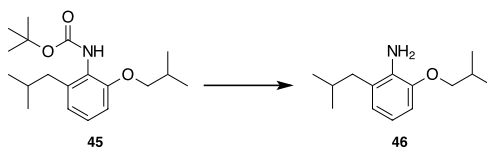
The reaction was carried out as described by Andrew Bayly. *tert*-Butyl *N*-[2-(methylpropoxy)-6-(2-methylpropyl)phenyl] carbamate **45** (431 mg, 1.34 mmol, 1.0 eq.) was dissolved in CH₂Cl₂ (5 mL). TFA (7.00 mL, high excess) was added and the reaction mixture was stirred for 15 minutes at RT. The excess of TFA and solvent was removed under reduced pressure. The pure product **46** was obtained as a brown oil (156 mg, 0.70 mmol, 52%) without further purification needed. The spectra obtained are in correspondence to the reported data by Andrew Bayly. [62] δ$_H$ (CDCl₃, 400 MHz) 0.98 (2H, d, *J* 6.6 Hz, Ar-CH₂CH(C*H*₃)₂), 1.07 (6H, d, *J* 6.7 Hz, OCH₂CH(C*H*₃)₂), 1.98 (1H, dq, *J* 6.8, 6.7 Hz, Ar-CH₂C*H*), 2.15 (1H, dq, *J* 6.8, 6.6

Hz, OCH$_2$CH), 2.42 (2H, d, J 7.2 Hz, Ar-CH_2), 3.78 (2H, d, J 6.5 Hz, OCH_2), 6.55-6.83 (3H, m, Ar-H); m/z 222 (M+H$^+$, 100%).

### N-[2-(2-Methylpropoxy)-6-(2-methylpropyl)phenyl] maleimide 47 [62]

The reaction was carried out as described in the PhD thesis by Ardrew Bayly. 2-(2-Methylpropoxy)-6-(2-methylpropyl)anline **46** (313 mg, 1.4 mmol, 1.0 eq.) and maleic anhydride (137 mg, 1.4 mmol, 1.0 eq.) were heated neat to 120 °C for 1 h. Then, the glassy product was dissolved in toluene (0.4 mL) and DMSO (0.1 mL) and H$_2$SO$_4$ (8 µL, 0.14 mmol, 0.1 eq.) was added. The reaction mixture was heated to 135 °C for 20 h. The crude product was purified by column chromatography to afford the product **47** as a yellow solid (371 mg, 123 mmol, 88%). The spectra were in agreement to the reported data by Andrew Bayly. [62] δ$_H$ (CDCl$_3$, 400 MHz) 0.85 (6H, d, J 6.6 Hz, Ar-CH$_2$CH(CH_3)$_2$), 0.89 (6H, d, J 6.7 Hz, OCH$_2$CH(CH_3)$_2$), 1.76 (1H, dq, J 13.6 and 6.8 Hz, Ar-CH$_2$CH), 1.94 (1H, dq, J 13.6 and 6.6 Hz, OCH$_2$CH), 2.33 (2H, d, J 7.3 Hz, Ar-CH_2), 3.67 (2H, d, J 6.2 Hz, OCH_2), 6.79 (1H, dd, J 8.3 and 1.2 Hz, Ar-H), 6.83-6.90 (3H, m, CH=CH, Ar-H), 7.27 (1H, t, J 8.02 Hz, Ar-H); m/z 302 (M+H$^+$, 5%).

3-(2-Methylbutyl)-N-benzylpyridinium bromide 60
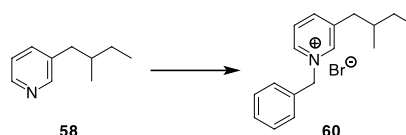
Benzyl bromide (0.45 mL, 3.7 mmol, 1.1 eq.) was dissolved in toluene, and added drop wise to a solution of 3-alkyl pyridine **58** (500 mg, 3.35 mmol, 1.0 eq.) in acetone (0.4 mL). The reaction mixture was stirred at RT for 16 h. The remaining solvent and benzyl bromide were removed *in vacuo* to afford the pure product **60** as a white solid (867 mg, 2.7 mmol, 81%). R$_f$: 0.0 (2% MeOH/ CH2Cl2); mp: 209-212 °C; v/cm^{-1} (neat) 2961, 2932, 1630, 1497, 1448, 1455, 1381, 1359, 1196, 1144, 740, 707, 691; δ$_H$ (CDCl$_3$, 400 MHz) 0.75 (3H, d, J 6.6 Hz, CH$_2$CH_3), 0.81 (3H, t, J 7.4 Hz, CH$_2$CH_3CH$_2$), 1.05-1.18 (1H, m, CH_2CH$_3$), 1.20-1.33 (1H, m, CH_2CH$_3$), 1.61-1.82 (1H, m, CH$_2$CHCH$_2$), 2.57 (1H, dd, J 13.8 and 8.2 Hz, Ar-CH_2), 2.80 (1H, dd, J 13.8 and 6.1 Hz, Ar-CH_2), 6.26 (2H, s, PhCH_2), 7.10-7.50 (3H, m, Ar-H), 7.69 (2H, ddd, J 5.4, 2.8 and 1.6 Hz, Ar-H), 7.92 (1H, dd, J 8.0 and 5.9, Ar-H), 8.09 (1H, dt, J 8.0 and 1.3 Hz, Ar-H), 9.49 (2H, dt, J 7.2 and 1.7 Hz, Ar-H); δ$_C$ (CDCl$_3$, 100 MHz) 11.3, 18.5, 28.8, 35.9, 39.7, 63.6, 127.8, 129.53, 129.6, 129.8, 133.4, 142.5, 143.1, 144.6, 145.4; The mass spectrum could not be obtained.

3-(2-Methylbutyl)-*N*-benzyl tetrahydropyridine 61
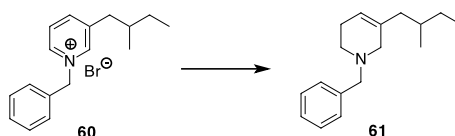
The reaction was carried out as described by Maranzano *et al*. [120] The benzyl pyridinium salt **60** (857 mg, 2.67 mmol, 1.0 eq.) was dissolved in dry MeOH (16 mL). The reaction mixture was cooled to 0 °C and NaBH$_4$ (404 mg, 10.68 mmol, 4.0 eq.) was added in small portions. The reaction mixture was heated to 65 °C for 16 h. after that time, the reaction mixture was cooled to RT and the solvent was removed under reduced pressure. The remaining solid was re-dissolved in CH$_2$Cl$_2$ and H$_2$O was added. The phases were separated and the aqueous layer was extracted with CH$_2$Cl$_2$. The combined organic layer was dried over Na$_2$SO$_4$ and the solvent was removed *in vacuo*. Purification by column chromatography afforded the pure product **61** as a colourless oil (344 mg, 1.14 mmol, 53%). R$_f$: 0.5 (6% MeOH/CH$_2$Cl$_2$); v/cm^{-1} (neat) 2958, 2913, 1660, 1494, 1453, 1377, 1359, 969, 737, 698; δ$_H$ (CDCl$_3$, 400 MHz) 0.84 (3H, d, *J* 6.8 Hz, C*H*$_3$), 0.87 (3H, t, *J* 7.37 Hz, C*H*$_3$), 0.91-0.97 (1H, m, C*H*$_2$CH$_3$), 1.02-1.19 (1H, m, C*H*$_2$CH$_3$), 1.29-1.40 (1H, m, Ar-C*H*$_2$), 1.40-1.50 (1H, m, Ar-C*H*$_2$), 1.72 (1H, dd *J* 13.33 and 8.60, CH$_2$C*H*CH$_2$), 1.95 (1H, dd, *J* 13.24 and 4.50, CH$_2$C*H*CH$_2$), 2.15 (2H, s, H-5), 2.43-2.62 (2H, m, H-6), 2.85 (2H, d, *J* 2.4 Hz, H-2), 3.59 (2H, s, PhC*H*$_2$), 5.44 (1H, s, H-4), 7.23-7.29 (1H, m, Ar-*H*), 7.41 (4H, m, Ar-*H*), δ$_C$ (CDCl$_3$, 100 MHz) 11.6, 19.2, 26.1, 29.5, 32.6, 43.5, 49.8, 56.1, 62.9, 120.3, 127.1, 128.3, 135.3, 138.6; *m/z* 244 (M+H, 100%); HRMS (ES$^+$) 244.2065 calculated for C$_{17}$H$_{26}$N$^+$ (M+H$^+$), found 244.2065, Δ= 0.0 ppm.

3-(2-Methylbutyl)-*N*-benzyl-*N*-oxide tetrahydropyridine 62
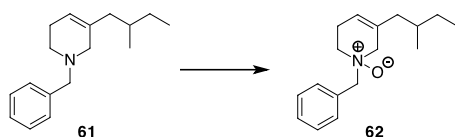
The reaction was carried out following a procedure by Maranzano *et al*. [121] The 3-alkyl tetrahydropyridine **61** (264 mg, 1.08 mmol, 1.0 eq.) and *m*-CPBA (205 mg, 1.18 mmol, 1.1 eq.) were dissolved in CH$_2$Cl$_2$ (5 mL). The reaction mixture was stirred at RT for 16 h. The crude product was concentrated and filtered through a short column of basic silica using a concentration gradient starting from 2% MeOH/CH$_2$Cl$_2$ to 10% MeOH/CH$_2$Cl$_2$ to give the product **62** as a yellow oil (117 mg, 0.45 mmol, 42%). R$_f$: 0.2 (6% MeOH/CH$_2$Cl$_2$); v/cm^{-1} (neat) 3262, 2959, 2921, 1659, 1454, 1378, 1033, 916, 728, 700; δ$_H$ (CDCl$_3$, 400 MHz) 0.75-0.87 (6H, 2xC*H*$_3$), 0.99-1.18 (C*H*$_2$CHCH$_2$), 1.24-1.48 (3H, m, alkyl), 1.75 (1H, dd, *J* 14.2 and 8.2 Hz, Ar-C*H*$_2$), 1.97 (1H, dd, *J* 14.3, 6.59 Hz, ArC*H*$_2$), 2.23-2.44 (1H, m, H-6), 2.53-2.69 (1H, m, H-5), 3.14-3.43 (1H, m, H-2), 3.94 (1H, d, *J* 40.4 Hz, H-2), 4.28-4.54 (2H, m, PhC*H*$_2$), 5.55 (1H, dd, *J* 3.3 and 1.7 Hz, H-4), 7.32-7.45 (3H, m, Ar-*H*), 7.52-7.58 (2H, m, Ar-*H*); δ$_C$ (CDCl$_3$, 100 MHz) 11.4, 18.9, 19.1, 23.4, 29.2, 29.5, 32.2, 42.5, 61.0, 66.7, 70.3, 70.5, 119.1, 128.6,

129.8, 131.4, 132.7; *m/z* 260 (M+H, 100%); HRMS (ES$^+$) 260.2014 calculated for $C_{17}H_{26}NO^+$ (M+H$^+$), found 260.2008, Δ= -2.3 ppm.

Diels-Alder adduct 64
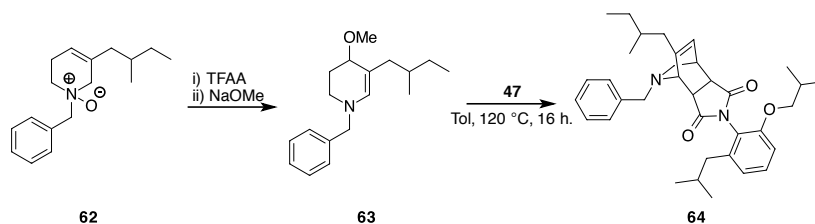
The reaction was carried out in accordance to the procedure described by Maranzano *et al*. [121] The *N*-oxide **62** (12 mg, 0.046 mmol, 1.0 eq.) was dissolved in dry toluene (0.13 mL). the reaction mixture was cooled to 0 °C and TFAA (13 µL, 0.092 mmol, 2.0 eq.) was added to the solution. The reaction mixture was stirred at RT for 1.5 h before NaOMe (12.4 mg, 0.23 mmol, 5.0 eq.) was added. The reaction mixture was stirred for another 1 h. The solvent was removed under reduced pressure and used crude for the next reaction. The *p*-methoxy tetrahydropyridine **63** (16 mg, 0.05 mmol, 1.0 eq.) and alkyl-substitued *N*-aryl maleimide **47** (13 mg, 0.07 mmol, 1.4 eq.) were dissolved in toluene (1 mL). The solvent was degassed (freeze-pump-thaw, 3 cycles) the reaction mixture was heated to reflux for 16 h. Purification by column chromatography gave the product **64** as a brown oil (3 mg, 0.006 mmol, 13%). Rf: 0.4 (PE/EtOAc 5:1); δ$_H$ (CDCl$_3$, 400 MHz) 0.83-1.33 (29H, m, alkyl), 3.11-3.24 (3H, m, NC*H*, NCHC*H*, NCHCHC*H*), 3.29-3.41 (2H, NC*H$_2$*), 4.93-4.97 (1H, m, CH$_2$C*H*), 5.50-5.64 (2H, m, ArC*H$_2$*), 6.16 (1H, s br, CH=C*H*), 7.28-7.67 (8H, m, Ar-H); δ$_C$ (CDCl$_3$, 100 MHz) 11.11 (s), 14.09 (s), 19.07 (s), 22.66 (s), 29.67 (s), 109.99 (s), 122.17 (s), 129.37-130.01 (m).

Protein Expression

In an eppendorf tube a stock solution (20 µL) of *E.coli* bacterial cells was defrosted on ice. The plasmid (3 µL) was added and the cells gently mixed. The tube was heated to 42 °C for 45 seconds and immediately put back on ice for 2 min. Media (700 µL) was added and the cells incubated for 30 min at 37 °C. Then, the solution was spread on agar plates, which were treated with chloramphenicol and ampicillin, and incubated overnight. From the grown colonies a single colony was picked and inoculated in media (2 mL). The falcon tube was incubated at 37 °C for 6 h, before the culture was transferred into a 100 mL of media. The culture was incubated over night. After that, this culture was divided into 5 times 1L of media. The cultures were grown until an optical density of 0.6 was achieved. Then, the cultures were induced with IPTG and incubated at 25 °C over night. To obtain the protein the cuture was divided into 4 centrifuge flasks and spun for 30 min at 5000 rpm. The supernatant was discarded, the obtained cell pellet was resuspended in water. The obtained slurry was sonicated in 30 sec intervals with 30 sec breaks for 3 min total sonication time. The resulting mixture was spun at 15000 rpm. The protein-containing supernatant was treated with DNAse and and MgCl$_2$ and left on ice for 30 min. Then, the protein was loaded onto a Hi-trap column

for purification. The crude protein was purified by FPLC using a Hepes buffer with an increasing gradient of imidazole. The protein-containing fractions were conbined and split in aliquots of 100 µL. The aliquots were rapidly frozen in liquid nitrogen and stored at -80 °C.

Determination of the Protein Concentration (Bicinchoninic Acid Assay)

A stock solution of BSA (10.5 mg in 1060 mL water) was prepared. An aliquot of this solution (50 µL) was transferred into the first well of a 96 well plate. Water (25 µL) was added to the remaining wells in the row. A 1-in-2 serial dilution was carried out. Bicinchoninic acid (5 mL) and $CuSO_4$ (1M, 100 µL) were mixed and added to the wells (200 µL). In the next row of the plate the protein solution (25 µL) and a 1 in 10 dilution were added. 200 µL of the bichinoic acid/$CuSO_4$ mix were added and the plate was incubated for 30 min. The absorbance was measured and the protein concentration calculated from the obtained graph.

AlphaScreen[®] Assay

Of all compounds and peptides stock solutions (10 mM in DMSO) were prepared. On a 384 well plate a 10 point 1-in-3 serial dilution of the compounds was carried out: To the first well of the row 15 µL of the compound stock was added. To the remaining wells of the row DMSO (10 µL) was added. Then, 5 µL of the compound stock was added to the second well of the row and mixed. From that well 5 µL were taken and added to the third well. This procedure continued until the last well. The 5 µL excess taken from the 10th well were discarded.

The compound controls (Whitby's **5a** and **Scripps** compound) were treated as compounds. A baseline control and negative control was implemented into the plate.

An aliquot (5 µL) of all concentrations was transferred to the assay plate. A dilution of protein and the respective peptide were added to each well. Nickel-chelate beads (20 µL beads in 980 µL buffer) were added to each well and the plate centrifuged for 20 sec to enhance mixing. The plate was placed on a shaker in the dark for 30 min at RT. Then, the streptavidine beads (20 µL beads in 980 µL buffer) were added. The plate was again centrifuged for 20 sec and placed on a shaker in the dark for another 1 h. The fluorescence was measured using a Pherastar plate reader (excitation 680 nm, emission 520-620 nm).

6. References

[1]   http://www.macmillan.org.uk (accessed August 2013).

[2]   Peepliwal, A. K.; Tandale, P. *J. Med. Heal. Sci.* **2013**, *2*, 31–42.

[3]   Klijn, J. G. .; Meijers-Heijboer, H. *Eur. J. Cancer Suppl.* **2003**, *1*, 13–23.

[4]   http://www.breastcancer.org (accessed August 2013).

[5]   http://seer.cancer.gov/csr/1975_2009_pops09/index. SEER Cancer Statistics Review , 1975-2009 (Vintage 2009 Populations) Contents in PDF (accessed August 2013).

[6]   Richie, R. C.; Swanson, J. O. *J. Insur. Med.* **2003**, *35*, 85–101.

[7]   Norman, S. A.; Potashnik, S. L.; Galantino, M. Lou; De Michele, A. M.; House, L.; Localio, A R. *J. Women's Heal.* **2007**, *16*, 177–190.

[8]   http://www.cancer.gov/cancertopics/types/breast (accessed August 2013).

[9]   Park, W.-C.; Jordan, V. C. *Trends Mol. Med.* **2002**, *8*, 82–88.

[10]   Friedman, M. A. *FDA News Events, Tamoxifen* **1998**.

[11]   Smith, I. E.; Dowsett, M. *N. Engl. J. Med.* **2003**, *348*, 2431–42.

[12]   Gunther, J. R.; Du, Y.; Rhoden, E.; Lewis, I.; Revennaugh, B.; Moore, T. W.; Kim, S. H.; Dingledine, R.; Fu, H.; Katzenellenbogen, J. A *J. Biomol. Screen.* **2009**, *14*, 181–193.

[13]   Ring, A.; Dowsett, M. *Endocr. Relat. Cancer* **2004**, *11*, 643–658.

[14]   Benoit, R.; Cooney, A.; Giguere, V.; Ingraham, H.; Lazar, M.; Muscat, G. *Pharmacol. Rev.* **2006**, *58*, 798–836.

[15]   Riggins, R. B.; Mazzotta, M. M.; Maniya, O. Z.; Clarke, R. *Endocr. Relat. Cancer* **2010**, *17*, R213–R231.

[16]   Piskunov, A.; Rochette-Egly, C. In *MSKs*; Arthur, S. C., Ed.; Landes Bioscience: Austin, **2012**; pp. 1–13.

[17]   Bain, D. L.; Heneghan, A. F.; Connaghan-Jones, K. D.; Miura, M. T. *Annu. Rev. Physiol.* **2007**, *69*, 201–220.

[18]   Annicotte, J.-S.; Chavey, C.; Servant, N.; Teyssier, J.; Bardin, A.; Licznar, A.; Badia, E.; Pujol, P.; Vignon, F.; Maudelonde, T.; Lazennec, G.; Cavailles, V.; Fajas, L. *Oncogene* **2005**, *24*, 8167–8175.

[19]   Fayard, E.; Auwerx, J.; Schoonjans, K. *Trends Cell Biol.* **2004**, *14*, 250–260.

[20]   Krylova, I. N.; Sablin, E. P.; Moore, J.; Xu, R. X.; Waitt, G. M.; MacKay, J. A.; Juzumiene, D.; Bynum, J. M.; Madauss, K.; Montana, V.; Lebedeva, L.; Suzawa, M.;

Williams, J. D.; Williams, S. P.; Guy, R. K.; Thornton, J. W.; Fletterick, R. J.; Willson, T. M.; Ingraham, H. A. *Cell* **2005**, *120*, 343–355.

[21] Benod, C.; Vinogradova, M. V; Jouravel, N.; Kim, G. E.; Fletterick, R. J.; Sablin, E. P. *Proc. Natl. Acad. Sci. U. S. A.* **2011**, *108*, 16927–16931.

[22] Lee, J. M.; Lee, Y. K.; Mamrosh, J. L.; Busby, S. a; Griffin, P. R.; Pathak, M. C.; Ortlund, E. A.; Moore, D. D. *Nature* **2011**, *474*, 506–510.

[23] Safi, R.; Kovacic, A.; Gaillard, S.; Murata, Y.; Simpson, E. R.; McDonnell, D. P.; Clyne, C. D. *Cancer Res.* **2005**, *65*, 11762–11770.

[24] Chand, A. L.; Wijayakumara, D. D.; Knower, K. C.; Herridge, K. A.; Howard, T. L.; Lazarus, K. A.; Clyne, C. D. *PLoS One* **2012**, *7*, e31593.

[25] Lazarus, K. A.; Wijayakumara, D.; Chand, A. L.; Simpson, E. R.; Clyne, C. D. *J. Steroid Biochem. Mol. Biol.* **2012**, *130*, 138–146.

[26] Heng, J.-C. D.; Feng, B.; Han, J.; Jiang, J.; Kraus, P.; Ng, J.-H.; Orlov, Y. L.; Huss, M.; Yang, L.; Lufkin, T.; Lim, B.; Ng, H.-H. *Cell Stem Cell* **2010**, *6*, 167–174.

[27] Wagner, R. T.; Xu, X.; Yi, F.; Merrill, B. J.; Cooney, A. J. *Stem Cells* **2010**, *28*, 1794–1804.

[28] Botrugno, O. a; Fayard, E.; Annicotte, J.-S.; Haby, C.; Brennan, T.; Wendling, O.; Tanaka, T.; Kodama, T.; Thomas, W.; Auwerx, J.; Schoonjans, K. *Mol. Cell* **2004**, *15*, 499–509.

[29] Miki, Y.; Clyne, C. D.; Suzuki, T.; Moriya, T.; Shibuya, R.; Nakamura, Y.; Ishida, T.; Yabuki, N.; Kitada, K.; Hayashi, S.; Sasano, H. *Cancer Lett.* **2006**, *244*, 24–33.

[30] Zhou, J.; Suzuki, T.; Kovacic, A.; Saito, R.; Miki, Y.; Ishida, T.; Moriya, T.; Simpson, E. R.; Sasano, H.; Clyne, C. D. *Cancer Res.* **2005**, *65*, 657–663.

[31] Wang, S.-L.; Zheng, D.-Z.; Lan, F.-H.; Deng, X.-J.; Zeng, J.; Li, C.-J.; Wang, R.; Zhu, Z.-Y. *Mol. Cell. Biochem.* **2008**, *308*, 93–100.

[32] Huang, P.; Chandra, V.; Rastinejad, F. *Annu. Rev. Physiol.* **2010**, *72*, 247–272.

[33] Mangelsdorf, D. J.; Thummel, C.; Beato, M.; Herrlich, P.; Schütz, G.; Umesono, K.; Blumberg, B.; Kastner, P.; Mark, M.; Chambon, P.; Evans, R. M. *Cell* **1995**, *83*, 835–839.

[34] Solomon, I. H.; Hager, J. M.; Safi, R.; McDonnell, D. P.; Redinbo, M. R.; Ortlund, E. A. *J. Mol. Biol.* **2005**, *354*, 1091–1102.

[35] Mangelsdorf, D. J.; Evanst, R. M. *Cell* **1995**, *83*, 841–850.

[36] Sablin, E. P.; Krylova, I. N.; Fletterick, R. J.; Ingraham, H. A. *Mol. Cell* **2003**, *11*, 1575–1585.

[37] Benecke, A.; Gronemeyer, H. *Gene Ther. Mol. Biol.* **1999**, *3*, 379–385.

[38] Wahli, W.; Desvergne, B. *Endocr. Rev.* **1999**, *20*, 649–688.

[39] Thiruchelvam, P. T. R.; Lai, C.-F.; Hua, H.; Thomas, R. S.; Hurtado, A.; Hudson, W.; Bayly, A. R.; Kyle, F. J.; Periyasamy, M.; Photiou, A.; Spivey, A. C.; Ortlund, E. A; Whitby, R. J.; Carroll, J. S.; Coombes, R. C.; Buluwela, L.; Ali, S. *Breast Cancer Res. Treat.* **2011**, *127*, 385–396.

[40] Chand, A. L.; Herridge, K. A.; Thompson, E. W.; Clyne, C. D. *Endocr. Relat. Cancer* **2010**, *17*, 965–975.

[41] Chand, A. L.; Herridge, K. A.; Howard, T. L.; Simpson, E. R.; Clyne, C. D. *Steroids* **2011**, *76*, 741–744.

[42] Ottow, E.; Weinmann, H. In *Nuclear Receptors as Drug Targets*; Ottow, E.; Weinmann, H.; Mannhold, R.; Kubinyi, H.; Folkers, G., Eds.; Wiley-VCH: Weinheim, **2008**; pp. 1–24.

[43] Mühl, H.; Pfeilschifter, J. *Pharm. Unserer Zeit* **2003**, *32*, 284–287.

[44] Meyer, U. *Pharm. Unserer Zeit* **2004**, *33*, 352–356.

[45] Quinkert, G. *Eur. J. Org. Chem.* **2004**, *2004*, 3727–3748.

[46] Gronemeyer, H.; Gustafsson, J.-A.; Laudet, V. *Nat. Rev. Drug Discov.* **2004**, *3*, 950–64.

[47] Osborne, Kent, C. *N. Engl. J. Med.* **1998**, *339*, 1609–1618.

[48] Shin, D.-J.; Osborne, T. F. *J. Biol. Chem.* **2008**, *283*, 15089–15096.

[49] Fayard, E.; Schoonjans, K.; Annicotte, J.-S.; Auwerx, J. *J. Biol. Chem.* **2003**, *278*, 35725–35731.

[50] Yazawa, T.; Inaoka, Y.; Okada, R.; Mizutani, T.; Yamazaki, Y.; Usami, Y.; Kuribayashi, M.; Orisaka, M.; Umezawa, A.; Miyamoto, K. *Mol. Endocrinol.* **2010**, *24*, 485–496.

[51] Clyne, C. D.; Speed, C. J.; Zhou, J.; Simpson, E. R. *J. Biol. Chem.* **2002**, *277*, 20591–20597.

[52] Clyne, C. D.; Kovacic, A.; Speed, C. J.; Zhou, J.; Pezzi, V.; Simpson, E. R. *Mol. Cell. Endocrinol.* **2004**, *215*, 39–44.

[53] Ortlund, E. A.; Lee, Y.; Solomon, I. H.; Hager, J. M.; Safi, R.; Choi, Y.; Guan, Z.; Tripathy, A.; Raetz, C. R. H.; McDonnell, D. P.; Moore, D. D.; Redinbo, M. R. *Nature* **2005**, *12*, 357–363.

[54] Whitby, R. J.; Dixon, S.; Maloney, P. R.; Delerive, P.; Goodwin, B. J.; Parks, D. J.; Willson, T. M. *J. Med. Chem.* **2006**, *49*, 6652–6655.

[55] Whitby, R. J.; Stec, J.; Blind, R. D.; Dixon, S.; Leesnitzer, L. M.; Orband-Miller, L. A.; Williams, S. P.; Willson, T. M.; Xu, R.; Zuercher, W. J.; Cai, F.; Ingraham, H. A. *J. Med. Chem.* **2010**, *54*, 2266–2281.

[56] Benod, C.; Carlsson, J.; Uthayaruban, R.; Hwang, P.; Irwin, J. J.; Doak, A. K.; Shoichet, B. K.; Sablin, E. P.; Fletterick, R. J. *J. Biol. Chem.* **2013**, *288*, 19830–44.

[57] Norris, J. D. *J. Biol. Chem.* **1998**, *273*, 6679–6688.

[58] Norris, J. D. *Science (80-.).* **1999**, *285*, 744–746.

[59] Leduc, A.-M.; Trent, J. O.; Wittliff, J. L.; Bramlett, K. S.; Briggs, S. L.; Chirgadze, N. Y.; Wang, Y.; Burris, T. P.; Spatola, A. F. *Proc. Natl. Acad. Sci. U. S. A.* **2003**, *100*, 11273–8.

[60] Williams, A. B.; Weiser, P. T.; Hanson, R. N.; Gunther, J. R.; Katzenellenbogen, J. A. *Org. Lett.* **2012**, *11*, 5370–5373.

[61] McDonnell, D. P.; Chang, C. Y.; Norris, J. D. *J. Steroid Biochem. Mol. Biol.* **2000**, *74*, 327–35.

[62] Bayly, A. R. PhD Thesis, Spivey, Imperial College London, **2011**.

[63] Topliss, J. G. *J. Med. Chem.* **1972**, *15*, 1006–11.

[64] Hobrecker, F. *Berichte der Dtsch. Chem. Gesellschaft* **1872**, *5*, 920–924.

[65] Wright, J. B. *Chem. Rev.* **1951**, *48*, 397–541.

[66] Ladenburg, A. *Berichte der Dtsch. Chem. Gesellschaft* **1875**, *8*, 535–536.

[67] Bahrami, K.; Khodaei, M.; Kavianinia, I. *Synthesis (Stuttg).* **2007**, *2007*, 547–550.

[68] Bastug, G.; Eviolitte, C.; Markó, I. E. *Org. Lett.* **2012**, *14*, 3502–5.

(69) Guru, M. M.; Ali, M. A.; Punniyamurthy, T. *J. Org. Chem.* **2011**, *76*, 5295–308.

[70] Kim, Y.; Kumar, M. R.; Park, N.; Heo, Y.; Lee, S. *J. Org. Chem.* **2011**, *76*, 9577–83.

[71] Li, J.; Bénard, S.; Neuville, L.; Zhu, J. *Org. Lett.* **2012**, *14*, 5980–3.

[72] Peng, J.; Ye, M.; Zong, C.; Hu, F.; Feng, L.; Wang, X.; Wang, Y.; Chen, C. *J. Org. Chem.* **2011**, *76*, 716–9.

[73] Wray, B. C.; Stambuli, J. P. *Org. Lett.* **2010**, *12*, 4576–9.

[74] Kedar, M. S.; Dighe, N. S.; Pattan, S. R.; Musmade, D. S. *Der Pharma Chim.* **2010**, *2*, 249–256.

[75] Praetorius, J. M.; Wang, R.; Crudden, C. M. *Organometallics* **2010**, *29*, 554–561.

[76] Labarbera, D. V; Skibo, E. B. *Bioorg. Med. Chem.* **2005**, *13*, 387–95.

[77] Thimmegowda, N. R.; Nanjunda Swamy, S.; Kumar, C. S. A.; Kumar, Y. C. S.; Chandrappa, S.; Yip, G. W.; Rangappa, K. S. *Bioorg. Med. Chem. Lett.* **2008**, *18*, 432–5.

[78] Kopańska, K.; Najda, A.; Zebrowska, J.; Chomicz, L.; Piekarczyk, J.; Myjak, P.; Bretner, M. *Bioorg. Med. Chem.* **2004**, *12*, 2617–24.

[79] Kosano, H.; Kayanuma, T.; Nishigori, H. *Biochim. Biophys. Acta* **2000**, *1499*, 11–18.

[80] Hwu, J. R.; Singha, R.; Hong, S. C.; Chang, Y. H.; Das, A. R.; Vliegen, I.; De Clercq, E.; Neyts, J. *Antiviral Res.* **2008**, *77*, 157–62.

[81] Tatsuta, M.; Kataoka, M.; Yasoshima, K.; Sakakibara, S.; Shogase, Y.; Shimazaki, M.; Yura, T.; Li, Y.; Yamamoto, N.; Gupta, J.; Urbahns, K. *Bioorg. Med. Chem. Lett.* **2005**, *15*, 2265–9.

[82] Murru, S.; Patel, B. K.; Bras, J. Le; Muzart, J. *J. Org. Chem.* **2009**, *74*, 2217–2220.

[83] Kline, T.; Felise, H. B.; Barry, K. C.; Jackson, S. R.; Nguyen, H. V; Miller, S. I. *J. Med. Chem.* **2008**, *51*, 7065–74.

[84] Klimesová, V.; Kocí, J.; Pour, M.; Stachel, J.; Waisser, K.; Kaustová, J. *Eur. J. Med. Chem.* **2002**, *37*, 409–18.

[85] Topliss, J. G. *J. Med. Chem.* **1977**, *20*, 463–469.

[86] Fujita, T.; Iwasa, J.; Hansch, C. *J. Med. Chem.* **1964**, *86*, 5175–5180.

[87] Sreedhar, B.; Venkanna, G.; Shiva Kumar, K.; Balasubrahmanyam, V. *Synthesis (Stuttg).* **2008**, *2008*, 795–799.

[88] Klapars, A.; Antilla, J. C.; Huang, X.; Buchwald, S. L. *J. Am. Chem. Soc.* **2001**, *123*, 7727–7729.

[89] Kiyomori, A.; Marcoux, J.; Buchwald, S. L. *Tetrahedron Lett.* **1999**, *40*, 2657–2660.

[90] Maxted, E, B. *J. Soc. Chem. Ind.* **1948**, *67*, 93–97.

[91] Dannhardt, G.; Kohl, B. K. *Arch. Pharm. (Weinheim).* **2000**, *333*, 123–9.

[92] Blythin, D. J.; Kaminski, J. J.; Domalski, M. S.; Spitler, J.; Solomon, D. M.; Conn, D. J.; Wong, S.; Verbiar, L. L.; Bober, L. A.; Chiu, P. J. S.; Watnick, A. S.; Siegel, M. I.; Hilbert, J. M.; Mcphailt, A. T. *J. Med. Chem.* **1986**, *29*, 1099–1113.

[93] Schelhaas, M.; Waldmann, H. *Angew. Chemie Int. Ed. English* **1996**, *35*, 2056–2083.

[94] Matsoukas, J.; Maragoudakis, M.; Vlaxakos, D. WO2008142576A2, **2008**.

[95) Grice, C. a; Tays, K. L.; Savall, B. M.; Wei, J.; Butler, C. R.; Axe, F. U.; Bembenek, S. D.; Fourie, A. M.; Dunford, P. J.; Lundeen, K.; Coles, F.; Xue, X.; Riley, J. P.; Williams, K. N.; Karlsson, L.; Edwards, J. P. *J. Med. Chem.* **2008**, *51*, 4150–69.

[96] Bamberg, J.; Hermann, J. C.; Lemoine, R.; Soth, M. WO2010063634, **2010**.

[97] Nicolaou, K. C.; Bulger, P. G.; Sarlah, D. *Angew. Chemie Int. Ed. English* **2005**, *44*, 4442–89.

[98] Kurti, L.; Czako, B. *Strategic Applications of Named Reactions in Organic Synthesis*; Hayhurst, J., Ed.; Elsevier Academic Press: Amsterdam, Boston, Heidelberg, London, New York, Oxford, Paris, San Diego, San Francisco, Singapore, Sydney, Tokyo, **2005**; p. 809.

[99] Cheung, W. S.; Parks, D. J.; Parsons, W. H.; Patel, S.; Player, M. R. US2008146637A1, **2008**.

[100] http://www.accessexcellence.org/RC/VL/GG/plasmid.php (accessed August 2013).

[101] Arkin, M. R.; Glicksman, Marcie, A.; Haian, F.; Havel, J.; Du, Y. In *Assay Guidance Manual*; Sittampalam, S. G.; Gal-Edd, N.; Arkin, M.; Auld, D.; Austin, C.; Bejcek, B.; Glicksman, Marcie, A.; Inglese, J.; McManus, O.; Minor, L.; Napper, A.; Riss, T.; Trask, J. J.; Weidner, J., Eds.; Bethesda (MD): Eli Lilly and Company and the National Centre for Advancing Translational Sciences, **2012**; pp. 1–25.

[102] http://www.iaszoology.com/elisa (accessed August 2013).

[103] : http://www.phenex-pharma.com/en/discovery-services/nr-screening-services (accessed August 2013).

[104] http://www.perkinelmer.co.uk/CMSResources/Images/44-73574MAN_AlphaScreenTruHitsKit.pdf (accessed August 2013).

[105] Rey, J.; Hu, H.; Kyle, F.; Lai, C.-F.; Buluwela, L.; Coombes, R. C.; Ortlund, E. A; Ali, S.; Snyder, J. P.; Barrett, A. G. M. *ChemMedChem* **2012**, *1*, 1909–1914.

[106] A Practical Guide to Working with the AlphaScreen; http://www.perkinelmer.co.uk/CMSResources/Images/44-73574MAN_AlphaScreenTruHitsKit.pdf (accessed August 2013).

[107] Busby, A. S.; Nuhant, P.; Cameron, M.; Mercer, B. A.; Hodder, P.; Roush, W. R.; Griffin, P. R.; Florida, S.; Way, C. S. *Discovery of Inverse Agonists for the Liver Receptor Homologue-1 (LRH-1; NR5A2)*; **2010**; Vol. 1, pp. 1–55.

[108] Davis, J. M.; Tsou, L. K.; Hamilton, A. D. *Chem. Soc. Rev.* **2007**, *36*, 326–34.

[109] Lehnert, U.; Xia, Y.; Royce, T. E.; Goh, C. S.; Liu, Y.; Senes, A.; Yu, H.; Zhang, Z. L.; Engelman, D. M.; Gerstein, M. *Q. Rev. Biophys.* **2004**, *37*, 121–146.

[110] Jochim, Andrea, L.; Arora, Paramjit, S. *ACS Chem. Biol.* **2010**, *5*, 919–923.

[111] Azzarito, V.; Long, K.; Murphy, N. S.; Wilson, A. J. *Nat. Chem.* **2013**, *5*, 161–173.

[112] Abell, A. D. *Lett. Pept. Sci.* **2002**, *8*, 267–272.

[113] Vagner, J.; Qu, H.; Hruby, V. *Curr. Opin. Chem. Biol.* **2008**, *12*, 292–296.

[114] Fletcher, S.; Hamilton, A. D. *J. R. Soc. Interface* **2006**, *3*, 215–233.

[115] Haridas, V. *Eur. J. Org. Chem.* **2009**, *30*, 5112–5128.

[116] Orner, B. P.; Ernst, J. T.; Hamilton, A D. *J. Am. Chem. Soc.* **2001**, *123*, 5382–3.

[117] Sundberg, R. J.; Hamilton, G.; Trindle, C. *J. Org. Chem.* **1986**, *51*, 3672–3679.

[118] Oshima, K.; Ohmura, T.; Suginome, M. *J. Am. Chem. Soc.* **2012**, *3*, 4–7.

[119] Li, F. MSci Report, Spivey, Imperial College London, **2012**.

[120] Gii, L.; Gateau-Olesker, A.; Marazano, C.; Das, B. C. *Tetrahedron Lett.* **1995**, *36*, 707–710.

[121] Leal Badaró Trindade, A. C.; dos Santos, D. C.; Gil, L.; Marazano, C.; Pereira de Freitas Gil, R. *European J. Org. Chem.* **2005**, *6*, 1052–1057.

[122]   Bayly, A. R.; White, A. J. P.; Spivey, A. C. *Eur. J. Org. Chem.* **2013**, *25*, 5566–5569.

[123]   Still, W. C.; Kahn, M.; Mitra, A. *J. Org. Chem.* **1978**, *43*, 2923–2925.

Appendix

Page Number	Type of work: text, figure, map, etc.	Source work	Copyright holder & year	Work out of copyright	Permission to re-use	Permission requested	permission refused	Orphan work
Page 1	Figure	McMillan.org.uk	McMillan Cancer Support 2014			✓		
Page 2	Figures (2)	Breastcancer.org	Breastcancer.org 2014		✓			
Page 5	Figure	Cancer.gov	Cancer.gov			✓		
Page 11	Figure	*J. Mol. Biol.* 2005, *354*, 1091–1102.	Elsevier 2005		✓			
Page 19	Scheme	*J. Biomol. Screen.* 2009, *14*, 181– 193.	Sage Publications 2009		✓			
Page 19	Figure	*Org. Lett. 2012, 11,* 5370–5373.	ACS Publications 2009		✓			
Page 32	Scheme	*J. Med. Chem.* 1972, *15*, 1006–11.	ACS Publications 1972		✓			
Page 53	Scheme	http://www.access excellence.org	http://www.accessexce llence.org					✓
Page 54	Scheme 2x	http://www.access excellence.org	http://www.accessexce llence.org					✓
Page 57	Scheme	http://www.iaszool ogy.com/elisa		✓				

Page Number	Type of work: text, figure, map, etc.	Source work	Copyright holder & year	Work out of copyright	Permission to re-use	Permission requested	permission refused	Orphan work
Page 58	Scheme	*Assay Guidance Manual*; Bethesda (MD): Eli Lilly and Company and the National Centre for Advancing Translational Sciences, 2012; pp. 1–25.	Bethesda (MD): Eli Lilly and Company and the National Centre for Advancing Translational Sciences, 2012; pp. 1–25.	✓		(✓)		
Page 59	Scheme	http://www.phenex-pharma.com	http://www.phenex-pharma.com 2014		✓			
Page 59	Scheme	PerkinElmer.co.uk	PerkinElmer 2014		✓			
Page 60	Scheme	PerkinElmer.co.uk	PerkinElmer 2014		✓			
Page 72	Figure	*J. Am. Chem. Soc.* 2001, *123*, 5382–3.	ACS Publications 2001		✓			

Left column:

permission to use a picture
3 messages

Melanie Mueller <m.mueller07@imperial.ac.uk>   20 January 2014 20:26
To: comments@breastcancer.org

Dear Sir or Madam,

I currently write my PhD thesis about breast cancer and I was wondering if I could have the permission to use a picture I found on your website in my introduction?

Many thanks and best wishes,

Melanie Müller

Melissa Jenkins <MJenkins@breastcancer.org>   20 January 2014 20:44
To: Melanie Mueller <m.mueller07@imperial.ac.uk>
Cc: comments <comments@breastcancer.org>

Yes, thanks for asking. Just please credit Breastcancer.org.

Best, Melissa Bollmann-Jenkins
[Quoted text hidden]

Melanie Mueller <m.mueller07@imperial.ac.uk>   20 January 2014 21:28
To: Melissa Jenkins <MJenkins@breastcancer.org>

Thanks a lot!

I certainly will do.

With best wishes,

Melanie
[Quoted text hidden]

Right column:

permission to use a picture in my PhD thesis [Inquiry: 140120-000065]
1 message

NCI Cancer.gov Staff <cancer.gov_staff@mail.nih.gov>   22 January 2014 13:23
Reply-To: "NCI Cancer.gov Staff" <cancer.gov_staff@mail.nih.gov>
To: m.mueller07@imperial.ac.uk

Thank you for contacting the National Cancer Institute. Below is a response to your recent request for information.

Subject
permission to use a picture in my PhD thesis

Discussion Thread
Response Via Email (NCI Agent)   01/22/2014 05:23 AM
Dear Ms. Müller:

Thank you for your e-mail to the National Cancer Institute (NCI) regarding permission to use an image from the NCI's website.

Some of the artwork that appears on NCI's website is owned by the artist, and permission must be obtained from the artist to use the images. We encourage you to explore NCI's Visuals Online website (http://visualsonline.cancer.gov) to locate images of interest. The image details for each image include information about any reuse restrictions and contact information for the rights holder.

Most of the information on the NCI website is in the public domain and is not subject to copyright restrictions. For more information, you may wish to refer to the Copyright and Reuse of Graphics and Text section of the NCI's Web Policies webpage, which includes information about reusing NCI information, registered trademarks, and copyrighted material. This resource is located at http://www.cancer.gov/policies/page5.

We hope this information is helpful.

National Cancer Institute Staff

If you get an error message when you click on the URLs in this e-mail, copy the full URL and paste it into your browser.

Customer By Email (Melanie Mueller)   01/20/2014 12:33 PM
Dear Sir or Madam,

I currently write my PhD thesis about breast cancer and I was wondering if I could have the permission to use a picture I found on your website in my introduction?

Many thanks and best wishes,

License Details — Elsevier

Copyright Clearance Center — RightsLink®

My Orders | My Library | My Profile | My Orders | My Library | My Profile | Log out | Help

My Orders > Orders > All Orders

License Details

Thank you very much for your order.

This is a License Agreement between melanie muller ("You") and Elsevier ("Elsevier"). The license consists of your order details, the terms and conditions provided by Elsevier, and the payment terms and conditions.

Get the printable license.

License Number	3313230295083
License date	Jan 20, 2014
Licensed content publisher	Elsevier
Licensed content publication	Journal of Molecular Biology
Licensed content title	Crystal Structure of the Human LRH-1 DBD–DNA Complex Reveals Ftz-F1 Domain Positioning is Required for Receptor Activity
Licensed content author	Isaac H. Solomon,Janet M. Hager,Rachid Safi,Donald P. McDonnell,Matthew R. Redinbo,Eric A. Ortlund
Licensed content date	16 December 2005
Licensed content volume number	354
Licensed content issue number	5
Number of pages	12
Type of Use	reuse in a thesis/dissertation
Portion	figures/tables/illustrations
Number of figures/tables/illustrations	1
Format	both print and electronic
Are you the author of this Elsevier article?	No
Will you be translating?	No
Title of your thesis/dissertation	Towards the Development of Modulators of LRH-1 as Potential Anti-Cancer Therapeutic Leads
Expected completion date	Jan 2014
Estimated size (number of pages)	130
Elsevier VAT number	GB 494 6272 12
Permissions price	0.00 GBP
VAT/Local Sales Tax	0.00 GBP / 0.00 GBP
Total	**0.00 GBP**

◄ Back

Copyright © 2014 Copyright Clearance Center, Inc. All Rights Reserved. Privacy statement . Comments? We would like to hear from you. E-mail us at customercare@copyright.com

---

SAGE

Copyright Clearance Center — RightsLink®

Home | Account Info | Help

Title: A Set of Time-Resolved Fluorescence Resonance Energy Transfer Assays for the Discovery of Inhibitors of Estrogen Receptor-Coactivator Binding:

Author: Jillian R. Gunther, Yuhong Du, Eric Rhoden, Iestyn Lewis, Brian Revennaugh, Terry W. Moore, Sung Hoon Kim, Raymond Dingledine, Haian Fu, John A. Katzenellenbogen

Publication: Journal of Biomolecular Screening

Publisher: SAGE Publications

Date: 02/01/2009

Copyright © 2009, Society for Laboratory Automation and Screening

Logged in as: melanie muller

LOGOUT

Gratis

Permission is granted at no cost for sole use in a Master's Thesis and/or Doctoral Dissertation. Additional permission is also granted for the selection to be included in the printing of said scholarly work as part of UMI's "Books on Demand" program. For any further usage or publication, please contact the publisher.

BACK | CLOSE WINDOW

Copyright © 2014 Copyright Clearance Center, Inc. All Rights Reserved. Privacy statement. Comments? We would like to hear from you. E-mail us at customercare@copyright.com

---

ACS Publications

Copyright Clearance Center — RightsLink®

Home | Account Info | Help

Title: Synthesis of Biphenyl Proteomimetics as Estrogen Receptor-α Coactivator Binding Inhibitors

Author: Anna B. Williams, Patrick T. Weiser, Robert N. Hanson, Jillian R. Gunther, and John A. Katzenellenbogen

Publication: Organic Letters

Publisher: American Chemical Society

Date: Dec 1, 2009

Copyright © 2009, American Chemical Society

Logged in as: melanie muller

LOGOUT

PERMISSION/LICENSE IS GRANTED FOR YOUR ORDER AT NO CHARGE

This type of permission/license, instead of the standard Terms & Conditions, is sent to you because no fee is being charged for your order. Please note the following:

- Permission is granted for your request in both print and electronic formats, and translations.
- If figures and/or tables were requested, they may be adapted or used in part.
- Please print this page for your records and send a copy of it to your publisher/graduate school.
- Appropriate credit for the requested material should be given as follows: "Reprinted (adapted) with permission from (COMPLETE REFERENCE CITATION). Copyright (YEAR) American Chemical Society." Insert appropriate information in place of the capitalized words.
- One-time permission is granted only for the use specified in your request. No additional uses are granted (such as derivative works or other editions). For any other uses, please submit a new request.

If credit is given to another source for the material you requested, permission must be obtained from that source.

BACK | CLOSE WINDOW

Copyright © 2014 Copyright Clearance Center, Inc. All Rights Reserved. Privacy statement. Comments? We would like to hear from you. E-mail us at customercare@copyright.com

---

ACS Publications

Copyright Clearance Center — RightsLink®

Home | Account Info | Help

Title: Utilization of operational schemes for analog synthesis in drug design

Author: John G. Topliss

Publication: Journal of Medicinal Chemistry

Publisher: American Chemical Society

Date: Oct 1, 1972

Copyright © 1972, American Chemical Society

Logged in as: melanie muller

LOGOUT

PERMISSION/LICENSE IS GRANTED FOR YOUR ORDER AT NO CHARGE

This type of permission/license, instead of the standard Terms & Conditions, is sent to you because no fee is being charged for your order. Please note the following:

- Permission is granted for your request in both print and electronic formats, and translations.
- If figures and/or tables were requested, they may be adapted or used in part.
- Please print this page for your records and send a copy of it to your publisher/graduate school.
- Appropriate credit for the requested material should be given as follows: "Reprinted (adapted) with permission from (COMPLETE REFERENCE CITATION). Copyright (YEAR) American Chemical Society." Insert appropriate information in place of the capitalized words.
- One-time permission is granted only for the use specified in your request. No additional uses are granted (such as derivative works or other editions). For any other uses, please submit a new request.

If credit is given to another source for the material you requested, permission must be obtained from that source.

BACK | CLOSE WINDOW

Copyright © 2014 Copyright Clearance Center, Inc. All Rights Reserved. Privacy statement. Comments? We would like to hear from you. E-mail us at customercare@copyright.com

ACCESS EXCELLENCE
@ the national health museum
ABOUT AE

Note: the "Contact us" link did not work any longer.

Gmail by Google

Melanie Muller <melanie.muller.ic@gmail.com>

AW: Fwd: Phenex Pharmaceuticals AG - Contact Form
2 messages

Thomas Schlueter <Thomas.Schlueter@phenex-pharma.com>   22 January 2014 10:17
To: m.mueller07@imperial.ac.uk

Dear Melanie,

no problem, please feel free to use that picture.

I also attached some more recent slides - just in case.

Best

Thomas

Phenex Pharmaceuticals AG
Dr. Thomas Schlueter
VP Discovery Services
Waldhofer Strasse 104
D-69123 Heidelberg
Germany
Phone: ++49-(0)6221-65282-21
Fax : ++49-(0)6221-65282-10
thomas.schlueter@phenex-pharma.com

P Sustainable development – Do you really need to print this email?

Von: Services [mailto:services@phenex-pharma.com]
Gesendet: Dienstag, 21. Januar 2014 21:38
An: Thomas Schlueter
Betreff: Fwd: Phenex Pharmaceuticals AG - Contact Form

> ---------- Ursprüngliche Nachricht ----------
> Von: Melanie Muller <m.mueller07@imperial.ac.uk>
> An: info@phenex-pharma.com
> Datum: 20. Januar 2014 um 22:39
> Betreff: Phenex Pharmaceuticals AG - Contact Form
>
> Dear Sir or Madam,
>
> I currently write my PhD thesis and I was wondering if I could have your permission to use a picture of a FRET assay I found on your website in my introduction?
>
>
> Many thanks and best wishes,
>
> Melanie Müller
>

Gmail by Google

Melanie Muller <melanie.muller.ic@gmail.com>

RE: permission to use AlphaScreen pictures from your website
3 messages

LAS-EU CC UK <LAS-EUCCUK@perkinelmer.com>   21 January 2014 14:18
To: Melanie Muller <melanie.muller.ic@gmail.com>

Dear Ms. Muller,

I have received the relevant approval, hence you may use the pictures of AlphaScreen

Kind regards,

Magdalena Nocuń | Customer Care UK & Ireland

PerkinElmer | For the Better

cc.uk@perkinelmer.com

Phone: 0800 896 046 | Fax: 0800 891 714 |

Chalfont Road, Seer Green, Beaconsfield, Bucks, HP9 2FX

cc.ie@perkinelmer.com

Phone: 1800 932 886 | Fax: 1800 932 884 |

C17 The Exchange, Calmount Park, Ballymount, Dublin 12

www.perkinelmer.com

Follow us on facebook and twitter

Please consider the environment before printing this e-mail.

This e-mail message and any attachments are confidential and proprietary to PerkinElmer, Inc. If you are not the intended recipient of this message, please inform the sender by replying to this email or sending a message to the sender and destroy the message and any attachments. Thank you.

From: Melanie Muller [mailto:melanie.muller.ic@gmail.com]
Sent: Monday, January 20, 2014 10:54 PM
To: LAS-EU CC UK
Subject: permission to use AlphaScreen pictures from your website

Dear Sir or Madam,

I currently write my PhD thesis and I was wondering if I could get permission use 2 explanatory pictures of the AlphaScreen I found on your website?

Many thanks and best wishes,

Melanie Müller

LAS-EU CC UK <LAS-EUCCUK@perkinelmer.com>
To: Melanie Muller <melanie.muller.ic@gmail.com>   22 January 2014 08:27

Dear Ms. Muller,

Following my yesterday's e-mail please kindly acknowledge the images of PerkinElmer when using them by:

Images used with permission of PerkinElmer. © 2014 PerkinElmer.

Thank you.

Kind regards,

Magdalena Nocuń | Customer Care UK & Ireland
PerkinElmer | For the Better
cc.uk@perkinelmer.com
Phone: 0800 896 046 | Fax: 0800 891 714 |
Chalfont Road, Seer Green, Beaconsfield, Bucks, HP9 2FX
cc.ie@perkinelmer.com
Phone: 1800 932 886 | Fax: 1800 932 884 |
C17 The Exchange, Calmount Park, Ballymount, Dublin 12
www.perkinelmer.com
Follow us on facebook and twitter
Please consider the environment before printing this e-mail.

From: LAS-EU CC UK
Sent: Tuesday, January 21, 2014 3:18 PM
To: 'Melanie Muller'
Subject: RE: permission to use AlphaScreen pictures from your website

[Quoted text hidden]

Melanie Muller <melanie.muller.ic@gmail.com>
To: LAS-EU CC UK <LAS-EUCCUK@perkinelmer.com>   22 January 2014 11:03

Dear Magdalena,

Yes I will certainly do this.

Many thanks and best wishes,

Melanie
[Quoted text hidden]

Copyright Clearance Center **RightsLink®**   Home Account Info Help

ACS Publications High quality. High impact.

Title: Toward Proteomimetics: Terphenyl Derivatives as Structural and Functional Mimics of Extended Regions of an α-Helix

Author: Brendan P. Orner, Justin T. Ernst, and, and Andrew D. Hamilton*

Publication: Journal of the American Chemical Society

Publisher: American Chemical Society

Date: Jun 1, 2001

Copyright © 2001, American Chemical Society

Logged in as:
melanie muller

LOGOUT

PERMISSION/LICENSE IS GRANTED FOR YOUR ORDER AT NO CHARGE

This type of permission/license, instead of the standard Terms & Conditions, is sent to you because no fee is being charged for your order. Please note the following:

- Permission is granted for your request in both print and electronic formats, and translations.
- If figures and/or tables were requested, they may be adapted or used in part.
- Please print this page for your records and send a copy of it to your publisher/graduate school.
- Appropriate credit for the requested material should be given as follows: "Reprinted (adapted) with permission from (COMPLETE REFERENCE CITATION). Copyright (YEAR) American Chemical Society." Insert appropriate information in place of the capitalized words.
- One-time permission is granted only for the use specified in your request. No additional uses are granted (such as derivative works or other editions). For any other uses, please submit a new request.

If credit is given to another source for the material you requested, permission must be obtained from that source.

BACK   CLOSE WINDOW